

Retinal and Optic Nerve Head Vascular Reactivity in Primary Open Angle Glaucoma

by

Subha Trichy Venkataraman

A thesis

presented to the University of Waterloo

in fulfillment of the

thesis requirement for the degree of

Doctor of Philosophy

in

Vision Science

Waterloo, Ontario, Canada, 2009

©Subha Trichy Venkataraman 2009

I hereby declare that I am the sole author of this thesis. This is a true copy of the thesis including any final revisions, as accepted by my examiners.

I understand that my thesis may be made electronically available to the public.

Abstract

The global aim of this thesis was to assess retinal vascular reactivity in glaucoma patients using a standardised hypercapnic stimulus. There is a suggestion of disturbance in the regulation of retinal and optic nerve head (ONH) hemodynamics in patients with Primary Open Angle Glaucoma (POAG), although much of the work to-date has either been equivocal or speculative. Previous studies have used non-standardised hypercapnic stimuli to assess vascular reactivity. To explain, hypercapnia induces hyperventilation which disturbs arterial oxygen concentration, an effect that varies between individuals resulting in the non-standardised provocation of vascular reactivity. Therefore, a normoxic hypercapnic provocation was developed to avoid additional and potentially uncontrolled vasoconstriction in what is thought to be a vasospastic disease. The development of a safe, sustained and stable normoxic hypercapnic stimulus was essential for the assessment of retinal arteriolar vascular reactivity so that repeated hemodynamic measurements could be obtained. Furthermore, most techniques used to measure vascular reactivity do not comprehensively assess retinal hemodynamics, in terms of the simultaneous measurement of vessel diameter and blood velocity in order to calculate flow. In this respect, this study utilized a technique that quantitatively assesses retinal blood flow and vascular reactivity of the major arterioles in close proximity to the ONH. The stimulus and vascular reactivity quantification technique was validated in healthy controls and then was clinically applied in patients with POAG. Newly diagnosed patients with untreated POAG (uPOAG) were recruited in order to avoid any confounding pharmacological effects and patients with progressive POAG (pPOAG) were also selected since they are thought to likely manifest vascular dysregulation. Finally, the results of the functional vascular reactivity assessment were compared to those of

systemic biochemical markers of endothelial function in patients with untreated and progressive POAG and in healthy controls.

Overall summary

A safe, sustained, stable and repeatable normoxic hypercapnic stimulus was developed, evaluated and validated. In terms of the physiology of retinal vascular regulation, the percent magnitude of vascular reactivity of the arterioles and capillaries was found to be comparable in terms of flow. The new stimulus was successfully applied in POAG and in healthy controls to assess vascular reactivity and was also compared to plasma levels of ET-1 and cGMP. In terms of the patho-physiology of POAG, the study revealed a clear impairment of vascular reactivity in the uPOAG and pPOAG groups. There were reduced levels of plasma ET-1 in the uPOAG and ntPOAG groups. In addition, treatment with Dorzolamide improved vascular reactivity in the ntPOAG group in the absence of any change in the expression of plasma ET-1 or cGMP. Future work will address this apparent contradiction between the outcome of the functional vascular reactivity assessment and the biochemical markers of endothelial function in newly diagnosed POAG patients treated with Dorzolamide.

Aims of chapters

- Chapter 3: To determine the effect of hypercapnia on retinal capillary blood flow in the macula and ONH using scanning laser Doppler flowmetry (SLDF) in young healthy subjects.
- Chapter 4: To describe a new manual methodology that permits the comprehensive assessment of retinal arteriolar vascular reactivity in response to a sustained and stable hypercapnic stimulus. The secondary aim was to determine the magnitude of the vascular reactivity response of the retinal arterioles to hypercapnic provocation in young healthy subjects.
- Chapter 5: To compare the magnitude of vascular reactivity of the retinal arterioles in terms of percentage change of flow to that of the retinal capillaries using a novel automated standardized methodology to provoke normoxic, or isoxic, hypercapnia.
- Chapter 6: To determine the magnitude of retinal arteriolar vascular reactivity to normoxic hypercapnia in patients with untreated POAG (uPOAG), progressive POAG (pPOAG) and controls. The secondary aim was to determine retinal vascular reactivity in newly treated POAG (ntPOAG, i.e. after treatment with 2% Dorzolamide, twice daily for 2 weeks).
- Chapter 7: To compare plasma endothelin-1 (ET-1) and cyclic guanosine monophosphate (cGMP) between groups of patients with untreated primary open angle glaucoma (uPOAG), progressive POAG (pPOAG), newly treated POAG (ntPOAG) and controls. The effect of normoxic hypercapnia on plasma ET-1 and cGMP was also assessed. The functional measures of retinal blood flow and vascular reactivity were correlated with systemic biochemical markers of endothelial function.

Methods

Chapters 3, 4 and 5 were conducted on young healthy control subjects, where as Chapters 6 and 7 were conducted on patients with glaucoma and healthy controls.

- Chapter 3: Subjects breathed unrestricted air for 15 minutes (baseline) via a sequential gas delivery circuit and then the fractional (percent) end-tidal concentration of CO₂ (FETCO₂) was manually raised for 15 minutes by adding a low flow of CO₂ to the inspired air. For the last 15 minutes, FETCO₂ was returned to baseline values to establish a recovery period. Heidelberg Retina Flowmeter (HRF) images centered on both the ONH and the macula were acquired during each phase.
- Chapter 4: Subjects breathed air via a sequential gas delivery circuit for 15 minutes and the air flow was then manually decreased so that subjects inspired gases from the rebreathing reservoir until a stable 10-15% increase in FETCO₂ concentration was achieved for 20 minutes. Air flow rate was then manually elevated so that subjects breathed primarily from the fresh gas reservoir to return FETCO₂ back to baseline for the last 15 minutes. Retinal arteriolar hemodynamics was assessed using the Canon Laser Blood Flowmeter (CLBF) during all three breathing phases.
- Chapter 5: Normoxic, or isoxic, hypercapnia was induced using an automated gas flow controller (RespirAct™, Thornhill Research Inc. Toronto, Canada). Subjects breathed air with PETCO₂ normalized at 38 mmHg. An increase in PETCO₂ of 15% above baseline, whilst maintaining normoxia, was then implemented for 20 minutes and then PETCO₂ was returned to baseline conditions for 10 minutes. Retinal and ONH hemodynamic measurements were performed using the CLBF and HRF in random order across sessions.

- Chapter 6: Retinal arteriolar vascular reactivity was assessed in patients with uPOAG, pPOAG (defined by the occurrence of optic disc hemorrhage within the past 24 months) and controls during normoxic hypercapnia. Using the automated gas flow controller, patients breathed air for 10 mins and PETCO₂ was maintained at 38mmHg. Following this normoxic hypercapnia (a 15% increase in PETCO₂ while PETO₂ was maintained at resting levels) was induced for 15 mins and then for the last 10 mins PETCO₂ was returned to baseline (post-hypercapnia) to establish recovery blood flow values. Retinal arteriolar diameter, blood velocity and blood flow was assessed using the CLBF in both patient groups and controls. A similar paradigm was repeated in the newly treated POAG group (ntPOAG, i.e. after treatment with 2% Dorzolamide, twice daily for 2 weeks).
- Chapter 7: Blood samples were collected from the cubital vein of all participants (uPOAG, pPOAG, ntPOAG and controls) during baseline conditions (PETCO₂=38mmHg) and then during normoxic hypercapnia (i.e. a 15% increase in PETCO₂ relative to the baseline) using the paradigm described for Chapter 6. ET-1 and cGMP was assessed using immunoassay.

Results

- Chapter 3: The group mean nasal macula capillary blood flow increased from 127.17 a.u. (SD 32.59) at baseline to 151.22 a.u. (SD 36.67) during hypercapnia (p=0.028), while foveal blood flow increased from 92.71 a.u. (SD 28.07) to 107.39 a.u. (SD 34.43) (p=0.042). There was a concomitant and uncontrolled +13% increase in the group mean PETO₂ during the hypercapnic provocation of +14% increase in PETCO₂.
- Chapter 4: Retinal arteriolar diameter, blood velocity and blood flow increased by 3.2% (p=0.0045), 26.4% (p<0.0001) and 34.9% (p<0.0001), respectively during hypercapnia.

There was a stable +12% increase in PETCO₂ during hypercapnia and a concomitant -6% decrease in PETO₂.

- Chapter 5: Using an automated gas flow controller the co-efficient of repeatability (COR) was 5% of the average PETCO₂ at baseline and during normoxic hypercapnia. The COR for PETO₂ was 10% and 7% of the average PETO₂ at baseline and during normoxic hypercapnia, respectively. Group mean PETCO₂ increased by approximately +14.4% and there was only a +4.3% increase in PETO₂ during hypercapnia across both study sessions. Retinal arteriolar hemodynamics increased during hypercapnia (p<0.001). Similarly, there was an increase in the capillary blood flow of the temporal rim of the ONH (p<0.001), nasal macula (p<0.001) and foveal areas (p<0.006) during hypercapnia. A non-significant trend for capillary blood flow to increase in the macula temporal area (+8.2%) was noted. In terms of percentage change of blood flow, retinal capillary vascular reactivity (i.e. all 4 analyzed areas = 22.4%) was similar to the magnitude of arteriolar (= 24.9%) vascular reactivity.
- Chapter 6: Retinal arteriolar diameter, blood velocity and flow did not increase during normoxic hypercapnia in uPOAG compared to controls. Diameter and blood velocity did not change in pPOAG during normoxic hypercapnia but there was a significant increase in blood flow (+9.1%, p=0.030). After treatment with 2% Dorzolamide for 2 weeks there was a 3% (p=0.040), 19% (p<0.001) and 26% (p<0.001) increase in diameter, velocity and flow, respectively, in the ntPOAG group. Group mean PETCO₂ increased by approximately +15% in all the groups and there was only a +3% increase in PETO₂ during hypercapnia.
- Chapter 7: Plasma ET-1 levels were significantly different across groups at baseline (one way ANOVA; p=0.0012) and this was repeated during normoxic hypercapnia (one way ANOVA; p=0.0014). ET-1 levels were lower in uPOAG compared to pPOAG and controls at

baseline and during normoxic hypercapnia (Tukey's honestly significant difference test). Similarly, ntPOAG group also showed lower ET-1 levels compared to the pPOAG and controls at baseline and during normoxic hypercapnia (Tukey's honestly significant difference test). The cGMP at baseline and during normoxic hypercapnia across all groups was not different. In the control group, the change in ET-1 during normoxic hypercapnia was negatively correlated with change in retinal arteriolar blood flow ($r = -0.52$, $p=0.04$), that is, as the change in ET-1 reduced, the change in blood flow increased. A weak correlation was noted between change in cGMP during normoxic hypercapnia and the change in arteriolar blood flow ($r = +0.45$, $p=0.08$).

Conclusions

- Chapter 3: Hypercapnia resulted in a quantifiable capillary vascular reactivity response in 2 of the 3 assessed retinal locations (i.e., nasal macula and fovea). There was no vascular reactivity response of the ONH. It is critical to minimise the concomitant change in $PETO_2$ during hypercapnia in order to obtain robust vascular reactivity responses.
- Chapter 4: A technique to comprehensively assess vascular reactivity during stable and sustained hypercapnia was described. Retinal arteriolar diameter, blood velocity and blood flow increased in response to hypercapnia. The vascular reactivity results of this study served as a reference for future studies using the hypercapnic provocation and CLBF. Also, the concomitant change in $PETO_2$ using the partial rebreathing technique was reduced compared to the manual addition of CO_2 technique described in Chapter 3 but was still greater than optimal.

- Chapter 5: A new automated gas flow controller was used to induce standardised normoxic, or isoxic, hypercapnia. The magnitude of vascular reactivity in both retinal arterioles and capillaries in response to the new hypercapnic stimulus was robust compared to the previous stimuli. There was a clear ONH vascular reactivity response in this study, unlike the result attained in Chapter 3. Although theoretically it is predictable that the percent magnitude of vascular reactivity of the arterioles and capillaries should be similar, this is the first study to show that they are indeed comparable. The magnitude of hypercapnia was repeatable and the concomitant change in $P_{ET}O_2$ was minimal and physiologically insignificant.
- Chapter 6: The normal response of the retinal arterioles and capillaries to normoxic hypercapnia is impaired in both uPOAG and pPOAG compared to controls. Short term treatment with 2% topical Dorzolamide for two weeks improved retinal vascular reactivity in ntPOAG. However, it is still unclear whether this improvement is a direct effect of Dorzolamide or as a secondary effect of the decrease in intraocular pressure (IOP).
- Chapter 7: We found a reduction in the plasma ET-1 at baseline and during normoxic hypercapnia in the uPOAG and in the ntPOAG groups. This is the first study to show a lower plasma ET-1 level in uPOAG. The fact that this finding was repeated after 2 weeks treatment with Dorzolamide in the ntPOAG group further validates these results. It also suggests that Dorzolamide treatment does not impact ET-1 and cGMP measures, although it clearly results in an improvement of vascular reactivity. Correlation results suggest that as the change in ET-1 reduced during normoxic hypercapnia, the change in blood flow increased in the controls.

Acknowledgements

I sincerely thank my supervisors Dr. Chris Hudson and Dr. John Flanagan for their continuous guidance, support and encouragement throughout my graduate program at Waterloo. I appreciate their time and efforts and I am grateful for their assistance.

I would like to extend my gratitude to my committee members Dr. Tony Cullen and Dr. Richard Hughson for their invaluable suggestions that significantly improved the quality of this thesis work.

I would like to express my sincere gratitude to Dr. Joseph Fisher and his lab members (Isocapnia Research Laboratory) for always being there to clarify my doubts.

I would like to thank Dr. Graham Trope and Dr. Yvonne Buys for their guidance and help in recruiting participants in the study. I also thank Dr. Markowitz for helping in the recruitment process.

My special thanks to Tien Wong for his help in the study procedure. I would also like to thank Mariel Escover, Dr. Rony Rachmiel, Dr. Taher Ahmed, Shelley Culp-Stewart, Rudy Vogl and Dr. Tong for their help in various study procedures.

I thank the graduate officers, graduate coordinators, staff and faculty at the School of Optometry and fellow graduate students in vision science. Thanks to Robin Jones for his help in instrumentation and Erin Harvey for statistical help.

I would like to thank fellow graduate students in Dr.Hudson's lab and also Dr. Edward Gilmore and Marie O'Brien Stockie for their support throughout my graduate program.

Thanks to the American Optometric Foundation (AOF) for providing me the Ezell fellowship and also Glaucoma Research Society of Canada and Canadian Institutes of Health Research (CIHR) for funding this research.

Finally, I would like to thank my parents, brother & sisters and their family for their love and emotional support that helped me get this far. I also thank my in-laws for their encouragement and support. Special thanks to my husband Raj for his love, patience, support and continuous motivation. I could not have done this without you.

Dedication

This work is dedicated to my parents, brother & sisters and their family, my husband Raj and our one year old son Keshav.

Table of Contents

<i>List of Tables</i>	xxiv
<i>List of Figures</i>	xxvii
<i>List of Abbreviations</i>	xxxii
1 Introduction.....	1
1.1 Anatomy and blood supply of the retina.....	1
1.2 Anatomy and blood supply of the ONH.....	2
1.3 Regulation of blood flow in the retina and ONH.....	3
1.4 Vascular endothelial factors.....	6
1.4.1 Endothelial derived constricting factors.....	8
1.4.2 Endothelial derived relaxing factors.....	11
1.5 Physiological provocations and ocular vascular reactivity.....	13
1.5.1 Blood pressure.....	14
1.5.2 Intra ocular pressure.....	15
1.5.3 Ocular perfusion pressure (OPP).....	15
1.5.4 Flicker stimulation.....	16
1.6 Ocular blood flow measurement techniques.....	17
1.6.1 Color doppler imaging (CDI).....	17
1.6.2 Pulsatile ocular blood flowmeter (POBF).....	17
1.6.3 Blue field entoptic phenomenon.....	18
1.6.4 Laser interferometry (Fundus pulsation technique).....	18
1.6.5 Retinal vessel analyzer (RVA).....	19
1.6.6 Laser Doppler effect.....	20

1.6.7	Heidelberg retina flowmeter (HRF).....	21
1.6.7.1	HRF calculation of volumetric blood flow	21
1.6.8	Bidirectional laser Doppler velocimetry.....	23
1.6.9	Canon laser blood flowmeter (CLBF -Model 100).....	25
1.7	Gas provocations.....	30
1.7.1	Respiration	30
1.7.2	Pulmonary anatomy	30
1.7.3	Mechanism of breathing	31
1.7.4	Ventilation and gas exchange	31
1.7.5	CO ₂ exchange.....	31
1.7.6	Normoxic/isoxic hypercapnia	32
1.7.7	Isocapnic hyperoxia	33
1.7.8	Manipulation of CO ₂ concentration in ocular blood flow studies	34
1.8	Summary.....	35
1.9	Glaucoma	36
1.9.1	Classification of Glaucoma.....	37
1.10	Risk factors of POAG	38
1.10.1	Age.....	38
1.10.2	IOP	39
1.10.3	Cup-to-disc ratio	39
1.10.4	Central corneal thickness (CCT).....	39
1.10.5	Race.....	40
1.10.6	Family history	40

1.10.7	Blood pressure	40
1.10.8	Diabetes.....	41
1.10.9	Migraine.....	41
1.10.10	Vasospasm	41
1.11	Etiology and patho-physiology of POAG.....	42
1.11.1	Biochemical factors	42
1.11.2	Mechanical theory.....	43
1.11.3	Vascular theory	44
1.12	Clinical diagnosis of glaucoma.....	47
1.13	Diagnostic imaging techniques.....	47
1.14	Management of glaucoma.....	47
1.14.1	Pharmacological agents	47
1.14.2	Laser.....	48
1.14.3	Surgical management.....	48
1.15	Effect of IOP lowering medications on ocular blood flow	49
1.15.1	Beta-blockers	49
1.15.2	Parasympathomimetic agents.....	50
1.15.3	Alpha agonists.....	50
1.15.4	Prostaglandin analogues.....	50
1.15.5	Carbonic anhydrase inhibitor.....	51
1.15.5.1	Acetazolamide.....	51
1.15.5.2	Dorzolamide.....	51
1.15.5.3	Brinzolamide.....	53

1.16	Summary	53
1.17	Autoregulation and vascular reactivity in glaucoma	54
1.17.1	Homeostatic blood flow in POAG	54
1.17.1.1	Pulsatile ocular blood flowmeter and fundus pulsation amplitude... ..	55
1.17.1.2	Scanning laser Doppler flowmetry	55
1.17.1.3	Color Doppler imaging	56
1.18	Regulation of blood flow in POAG	57
1.18.1	Regulation of blood flow to perfusion pressure provocation.....	58
1.19	Vascular reactivity response to provocations in glaucoma.....	58
1.19.1	Hypercapnia	59
1.19.2	Hyperoxia.....	61
1.19.3	Flicker stimulation	62
1.19.4	Cold stress test	63
1.20	Conclusions.....	64
1.21	References.....	67
2	Rationale	113
2.1	Development of a safe, sustained and stable normoxic/isoxic hypercapnic provocation	113
2.2	Quantitative assessment of retinal hemodynamics	114
2.3	Evaluation, validation and repeatability	115
2.4	Judicious selection of glaucoma patients to investigate vascular reactivity ...	117
2.5	Relationship between functional vascular response and biochemical measures in POAG.....	118

3	The Impact of Hypercapnia on Retinal Capillary Blood Flow Assessed by Scanning Laser Doppler Flowmetry	120
3.1	Abstract	120
3.2	Introduction	122
3.3	Materials and methods	124
3.3.1	Subjects	124
3.3.2	Visits	124
3.3.3	Scanning laser Doppler flowmetry	125
3.3.4	Procedures	126
3.3.5	Statistical analysis	129
3.4	Results	130
3.5	Discussion	134
3.6	Conclusions	137
3.7	References	139
4	Novel Methodology to Comprehensively Assess Retinal Arteriolar Vascular Reactivity to Hypercapnia	145
4.1	Abstract	145
4.2	Introduction	147
4.3	Materials and methods	150
4.3.1	Sample	150
4.3.2	Visits	150
4.3.3	Instrumentation	151
4.3.3.1	Quantitative retinal blood flow assessment	151

4.3.3.2	Sequential re-breathing circuit.....	152
4.3.4	Procedures.....	153
4.3.5	Analysis.....	154
4.3.5.1	CLBF velocity waveform analysis.....	154
4.3.5.2	Statistical Analysis.....	154
4.4	Results.....	155
4.5	Discussion.....	159
4.6	Conclusions.....	163
4.7	References.....	164
5	Retinal Arteriolar and Capillary Vascular Reactivity in Response to Isoxic Hypercapnia.....	170
5.1	Abstract.....	170
5.2	Introduction.....	172
5.3	Materials and methods.....	174
5.3.1	Sample.....	174
5.3.2	Instrumentation.....	174
5.3.2.1	Gas delivery system.....	174
5.3.2.2	Retinal blood flow assessment.....	175
5.3.2.2.1	Scanning Laser Doppler Flowmetry of Capillaries.....	175
5.3.2.2.2	Laser Doppler Flowmetry of Arterioles.....	176
5.3.3	Procedures.....	176
5.3.4	Analysis.....	179
5.3.4.1	Gas parameters analysis.....	179

5.3.4.2	SLDF image analysis	179
5.3.4.3	CLBF velocity waveform analysis.....	180
5.3.4.4	Statistical Analysis.....	180
5.4	Results.....	181
5.5	Discussion.....	188
5.6	Conclusions.....	193
5.7	References.....	194
6	Retinal Arteriolar Vascular Reactivity in Untreated and Progressive Primary Open Angle Glaucoma	201
6.1	Abstract.....	201
6.2	Introduction.....	203
6.3	Methods.....	206
6.3.1	Sample.....	206
6.3.2	Gas delivery system	207
6.3.3	Retinal blood flow assessment.....	207
6.3.4	Procedures.....	207
6.3.5	Analysis.....	209
6.3.5.1	Retinal Blood Flow Analysis	209
6.3.5.2	Gas Parameters Analysis.....	209
6.3.5.3	Statistical Analysis.....	209
6.4	Results.....	211
6.5	Discussion.....	218
6.6	Conclusions.....	225

6.7	References.....	226
7	Plasma Endothelin-1 and Cyclic GMP in Response to Normoxic Hypercapnia in Primary Open Angle Glaucoma.....	236
7.1	Abstract.....	236
7.2	Introduction.....	238
7.3	Methods.....	240
7.3.1	Sample.....	240
7.3.2	Procedures.....	241
7.3.2.1	ET-1 and cGMP assays.....	241
7.3.2.2	Normoxic hypercapnia provocation.....	241
7.3.3	Procedures.....	242
7.3.4	Statistical Analysis.....	242
7.4	Results.....	244
7.5	Discussion.....	253
7.6	Conclusions.....	258
7.7	References.....	260
8	General Discussion.....	268
8.1	Future work.....	274
8.2	Summary of new knowledge and findings from this work.....	275
9	Appendix A: Impact of Simulated Light Scatter on Scanning Laser Doppler Flowmetry.....	277
9.1	Abstract.....	277
9.2	Introduction.....	279

9.3	Materials and methods	280
9.3.1	Sample.....	280
9.3.2	Scanning laser Doppler flowmetry	280
9.3.3	Simulated light scatter model.....	281
9.3.4	Procedures.....	282
9.3.5	Analysis.....	284
9.4	Results.....	286
9.5	Discussion.....	291
9.6	Conclusion	293
9.7	References.....	294
10	Appendix B: Endothelin – 1 (ET- 1) assay procedure.....	297
10.1	Sample preparation	297
10.2	Principle of the assay	297
10.3	Reagent preparation	298
10.4	Assay procedure.....	299
11	Appendix C: 3',5' cyclic guanosine monophosphate (cGMP) assay procedure	301
11.1	Sample preparation	301
11.2	Reagents used for the assay procedure and other contents in the Enzyme Immunoassay (EIA) kit.....	301
11.3	Principle of the assay	302
11.4	Definition of terminologies in the assay procedure	302
11.5	Reagent preparation	303
11.6	Sample preparation	303

11.7	Standard preparation	304
11.8	Acetylation procedure	304
11.9	Assay procedure	305
11.10	Calculation of results	306

List of Tables

Table 1.1 Summary of findings from various studies that investigated plasma ET-1 levels in NTG	10
Table 1.2 Summary of findings from various studies that investigated plasma ET-1 levels in POAG compared to controls and/or capsular glaucoma†.....	10
Table 1.3 Summary of findings from various studies that investigated aqueous NO levels (indirect markers of NO such as cGMP, nitrates and nitrites) in POAG compared to controls and/or patients with angle closure glaucoma.	12
Table 1.4 Summary of findings from various studies that investigated plasma NO levels (indirect markers of NO such as cGMP and nitrites) in POAG, NTG* and NVG** compared to controls and/or patients with chronic angle closure glaucoma†.	13
Table 3.1 Statistical significance values for correlation between change in relevant gas parameters over time and change in blood flow in the optic nerve head, macula nasal, foveal and macula temporal areas of the retina.	130
Table 3.2 The group mean magnitude of fractional (i.e. %) end-tidal concentrations of CO ₂ and O ₂ for baseline, hypercapnia and post-hypercapnia (± SD).	133
Table 3.3 The group mean percentage heart rate, systolic and diastolic blood pressure, respiration rate and oxygen saturation (± SD) as a function of condition (i.e. baseline, hypercapnia and post-hypercapnia).	134
Table 4.1 The group mean fractional concentration of expired CO ₂ and O ₂ (± SD) as a function of condition (i.e. baseline, hypercapnia and post-hypercapnia) expressed as per cent.	155

Table 4.2 The group mean (\pm SD) pulse rate, systolic and diastolic blood pressure, respiration rate and oxygen saturation as a function of condition (i.e. baseline, hypercapnia and post-hypercapnia).	158
Table 5.1 Group mean (\pm SD) end-tidal partial pressure of CO ₂ & O ₂ , respiration rate, pulse rate, systolic & diastolic blood pressure and oxygen saturation across different breathing conditions (i.e., baseline, isoxic hypercapnia and recovery) in the first session.	185
Table 5.2 Group mean (\pm SD) end-tidal partial pressure of CO ₂ & O ₂ , respiration rate, pulse rate, systolic & diastolic blood pressure and oxygen saturation across different breathing conditions (i.e., baseline, isoxic hypercapnia and recovery) in the second session.	186
Table 6.1 The group mean \pm SD of the age, IOP and MOPP in all the groups.	213
Table 6.2 The group mean \pm SD of PETCO ₂ , PETO ₂ , respiration rate, pulse rate, systolic and diastolic BP and O ₂ saturation in uPOAG.	214
Table 6.3 The group mean \pm SD of PETCO ₂ , PETO ₂ , respiration rate, pulse rate, systolic and diastolic BP and O ₂ saturation in ntPOAG.	215
Table 6.4 The group mean \pm SD of PETCO ₂ , PETO ₂ , respiration rate, pulse rate, systolic and diastolic BP and O ₂ saturation in pPOAG.	216
Table 6.5 The group mean \pm SD of PETCO ₂ , PETO ₂ , respiration rate, pulse rate, systolic and diastolic BP and O ₂ saturation in controls.	217
Table 7.1 Represents group mean \pm SD of the ET-1 values (pg/mL) at baseline and during normoxic hypercapnia in uPOAG (untreated POAG), ntPOAG (newly treated POAG), pPOAG (progressive POAG), and controls.	245

Table 7.2 Represents group mean \pm SD of the cGMP values (pmol/mL) at baseline and during normoxic hypercapnia in uPOAG (untreated POAG), ntPOAG (newly treated POAG), pPOAG (progressive POAG), and controls.....	245
Table 9.1 Group mean baseline capillary blood flow values (\pm SD) of the ONH, nasal macula, fovea and temporal macula using the AFFPIA and HRF custom analysis.	286
Table 10.1 Details the various reagents in the endothelin-1 (ET-1) assay kit provided by the manufacturer that was used for the ET-1 assay procedure.	298
Table 11.1 Details the serial dilution procedure that was followed to prepare various concentrations of working standards.	304

List of Figures

Figure 1.1 Blood Supply of the ONH.	3
Figure 1.2 Schematic representation of the vasoconstricting and vasodilating factors released by the vascular endothelium in response to local physiological provocations.	7
Figure 1.3 Schematic representation of the Doppler effect.	20
Figure 1.4 Photograph of the Heidelberg Retina Flowmeter.	22
Figure 1.5 Schematic representation of the bi-directional laser Doppler effect.	24
Figure 1.6 Photograph of the Canon laser blood flowmeter (model 100).	27
Figure 1.7 Densitometry signal of a cross-sectional image acquired from a retinal arteriole.	28
Figure 1.8 Photograph of the fundus acquired using the Canon laser blood flowmeter. ...	28
Figure 1.9 An example of a CLBF measurement showing poor velocity waveform due to eye movements.	29
Figure 1.10 A typical measurement output that appears on the CLBF computer after data acquisition.	29
Figure 1.11 Flow diagram showing the possible factors responsible for the pathogenesis of POAG.	45
Figure 1.12 Schematic representation of the juxtacanalicular layer and schlemms canal.	46
Figure 3.1 Schematic representation of the sequential rebreathing system.	127
Figure 3.2 Scanning laser Doppler flowmetry image of the left macula of an individual showing the AFFPIA analysis circle centered on the fovea.	129
Figure 3.3 Normalised blood flow for each individual of the optic nerve head (open diamond; 5 plot symbols are overlapping), (macula nasal open triangle, 4 plot symbols	

are overlapping), foveal (open circle, 2 plot symbols are overlapping) and macula temporal (open inverted triangle, 5 plot symbols are overlapping) locations relative to the baseline (open square)..... 132

Figure 3.4 FETCO₂ plotted against time for a single individual. 133

Figure 4.1 Change in F_{ET}CO₂ (open circles) and F_{ET}O₂ (open squares) of a single individual over the course of the study. 156

Figure 4.2 Box plot of group mean change in: A). Retinal arteriolar diameter; B). Blood velocity; and C). Blood flow as a function of condition (i.e. baseline, hypercapnia and post-hypercapnia)..... 157

Figure 5.1 Schematic representation of the gas flow controller attached to a sequential gas delivery system. 175

Figure 5.2 Change in P_{ET}CO₂ (upper) and simultaneous constant P_{ET}O₂ (lower) in one individual using the gas flow controller..... 178

Figure 5.3 Box plot represents the group mean: A) retinal arteriolar diameter; B) blood velocity; and C) blood flow at baseline, isoxic hypercapnia and recovery. 181

Figure 5.4 Box plot represents the group mean capillary blood flow at the temporal rim of the ONH at baseline, isoxic hypercapnia and recovery. 182

Figure 5.5 Box plot represents the group mean capillary blood flow at the macula nasal, foveal and macula temporal areas at baseline, isoxic hypercapnia and recovery. 183

Figure 5.6 Bland and Altman plot of the difference (V1-V2) (mmHg) plotted against the mean $\{[V1 + V2]\} / 2$ (mmHg) across the two study sessions..... 187

Figure 6.1 The percentage change from baseline in group mean A) retinal arteriolar diameter; B) blood velocity; and C) blood flow in response to normoxic hypercapnia in patients with uPOAG, ntPOAG, pPOAG and controls..... 212

Figure 6.2 The percentage change from baseline in group mean temporal rim ONH blood flow in response to normoxic hypercapnia in patients with uPOAG and ntPOAG, pPOAG and controls..... 221

Figure 7.1 Correlation analysis of the baseline cGMP and retinal arteriolar blood flow in A) uPOAG (untreated POAG) and B) ntPOAG (newly treated POAG). 247

Figure 7.2 Correlation analysis of the baseline ET-1 concentration and retinal arteriolar blood flow in A) uPOAG (untreated POAG) and B) ntPOAG (newly treated POAG). 248

Figure 7.3 Correlation analysis of the hypercapnic ET-1 and retinal arteriolar blood flow in A) uPOAG (untreated POAG) and B) ntPOAG (newly treated POAG). 249

Figure 7.4 Correlation analysis of the change in response to normoxic hypercapnia of A) ET-1 and B) cGMP to the change in arteriolar blood flow in controls..... 250

Figure 7.5 Box plots represent change in plasma ET-1 in response to normoxic hypercapnia in uPOAG (untreated POAG), ntPOAG (newly treated POAG), pPOAG (progressive POAG) and controls..... 251

Figure 7.6 Box plots represent change in plasma cGMP in response to normoxic hypercapnia in uPOAG (untreated POAG), ntPOAG (newly treated POAG), pPOAG (progressive POAG) and controls..... 252

Figure 9.1 Schematic representation of the light scatter cell mounted in front of the objective of the HRF using a custom designed adaptor to produce a standard 20° tilt. . 282

Figure 9.2 Group mean capillary blood flow (+SD) with no cell, water only, 0.01%, 0.02%, 0.03%, 0.05% microsphere concentrations of the A) optic nerve head B) macula nasal C) foveal and D) macula temporal areas using SLDF (grey bars) and custom HRF (black bars) analysis..... 287

Figure 9.3 Group mean DC values for all the measured regions with no cell, water only, 0.01%, 0.02%, 0.03%, 0.05% microsphere concentrations. 289

Figure 9.4 Fundus image of a normal subject acquired with various cell microsphere concentrations placed in front of a digital fundus camera. 290

Figure 11.1 Map of the microplate wells used for cGMP assay procedure..... 306

List of Abbreviations

AFFPIA	Automated full field perfusion image analysis
AGIS	Advance Glaucoma Intervention Study
AT	Angiotensin
AVP	Arteriovenous passage time
BP	Blood pressure
CAI	Carbonic anhydrase inhibitor
cAMP	Cyclic adenosine monophosphate
CCT	Central corneal thickness
CDI	Color Doppler imaging
cGMP	Cyclic guanosine monophosphate
CIGTS	Collaborative Initial Glaucoma Treatment Study
CLBF	Canon laser blood flowmeter
CO ₂	Carbon dioxide (CO ₂)
CPV	Cerebral plasma volume
CRA	Central retinal artery
EDCF	Endothelial derived constricting factors
EDRF	Endothelial derived relaxing factors
EMGT	Early manifest glaucoma trial
eNOS	Endothelial NOS
ET-1	Endothelin-1
FACO ₂	Fractional alveolar concentration of CO ₂

FETCO ₂	Fractional end-tidal concentration of CO ₂
FETO ₂	Fractional end-tidal concentration of O ₂
FFT	Fast Fourier transformation
FPA	Fundus pulsation amplitude
GON	Glaucomatous optic neuropathy
HRF	Heidelberg Retina Flowmeter
HRP	Horse radish peroxidase
HRT	Heidelberg Retina Tomograph
iNOS	Inducible NOS
IOP	Intra ocular pressure
LC	Lamina cribrosa
LOCS	Lens opacity classification system
LPM	Litres per minute
MAP	Mean arterial pressure
MCI	Major circle of iris
MOPP	Mean OPP
nNOS	Neuronal NOS
NO	Nitric oxide
NOS	Nitric oxide synthase
NTG	Normal tension glaucoma
ntPOAG	Newly treated POAG
NVG	Neovascular glaucoma
O ₂	Oxygen

OA	Ophthalmic artery
OHT	Ocular hypertension
OHTS	Ocular hypertensive treatment study
ONH	Optic nerve head
OPP	Ocular perfusion pressure
PaCO ₂	Partial pressure of arterial concentration of CO ₂
PaO ₂	Partial pressure of arterial concentration of O ₂ (PaO ₂)
PETCO ₂	End-tidal partial pressure of CO ₂
PETO ₂	End-tidal partial pressure of O ₂
PGH2	Prostaglandins
POAG	Primary open angle glaucoma
pPOAG	Progressive POAG
POBF	Pulsatile ocular blood flowmeter
RNFL	Retinal nerve fibre layer
ROS	Reactive oxygen species
RVA	Retinal vessel analyzer
SLDF	Scanning laser Doppler flowmetry
SPCA	Short posterior ciliary artery
uPOAG	Untreated POAG
V _A	Alveolar ventilation
VCO ₂	Minute ventilation of CO ₂
V _E	Total ventilation
Δf _{max}	Maximum frequency shift

1 Introduction

The inner retina and optic nerve head (ONH), and also the choroid, are nourished by different blood supplies and therefore the measurement of all aspects of hemodynamic parameters using a single blood flow assessment technique is difficult.

1.1 Anatomy and blood supply of the retina

The inner, or neural, retina receives its blood supply through the common carotid artery, internal carotid artery, ophthalmic artery (OA) and finally the central retinal artery (CRA) ¹. The CRA divides into four major arterioles usually at the surface of the ONH. The outer retina, or choroid, is nourished by the choriocapillaries via the common carotid artery, internal carotid artery, OA and the posterior ciliary arteries (PCAs) ². The short PCAs (SPCA) supply the posterior choriocapillaries and the long PCAs supply the anterior choriocapillaries. The long PCAs and anterior ciliary arteries derived from the muscular branches of the OA combine to form the major circle of the iris (MCI) ¹. The retinal venules drain blood from the retina into the central retinal vein. Venous blood eventually drains into the ophthalmic vein (mostly into the superior ophthalmic vein) to exit the orbit. The ophthalmic vein passes through the superior orbital fissure and drains into venous sinuses in particular, the cavernous sinus ^{1,3}.

1.2 Anatomy and blood supply of the ONH

The ONH is stratified into 4 layers (Figure 1.1). The superficial nerve fibre layer (NFL) consists primarily of neurons and is predominantly supplied by the inner retinal circulation and, in part, by the SPCAs in the temporal area ^{4, 5}. The prelaminar region in most eyes is seen clinically in the central optic cup. This layer comprises neurons and astrocytes. It receives its blood supply from the branches of the peripapillary choroid and from the SPCAs. The third layer is the lamina cribrosa (LC), consisting of fenestrated connective tissue and elastic fibres through which axons transit to and from the eye. The LC is principally supplied by the SPCAs. The retrolaminar region lies outside the globe and is posterior to the LC. As the axons leave the globe and exit the lamina cribrosa they are invested with myelin and the optic nerve increases in diameter. The lamina is nourished by both the pial vessels and the SPCAs ⁵⁻⁸. The venous drainage of the ONH is primarily through the central retinal vein and its branches ^{1, 3, 5}. Hayreh S.S. (2001) and Buchi E.R. (1996) have reported that the prelaminar region of the ONH also drains through the choroidal veins ^{3, 5}. The choroidal circulation drains through the vortex veins and empties into the superior ophthalmic and inferior ophthalmic veins ^{1,3}.

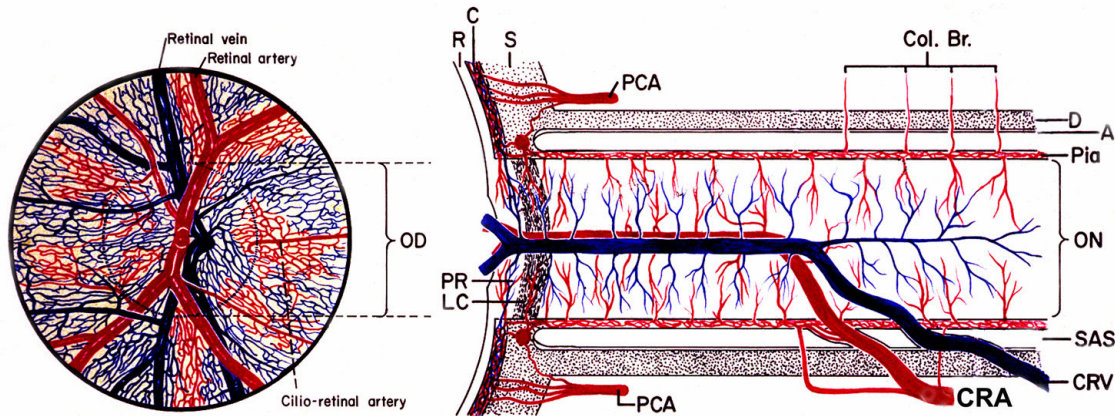


Figure 1.1 Blood Supply of the ONH.

Abbreviations used in figure: A = arachnoid, C = choroid, CRA = central retinal artery, Col Br. = collateral branches, CRV = central retinal vein, D = dura, LC = lamina cribrosa, OD = optic disc, ON = optic nerve, ONH = optic nerve head, PCA = posterior ciliary artery, PR = prelaminar region, R = retina, S = sclera, SAS = subarachnoid space.

Reprinted by permission, Progress in Retinal and Eye Research 20: 563-593, Copyright (2001).

1.3 Regulation of blood flow in the retina and ONH

The eye is supplied with autonomic nerves within the uvea and the posterior ciliary arteries ⁹, ¹⁰. The retina lacks autonomic innervation and blood flow is regulated as a result of a myogenic driven negative feedback mechanism and by local tissue demands. In most tissues, arterioles are thought to be the major site for regulation of perfusion ^{5, 11, 12}. However, there is also increasing evidence that the pericytes in retinal capillaries might also regulate perfusion at a local level ^{11, 13-16}.

Autoregulation is defined as the ability of a tissue to maintain perfusion despite changes in perfusion pressure. Guyton and co-workers (1964) expanded the original definition of autoregulation to include tissue responses to changes in blood gas concentrations, sometimes

referred to as metabolic autoregulation ¹⁷. The change in hemodynamic parameters in response to physiological provocation such as carbon dioxide (CO₂) ¹⁸⁻²¹, oxygen (O₂) ²²⁻²⁵, cold stress ²⁶⁻³⁰ or light flicker ³¹⁻³⁵ is often referred to as vascular reactivity, particularly in the cerebral blood flow literature.

Regulation of blood flow in the eye is achieved through metabolic, myogenic, neural and hormonal mechanisms. Metabolic autoregulation is the regulation of the retinal and ONH vasculature by the local concentration of O₂, CO₂, potassium or hydrogen ^{5, 12, 36}. The mechanism of metabolic autoregulation is not well established but certain endothelial derived relaxing and constricting factors are thought to play an important role ^{11, 24, 36-42}.

An increase in blood pressure leads to vasoconstriction of arterioles, and vice versa and thereby maintains blood flow and this is termed as myogenic autoregulation. Myogenic autoregulation occurs secondary to the activation of stretch activated ion channels in vascular smooth muscle cells that, in turn, allow calcium ions to enter the smooth muscle cell to induce contraction. Myogenic autoregulation has been shown in both retinal ^{11, 43-45} and ONH circulation ⁴⁶⁻⁴⁸ in a variety of animal models.

Neurogenic factors are also thought to control blood supply in certain vascular beds of the ocular vasculature ¹² and also in response to light flicker simulation ⁴⁹. However, the inner retina and the pre-laminar portion of the ONH lack autonomic nerve supply and the resistance of these vessels is altered primarily based on myogenic influences and local metabolic needs ^{1, 36}. A few studies have shown that nitric oxide (NO), a potent neural

vasodilator, might play an important role in the regulation of inner retinal vessels ^{37, 50-56}. However, earlier studies in pigs ⁵⁷⁻⁵⁹ and in humans ⁵⁴ do not support the regulatory role of NO in the retina and ONH.

Hormonal factors also participate in the regulation of blood flow by the signalling of blood vessel smooth muscle cells, endothelial cells and also pericytes ^{12, 60}. In particular the renin-angiotensin system activates angiotensin I (AT-I) to form angiotensin II (AT-II) by the action of angiotensin converting enzyme (ACE) ^{61, 62}. AT-II infusion has been shown to decrease ONH blood flow in cats ⁶³. Inhibition of ACE improved retinal endothelial function in rats with O₂ induced diabetic retinopathy ⁶⁴ and in healthy humans ⁶⁵. In addition, an enhanced increase in retinal capillary blood flow in response to flicker stimulation was shown in patients with reduced blood pressure (after treatment) compared to those with normal blood pressure ⁶⁵. Epinephrine is produced by the adrenal medulla and can produce tissue vasoconstriction in the eye through adrenergic receptors ^{60, 66}. However, the effect of epinephrine on retinal and ONH circulation is not well understood. High levels of circulating epinephrine fail to produce greater changes in the retinal vascular tone ⁶⁷. Similarly, the role of other hormonal regulators such as vasopressin and natriuretic peptides are not well established in the retina and ONH ¹².

In the eye, the retina and the ONH have been generally shown to autoregulate up to an intraocular pressure (IOP) increase of 30-40mmHg in clinically normal human subjects ⁶⁸⁻⁷¹. Sehi and co-workers (2005) showed effective autoregulation of the ONH capillaries during diurnal changes in IOP and MOPP ⁷². In addition, Lovasik and co-workers (2003) showed that

choroidal blood vessels also autoregulate during an ocular perfusion pressure (OPP) increase of 43% achieved using isometric exercise ⁷³. Several review papers have suggested a disturbance of autoregulation in primary open angle (POAG) ^{40, 74-79}. There is, however, a lack of an adequate evidence base to prove the association between altered autoregulation and POAG.

1.4 Vascular endothelial factors

The vascular endothelium lines the lumen of blood vessels and, in terms of arterioles, is enveloped in the vascular smooth muscle cells ^{1, 60}. It regulates blood flow by producing vasoactive substances such as Endothelial Derived Constricting Factors (EDCF) and Endothelial Derived Relaxing Factors (EDRF) (Figure 1.2). In healthy individuals, the endothelial factors respond to various provocative stimuli to maintain local blood flow, in the face of change in blood pressure by exercise ^{73, 80-83} or changes in IOP induced using a suction cup or after exercise ^{43, 69, 71, 80, 82}. These factors also maintain the supply of nutrients based on local metabolic demands ^{11, 12, 36, 38, 55, 84}.

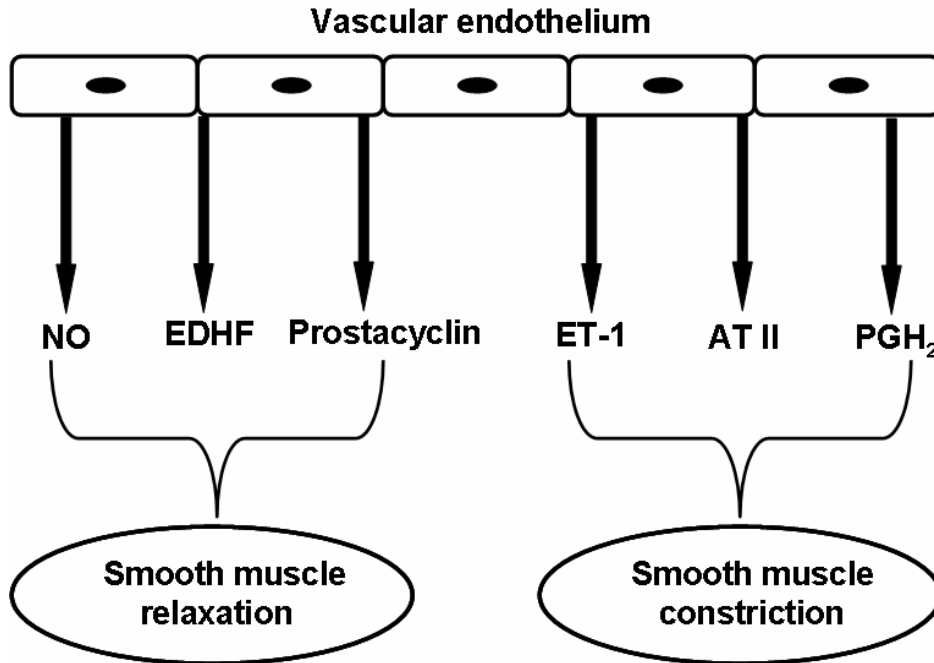


Figure 1.2 Schematic representation of the vasoconstricting and vasodilating factors released by the vascular endothelium in response to local physiological provocations.

Abbreviations used: AT = angiotensin, EDHF = endothelium derived hyperpolarising factor, ET = endothelin, NO = nitric oxide, PG = prostaglandin.

The EDCFs include contracting factors such as prostaglandin H₂ (PGH₂) and thromboxane A₂, derived from the cyclooxygenase pathway as studied in the cerebral vasculature⁸⁵⁻⁸⁷. The cyclooxygenase pathway, however, also produces prostacyclin by the activation of the enzyme phospholipase A₂ and results in vasodilation through an increase in cyclic adenosine monophosphate (cAMP)¹². In addition, AT-I after conversion into AT-II by ACE can also result in vasoconstriction in the retinal circulation⁸⁷.

Among the various dilating and constricting factors, evidence suggests that NO (EDRF) and endothelin-1 (ET-1) (EDCF) represent major players responsible for modulation of blood flow in the eye. A constant balance between these two opposing factors is critical for proper regulation of the vascular system⁸⁸⁻⁹⁰. NO and ET-1 are continually secreted by the

endothelium. Up-regulation of ET-1 is thought to result in vasoconstriction, as will down-regulation of NO, and vice versa. A possible disturbance of this balance between NO and ET-1 has been proposed in glaucoma, in particular in POAG, and this disturbance has been suggested to trigger a series of events that lead to the apoptotic loss of retinal ganglion cells and glaucomatous optic neuropathy (GON)^{39, 41, 78, 91-93}.

1.4.1 Endothelial derived constricting factors

The endothelial cells produce endothelin, a 21 amino acid peptide. There are three isoforms of endothelin, namely ET-1, ET-2 and ET-3^{12, 41, 94}. ET-1 is the primary constricting factor that has been widely studied and is thought to be produced in large amounts in the ocular circulation. ET-1 mainly causes vasoconstriction by the stimulation of the ET-A receptor that is present in the vascular smooth muscle cells and pericytes^{60, 95, 96}. ET-1 dependent vasoconstriction is thought to occur by an increase in intracellular calcium. Under normal conditions, at lower concentrations, ET-1 through the stimulation of the ET-B receptors, can result in vasodilatation via the NO/prostacyclin pathways⁹⁵.

Recently, a link between IOP and factors that might drive glaucomatous optic neuropathy (GON) was investigated. The aqueous ET-1 concentration increased as a result of an increase in IOP in a rat model, suggesting a possible role of ET-1 in GON⁹⁷. Interestingly, higher ET-B receptors have been located in pathological conditions in the astrocytes of both brain⁹⁸ and ONH^{99, 100}. Also, higher ET-B receptor immunoreactivity was observed in patients with glaucoma than in controls¹⁰⁰. Hyperoxia results in vasoconstriction of retinal blood vessels and this is thought to be primarily mediated by ET-1^{24, 101, 102}. Intravitreal injection of

endothelin has been shown to decrease retinal blood flow in animals ^{103, 104} and in humans ¹⁰⁵. Endothelin can also reduce the bio-availability of NO, thereby leading to exaggerated vasoconstriction ⁸⁹. ET-1 has been suggested to be present in higher amounts in the plasma and / or aqueous of patients with normal tension glaucoma (NTG) ^{106, 107} and in POAG with visual field progression ¹⁰⁸, while there was no difference in ET-1 reported by another study in POAG ¹⁰⁹ and in NTG ¹¹⁰. An increased aqueous level of ET-1 was also reported in glaucomatous dog models ¹¹¹. Similarly, Tezel and co-workers (1997) showed higher levels of aqueous ET-1 in humans with POAG ¹¹². However, other studies have failed to show higher levels of plasma ET-1 in NTG or POAG ^{26, 28, 109, 112} (Table 1.1a & 1.1b). Nicoleta and co-workers (2003) were the first to investigate plasma ET-1 concentration following cold provocation and showed higher ET-1 levels in patients with open angle glaucoma after provocation ²⁸. The discrepancy in the results of these studies might be due to the difference in the characteristics of the sample studied, differences in the procedures of the assay used (i.e. radioimmunoassay and enzyme immunoassay) and also individual variations in the cross-reactivities of the immunoassays. The findings of Kunimatsu and co-workers (2006) ¹⁰⁹ might differ from other studies in the respect that ET-1 levels were assessed in a Japanese population and also in patients of <60 years of age. It is thought that ET-1 levels might increase with age, however, this needs to be confirmed ¹¹².

Most of these studies have included patients receiving IOP lowering treatment prior to ET-1 assessment. The influence of IOP lowering medications on endothelial vasoactive factors is not known, however, we cannot rule out the possible effect of treatment on these findings. Other vasoconstricting factors are present in the cerebral circulation such as prostaglandins,

superoxide anions and thromboxane A₂¹¹³; however, there is no evidence of the involvement of these factors in the regulation of ocular circulation.

Author & year	Findings
Kunimatsu S. 2006	No difference in ET-1 levels.
Cellini M. 1997	Higher ET-1 levels.
Kaiser HJ. 1995	No difference in ET-1 levels †.
Sugiyama T. 1995	Higher ET-1 levels.

Table 1.1 Summary of findings from various studies that investigated plasma ET-1 levels in NTG compared to controls and/or high tension glaucoma †.

Author & year	Findings
Kunimatsu S. 2006	No difference in ET-1 levels.
Emre M. 2005	Patients with progressive visual fields had higher ET-1 levels.
Nicolela MT. 2003	No difference in ET-1 levels.
Hollo G. 1998	No difference in ET-1 levels †.
Tezel G. 1997	No difference in ET-1 levels.

Table 1.2 Summary of findings from various studies that investigated plasma ET-1 levels in POAG compared to controls and/or capsular glaucoma †.

1.4.2 Endothelial derived relaxing factors

The vascular endothelium produces NO, a potent vasodilator, under basal conditions and also in response to physiological provocation^{37, 50, 60, 90, 114}. NO is formed from L-arginine by the enzyme nitric oxide synthase (NOS)^{115, 116}. There are three types of nitric oxide synthase (NOS) namely, endothelial NOS (eNOS), inducible NOS (iNOS) and neuronal NOS (nNOS). eNOS is the most widely available form in the vascular endothelium and is responsible for regulation of blood flow in a tissue^{117, 118}. The release of NO during physiological provocation results in the increased production of cyclic guanosine monophosphate (cGMP) leading to a decrease in calcium thereby causing vasodilatation¹¹⁹⁻¹²¹.

Previous research has already shown the effect of NO on the regulation of choroidal blood flow^{54, 122}. It is well established in the cerebral circulation that NO contributes to hypercapnia induced vasodilatation¹²³⁻¹²⁷. However, a few recent studies do not support the above results^{128, 129}. The effect of NO on the ocular circulation, however, has not been as extensively studied. NOS inhibition was shown not to decrease the hypercapnia induced retinal vasodilatation in humans¹²⁴, while a positive role of NO during hypercapnic vasodilation was reported in cats¹³⁰. Recently, it was reported that NO plays a role in the recovery (i.e. post-vasoconstriction) of retinal arterioles after hyperoxia¹³¹.

Nitric oxide has a very short half-life and direct measurement is challenging. As a result, previous studies have investigated the presence of cGMP or levels of nitrites and nitrates in the aqueous and plasma as a surrogate to ascertain the level of NO expression. The findings of the levels of NO in glaucoma are inconclusive. There is some evidence for decreased

levels of NO in the plasma/aqueous of POAG ^{121, 132-134}. However, other researchers have reported no difference in the plasma levels of NO ^{111, 135}. Increased levels of nitrites have been noted in the aqueous and vitreous of dogs with POAG ¹¹¹. Studies using other types of glaucoma, such as juvenile and neovascular glaucoma (NVG), showed that NO levels in the aqueous were higher in NVG, while they were lower in juvenile glaucoma ¹³⁶. Similarly, Tsai and co-workers (2002) showed increased levels of nitrites in the aqueous of patients with NVG ¹¹¹ (Table 1.2a & 1.2b). NVG, a secondary glaucoma, is generally associated with other systemic conditions, in particular diabetes ¹³⁷. It is known that the ocular blood vessels are in a dilated state due to the hypoxic environment in NVG ¹³⁸ and that is the possible reason for the increase in NO or its surrogate marker levels in NVG.

Author & year	Findings
Kallberg ME. 2007	Increased levels of nitrites in dog models
Galassi F. 2004	Decreased levels of cGMP
Kosior-Jarecka E. 2004	Decreased levels of nitrites †
Doganay S. 2002	Decreased levels of nitrites
Kotikoski H. 2002	Trend to increase in nitrite & cGMP levels
Tsai DC. 2002	Increase in NO levels †

Table 1.3 Summary of findings from various studies that investigated aqueous NO levels (indirect markers of NO such as cGMP, nitrates and nitrites) in POAG compared to controls and/or patients with angle closure glaucoma.

There is evidence of imbalance of NO or its surrogate markers in glaucoma compared to healthy controls. The measurement of indirect markers to represent NO has some disadvantages as it is hard to eliminate the influence of diet rich in nitrates that will artificially elevate nitrites, nitrates and or cGMP levels in the plasma. Previous reports lack details about any diet restrictions imposed in study patients other than the study by Galassi and co-workers (2004)¹²¹. It is yet to be confirmed whether the levels of nitrates, nitrites or cGMP reflect the presence of NO.

Author & year	Findings
Galassi F. 2004	Decrease in cGMP levels.
O'Brien C.1999*	Decreased concentration of cGMP.
Kotikoski H. 2002	Increase in cGMP levels.
Tsai DC. 2002**	Increase in NO levels†

Table 1.4 Summary of findings from various studies that investigated plasma NO levels (indirect markers of NO such as cGMP and nitrites) in POAG, NTG* and NVG** compared to controls and/or patients with chronic angle closure glaucoma†.

1.5 Physiological provocations and ocular vascular reactivity

The hemodynamic response of ocular blood vessels to physiological provocation has been widely studied in the past. Measurement of hemodynamic parameters under normal circumstances may not provide adequate information about vascular regulation ¹³⁹. In addition, it is clear that there is a wide variability in homeostatic hemodynamic variables

amongst individuals, while the assessment of change in hemodynamics in response to some form of provocation results in a markedly reduced variability ¹⁴⁰. There are various provocation techniques that are currently available to study the ocular hemodynamics in both normal and in pathological conditions.

1.5.1 Blood pressure

Blood pressure (BP) is the force exerted on the walls of the arteries as the heart pumps blood throughout the body. The maximum pressure exerted on the arteries during ventricular contraction is the systolic pressure and the minimum pressure during ventricular relaxation is the diastolic pressure. Average normal values of systolic and diastolic blood pressures are 120 and 80mmHg in young healthy subjects. BP is measured using a sphygmomanometer and a stethoscope. Mean arterial pressure (MAP) can be calculated from the BP using the following relationship

$$\text{MAP} = \text{Diastolic pressure} + 1/3 (\text{Systolic-Diastolic})$$

Previous research has shown that ocular blood flow remains stable with increase in BP during dynamic exercise ⁸². Another study showed a 2.5% decrease in retinal arteriolar diameter with change in MAP of 21.8mmHg relative to baseline in normal volunteers, i.e. suggesting a resistance to vasodilation in the face of a large increase in MAP. Not surprisingly, there was a weak correlation between increase in BP and decrease in retinal arteriolar diameter ⁴⁸.

1.5.2 Intra ocular pressure

IOP is the pressure induced by the constant renewal of aqueous humor from the posterior chamber of the eye. Aqueous humor is secreted by the non-pigmented epithelium of the ciliary body into the posterior chamber and passes through the pupil to drain through the anterior chamber via the trabecular meshwork and finally into the Schlemm's canal. It is the resistance to outflow of aqueous humor at the site of the trabecular meshwork, along with the constant secretion of aqueous humor that generates the IOP. In addition, aqueous humor also drains through the anterior ciliary body into the suprachoroidal space known as the uveoscleral drainage but this represents only 20% of aqueous outflow. The distribution of normal IOP values is essentially Gaussian but with a positive skew and a range of 10-21mmHg, with a mean of 15mmHg. The IOP exerts a uniquely high external tissue pressure on the retinal vessels which must be opposed with sufficient force to preserve lumen integrity.

Riva and co-workers (1981) studied autoregulation of the retinal circulation using the blue field entoptic technique and showed that the retinal vessels autoregulated up to a 36% decrease in perfusion pressure (as defined below)⁶⁸. In a recent study, choroidal blood flow showed a negative correlation with increase in IOP and MAP. However, choroidal blood flow did not change until an IOP increase of 40mmHg was achieved using a suction cup⁸⁰.

1.5.3 Ocular perfusion pressure (OPP)

OPP is defined as the resultant pressure of blood entering the eye. It can be calculated using the following relationship:

$$\text{OPP} = 2/3 \text{ MAP} - \text{IOP}$$

An increase in OPP of 43% from baseline was found not to change choroidal blood flow measured using Laser Doppler Flowmetry⁷³. Also, other studies have shown effective autoregulation up to a 67%¹⁴¹ and 69%¹⁴² increase in OPP after isometric exercise. Conversely, some studies have shown that an increase in OPP after dynamic exercise results in an increase in ocular blood flow using the Scanning Laser Blood Flowmeter (SLDF) and the Pulsatile Ocular Blood Flowmeter (POBF) in healthy subjects i.e. no effective autoregulation within the autoregulatory range^{56, 83}.

1.5.4 Flicker stimulation

The retinal vasculature regulates blood flow as a result of various metabolic demands. The regulation of choroidal vessels in response to flicker stimulation is not well understood. Flicker of different frequencies can be produced using a photo stimulator that can emit flashes at a pre-determined time interval. Studies have shown that there is a significant increase in blood volume in the ONH during flicker stimulation^{35, 143}. A few studies have shown no change in retinal and choroidal perfusion in response to flicker^{143, 144}. The mechanism by which retinal vessels regulate their blood supply during flicker stimulation is not completely clear but it is thought to be due to coupling of neural activity with blood flow to increase ganglion cell activity^{32, 145}. It has been suggested that flicker stimulation of change in retinal blood flow is a measure of endothelial function, although the evidence to support this theory is currently equivocal.

1.6 Ocular blood flow measurement techniques

1.6.1 Color doppler imaging (CDI)

CDI is a non-invasive technique based on the principle of ultrasound that is used to measure blood velocity in extra ocular vessels i.e., OA, CRA and SPCAs. Sound waves from a stationary object reflect with an unchanged frequency, while those from moving particles have a shift in frequency. Blood velocity can be calculated from the frequency shift of the sound waves that reflect from the moving blood. This technique cannot measure the diameter of blood vessels and therefore the quantification of blood flow is not possible. Previously, disturbed homeostatic blood velocity in the CRA and/or OA, SPCAs in patients with POAG has been shown ¹⁴⁶. Importantly, the angle at which the probe is held in relation to the eye will impact the velocity values since the measured Doppler shift depends upon the angle between the moving object and the reflected sound wave. Patients with POAG in response to hypercapnia have shown a decreased magnitude of vascular reactivity compared to ocular hypertensive patients and controls ¹⁴⁷.

1.6.2 Pulsatile ocular blood flowmeter (POBF)

The POBF instrument measures the pulsatile component of the arterial blood flow and primarily reflects the choroidal circulation since this is by far the predominant circulatory component in the eye. IOP is sampled at 200Hz in 5-20seconds using a pneumatic probe attached to a disposable tip. The resulting pulsatile waveform provides information about IOP, systolic and diastolic time, ocular pulse amplitude and heart rate. The pulsatile ocular blood flow is automatically calculated by the instrument by the analysis of the IOP

waveforms between systolic and diastolic IOP assuming standard ocular rigidity and constant aqueous humor outflow. POBF measurements are influenced by axial length and refractive error. The blood flow measurements are not obtained through direct assessment of ocular blood flow. They are derived mathematically by estimating ocular pulse volume change on the basis of a preset equation relating ocular volume to IOP. This assumes a uniform and stable ocular rigidity. POBF measurements have been shown to be reduced in patients with NTG^{134, 148}.

1.6.3 Blue field entoptic phenomenon

This non-invasive psychophysical technique is used to measure retinal macular capillary velocity. The blue-field entoptic phenomenon can be best perceived at a narrow band of blue light of wavelength 430nm. The movement of white blood cells (WBC's) can be seen as a flying corpuscle at 10-15 degrees around the fovea. To determine mean blood velocity, subjects are shown a stimulated particle field and asked to match a comparison field to the speed of their perceived moving corpuscles. In the past, retinal vascular reactivity in response to various provocation stimuli has been studied using this technique^{19, 25, 149}. The major limitation of this technique is that it is subjective, quantifies movement of only WBC's and also has very poor reproducibility.

1.6.4 Laser interferometry (Fundus pulsation technique)

The laser interferometry is a technique used to determine the pulsatility of the choroidal blood flow¹⁵⁰. The eye is illuminated using a single mode-diode laser of wavelength 783nm.

The light is reflected from the front surface of the cornea and the retina. This results in an interference pattern from which the distance between the cornea and the retinal surfaces are calculated along the cardiac cycle. The maximum change in distance between the systolic and the diastolic phase is referred to as the fundus pulsation amplitude (FPA) ^{118, 151}. The change in the interference pattern is measured in micrometers. A decrease in choroidal blood flow has been shown in POAG using the fundus pulsation technique¹⁵².

1.6.5 Retinal vessel analyzer (RVA)

The RVA measures retinal arteriolar and venular diameter in relative units. It consists of a fundus camera, a charge-coupled device and a computer. An area in the retina is defined by the examiner and the diameter of the vessel (arteriole, venule, or both) inside this region is determined using an algorithm that detects the edges of the vessel at a maximum frequency of 50Hz ¹⁵³. The fundus is imaged onto the charge-coupled device (CCD) chip of the video camera. There are a total of 25 diameter measurements performed every second ^{19, 154}. The system automatically stops the measurement if the readings are affected due to eye movements or blinks and restarts as soon as a clear fundus image is obtained ¹⁵³. This instrument does not measure blood velocity and flow in the retinal vasculature, rather it infers a direct relationship between diameter and retinal blood flow. RVA has been used in clinically healthy subjects to assess retinal arteriolar and venular diameter in response to hypercapnia and hyperoxia ^{19, 154}. There is lack of information on retinal vascular response in POAG using the RVA.

1.6.6 Laser Doppler effect

The Doppler effect is the observed change in frequency, often termed frequency shift, that a light or sound wave undergoes when reflected from a moving object, relative to the frequency of the wave prior to reflection (or relative to neighbouring non-moving tissue).

The velocity of the moving object is directly proportional to the change in frequency

(Figure 1.3).

Doppler effect can be approximated as:

$$\frac{df}{f} = \frac{v \cos a}{c}$$

df is the frequency shift, f is the frequency of the light wave; v is the velocity of the moving object; c is the speed of light; a is the angle between the velocity vector of the moving object and the direction of observation.

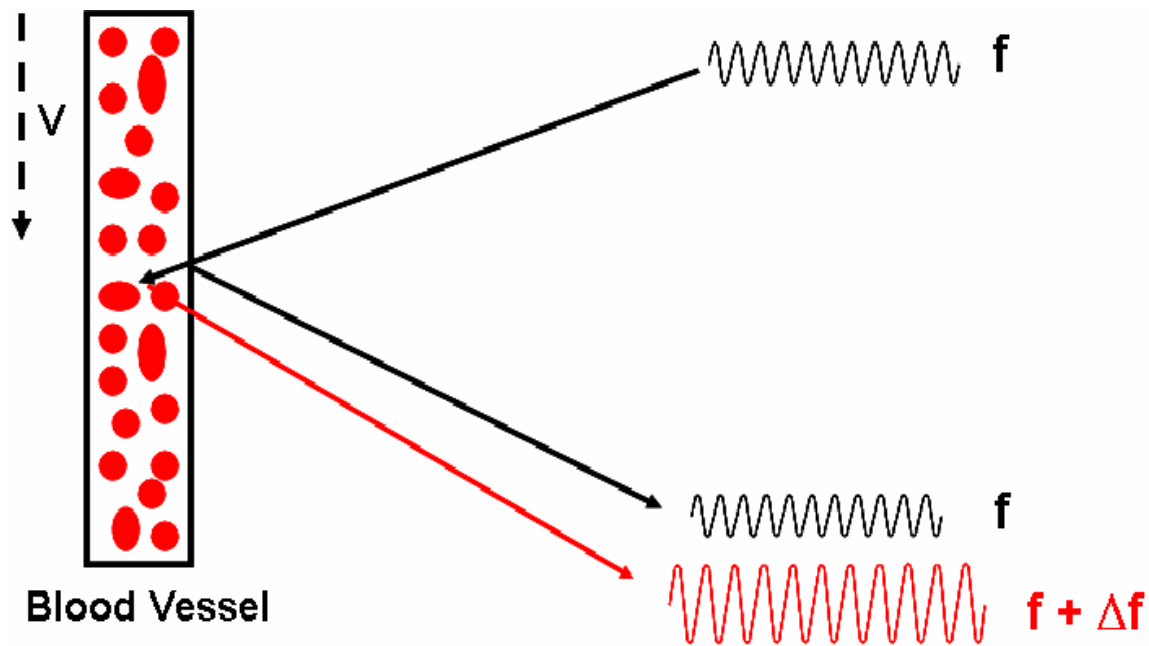


Figure 1.3 Schematic representation of the Doppler effect.

Laser beam of frequency (f) strikes the red blood cells moving with a velocity (V) and the resulting Doppler-shifted frequency (Δf) is detected by the photodetector.

1.6.7 Heidelberg retina flowmeter (HRF)

The principle of the HRF is based on the combination of confocal scanning laser and the Doppler effect. The HRF is used to measure blood velocity, volume and flow (arbitrary units) in the retinal and ONH capillaries (Figure 1.4). The fundus is illuminated using a diode laser source of 780nm wavelength with a power of 180 μ W. After the laser beam is centered on the area of interest, instrument focus is adjusted to produce maximal brightness within that area but without “pixel burnout”. The scan field is 10° wide and 2.5° high with a total area of 2.88x0.72mm and a scan resolution of 256 pixels (horizontal) by 64 lines. Each line of 256 pixels is sequentially scanned 128 times at a frequency of 4000Hz. The incident and reflected light interfere resulting in an oscillation, or “beat”, of the measured light intensity. The resulting “beat” is converted using a digitizer to obtain 256 pixels in each measurement line. The intensity of back-scattered laser light from the retina is measured as a function of time (to produce an intensity-time curve) for each pixel within the image. The intensity obtained at each pixel undergoes Fast Fourier Transformation (FFT) to generate a power spectrum (as a function of frequency). Volume, flow and velocity are calculated based on this power spectrum. The point in the power spectrum where the frequency is zero $P(0; x,y)$ is the direct current (DC) value. The power spectra is corrected for noise and normalised to the DC component to avoid dependence of reflectance^{155, 156}.

1.6.7.1 HRF calculation of volumetric blood flow

Volume is calculated as an integral of the power spectrum over all frequencies and is proportional to the total number of red blood cells in the measured volume. Flow is calculated as the integral of power times the frequency and is proportional to the number of

red blood cells multiplied by their velocity. Velocity is calculated using flow divided by volume, normalised by the DC value. The upper limit of the integral equation = 2000Hz and the lower limit =125. The upper limit in the equation is determined based on the Nyquist sampling theorem (sampling rate is twice the frequency i.e. the HRF samples at a rate of 4000Hz in order to obtain all range of frequencies to calculate volume, velocity and flow). The lower limit is chosen such as to eliminate intensity variations that are due to eye movements, heart beat and respiration ¹⁵⁵.

Studies have shown SLDF measurements of the ONH and / or temporal retinal area to be lower in patients with POAG compared to controls ^{152, 157-159}. There are a number of limitations noted in previous studies using this instrument. There is an artificial flow value produced even when no cells are moving ^{160, 161}. Research from our lab has shown an artifactual increase in HRF flow values using a simulated light scatter model ¹⁶². However, the HRF can be used as a follow-up tool to measure flow at one site across time ^{160, 161}.



Figure 1.4 Photograph of the Heidelberg Retina Flowmeter.
Laser head of the instrument mounted on a table and attached to a chin rest.

1.6.8 Bidirectional laser Doppler velocimetry

The use of two photo-detectors separated by a known angle permits the quantification of absolute centre-line blood velocity, irrespective of the angle between the moving particle and incident beam^{163, 164}. The previous optical set-up described by Feke and Riva (1978)¹⁶⁵ did not measure absolute velocity due to the difficulty in determining the angles between the incident laser light and the moving blood cells. When an incident beam strikes the moving red blood cells (RBC) it is known that a vessel that exhibits Poiseuille flow will result in a frequency shift of up to a maximum Δf_{\max} ^{163, 166}. This shift Δf_{\max} corresponds to the maximum velocity at the centre of the vessel lumen.

$$\Delta f_{\max} = f_{\max 2} - f_{\max 1} = (\alpha 2 - \alpha 1).n/\lambda$$

where $\alpha 1$ and $\alpha 2$ are the angles between the velocity vector V_{\max} and K_1 and K_2 , respectively. $f_{\max 1}$ and $f_{\max 2}$ are the maximum frequency shifts at K_1 and K_2 , respectively, n is the refractive index of the medium and λ is the wavelength of the incident light (Figure 1.5).

$$V_{\max} = \lambda.\Delta f / n.\Delta\alpha.\cos\beta$$

where $\Delta\alpha$ is the angle between K_1 and K_2 and β is the angle between the vector V_{\max} and the incident beam.

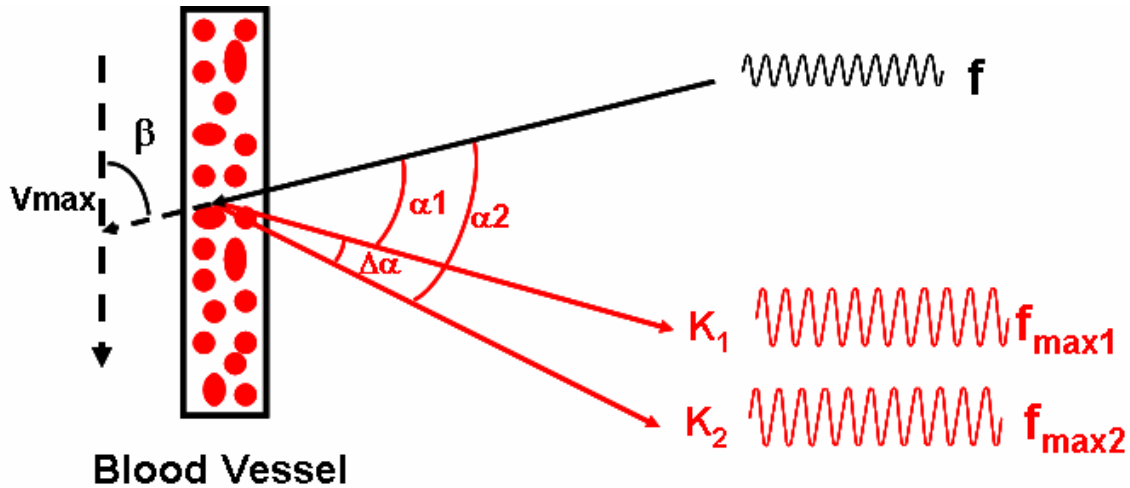


Figure 1.5 Schematic representation of the bi-directional laser Doppler effect.

Laser beam of frequency (f) strikes the red blood cells moving with a velocity (V_{max}) and the resulting Doppler-shifted frequencies f_{max1} and f_{max2} is detected by two photodetectors separated by a known angle.

In a vessel that exhibits Poiseuille flow, mean velocity can be calculated using the following relationship¹⁶⁷.

$$V_{mean} = V_{max} / 2$$

Flow rate (F) = $V_{max} S/2$ where S is the cross sectional area of the vessels at the measurement site.

Retinal blood flow can be calculated based on the diameter and maximum velocity (V_{max}) measured.

$$F = \frac{1}{2} \cdot \pi \cdot D^2 / 4 \cdot \frac{1}{T} \int V_{max}(t) dt$$

where $V_{max}(t)$ is maximum RBC velocity, D is vessel diameter, T is the observation period, and $\frac{1}{T} \int V_{max}(t) dt$ is the average of V_{max} during T ¹⁶⁸. This formula assumes that blood flow is according to Poiseuille flow and that the blood vessel exhibits a circular cross section.

1.6.9 Canon laser blood flowmeter (CLBF -Model 100)

The CLBF simultaneously measures vessel diameter (μm) and blood velocity (mm/sec) to calculate the rate of blood flow ($\mu\text{L}/\text{min}$)^{22, 168-171} (Figure 1.6). Retinal vessel diameter is determined by projecting a rectangular ($1500 \times 150 \mu\text{m}$) green (543 nm) HeNe diode laser perpendicular to the vessel segment measurement site. Densitometry analysis of the cross-sectional vessel image on the CLBF array sensor is used to calculate vessel diameter. The minimum point (Min_1) in the central portion of the image is designated as the nominal vessel center with D_1 being its signal level from the background level. When mirror reflection occurs from the vessel wall, the second minimum point is observed in the neighborhood of Min_1 with signal level D_2 . The maximum points on either side are detected as the vessel edges with D_3 and D_4 signal levels. The half-height points (X_1 and X_2) are points on the image whose signal levels are $(D_1 + D_3)/2$ and $(D_2 + D_4)/2$, respectively. The width between X_1 and X_2 is taken to represent the uncorrected vessel diameter and is converted into micron units after correction for axial and refractive magnification effects¹⁷¹⁻¹⁷³ (Figure 1.7). Diameter measurements are acquired every 4 ms during the first and last 60 ms of the 2secs velocity acquisition window. An integral “eye tracking” mechanism stabilizes the laser system on the selected measurement site. Light from the red laser is projected into the center of the green rectangle¹⁶¹. The green laser is manually adjusted perpendicular to the vessel segment (Figure 1.8). The resulting cross-sectional image of the vessel is focused on the CLBF array sensor. The array sensor detects any lateral motion of the vessel and, via a negative feedback loop, controls the galvanometer steering system to stabilize the green tracking laser on the selected measurement site. This system also enables identification and post-acquisition rejection of velocity measurements impacted by significant saccades (Figure 1.9).

A red diode laser (675nm, 80 μ m x 50 μ m oval), positioned in the centre of the green laser, is used to acquire bi-directional velocity measurements every 0.02secs throughout the 2secs measurement window resulting in a velocity-time trace that depicts the systolic-diastolic variation of blood velocity (Figure 1.10). A vessel that exhibits Poiseuille flow will have a range of velocities and thus a range of frequency shifts up to a maximum frequency shift (Δf_{\max}) that corresponds to the maximum velocity of the blood moving at the centre of the vessel lumen. Δf_{\max} can be referenced to the frequency of laser light reflected from stationary tissue to calculate relative change in velocity¹⁶⁵. By utilizing two photo-detectors separated by a known angle, the maximum frequency shift detected by each photo-detector is subtracted to allow the absolute quantification of centre-line blood velocity, irrespective of the angle between the moving particle and reflected beam^{163, 164}. The resulting Doppler signal is analysed using a previously described algorithm^{163, 166}. The frequency shift is determined as the frequency at which there is an abrupt reduction in the amplitude of the fluctuations in the Doppler-shift power spectrum. This determination does not depend on any presumed shape of the average power spectral density curve.

Two sequential measurements (Path 1 & Path 2) of diameter and velocity are taken to ensure consistency and averaged to give one reading (Figure 1.10). Hemodynamic measurements are corrected for magnification effects associated with axial and refractive ametropia^{27, 168}. In combination with the average velocity (V_{mean}) over a pulse cycle and diameter (D), flow (F) through the vessel can be calculated using the formula:

$$F = \frac{1}{2} (\pi \times D^2/4) (V_{\max} \times 60 \text{ sec})$$

D = vessel diameter (μm) and V_{max} = maximum centreline blood velocity across a cardiac cycle (mm/sec).

Although the only instrument capable of measuring retinal blood flow in absolute units, the CLBF has a number of disadvantages. The measurement is limited to a single location in the vascular tree. In this respect, it can be assumed that all branches of the vascular tree react similarly to provocation¹⁷⁴. Also, the measurement is not continuous but limited to a 2 second window. For this reason, we were aware from the infancy of the work described in this thesis of the need to develop a sustainable and stable provocation. The flow calculated using the CLBF assumes that blood flows according to Poiseuille flow (i.e. maximum velocity is in the centre of the vessel) and that blood vessel exhibits a circular cross section.



Figure 1.6 Photograph of the Canon laser blood flowmeter (model 100).

Fundus camera like laser head mounted on a table and attached to a chin rest (left). The measurements acquired by the CLBF are displayed on a computer (right) and analysed using custom software provided by the manufacturer.

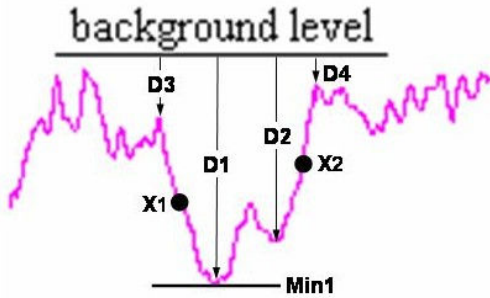


Figure 1.7 Densitometry signal of a cross-sectional image acquired from a retinal arteriole.

Min_1 , minimum point in the central portion of the image designated as the nominal vessel center; D_1 , signal level of Min_1 from the background level; D_2 , signal level of the second minimum point in the neighborhood of Min_1 ; D_3 and D_4 , signal levels of the maximum points on either side designated as the vessel edges; X_1 and X_2 , the half-height points whose signal levels are $(D_1+D_3)/2$ and $(D_2+D_4)/2$, respectively. The width between X_1 and X_2 is taken to represent the uncorrected vessel diameter.

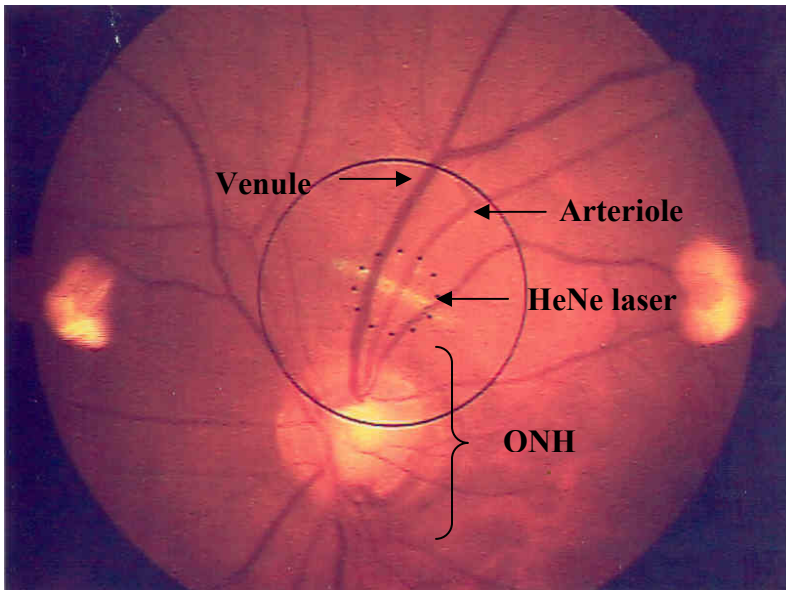


Figure 1.8 Photograph of the fundus acquired using the Canon laser blood flowmeter.

Photograph shows the ONH - optic nerve head, superior temporal arteriole and venule. A HeNe laser of 543nm wavelength is centered on the arteriole of interest and oriented perpendicular to the vessel segment for measurement of diameter.

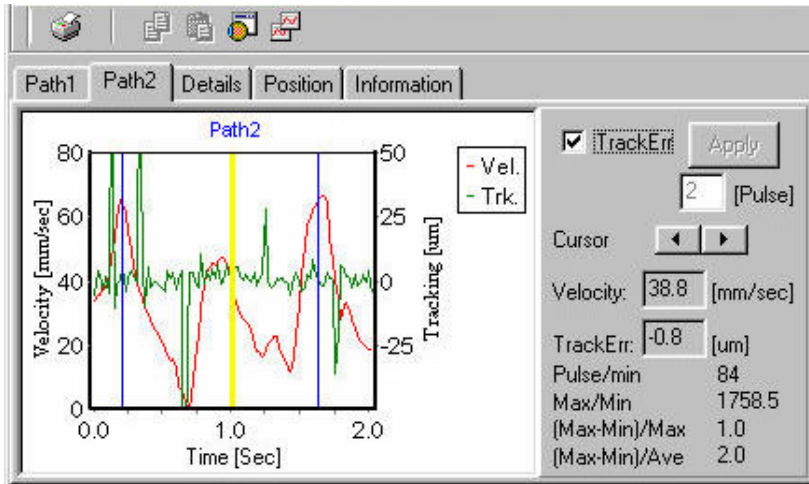


Figure 1.9 An example of a CLBF measurement showing poor velocity waveform due to eye movements. The middle line in the figure is the cursor that can be moved on either side to read velocity measurement at one particular point on the waveform.

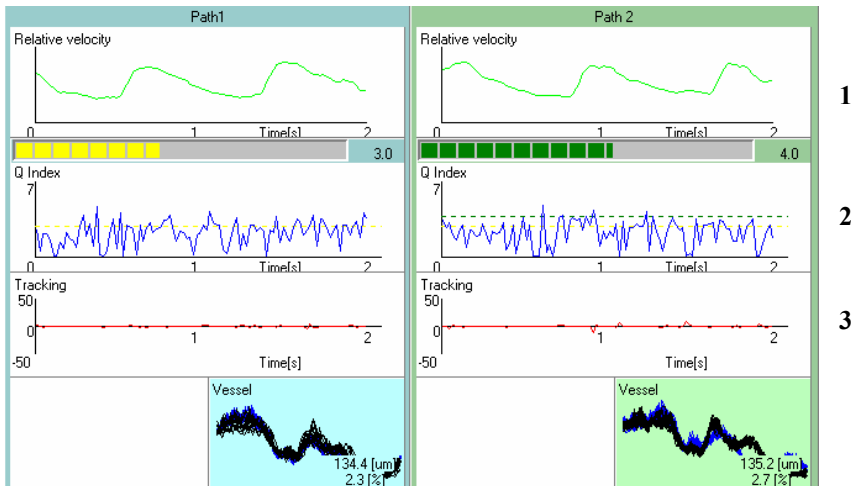


Figure 1.10 A typical measurement output that appears on the CLBF computer after data acquisition. 1) relative velocity profile of the CLBF measurement, that is variation of the centreline blood velocity during cardiac cycle 2) quality index of the measurement (Q index) that provides information about the overall quality of a reading as a numerical score 3) eye tracking measures across the 2 seconds window, in path 1 (left) and path 2 (right). The two paths represent measurements obtained at two different angles of incidence of the measurement beam. The diameter measurements and the co-efficient of variability (CoV) are shown at the bottom right of the CLBF output in each path.

1.7 Gas provocations

The hemodynamic effect of gas provocations in healthy volunteers has been extensively studied. The results of the effect of gas provocations in patients with POAG are discussed later in this chapter.

1.7.1 Respiration

The process of supplying O₂ to the cells in the body and the removal of CO₂ is defined as respiration. The first stage of respiration is gas exchange where O₂ and CO₂ are transferred between the atmosphere and the pulmonary capillaries followed by exchange between the systemic blood and the tissue. The second stage is cellular respiration and this involves various chemical processes that break down food to release energy and CO₂.

1.7.2 Pulmonary anatomy

The lungs are the primary organs of gas exchange. During each inspiration, air passes through the nose or mouth and initially reaches the pharynx. It then travels to the larynx through the vocal cords and reaches the trachea that branches into two bronchi. Each bronchus enters the lungs that branch into further smaller structures known as bronchioles. The terminal bronchioles then branch into smaller structures called alveoli that are the site of gas exchange. Each alveolus is surrounded by pulmonary capillaries that facilitate gas exchange. O₂ from the inhaled air diffuses through the alveolus into the blood and CO₂ is diffused from the blood into the alveolus¹⁷⁵.

1.7.3 Mechanism of breathing

The primary muscle involved during inspiration is the diaphragm (a structure that separates the abdomen from the thoracic cavity). The process of inspiration contracts the diaphragm leading to the contraction of external intercostal muscles that are attached to the ribs. This results in upward and outward movement of the ribs thereby increasing the thoracic volume and decreases alveolar pressure during inspiration. Inspiration is followed by expiration which is generally a passive process. The diaphragm and the intercostal muscles relax and decrease the alveolar volume thereby forcing out air from the lungs ¹⁷⁶.

1.7.4 Ventilation and gas exchange

The amount of air exhaled at a given time is defined as total ventilation (V_E). During inspiration, the total amount of air does not participate in alveolar gas exchange. The component that is not part of gas exchange forms the physiological dead space ($V_{D\text{physiol}}$). The portion of air that remains in the airways gets exhaled first during expiration. Alveolar ventilation is defined as the volume of air that participates in alveolar gas exchange (V_A). It can be calculated using the following relationship:

$$V_A = V_E - V_{D\text{physiol}}$$

1.7.5 CO₂ exchange

CO₂ is eliminated by the process of ventilation. The minute ventilation of CO₂ (V_{CO_2}) is the difference between the exhaled and the inhaled amount of CO₂ in a minute. As the amount of CO₂ inhaled is negligible, the CO₂ in expired gas represents the alveolar concentration of CO₂ (F_{ACO_2}). The F_{ACO_2} is equal to F_{ETCO_2} i.e., the fractional concentration of CO₂ in

expired air measured in percent. The partial pressure of arterial CO₂ (PaCO₂) can be derived from VCO₂ and is usually 40mmHg ± 3mmHg. The measurement of PaCO₂ requires sampling from an arterial blood line and has only been used by a few studies in the past to measure manipulated changes in arterial partial pressure of CO₂. The surrogate marker of PaCO₂ is PETCO₂ (end-tidal partial pressure of CO₂: the amount of CO₂ present in each exhaled breath, measured in mmHg) and is considered to be directly proportional to PaCO₂. However, it has been recently shown that there is a large variation between PETCO₂ and PaCO₂ measurements achieved using non-standardised gas provocations (i.e. use of non-rebreathing circuit and manual addition of CO₂ to inspired air) ¹⁷⁷⁻¹⁷⁹.

1.7.6 Normoxic/isoxic hypercapnia

Breathing increased amounts of CO₂ without any significant change in the partial pressure of O₂ is defined as isoxic hypercapnia (i.e. PETO₂ unchanged). Normoxic hypercapnia is the increase in PETCO₂ while the PETO₂ remains constant at physiological resting levels (change that does not result in any physiologically measurable impact). The increase in the systemic partial pressure of arterial CO₂ has been shown to increase blood flow in retinal vessels in humans ^{19, 20, 154, 170, 180-182} but the majority of these studies have failed to adequately consider O₂ control during hypercapnia. The use of a standardised and a repeatable normoxic/isoxic hypercapnic stimulus is essential to assess vascular reactivity in order to avoid any confounding effects of O₂ induced vasoconstriction. In this thesis, a safe, sustained and a stable normoxic hypercapnic stimulus was developed to assess retinal arteriolar and ONH vascular reactivity in patients with POAG. It is established that an increase in the arterial O₂ causes reduction in blood flow ^{20, 22, 23, 183-186}. Similarly, the concomitant change in PETO₂

during hypercapnia can reduce the overall magnitude of vascular reactivity obtained in response to the increase in PETCO₂. It is widely accepted in the cerebral literature that NO might be an important factor that causes vasodilation. A few studies have shown the involvement of NO (a potent vasodilator) that leads to an increase in the retinal¹³⁰ and choroidal blood flow¹²⁴ in hypercapnia induced vasodilation. However, the exact mechanism of action is still not clear.

1.7.7 Isocapnic hyperoxia

Breathing increased amounts of O₂ without a physiologically significant change in partial pressure of arterial CO₂ is defined as isocapnic hyperoxia. The partial pressure of arterial O₂ (PaO₂) can be indirectly assessed by measuring the minimum amount of O₂ in each exhaled breath (PETO₂ in mmHg). A number of studies have shown vasoconstriction in ocular blood vessels in humans in response to an increase in arterial partial pressure of O₂^{20, 22, 154, 181, 183, 185-188} but many of these studies have not met isocapnic conditions. Addition of O₂ typically results in hyperventilation and thereby results in a decrease in pCO₂¹⁸⁹. Isocapnic hyperoxia generally results in accumulation of reactive oxygen species (ROS) thereby causing oxidative stress. Hyperoxia induced hyperventilation is thought to occur due to the stimulation of central chemoreceptors in the brain stem as a result of the increase in ROS¹⁹⁰. It is critical to control the concomitant change in CO₂ during hyperoxia in order to reduce variability in retinal vascular reactivity assessment²². The use of non-isocapnic hyperoxia can cause a compounded effect on vascular reactivity assessment^{23, 181, 191}. ET-1, a potent vasoconstrictor produced by the vascular endothelium, is thought to play an important role in the regulation of the retinal vasculature to isocapnic hyperoxia^{24, 38}.

1.7.8 Manipulation of CO₂ concentration in ocular blood flow studies

Studies in the past have manipulated the levels of PETCO₂ using various techniques in both humans and animals to assess its impact on ocular blood vessels. It is known that hypercapnia causes unpredictable hyperventilation and thereby affects PETO₂ in an unpredictable manner between individuals.¹⁷⁵ Inhalation of CO₂ enriched gas dilutes the inspired air and thereby reduces the O₂ concentration in the lungs and thus in the blood. However, this effect on the lung O₂ concentration is partly offset by the increased ventilation stimulated by hypercapnia, thereby resulting in an increased PETO₂. The mechanism involved in hypercapnia induced hyperventilation is thought to be mediated by the CO₂ sensitive central and peripheral chemoreceptors. These receptors provide feedback to the brain stem respiratory control system regarding arterial CO₂ levels. The increase in CO₂ during hypercapnia is detected by the chemoreceptors in the brain stem thereby resulting in hyperventilation¹⁹². As increase in PETO₂ has been shown to decrease ocular blood flow, it becomes important to simultaneously monitor PETO₂ during changes in CO₂. However, most of the previous studies lack information about PETO₂ during hypercapnia^{182, 193, 194}.

In this respect, we initially set-out to develop a normoxic/isoxic hypercapnic stimulus and assessed its effect on retinal vascular reactivity in young healthy subjects with the ultimate aim of using the standardised stimulus in patients with glaucoma. In this thesis, the use of a sequential rebreathing circuit along with the automated gas flow controller still resulted in a minimal change in PETO₂. Since the change in PETO₂ was minimal, the term normoxic hypercapnia (i.e. change that did not have any measureable physiological impact) was adopted rather than isoxic hypercapnia (i.e. unchanged). This stimulus was used in this work

to assess retinal vasodilatory capacity in patients with POAG. We chose normoxic hypercapnia because of concerns about provoking vasoconstriction in patients with a disease that might be triggered or exacerbated by transient peripheral vasoconstriction.

1.8 Summary

The blood supply to the retina and the ONH vary in terms of supply vessels and, in combination with differing anatomical conditions, this poses difficulty in measuring the hemodynamics at both sites using one instrument. The retinal vasculature is shown to exhibit autoregulation. Retinal arterioles are a major site of vascular resistance, however, recent evidence suggests that pericytes can also regulate blood flow in the eye. ET-1 and NO are thought to be the two major factors responsible for vascular regulation. There is some evidence for an increased expression of ET-1 in POAG.

The CLBF is the only instrument currently available that quantifies retinal arteriolar hemodynamics in absolute units. The CLBF measures diameter and blood velocity at a single point along the vessel. Also, the measurement is not continuous but limited to a 2 second window. Similarly, the HRF has been used in the past to assess ONH blood flow. This instrument has high measurement variability and requires repeated measurements to obtain valid blood flow values. Both the CLBF and the HRF has been used in this work to assess retinal and ONH vascular reactivity in patients with POAG. For this reason, we were aware from the infancy of this work of the need to develop a safe, sustainable and stable provocation. In this respect, we set-out to initially develop a normoxic/isoxic hypercapnic stimulus ultimately to assess retinal vasodilatory capacity in patients with POAG.

The majority of previous studies have quantified homeostatic blood flow in POAG/NTG. The studies that have looked at vascular reactivity of the retinal vessels have only used non-standardised provocation techniques (i.e. use of a non-rebreathing circuit to induce hypercapnia). The use of non-rebreathing circuit has been shown only to increase PETCO₂, while the arterial partial pressure of CO₂ failed to increase. In this thesis, the use of a sequential re-breathing circuit along with the automated gas flow controller resulted in a minimal change in PETO₂. Since the change in PETO₂ was minimal, the term normoxic hypercapnia (i.e. change that did not have any measureable physiological impact) was adopted rather than isoxic hypercapnia (i.e. unchanged).

We chose to use normoxic hypercapnia in our study because of the concerns about provoking vasoconstriction in patients with a disease that might be triggered or exacerbated by transient peripheral vasoconstriction. In addition, this work also aimed to determine plasma levels of biochemical markers of endothelial function in patients with untreated POAG, newly treated POAG (after Dorzolamide treatment), progressive POAG and age-matched controls both at baseline and during hypercapnic provocation. We correlated these biochemical markers to functional vascular responses in the same group of patients.

1.9 Glaucoma

Glaucoma is a condition characterized by loss of visual field, damage to the optic disc and an associated increase in IOP. It is the second leading cause of blindness in the world ¹⁹⁵ and also in Canada, according to the Canadian National Institute for the Blind (CNIB) ¹⁹⁶. A previous report showed an overall prevalence of 1.86% of open angle glaucoma (OAG) in

the US population ¹⁹⁷. According to the CNIB, at least 300,000 Canadians currently have glaucoma and 50% of them are undiagnosed. Recent reports suggest that glaucoma can occur at any level of IOP, which is not considered as the only risk factor for glaucoma. The prevalence of OAG increases with age and there is a greater percentage of African Americans affected by the disease ¹⁹⁸. A recent meta-analysis of the prevalence of OAG in patients over 40 years of age showed 4.2% in the African population, 2.1% in whites of European origin and 1.4% in Asians. A higher prevalence of OAG in females compared to males has also been reported ¹⁹⁹.

1.9.1 Classification of Glaucoma

There are various classification schemes used in the past to define glaucoma sub-types. Some have classified based on the etiology, mechanism and onset, while others have identified based on just mechanisms of outflow obstruction. The use of an appropriate classification system becomes clinically important in order to manage and treat this condition.

Glaucoma is primarily classified into three broad categories 1) Open angle 2) Angle closure and 3) Developmental glaucoma. The Open Angle and Closed Angle Glaucomas are further divided into primary and secondary glaucomas. Primary open-angle glaucoma (POAG) includes high tension and NTG. POAG usually presents with an increase in IOP in most cases due to obstruction of aqueous outflow. The etiology of this obstruction is generally at the sub-microscopic level and not due to any mechanical obstruction. POAG can also present with optic disc abnormalities and associated visual field loss without elevation of IOP in some patients and that is termed as NTG.

The secondary open angle glaucomas can occur due to a variety of ocular and systemic conditions. There is usually mechanical obstruction to aqueous outflow and it can be at the level of pre-trabecular, trabecular or post-trabecular meshwork. Primary angle closure glaucomas consist of acute, sub-acute and chronic angle closure, while the secondary angle closure glaucomas include those with or without pupillary block.

A malformation or an incomplete formation of the trabecular meshwork or Schlemm's canal during gestation is suggested to cause developmental glaucoma.

1.10 Risk factors of POAG

Careful identification of risk factors that aid in the progression of glaucoma is imperative to effectively manage glaucoma using medical therapy. Some of the earlier large scale clinical trials have provided evidence about the baseline risk factors that are involved in the progression of POAG.

1.10.1 Age

Increasing age has been proposed as one of the major risk factor for the prevalence of ocular hypertension (OHT) and development of POAG. The results of large clinical trials such as the Ocular Hypertension Treatment Study (OHTS), Early Manifest Glaucoma Trial (EMGT), Blue Mountain Eye Study (BMES), Advance Glaucoma Intervention Study (AGIS) and the Collaborative Initial Glaucoma Treatment Study (CIGTS)²⁰⁰⁻²⁰³ and some population based studies support this theory.^{204, 205}

1.10.2 IOP

IOP is consistently considered as the primary risk factor for POAG. The outcome of large scale clinical trials has provided information to help modify the treatment approach of patients with POAG and OHT. The results of the OHTS indicated that use of IOP lowering medications reduces the risk of glaucoma progression by approximately half, i.e. 9.5% to 4.4%²⁰⁶. IOP lowering is also effective in delaying progression of POAG in African American population. Further analysis revealed that for every 1mmHg increase in IOP there was a 10% increase in the risk of development of POAG²⁰⁷. Similarly, the EMGT also showed effective decrease in the progression rate after decrease in IOP in OHT (i.e. 65% in untreated OHTs to 45% in the treated OHT group). Large diurnal and nocturnal fluctuations of IOP are also proposed to be a factor for progression of POAG²⁰⁸.

1.10.3 Cup-to-disc ratio

Previous evidence suggests that increased cup-to-disc ratio is an independent risk factor for the progression of POAG. Based on the univariate analysis of the OHTS results, there is a 25% increase in the hazards ratio for every 0.1 increase in horizontal cup-to-disc ratio and a 32% increase for a 0.1 increase in vertical cup-to-disc ratio^{203, 206}.

1.10.4 Central corneal thickness (CCT)

There is also evidence for CCT as a risk factor for progression of POAG. According to the OHTS results, CCT is a stronger predictive factor for the development of POAG^{203, 206}.

1.10.5 Race

Studies have shown increased prevalence of POAG in the black race. However, it was not clear whether there are other associated factors that increase the prevalence in this race. The OHTS did not reveal any significant correlations to the progression of POAG and race using multivariate analysis ^{203, 206}. Conversely, a random survey of the urban Baltimore and Maryland residents showed increased prevalence in the black population. The study also revealed prevalence of POAG at an earlier age in the black population compared to the whites ²⁰⁹.

1.10.6 Family history

A positive family history is proposed to be associated with the incidence of POAG; however, there is no strong association with the progression of POAG. The Barbados Eye Study and the Rotterdam Study ^{204, 210} showed increased incidence of POAG in patients with a strong family history but this finding was not observed in OHTS.

1.10.7 Blood pressure

A positive association between IOP and blood pressure has been noted. The results of the EMGT study that assessed predictors of long term progression of POAG showed that low blood pressure is an independent risk factor for progression ²¹¹. Similar findings have been suggested by other studies and this leads to a possible vascular disturbance in patients with POAG ^{212, 213}.

1.10.8 Diabetes

Vascular dysregulation has also been proposed in diabetes. An increase in the prevalence of POAG has been noted in patients with diabetes. The BMES showed a 6.5% increase in POAG compared to 3.5% prevalence in patients without diabetes²¹⁴. The AGIS, Beaver Dam Study and EMGT also showed an association between diabetes and progression of POAG^{202, 211, 215}, while few other studies failed to show any association^{209, 216}.

1.10.9 Migraine

The BMES showed an association between history of migraine in different age groups and the prevalence of POAG. The results also suggested that history of migraine decreased with increasing age²¹⁷. In the OHTS analysis, however, there was no correlation between migraine and progression of POAG²⁰³.

1.10.10 Vasospasm

Presence of vasospasm is considered as risk factor for progression of POAG. However, this is not well established. Recently, the Canadian Glaucoma Study showed no association between vasospasm and progression of POAG²¹⁸. Conversely, another study that reviewed the potential risk factors suggests that vasospasm might be a risk factor in POAG^{78, 94}. The majority of other clinical trials have failed to evaluate vasospasm as one of the risk factors in POAG progression.

1.11 Etiology and patho-physiology of POAG

Glaucomatous optic neuropathy is characterised by progressive changes in the ONH caused either by an increase in IOP or as a result of vascular dysregulation leading to visual impairment (or possibly a mixture of both these mechanisms) ^{219, 220}. It is generally characterised by one or more of the following features; enlargement of the optic cup, optic disc hemorrhage, thinning of the nerve fibre layer, asymmetrical cupping and parapapillary atrophy. There are various theories suggested as the possible etiology for the occurrence of optic neuropathy in POAG. The most widely studied are the biochemical factors, mechanical theory and the vascular theory (Figure 1.11). However it is generally recognised that glaucoma is typically caused by a combination of these different theories, i.e. it is the ability of an individual ONH to maintain perfusion, no matter what the biomechanical and vascular stresses. For historical reasons the theories will be discussed separately.

1.11.1 Biochemical factors

Evidence suggests that structural alterations in POAG at the level of the trabecular meshwork could give rise to an increased resistance to the aqueous outflow resulting in an increase in IOP. It is possible that in POAG the balance between secretion of aqueous humor and the outflow resistance could be altered. A decrease in the number of endothelial cells in the trabecular meshwork with age has already been established ²²¹. However, in patients with POAG there might be an exaggerated decrease in cells leading to obstruction of the aqueous outflow and thereby causing an increase in IOP. Histopathological evidence also suggests that the loss of endothelial cells results in the enlargement and fusion of the remaining cells ²²¹, thereby blocking or reducing the size of the trabecular meshwork pores. In addition, there

is deposition of sheath-derived plaque material in the anterior chamber of patients with POAG.^{222, 223} However, it is not very clear whether the plaque formation could result in decreased aqueous outflow^{224, 225}. The presence of giant vacuoles lining the inner wall of Schlemm's canal has also been thought to play a role in aqueous drainage²²⁶ (Figure 1.12). In eyes with POAG, there is evidence for a decrease in the number of vacuoles thereby leading to a decrease in aqueous outflow. The presence of transforming growth factor β 2 (TGF) in the aqueous humor of patients with POAG might result in an increased deposition of extra cellular matrix leading to a decrease in aqueous outflow²²⁷. The exact mechanism of decreased aqueous outflow is not well understood although there is histo-pathological and biochemical evidence of several factors resulting in GON.

1.11.2 Mechanical theory

An increase in IOP causes mechanical stress on the lamina cribrosa and the retinal ganglion cells affecting both antero-grade and retrograde axonal transport. There are various neurotrophic factors that are transmitted from the lateral geniculate nucleus to the optic nerve. Compression of the lamina cribrosa results in axonal cell death due to lack of sufficient trophic factors. Using a biomechanical model, Sigal and co-workers (2007) have shown that the ONH predominantly undergoes compression followed by stretching and shearing as a result of an increase in IOP²²⁸. Also, the extent of scleral rigidity has been shown to be a primary factor for the development of POAG^{229, 230}. However, in patients with NTG, the optic nerve is affected even within the normal range of IOP²³¹.

1.11.3 Vascular theory

An instability in blood flow might play an important role in the obstruction of axoplasmic flow leading to GON. A wide range of change in IOP and BP are autoregulated by retinal vessels under normal conditions. The vascular theory suggests that there could be impairment of normal autoregulation in patients with POAG^{78, 94, 232}. There is evidence from previous studies that ONH blood flow is decreased in patients with POAG measured using fundus fluorescein angiography²³³ and Doppler techniques^{233, 234}, as well as histo-pathological evidence²³⁵. Atrophy of the peripapillary capillaries supplying the retinal nerve fibre layer (RNFL) has also been reported in POAG^{236, 237}. However, another study shows no correlation between atrophy of peripapillary capillaries and visual field²³⁸. Similarly, Michelson and co-workers (1996 & 1998) showed significant decrease in juxtapapillary and retinal capillary blood flow^{158, 239}. The presence of vascular alteration in POAG is not well understood and still remains controversial.

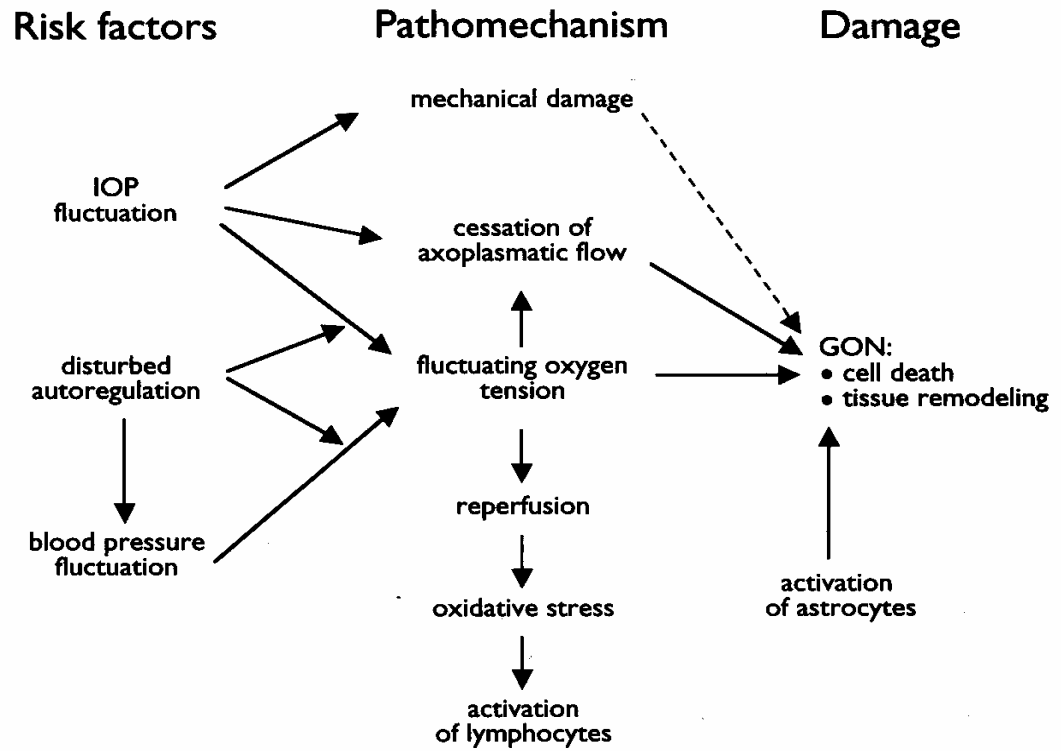


Figure 1.11 Flow diagram showing the possible factors responsible for the pathogenesis of POAG.
 Reprinted by permission from Taylor and Francis Group, Glaucoma Therapy, Current Issues and Controversies.

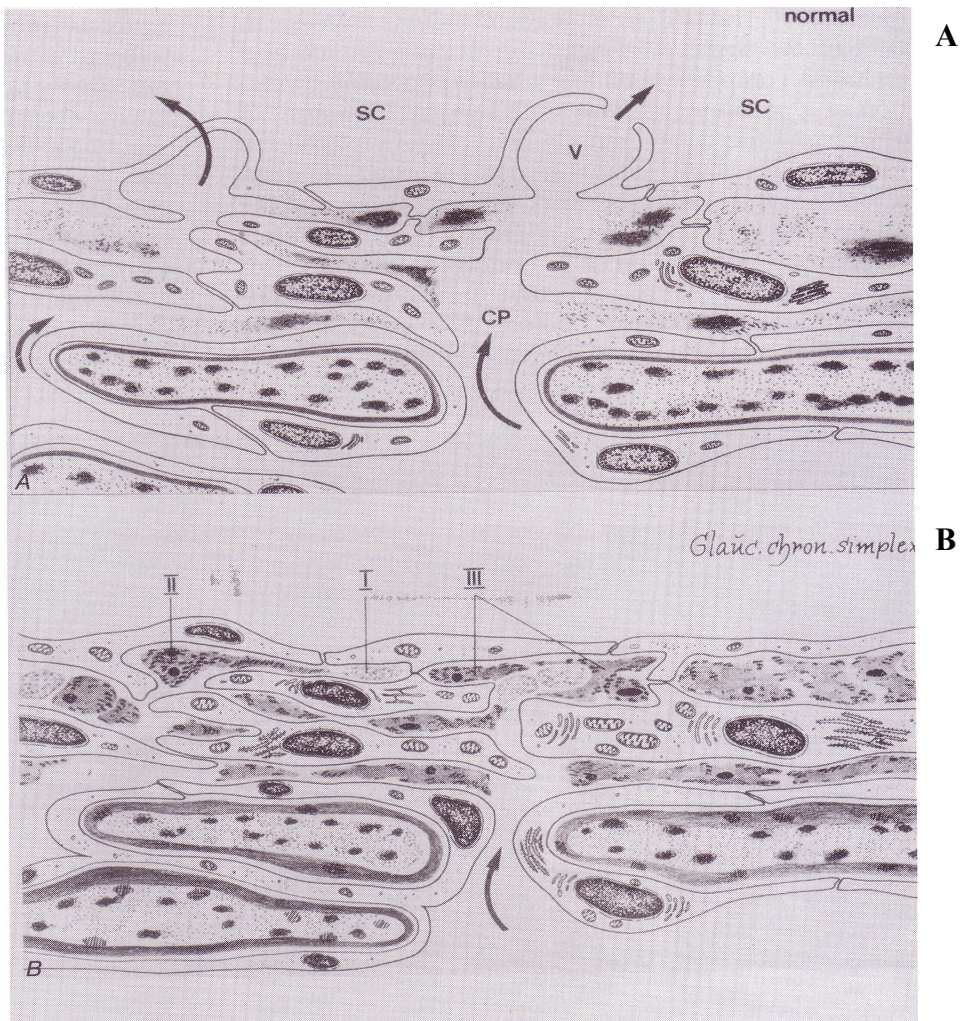


Figure 1.12 Schematic representation of the juxtacanalicular layer and schlemms canal.

A) Arrows show normal aqueous outflow (top). B) Accumulation of extracellular material (marked types I, II and III) along the juxtacanalicular tissue. Flow and partial blockade of aqueous outflow is shown by the arrow in glaucomatous eye (bottom).

Reprinted by permission from McGraw Hill Publishers.

1.12 Clinical diagnosis of glaucoma

The first important step in the diagnosis of any eye disease is to obtain a detailed ocular and systemic history of the patient. A positive family history of POAG is one of the major risk factors and it is therefore essential to rule out any possible genetic influence during history taking^{240, 241}. The clinical diagnosis of POAG is complex and outside the scope of this thesis. However, the following clinical tests are often undertaken to aid the clinician reach a diagnosis, including ONH and nerve fibre evaluation, gonioscopy, tonometry, fundus photography, measurement of CCT and visual field assessment.

1.13 Diagnostic imaging techniques

During the last decade, objective imaging techniques have been developed in order to effectively monitor the progression of POAG. The most common imaging techniques that are currently used to monitor progression of POAG are scanning laser tomography (SLT), time domain and spectral domain optical coherence tomography (OCT) and scanning laser polarimetry.

1.14 Management of glaucoma

1.14.1 Pharmacological agents

In the absence of optic disc damage and visual field loss, most clinicians initiate IOP reducing treatments when the baseline IOP reaches 30mmHg or close to this level. In general, target IOP is usually decided based on the extent of optic disc damage, visual field

deterioration and risk factor assessment. There are various groups of drugs used to treat glaucoma namely, beta-blockers, adrenergic agonists, miotics, carbonic anhydrase inhibitors (CAI), prostaglandin analogues and hyperosmotic agents. ²⁴².

1.14.2 Laser

Laser iridectomy is usually performed in angle closure glaucoma with pupillary block. On many occasions, a prophylactic iridectomy is indicated to avoid potential pupillary block. Argon or disruptive Nd:YAG laser is delivered using a slit lamp to create an iridectomy. Argon Laser Trabeculoplasty (ALT) is a technique used primarily to treat POAG. This technique lowers intraocular pressure by improving aqueous outflow ²⁴³. Recently, Selective Laser Trabeculoplasty (SLT) has been used as it targets only specific trabecular cells ^{244, 245}.

1.14.3 Surgical management

Filtering surgery is the most common technique to treat POAG. During the surgery a piece of the cornea or sclera is removed to help in the drainage of aqueous humor. In addition, anti-metabolites are used during filtration surgery to avoid post-operative fibrosis of episcleral and sub-conjunctival tissue. The most commonly used anti-metabolites are mitomycin (MMC) and 5-Fluorouracil. In conditions when filtration surgery fails, aqueous shunts are implanted to provide a pathway for the aqueous to drain into an exterior reservoir. In addition, cyclodestructive procedures are also used in patients where all other conventional therapy failed to decrease IOP. This procedure destroys the ciliary body to reduce aqueous production leading to reduction in IOP. ²⁴⁵.

1.15 Effect of IOP lowering medications on ocular blood flow

The currently available IOP lowering medications primarily decrease IOP to a target level. Recently, the possible involvement of vascular dysregulation in the development of glaucoma, in particular in POAG, has been widely studied. As a result, there is an interest and need to define any possible effect on ocular hemodynamics of the different groups of medications used to lower IOP. However, the results of these studies are still contradictory.

1.15.1 Beta-blockers

Beta-blockers decrease IOP by reducing aqueous production. The most commonly used beta blocker is timolol maleate and the majority of the studies using this medication on animal models have shown either no effect^{246, 247} or a decrease in choroidal blood flow²⁴⁸. Studies have shown no change in ocular blood flow in POAG/NTG after treatment with timolol²⁴⁹⁻²⁵³. Similarly, Betaxolol treatment in patients with POAG did not show any change in pulsatile ocular blood flow²⁵⁴. Another study showed a significant increase in retrobulbar hemodynamics in POAG with betaxolol compared to the other beta blockers²⁵⁵. Levobunolol, a non-selective beta-blocker, also showed an increase in POBF in patients with POAG^{256, 257}. These studies, however, failed to correlate the effect of IOP decrease on ocular blood flow changes. Similarly, treatment with carteolol showed a decrease in resistance index of CRA in POAG²⁵⁵.

1.15.2 Parasympathomimetic agents

Pilocarpine is one of the most commonly used parasympathomimetic and it decreases IOP through alteration of the trabecular meshwork configuration to facilitate an increase in aqueous outflow. In healthy volunteers treatment with pilocarpine showed no change in retrobulbar blood velocity of the CRA ²⁵⁸. A similar result was seen using the POBF in patients with POAG ²⁵⁹.

1.15.3 Alpha agonists

The primary mode of action of alpha agonists is to decrease IOP by a reduction in aqueous production without any alteration to the aqueous outflow. Intravenous administration of clonidine increased retinal arteriolar diameter measured using the RVA but decreased blood velocity and blood flow assessed using the laser Doppler velocimetry ²⁶⁰ in healthy volunteers. Using topical apraclonidine decreased blood velocity of the OA was noted in POAG ²⁶¹. Few studies have also looked at the treatment effect of brimonidine but have shown no change in ocular blood flow in POAG ²⁶²⁻²⁶⁶.

1.15.4 Prostaglandin analogues

This group of drugs decrease IOP by increasing the uveoscleral outflow. Studies in patients with POAG after treatment with latanoprost showed no effect on the retrobulbar blood velocity ²⁶⁷ and pulsatile ocular blood flow after correcting for the decrease in IOP ²⁶⁸. Similarly, no effect was seen with a combination of timolol and latanoprost treatment in early POAG using the SLO ²⁶⁹ and CDI/SLDF ²⁷⁰. Interestingly, treatment with latanoprost

demonstrated an initial increase in POBF but no significant change after 6 months of treatment²⁷¹. More recent studies have shown increase in ONH and retinal blood flow using the HRF in newly diagnosed POAG²⁷² and a decrease in end-diastolic velocity of the OA in POAG²⁷³.

1.15.5 Carbonic anhydrase inhibitor

Carbonic anhydrase enzyme is responsible for the production of aqueous humor by the non-pigmented ciliary epithelium. These isoenzymes are also found in corneal endothelium, retina and the ciliary processes. The CAI decrease IOP by inhibition of the carbonic anhydrase in the eye, thereby decreasing the production of aqueous humor.

1.15.5.1 Acetazolamide

Intravenous administration of acetazolamide in healthy volunteers showed an increase in choroidal blood flow²⁷⁴ and an increase in ocular pulse amplitude²⁷⁵ measured using the FPA. The effect of this drug on patients with glaucoma is not well studied.

1.15.5.2 Dorzolamide

Dorzolamide is not used as a “first line” treatment in patients with POAG, mainly due to the weak IOP lowering effect compared to the other group of IOP lowering drugs. Over the last decade, researchers have widely studied the possible hemodynamic effect of this drug in patients with POAG, an investigation concept that has been encouraged by the manufacturer. However, the results of these generally poorly controlled studies are contradictory. In

normal individuals, a single drop treatment of Dorzolamide did not show any short-term change in retinal arteriolar hemodynamics assessed using the CLBF²⁷⁶ and a similar result was observed after 3 days of treatment²⁷⁷. Another study showed a significant increase in ocular pulse amplitude in both normal subjects and patients with OHT²⁷⁸. In general, most previous studies have shown an increase in the retinal hemodynamics with topical Dorzolamide treatment in patients with POAG. Dorzolamide treatment for 4 weeks in POAG demonstrated a trend to increase diastolic velocity of the SPCAs²⁷⁹ and a decrease in the retinal arteriovenous passage time (AVP)^{269, 280, 281}. Assessment of neuroretinal rim blood flow and FPA showed an increase after 2 weeks treatment with topical Dorzolamide²⁵³, while there was an increase in ONH blood flow using the SLDF after 4 weeks treatment with a fixed combination of Dorzolamide and Timolol²⁸². However, Bergstrand and co-workers (2002) observed no effect after 2 weeks Dorzolamide treatment in retrobulbar hemodynamics²⁸³. Treatment with Dorzolamide is shown to stabilise and/or increase ocular perfusion in normal subjects during hypercapnia²⁸⁴. Intravenous injection of Dorzolamide 500mg in pigs resulted in retinal arteriolar dilation assessed using fundus photographs and also an increase in optic nerve oxygen tension²⁸⁵. The majority of previous studies have only assessed homeostatic blood flow in previously treated patients or in patients without an adequate drug wash-out period. The effect of previous treatment on retinal hemodynamics is poorly understood. In addition, a combination of drugs has been used in the past that will not give adequate information about the vascular effect of one drug. As a result, we set out to investigate the effect of treatment with Dorzolamide on retinal vascular reactivity (i.e. in response to normoxic/isoxic hypercapnia) in untreated POAG.

1.15.5.3 Brinzolamide

There is lack of adequate research on the treatment effect of Brinzolamide in patients with POAG. Sampolesi and co-workers (2001) showed no effect of Brinzolamide in advanced stages of POAG assessed using the SLDF ²⁶⁶. Similarly, there was no effect on the retrobulbar hemodynamics after 2 weeks brinzolamide treatment in healthy subjects but there was a decrease in AVP time noted ²⁸⁶.

1.16 Summary

The etiology of POAG is multi-factorial and previously two major theories were proposed, i.e. mechanical and vascular theories. Recent evidence suggests that the etiology of POAG is a combination of the two theories. However, the current treatment options available for POAG are only targeted to decrease IOP. The vascular beneficial effects of some of the IOP lowering medications have been studied. Some recent evidence suggests that CAI might improve ocular blood flow. However, those studies have not assessed the function of the retinal vessels in untreated POAG (uPOAG). The assessment of vascular reactivity in response to provocation is essential for a better understanding the patho-physiology of the disease. Accordingly, the work presented in this thesis is aimed at investigating the effect of normoxic hypercapnia on retinal arteriolar and ONH capillary vascular reactivity in uPOAG and also followed these patients after treatment with 2% Dorzolamide for 2 weeks. In addition, retinal and ONH vascular reactivity was also quantified in response to normoxic hypercapnia in patients with progressive POAG (pPOAG) as this group of patients have been suggested to more often exhibit ONH vascular dysregulation.

1.17 Autoregulation and vascular reactivity in glaucoma

A few recent studies have concentrated on the assessment of homeostatic levels of ocular blood flow and also the response of the retinal, choroidal and ONH vasculature to various physiological provocations including inspired gas, light flicker, cold stress testing and changes in perfusion pressure. The results of these studies have provided some basic understanding of the possible vascular abnormalities associated with GON. In addition, the vascular abnormalities seen in POAG are thought to be associated with the imbalance of certain vasoactive substances such as ET-1 and NO that are primarily produced by the smooth muscle cells of the vascular endothelium^{51, 287}.

1.17.1 Homeostatic blood flow in POAG

Recent developments in blood flow measurement techniques have made the quantification of hemodynamic parameters possible²⁸⁸. However, the measurement of blood flow in the eye is still challenging partly because of poor signal-to-noise ratio. The design and the principle of the various blood flow measurement techniques used to assess ocular hemodynamics in glaucoma have been described in detail elsewhere^{74, 288}. The majority of previous research has suggested a decrease in blood flow in various ocular tissue beds in patients with POAG/NTG. A decrease in perfusion assessed by measuring the retinal mean transit time has been found that is similar in both POAG and NTG²⁸⁹.

1.17.1.1 Pulsatile ocular blood flowmeter and fundus pulsation amplitude

Kerr and co-workers (2003) reported decreased levels of POBF-derived choroidal blood flow in uPOAG in comparison to patients with OHT and controls¹⁸. Other studies have also reported similar findings in patients with POAG²⁹⁰⁻²⁹⁴. Assessment of choroidal hemodynamics using FPA is in agreement with previous studies showing a decrease in pulsation amplitude in POAG^{118, 152, 295}.

1.17.1.2 Scanning laser Doppler flowmetry

Using the SLDF, a decrease in blood flow in the ONH has been shown in patients with POAG^{152, 157-159, 291, 295, 296}, NTG²⁹⁷ and glaucoma suspects²⁹⁸. Boehm and co-workers (1999) have shown regional variation in blood flow in healthy individuals using the HRF with the temporal neuroretinal rim of the ONH showing reduced blood flow compared to the nasal area²⁹⁹. Also, the area of blood flow reduction in the ONH corresponded to visual field defects in patients with NTG³⁰⁰. Sehi and co-workers (2005) determined the association between diurnal variation in IOP and MOPP to that of HRF measured ONH rim blood flow and showed an inverse correlation of blood flow to diurnal variation in IOP in untreated POAG⁷². These findings likely indicate a vascular abnormality in POAG and NTG, however, none of the above studies have determined retinal or ONH vascular reactivity in response to physiological provocations such as CO₂ or light flicker. The assessment of retinal and ONH vascular regulation provides additional information about ocular physiology and can be disturbed in the absence of disturbance of homeostatic retinal blood flow. Also, there is lack of a comprehensive assessment of ocular vascular hemodynamics in all the studies. Inner retinal blood flow might be normal in the presence of disturbed outer retinal blood

flow, or vice versa. More importantly, all the studies share the same limitation of using a surrogate parameter to indicate differences in blood flow, rather than measuring blood flow *per se*.

1.17.1.3 Color Doppler imaging

Using the CDI, a decrease has been found in retrobulbar hemodynamics in the OA and/or CRA in POAG^{296, 301-305} and NTG^{304, 306-309}. However, in patients with non-progressive POAG³¹⁰ and NTG³¹¹ no difference was found in retrobulbar blood velocity compared to controls. CDI has a number of significant limitations, including the requirement for an experienced operator to obtain reliable measurements, its inability to quantify volumetric blood flow and also the difficulty to differentiate responses between the CRA and SPCA²⁸⁸. Proper positioning of the probe on the eye is critical as the resulting blood velocity value depends on the angle between the incident beam and the direction of blood flow.

Another confounding factor that has been overlooked by the majority of the CDI-based and other studies is that homeostatic blood flow was assessed in treated POAG and/or in patients who had only recently stopped IOP lowering medication without an adequate washout period. The vascular effects of IOP lowering medications remain controversial. One study has shown no effect of medications on ocular blood flow²⁴⁹, while other studies report change in ocular blood flow as a result of IOP lowering medication^{256, 312, 313}. The average wash-out period for IOP lowering medications is 4 weeks, in order to return to original IOP levels^{314, 315}. However, there is lack of adequate evidence to support the assumption that any secondary vascular effects induced by these drugs return to baseline conditions after the

required wash-out period to normalize IOP. Also, the use of IOP lowering medications can influence MOPP resulting in disturbances of vascular regulation¹⁸. The presence of any residual vascular effects can thereby mask or exaggerate a true difference in measured baseline blood flow results. In addition, Costa and co-workers (2003) reported a negligible effect of IOP lowering medications on ocular blood flow³¹⁴. A more recent review on the impact of systemic medications on ocular blood flow reported beneficial vascular effects in various ocular beds³¹⁶. Another study showed that ONH blood flow was regulated with IOP lowering medications³¹⁷ in early POAG and failed to exhibit such a regulation of blood flow in advanced POAG. Nevertheless, it remains questionable as to whether a wash-out period of 2-4 weeks will normalize hemodynamics in POAG.

1.18 Regulation of blood flow in POAG

Autoregulation is the ability of a tissue to maintain constant blood flow despite constant changes in perfusion pressure^{318, 319}. This original definition has been modified to include other types of blood flow regulation such as metabolic regulation. The vascular endothelium is thought to release certain vasoactive factors that regulate blood flow in response to changes in trans-mural pressure and is termed as myogenic regulation. Metabolic autoregulation occurs in order to regulate blood flow to maintain adequate and optimal levels of critical nutrients such as O₂, CO₂ and K⁺ and to ensure the removal of unwanted metabolic waste products. In the eye, the inner retina and the superficial ONH vascular beds have been shown to autoregulate to an IOP increase of 30-40mmHg in clinically normal human subjects⁶⁸⁻⁷¹. Also, an abnormal vascular regulation has been suggested to occur in POAG^{40, 74-76}. There is however, a lack of definitive evidence to suggest altered autoregulation in POAG.

1.18.1 Regulation of blood flow to perfusion pressure provocation

The ONH blood flow regulation to myogenic provocation has been studied using various hemodynamic measurement techniques. Using laser Doppler flowmetry, the blood flow in the ONH did not show a significant change in normal controls or patients with NTG after 3 weeks wash-out of topical medications to a 28% increase in perfusion pressure during exercise ⁹¹. In NTG patients, however, there was an increase of vascular resistance to the alteration in perfusion pressure that might indicate some autoregulatory disturbance ⁹¹. A similar result was found in a study that measured change in choroidal pulsation using the fundus pulsation technique and ONH blood flow using the Laser Doppler Flowmetry in response to a 20mmHg change in IOP in patients with POAG ³²⁰. Similarly, altered autoregulation has been suggested to occur to changes in IOP in patients with POAG, as indicated by macular leucocyte velocity measured using the blue field entoptic phenomenon ³²¹. A short term increase in IOP has been shown to cause a reduced regulatory change in retinal arteriolar and venular diameter in POAG when assessed using the RVA in POAG ³²².

1.19 Vascular reactivity response to provocations in glaucoma

The change in hemodynamic parameters in response to physiological provocation such as CO₂, O₂, cold stress or light flicker is defined as vascular reactivity or metabolic autoregulation; this functional assessment of the ocular vasculature is thought, but not proven, to reflect vascular regulation capacity. Relatively few studies have been undertaken on the assessment of vascular reactivity in response to provocation in patients with glaucoma. However, several recent studies have provided some in-sight into the retinal vascular response in glaucoma.

1.19.1 Hypercapnia

Hypercapnia is the increase in the arterial partial pressure of CO₂ achieved by inspiring increased amounts of CO₂. In normal control subjects breathing CO₂ causes vasodilation and thereby leads to an increase of inner retinal and superficial ONH blood flow^{19, 170, 180, 182, 188, 323}. The mechanism involved in the vasodilation response of blood vessels to hypercapnia is controversial. Studies have shown a positive role of NO in humans¹²⁴ and animal models¹³⁰. Conversely, an absence of the role of NO during hypercapnia induced vasodilation has been reported in animal models^{58, 59}.

Hosking and co-workers (2004) showed an increase in blood velocity of the SPCA in response to hypercapnia measured using CDI in POAG, although a similar response was not found in the OA¹⁴⁶. Patients with uPOAG have been shown to demonstrate a normal increase in the blood velocity of the CRA to hypercapnia but a decrease in blood velocity in the OA¹⁴⁷. Interestingly, others have found an exaggerated response to hypercapnia in the CRA and short PCAs in NTG compared to control subjects³⁰⁷; the authors explain that this might be due to the reduced baseline blood velocity in the patient group compared to controls. A recent study has shown a decrease in the choroidal blood flow and an increase in ONH blood flow measured using the laser Doppler flowmeter in female subjects with vasospastic symptoms, such as cold hands and/or feet, in response to hypercapnia⁹² although, there was no increase in ONH blood flow in subjects without vasospasm. There was also a significant change in blood pressure during hypercapnia in all the groups, that is men, women without vasospasm and women with vasospasm. The reason for these unexpected results is unclear. The authors speculate that there might be either an increased

response of the ONH to hypercapnia in vasospasm or a lack of adequate autoregulation causing an increase in blood flow due to the associated change in blood pressure.

The majority of the hypercapnia studies have used a simple manual addition of CO₂ rather than a re-breathing circuit. The use of a standardised provocation is essential to minimise variability in the magnitude of vascular reactivity and the re-breathing circuit helps to minimise this variability¹⁷⁷. Breathing CO₂ results in an unpredictable increase in ventilation and thereby an unpredictable increase in PETO₂¹⁷⁶. The use of normoxic/isoxic hypercapnia is important in the assessment of retinal vascular reactivity in order to avoid the confounding effects of varying O₂, i.e. resulting in vasoconstriction. It has recently been shown that the use of a non-rebreathing circuit and the addition of CO₂ to inspired air to induce hypercapnia results in an increase in PETCO₂ to target levels, however, the arterial partial pressure of CO₂ remains unchanged¹⁷⁷. This potential problem is avoided by the use of a sequential gas breathing circuit and a newly developed automated gas flow controller^{21, 177}.

Recently, our laboratory has validated a normoxic hypercapnic stimulus that is induced using an automated gas flow controller²¹(see Chapter 5). Using this technique, partial pressures of CO₂ and O₂ can be manipulated independent of each other. This standardised stimulus is currently used in our laboratory for investigating the retinal arteriolar and ONH functional hemodynamic responses.

1.19.2 Hyperoxia

Hyperoxia is the increase in the arterial partial pressure of O₂. The ocular vasculature responds to this increase in O₂ level by vasoconstricting which results in a decrease in blood flow in healthy humans^{22, 23, 154, 182}. The response to hyperoxia in glaucoma has not been widely studied. This is likely due to the theory of a pre-existing vasospasm in glaucoma and that breathing O₂ would further decrease the blood supply to an already compromised ONH. Recently, retrobulbar velocities in patients with POAG have been shown to remain unaltered in response to hyperoxia suggesting that the pre-existing vasospasm prevents further decrease in blood velocity in this group¹⁴⁶. There is also evidence that glaucoma might be associated with reduced blood velocity in cerebral vessels, in particular, the middle cerebral artery and also a decrease in the magnitude of cerebral vascular reactivity to hyperoxia in POAG³²⁴.

The increase in PETO₂ during hyperoxia can generally result in a concomitant change in PETCO₂. Most previous studies have used non-standardised hyperoxic stimuli, including use of a non-rebreathing valve and the manual addition of small amounts of CO₂. This resulted in a high intrasubject variability. Gilmore and co-workers (2004) used a sequential re-breathing circuit and induced isocapnic hyperoxia to assess retinal vascular reactivity³²⁵. As a result, they demonstrated a reduced variability of PETCO₂ and this produced less variable vascular reactivity responses of the retinal vasculature to hyperoxia. However, although now experimentally feasible, the use of isocapnic hyperoxia has generally been avoided in patients with POAG due to the risk of further constriction of the vasculature of the retina and ONH.

1.19.3 Flicker stimulation

The retinal and ONH blood vessels respond to flicker provocation with an increase in diameter and blood flow^{31, 143, 326, 327} and a recent study has shown decreased vasodilation in response to flicker in patients with type 2 diabetes³²⁸. The mechanism of vasodilation response during flicker is not well understood. In the cerebral vasculature, however, it is believed that there is a tight neural coupling between the local metabolic demand and blood flow³²⁹. In addition, there are various vasoactive factors identified in the cerebral response to flicker stimulation, such as CO₂, potassium, adenosine and NO, that have been suggested to play a role in the vasodilatory response during neuronal driven activity in both the cerebral and retinal vessels^{330, 331}. It is suggested that the increase in blood flow in the ONH in response to flicker stimulation in healthy individuals might be an effect of increased retinal activity^{49, 332}. However, the mediators responsible for the vasodilation during this neural activity are still not clear, although NO might play an important role⁵³.

Recently, the response of the retina and the ONH to flicker stimulation has been widely studied in POAG. Horn and co-workers (2006) investigated temporal contrast sensitivity in patients with glaucoma and normal controls and showed a delayed recovery time after flicker stimulation in the patient group compared to controls³⁴. Vascular reactivity of the retinal and ONH blood vessels measured using laser Doppler flowmetry in response to flicker stimulation was reduced in patients with treated early OAG but did not show any deterioration in patients with OHT³³.

It has also been shown that short term increases in IOP in a group of normals does not alter the dilation response to flicker stimulation³²⁷. This is in agreement to previous experiments in animal models^{32, 53}. However, these findings cannot be directly compared to patients with glaucoma because the long term effect of increased IOP has not been studied. Recently, an abnormal autoregulatory response to flicker and pattern stimulation has also been reported in early OAG⁴⁹.

1.19.4 Cold stress test

Cold provocation is a technique used to assess the function of the autonomic nervous system (ANS). Disturbance in the ANS might be present in glaucoma, in particular in NTG³³³⁻³³⁵. Cold provocation generally produces vasoconstriction, decrease in peripheral blood flow and an increase in blood pressure

Previous studies in patients with POAG showed no significant alteration in ocular blood flow assessed using the SLDF and trans-cranial Doppler technique in the peripapillary retina²⁸ or in the OA²⁹. Recently, patients with POAG have been shown to exhibit a decrease in blood flow at the temporal neuroretinal rim in response to cold provocation, while no change was found in ocular blood flow in non-glaucomatous subjects³³⁶. The mechanisms responsible for the regulation of blood flow during cold provocation are not well understood. However, Nicolela and co-workers (2003) have shown increased levels of plasma ET-1 in POAG after cold provocation²⁸. This increase in ET-1 might be responsible for the vasoconstriction of peripheral blood flow in response to cold in POAG. The use of IOP lowering medications in

patients with POAG and vasospasm helped to improve ONH rim blood flow compared to those without vasospasm³³⁷.

A limiting factor in our interpretation of virtually all vascular reactivity studies is our lack of understanding of the impact of the provocation upon the cellular vasoactive factors that control ocular vasoconstriction and vasodilation.

1.20 Conclusions

The retina and the ONH autoregulate to a wide range of changes in ocular perfusion pressure. The vascular endothelium derived vasoconstricting and vasodilating factors play an important role in regulating the blood flow in the eye. Studies have used a number of techniques to assess ocular blood flow, however, previous studies have not performed a comprehensive assessment of retinal hemodynamics. The measurement of all aspects of hemodynamics is important to assess the autoregulatory status of the retina and ONH. The CLBF is the only instrument currently available that quantifies retinal arteriolar hemodynamics in absolute units. The CLBF measures diameter and blood velocity at a single point along the vessel and in this respect, it can be assumed that all branches of the vascular tree react similarly to provocation. Also, the measurement is not continuous but limited to a 2 second window. As glaucoma is a condition primarily affecting the ONH, assessment of the vascular reactivity of the ONH will provide a better understanding of the pathophysiology of the disease. In this work, the HRF will be used to assess ONH vascular reactivity in some patients with uPOAG, pPOAG and controls. The HRF has relatively high measurement variability and requires repeated measurements in order to obtain valid blood flow values.

For this reason, this work aimed to develop a safe, sustainable and stable provocation. We set-out to develop a normoxic/isoxic hypercapnic stimulus ultimately to assess retinal vasodilation capacity in patients with POAG.

Over the last few years, retinal vascular reactivity has been widely studied using various provocation techniques. Studies have used gas provocations, cold stress test and flicker stimulation to assess regulation of vascular reactivity. Under normal conditions, the retinal and the ONH vessels respond by an increase in diameter, velocity and blood flow to hypercapnia and a decrease in all the hemodynamic parameters in response to hyperoxia. There is a particular lack of adequate information on the regulation of retinal and ONH blood flow in disease such as patients with POAG, especially in untreated POAG. In addition, the few studies that have looked at the effect of hypercapnia in POAG have either not used a standardised hypercapnic stimulus or failed to monitor any concomitant changes in $P_{ET}O_2$. In our study we used a newly developed automated gas flow controller to induce normoxic hypercapnia via a sequential rebreathing circuit and this resulted in a robust vascular reactivity response in both normal controls and in patients with uPOAG and pPOAG.

Vascular dysregulation is suggested to be a factor in the progression of POAG. Current treatment for POAG involves the use of medication to lower the IOP. Recent studies have focused on the effect of certain IOP lowering medications on retinal and ONH blood flow. There is a need for more research on the assessment of hemodynamic characteristics of patients with POAG and also to establish a treatment modality to address any possible vascular disturbance. Previous studies have assessed the vascular effects of IOP lowering

medications by using a combination of drugs. However, it is difficult to determine any beneficial effect of an individual medication. Accordingly, in our study we investigated the effect of treatment with 2% Dorzolamide for 2 weeks on retinal arteriolar vascular reactivity in patients with newly diagnosed POAG.

The vascular endothelium releases both vasoconstricting and vasodilating factors such as ET-1 and NO respectively. Previously it has been shown that an exaggerated amount of ET-1 at baseline in patients with POAG thereby leading to vasospasm. In this work we therefore assessed plasma levels of ET-1/NO at baseline and during normoxic hypercapnic provocation in uPOAG, pPOAG and controls. Conversely, the results of this work show that there is a decrease in the plasma ET-1 at baseline in uPOAG. We also correlated functional vascular response in the above patients to endothelial biochemical markers. The approach to correlate between functional retinal vascular response and vascular endothelial biochemical markers will further improve our understanding of the pathophysiology of POAG.

1.21 References

1. Cioffi GA, Granstam E, Alm A. Ocular circulation. P. Kaufman and A. Alm. *In Adler's physiology of the eye*. Elsevier; 2002. 747-784 pp.
2. Yu DY, Cringle SJ. Oxygen distribution and consumption within the retina in vascularised and avascular retinas and in animal models of retinal disease. *Prog.Retin.Eye Res.* 2001;20:175-208.
3. Buchi ER. The blood supply to the optic nerve head. H. J. Kaiser, J. Flammer and Ph Hendrickson. *In Ocular Blood Flow; New Insights into the Pathogenesis of Ocular Diseases*. Basel: Karger Publications; 1996. 1-8 pp.
4. Cioffi GA. Vascular anatomy of the optic nerve. L. E. Pillunat, A. Harris, D. R. Anderson and I. L. Greve. *In Current Concepts on Ocular Blood Flow in Glaucoma*. The Hague, The Netherlands: Kugler Publications; 1999. 45-50 pp.
5. Hayreh SS. Blood flow in the optic nerve head and factors that may influence it. *Prog.Retin.Eye Res.* 2001;20:595-624.
6. Gupta D. Pathophysiology of glaucoma. Anonymous *In Glaucoma Diagnosis and Management*. Philadelphia: Lippincott Williams & Wilkins; 2004. 31-39 pp.
7. Cantor L, Fechtner R, Michael AJ, Simmons ST, Wilson MR, Brown SVL. Clinical evaluation; the optic nerve anatomy and pathology. M. Denny and J. Daniel. *In Glaucoma Basic and Clinical Science Course*. San Francisco: 2004. 39-42 pp.

8. Mackenzie PJ, Cioffi GA. Vascular anatomy of the optic nerve head. *Can.J.Ophthalmol.* 2008;43:308-312.
9. Alm A. The effect of sympathetic stimulation on blood flow through the uvea, retina and optic nerve in monkeys (*Macaca irus*). *Exp.Eye Res.* 1977;25:19-24.
10. Flugel-Koch C, Kaufman P, Lutjen-Drecoll E. Association of a choroidal ganglion cell plexus with the fovea centralis. *Invest.Ophthalmol.Vis.Sci.* 1994;35:4268-4272.
11. Pournaras CJ, Rungger-Brandle E, Riva CE, Hardarson SH, Stefansson E. Regulation of retinal blood flow in health and disease. *Prog.Retin.Eye Res.* 2008;27:284-330.
12. Orgul S, Gugleta K, Flammer J. Physiology of perfusion as it relates to the optic nerve head. *Surv.Ophthalmol.* 1999;43 Suppl 1:S17-S26.
13. Anderson DR. Glaucoma, capillaries and pericytes. 1. blood flow regulation. *Ophthalmologica* 1996;210:257-262.
14. Anderson DR, Davis EB. Glaucoma, capillaries and pericytes. 5. preliminary evidence that carbon dioxide relaxes pericyte contractile tone. *Ophthalmologica* 1996;210:280-284.
15. Lombard JH. A novel mechanism for regulation of retinal blood flow by lactate: Gap junctions, hypoxia, and pericytes. *Am.J.Physiol.Heart Circ.Physiol.* 2006;290:H921-2.
16. Peppiatt CM, Howarth C, Mobbs P, Attwell D. Bidirectional control of CNS capillary diameter by pericytes. *Nature* 2006;443:700-704.

17. Guyton AC, Carrier O, Jr, Walker JR. Evidence for tissue oxygen demand as the major factor causing autoregulation. *Circ.Res.* 1964;15:SUPPL:60-9.
18. Kerr J, Nelson P, O'Brien C. Pulsatile ocular blood flow in primary open-angle glaucoma and ocular hypertension. *Am.J.Ophthalmol.* 2003;136:1106-1113.
19. Dorner GT, Garhofer G, Zawinka C, Kiss B, Schmetterer L. Response of retinal blood flow to CO₂-breathing in humans. *Eur.J.Ophthalmol.* 2002;12:459-466.
20. Harris A, Anderson DR, Pillunat L, et al. Laser doppler flowmetry measurement of changes in human optic nerve head blood flow in response to blood gas perturbations. *J.Glaucoma* 1996;5:258-265.
21. Venkataraman ST, Hudson C, Fisher JA, et al. Retinal arteriolar and capillary vascular reactivity in response to isoxic hypercapnia. *Exp.Eye Res.* 2008; 87(6):535-542.
22. Gilmore ED, Hudson C, Preiss D, Fisher J. Retinal arteriolar diameter, blood velocity, and blood flow response to an isocapnic hyperoxic provocation. *Am J Physiol Heart Circ Physiol* 2005;288:H2912-H2917.
23. Kiss B, Polska E, Dorner G, et al. Retinal blood flow during hyperoxia in humans revisited: Concerted results using different measurement techniques. *Microvasc.Res.* 2002;64:75-85.
24. Dallinger S, Dorner GT, Wenzel R, et al. Endothelin-1 contributes to hyperoxia-induced vasoconstriction in the human retina. *Invest.Ophthalmol.Vis.Sci.* 2000;41:864-869.

25. Tomic L, Bjarnhall G, Maepea O, Sperber GO, Alm A. Effects of oxygen and carbon dioxide on human retinal circulation: An investigation using blue field simulation and scanning laser ophthalmoscopy. *Acta Ophthalmol.Scand.* 2005;83:705-710.
26. Hollo G, Lakatos P, Farkas K. Cold pressor test and plasma endothelin-1 concentration in primary open-angle and capsular glaucoma. *J.Glaucoma* 1998;7:105-110.
27. Nagaoka T, Mori F, Yoshida A. Retinal artery response to acute systemic blood pressure increase during cold pressor test in humans. *Invest.Ophthalmol.Vis.Sci.* 2002;43:1941-1945.
28. Nicolela MT, Ferrier SN, Morrison CA, et al. Effects of cold-induced vasospasm in glaucoma: The role of endothelin-1. *Invest.Ophthalmol.Vis.Sci.* 2003;44:2565-2572.
29. Rojanapongpun P, Drance SM. The response of blood flow velocity in the ophthalmic artery and blood flow of the finger to warm and cold stimuli in glaucomatous patients. *Graefes Arch.Clin.Exp.Ophthalmol.* 1993;231:375-377.
30. Prokopich CL, Flanagan JG. The association between a positive cold pressor test and vasospastic symptoms. *Invest.Ophthalmol.Vis.Sci.* 2003;44:E-Abstract 116.
31. Polak K, Schmetterer L, Riva CE. Influence of flicker frequency on flicker-induced changes of retinal vessel diameter. *Invest.Ophthalmol.Vis.Sci.* 2002;43:2721-2726.
32. Riva CE, Harino S, Shonat RD, Petrig BL. Flicker evoked increase in optic nerve head blood flow in anesthetized cats. *Neurosci.Lett.* 1991;128:291-296.

33. Riva CE, Salgarello T, Logean E, Colotto A, Galan EM, Falsini B. Flicker-evoked response measured at the optic disc rim is reduced in ocular hypertension and early glaucoma. *Invest.Ophthalmol.Vis.Sci.* 2004;45:3662-3668.
34. Horn FK, Link B, Dehne K, Lammer R, Junemann AG. Flicker provocation with LED full-field stimulation in normals and glaucoma patients. *Ophthalmologe* 2006;103:866-872.
35. Falsini B, Riva CE, Logean E. Flicker-evoked changes in human optic nerve blood flow: Relationship with retinal neural activity. *Invest.Ophthalmol.Vis.Sci.* 2002;43:2309-2316.
36. Harris A, Ciulla TA, Chung HS, Martin B. Regulation of retinal and optic nerve blood flow. *Arch.Ophthalmol.* 1998;116:1491-1495.
37. Dorner GT, Garhofer G, Kiss B, et al. Nitric oxide regulates retinal vascular tone in humans. *Am.J.Physiol.Heart Circ.Physiol.* 2003;285:H631-H636.
38. Polak K, Luksch A, Frank B, Jandrasits K, Polska E, Schmetterer L. Regulation of human retinal blood flow by endothelin-1. *Exp.Eye Res.* 2003;76:633-640.
39. Flammer J, Mozaffarieh M. Autoregulation, a balancing act between supply and demand. *Can.J.Ophthalmol.* 2008;43:317-321.
40. Flammer J, Mozaffarieh M. What is the present pathogenetic concept of glaucomatous optic neuropathy? *Surv.Ophthalmol.* 2007;52:S162-73.
41. Chauhan BC. Endothelin and its potential role in glaucoma. *Can.J.Ophthalmol.* 2008;43:356-360.

42. Mozaffarieh M, Grieshaber MC, Flammer J. Oxygen and blood flow: Players in the pathogenesis of glaucoma. *Mol.Vis.* 2008;14:224-233.
43. Grunwald JE, Sinclair SH, Riva CE. Autoregulation of the retinal circulation in response to decrease of intraocular pressure below normal. *Invest.Ophthalmol.Vis.Sci.* 1982;23:124-127.
44. Rassam SM, Patel V, Kohner EM. The effect of experimental hypertension on retinal vascular autoregulation in humans: A mechanism for the progression of diabetic retinopathy. *Exp.Physiol.* 1995;80:53-68.
45. Robinson F, Riva CE, Grunwald JE, Petrig BL, Sinclair SH. Retinal blood flow autoregulation in response to an acute increase in blood pressure. *Invest.Ophthalmol.Vis.Sci.* 1986;27:722-726.
46. Weinstein JM, Duckrow RB, Beard D, Brennan RW. Regional optic nerve blood flow and its autoregulation. *Invest.Ophthalmol.Vis.Sci.* 1983;24:1559-1565.
47. Weinstein JM, Funsch D, Page RB, Brennan RW. Optic nerve blood flow and its regulation. *Invest.Ophthalmol.Vis.Sci.* 1982;23:640-645.
48. Jeppesen P, Sanye-Hajari J, Bek T. Increased blood pressure induces a diameter response of retinal arterioles that increases with decreasing arteriolar diameter. *Invest.Ophthalmol.Vis.Sci.* 2007;48:328-331.
49. Riva CE, Falsini B. Functional laser doppler flowmetry of the optic nerve: Physiological aspects and clinical applications. *Prog.Brain Res.* 2008;173:149-163.

50. Haefliger IO, Flammer J, Luscher TF. Nitric oxide and endothelin-1 are important regulators of human ophthalmic artery. *Invest.Ophthalmol.Vis.Sci.* 1992;33:2340-2343.
51. Haefliger IO, Dettmann E, Liu R, et al. Potential role of nitric oxide and endothelin in the pathogenesis of glaucoma. *Surv.Ophthalmol.* 1999;43 Suppl 1:S51-S58.
52. Bertuglia S, Giusti A. Role of nitric oxide in capillary perfusion and oxygen delivery regulation during systemic hypoxia. *Am.J.Physiol.Heart Circ.Physiol.* 2005;288:H525-31.
53. Buerk DG, Riva CE, Cranstoun SD. Nitric oxide has a vasodilatory role in cat optic nerve head during flicker stimuli. *Microvasc.Res.* 1996;52:13-26.
54. Schmetterer L, Krejcy K, Kastner J, et al. The effect of systemic nitric oxide-synthase inhibition on ocular fundus pulsations in man. *Exp.Eye Res.* 1997;64:305-312.
55. Koss MC. Functional role of nitric oxide in regulation of ocular blood flow. *Eur.J.Pharmacol.* 1999;374:161-174.
56. Okuno T, Sugiyama T, Kohyama M, Kojima S, Oku H, Ikeda T. Ocular blood flow changes after dynamic exercise in humans. *Eye* 2006;20:796-800.
57. Bouzas EA, Donati G, Pournaras CJ. Distribution and regulation of the optic nerve head tissue PO₂. *Surv.Ophthalmol.* 1997;42 Suppl 1:S27-34.
58. Gidday JM, Zhu Y. Nitric oxide does not mediate autoregulation of retinal blood flow in newborn pig. *Am.J.Physiol.* 1995;269:H1065-72.

59. Donati G, Pournaras CJ, Munoz JL, Tsacopoulos M. The role of nitric oxide in retinal vasomotor regulation. *Klin.Monatsbl.Augenheilkd.* 1994;204:424-426.
60. Haefliger IO, Flammer J, Beny JL, Luscher TF. Endothelium-dependent vasoactive modulation in the ophthalmic circulation. *Prog.Retin.Eye Res.* 2001;20:209-225.
61. Reudelhuber TL. The renin-angiotensin system: Peptides and enzymes beyond angiotensin II. *Curr.Opin.Nephrol.Hypertens.* 2005;14:155-159.
62. Haefliger IO, Meyer P, Flammer J. Endothelium-dependent vasoactive factors. H. J. Kaiser, J. Flammer and P. Hendrickson. *In Ocular blood flow.* Glaucoma-meeting 1995. Basel, Karger; 1996. 51-63 pp.
63. Sossi N, Anderson DR. Blockage of axonal transport in optic nerve induced by elevation of intraocular pressure. effect of arterial hypertension induced by angiotensin I. *Arch.Ophthalmol.* 1983;101:94-97.
64. Clermont A, Bursell SE, Feener EP. Role of the angiotensin II type 1 receptor in the pathogenesis of diabetic retinopathy: Effects of blood pressure control and beyond. *J.Hypertens.Suppl.* 2006;24:S73-80.
65. Ott C, Schlaich MP, Harazny J, Schmidt BM, Michelson G, Schmieder RE. Effects of angiotensin II type 1-receptor blockade on retinal endothelial function. *J.Hypertens.* 2008;26:516-522.

66. Yu DY, Alder VA, Cringle SJ, Su EN, Yu PK. Vasoactivity of intraluminal and extraluminal agonists in perfused retinal arteries. *Invest.Ophthalmol.Vis.Sci.* 1994;35:4087-4099.
67. Jandrasits K, Luksch A, Soregi G, Dorner GT, Polak K, Schmetterer L. Effect of noradrenaline on retinal blood flow in healthy subjects. *Ophthalmology* 2002;109:291-295.
68. Riva CE, Sinclair SH, Grunwald JE. Autoregulation of retinal circulation in response to decrease of perfusion pressure. *Invest.Ophthalmol.Vis.Sci.* 1981;21:34-38.
69. Pillunat LE, Anderson DR, Knighton RW, Joos KM, Feuer WJ. Autoregulation of human optic nerve head circulation in response to increased intraocular pressure. *Exp.Eye Res.* 1997;64:737-744.
70. Schulte K, Wolf S, Arend O, Harris A, Henle C, Reim M. Retinal hemodynamics during increased intraocular pressure. *Ger.J.Ophthalmol.* 1996;5:1-5.
71. Riva CE, Grunwald JE, Petrig BL. Autoregulation of human retinal blood flow. an investigation with laser doppler velocimetry. *Invest.Ophthalmol.Vis.Sci.* 1986;27:1706-1712.
72. Sehi M, Flanagan JG, Zeng L, Cook RJ, Trope GE. Anterior optic nerve capillary blood flow response to diurnal variation of mean ocular perfusion pressure in early untreated primary open-angle glaucoma. *Invest.Ophthalmol.Vis.Sci.* 2005;46:4581-4587.

73. Lovasik JV, Kergoat H, Riva CE, Petrig BL, Geiser M. Choroidal blood flow during exercise-induced changes in the ocular perfusion pressure. *Invest.Ophthalmol.Vis.Sci.* 2003;44:2126-2132.
74. Flammer J, Orgul S, Costa VP, et al. The impact of ocular blood flow in glaucoma. *Prog.Retin.Eye Res.* 2002;21:359-393.
75. Evans DW, Harris A, Garrett M, Chung HS, Kagemann L. Glaucoma patients demonstrate faulty autoregulation of ocular blood flow during posture change. *Br.J.Ophthalmol.* 1999;83:809-813.
76. Flammer J, Haefliger IO, Orgul S, Resink T. Vascular dysregulation: A principal risk factor for glaucomatous damage? *J.Glaucoma* 1999;8:212-219.
77. Grieshaber MC, Flammer J. Blood flow in glaucoma. *Curr.Opin.Ophthalmol.* 2005;16:79-83.
78. Grieshaber MC, Mozaffarieh M, Flammer J. What is the link between vascular dysregulation and glaucoma? *Surv.Ophthalmol.* 2007;52:S144-54.
79. Chung HS, Harris A, Evans DW, Kagemann L, Garzosi HJ, Martin B. Vascular aspects in the pathophysiology of glaucomatous optic neuropathy. *Surv.Ophthalmol.* 1999;43 Suppl 1:S43-S50.
80. Polska E, Simader C, Weigert G, et al. Regulation of choroidal blood flow during combined changes in intraocular pressure and arterial blood pressure. *Invest.Ophthalmol.Vis.Sci.* 2007;48:3768-3774.

81. Dumskyj MJ, Eriksen JE, Dore CJ, Kohner EM. Autoregulation in the human retinal circulation: Assessment using isometric exercise, laser doppler velocimetry, and computer-assisted image analysis. *Microvasc.Res.* 1996;51:378-392.
82. Iester M, Torre PG, Bricola G, Bagnis A, Calabria G. Retinal blood flow autoregulation after dynamic exercise in healthy young subjects. *Ophthalmologica* 2007;221:180-185.
83. Lovasik JV, Kergoat H. Consequences of an increase in the ocular perfusion pressure on the pulsatile ocular blood flow. *Optom.Vis.Sci.* 2004;81:692-698.
84. Meyer P, Haefliger IO, Flammer J, Luscher TF. Endothelium-dependent regulation in ocular vessels. H. J. Kaiser, J. Flammer and P. Hendrickson. *In Ocular Blood Flow - New Insights into the Pathogenesis of Ocular Diseases.* Basel, Switzerland: Karger Publishers; 1996. 64-73 pp.
85. Faraci FM, Heistad DD. Central nervous system and eye, microcirculation of the brain. D. Shepro. *In Microvascular research Biology and Pathology.* San Diego, CA: Elsevier Academic Press Publications; 2006. 381-384 pp.
86. Luscher TF, Boulanger CM, Dohi Y, Yang ZH. Endothelium-derived contracting factors. *Hypertension* 1992;19:117-130.
87. Lu M, Adamis AP. Central nervous system and eye, the retinal microvasculature. D. Shepro. *In Microvascular research-Biology and Pathology.* San Diego, CA: Elsevier Academic Press; 2006. 401-403 pp.

88. Cardillo C, Kilcoyne CM, Cannon RO,3rd, Panza JA. Interactions between nitric oxide and endothelin in the regulation of vascular tone of human resistance vessels in vivo. *Hypertension* 2000;35:1237-1241.
89. Mather KJ, Lteif A, Steinberg HO, Baron AD. Interactions between endothelin and nitric oxide in the regulation of vascular tone in obesity and diabetes. *Diabetes* 2004;53:2060-2066.
90. Pechanova O, Simko F. The role of nitric oxide in the maintenance of vasoactive balance. *Physiol.Res.* 2007;56 Suppl 2:S7-S16.
91. Pournaras CJ, Riva CE, Bresson-Dumont H, De Gottrau P, Bechettoille A. Regulation of optic nerve head blood flow in normal tension glaucoma patients. *Eur.J.Ophthalmol.* 2004;14:226-235.
92. Gugleta K, Orgul S, Hasler P, Flammer J. Circulatory response to blood gas perturbations in vasospasm. *Invest.Ophthalmol.Vis.Sci.* 2005;46:3288-3294.
93. Resch H, Garhofer G, Fuchsjager-Mayrl G, Hommer A, Schmetterer L. Endothelial dysfunction in glaucoma. *Acta Ophthalmol.* 2008; 87(1):4-12.
94. Mozaffarieh M, Flammer J. Is there more to glaucoma treatment than lowering IOP? *Surv.Ophthalmol.* 2007;52 Suppl 2:S174-9.
95. Meyer P, Flammer J, Luscher TF. Endothelium-dependent regulation of the ophthalmic microcirculation in the perfused porcine eye: Role of nitric oxide and endothelins. *Invest.Ophthalmol.Vis.Sci.* 1993;34:3614-3621.

96. Prasanna G, Krishnamoorthy R, Clark AF, Wordinger RJ, Yorio T. Human optic nerve head astrocytes as a target for endothelin-1. *Invest.Ophthalmol.Vis.Sci.* 2002;43:2704-2713.
97. Prasanna G, Hulet C, Desai D, et al. Effect of elevated intraocular pressure on endothelin-1 in a rat model of glaucoma. *Pharmacol.Res.* 2005;51:41-50.
98. Nie XJ, Olsson Y. Endothelin peptides in brain diseases. *Rev.Neurosci.* 1996;7:177-186.
99. Rogers SD, Peters CM, Pomonis JD, Hagiwara H, Ghilardi JR, Mantyh PW. Endothelin B receptors are expressed by astrocytes and regulate astrocyte hypertrophy in the normal and injured CNS. *Glia* 2003;41:180-190.
100. Wang L, Fortune B, Cull G, Dong J, Cioffi GA. Endothelin B receptor in human glaucoma and experimentally induced optic nerve damage. *Arch.Ophthalmol.* 2006;124:717-724.
101. Takagi C, King GL, Takagi H, Lin YW, Clermont AC, Bursell SE. Endothelin-1 action via endothelin receptors is a primary mechanism modulating retinal circulatory response to hyperoxia. *Invest.Ophthalmol.Vis.Sci.* 1996;37:2099-2109.
102. Zhu Y, Park TS, Gidday JM. Mechanisms of hyperoxia-induced reductions in retinal blood flow in newborn pig. *Exp.Eye Res.* 1998;67:357-369.
103. Granstam E, Wang L, Bill A. Ocular effects of endothelin-1 in the cat. *Curr.Eye Res.* 1992;11:325-332.

104. Bursell SE, Clermont AC, Oren B, King GL. The in vivo effect of endothelins on retinal circulation in nondiabetic and diabetic rats. *Invest.Ophthalmol.Vis.Sci.* 1995;36:596-607.
105. Schmetterer L, Findl O, Strenn K, et al. Effects of endothelin-1 (ET-1) on ocular hemodynamics. *Curr.Eye Res.* 1997;16:687-692.
106. Cellini M, Possati GL, Profazio V, Sbrocca M, Caramazza N, Caramazza R. Color doppler imaging and plasma levels of endothelin-1 in low-tension glaucoma. *Acta Ophthalmol.Scand.Suppl.* 1997:11-13.
107. Sugiyama T, Moriya S, Oku H, Azuma I. Association of endothelin-1 with normal tension glaucoma: Clinical and fundamental studies. *Surv.Ophthalmol.* 1995;39 Suppl 1:S49-S56.
108. Emre M, Orgul S, Haufschild T, Shaw SG, Flammer J. Increased plasma endothelin-1 levels in patients with progressive open angle glaucoma. *Br.J.Ophthalmol.* 2005;89:60-63.
109. Kunimatsu S, Mayama C, Tomidokoro A, Araie M. Plasma endothelin-1 level in japanese normal tension glaucoma patients. *Curr.Eye Res.* 2006;31:727-731.
110. Kaiser HJ, Flammer J, Wenk M, Luscher T. Endothelin-1 plasma levels in normal-tension glaucoma: Abnormal response to postural changes. *Graefes Arch.Clin.Exp.Ophthalmol.* 1995;233:484-488.

111. Kallberg ME, Brooks DE, Gelatt KN, Garcia-Sanchez GA, Szabo NJ, Lambrou GN. Endothelin-1, nitric oxide, and glutamate in the normal and glaucomatous dog eye. *Vet.Ophthalmol.* 2007;10 Suppl 1:46-52.
112. Tezel G, Kass MA, Kolker AE, Becker B, Wax MB. Plasma and aqueous humor endothelin levels in primary open-angle glaucoma. *J.Glaucoma* 1997;6:83-89.
113. Vanhoutte PM, Rubanyi GM, Miller VM, Houston DS. Modulation of vascular smooth muscle contraction by the endothelium. *Annu.Rev.Physiol.* 1986;48:307-320.
114. Jarajapu YP, Grant MB, Knot HJ. Myogenic tone and reactivity of the rat ophthalmic artery. *Invest.Ophthalmol.Vis.Sci.* 2004;45:253-259.
115. Busse R, Luckhoff A, Bassenge E. Endothelium-derived relaxant factor inhibits platelet activation. *Naunyn Schmiedebergs Arch.Pharmacol.* 1987;336:566-571.
116. Ignarro LJ, Byrns RE, Buga GM, Wood KS. Endothelium-derived relaxing factor from pulmonary artery and vein possesses pharmacologic and chemical properties identical to those of nitric oxide radical. *Circ.Res.* 1987;61:866-879.
117. Neufeld AH, Hernandez MR, Gonzalez M. Nitric oxide synthase in the human glaucomatous optic nerve head. *Arch.Ophthalmol.* 1997;115:497-503.
118. Polak K, Luksch A, Berisha F, Fuchsjager-Mayrl G, Dallinger S, Schmetterer L. Altered nitric oxide system in patients with open-angle glaucoma. *Arch.Ophthalmol.* 2007;125:494-498.

119. Haefliger IO, Meyer P, Flammer J, Luscher TF. The vascular endothelium as a regulator of the ocular circulation: A new concept in ophthalmology? *Surv.Ophthalmol.* 1994;39:123-132.
120. Haefliger IO, Zschauer A, Anderson DR. Relaxation of retinal pericyte contractile tone through the nitric oxide-cyclic guanosine monophosphate pathway. *Invest.Ophthalmol.Vis.Sci.* 1994;35:991-997.
121. Galassi F, Renieri G, Sodi A, Ucci F, Vannozzi L, Masini E. Nitric oxide proxies and ocular perfusion pressure in primary open angle glaucoma. *Br.J.Ophthalmol.* 2004;88:757-760.
122. Deussen A, Sonntag M, Vogel R. L-arginine-derived nitric oxide: A major determinant of uveal blood flow. *Exp.Eye Res.* 1993;57:129-134.
123. Wang Q, Bryowsky J, Minshall RD, Pelligrino DA. Possible obligatory functions of cyclic nucleotides in hypercapnia-induced cerebral vasodilation in adult rats. *Am.J.Physiol.* 1999;276:H480-H487.
124. Schmetterer L, Findl O, Strenn K, et al. Role of NO in the O₂ and CO₂ responsiveness of cerebral and ocular circulation in humans. *Am.J.Physiol.* 1997;273:R2005-R2012.
125. Parfenova H, Shibata M, Zuckerman S, Leffler CW. CO₂ and cerebral circulation in newborn pigs: Cyclic nucleotides and prostanoids in vascular regulation. *Am.J.Physiol.* 1994;266:H1494-501.

126. Najarian T, Marrache AM, Dumont I, et al. Prolonged hypercapnia-evoked cerebral hyperemia via K(+) channel- and prostaglandin E(2)-dependent endothelial nitric oxide synthase induction. *Circ.Res.* 2000;87:1149-1156.
127. Lavi S, Gaitini D, Milloul V, Jacob G. Impaired cerebral CO₂ vasoreactivity: Association with endothelial dysfunction. *Am.J.Physiol.Heart Circ.Physiol.* 2006;291:H1856-61.
128. Harris AP, Ohata H, Koehler RC. Role of nitric oxide in cerebrovascular reactivity to NMDA and hypercapnia during prenatal development in sheep. *Int.J.Dev.Neurosci.* 2008;26:47-55.
129. Rosenblum WI, Wei EP, Kontos HA. Dilation of rat brain arterioles by hypercapnia in vivo can occur even after blockade of guanylate cyclase by ODC. *Eur.J.Pharmacol.* 2002;448:201-206.
130. Sato E, Sakamoto T, Nagaoka T, Mori F, Takakusaki K, Yoshida A. Role of nitric oxide in regulation of retinal blood flow during hypercapnia in cats. *Invest.Ophthalmol.Vis.Sci.* 2003;44:4947-4953.
131. Izumi N, Nagaoka T, Sato E, et al. Role of nitric oxide in regulation of retinal blood flow in response to hyperoxia in cats. *Invest.Ophthalmol.Vis.Sci.* 2008;49:4595-4603.
132. Doganay S, Evereklioglu C, Turkoz Y, Er H. Decreased nitric oxide production in primary open-angle glaucoma. *Eur.J.Ophthalmol.* 2002;12:44-48.

133. Kosior-Jarecka E, Gerkowicz M, Latalaska M, Koziol-Montewka M, Szczepanik A. Nitric oxide level in aqueous humor in patients with glaucoma. *Klin.Oczna* 2004;106:158-159.
134. Colm O' Brien. Pulsatile ocular blood flow in normal pressure glaucoma. Pillunat L.E, Harris A, Anderson D.R and Greve E.L. *In Current concepts on ocular blood flow in glaucoma*. The Hague, The Netherlands: Kugler Publications; 1999. 111-117 pp.
135. Kotikoski H, Moilanen E, Vapaatalo H, Aine E. Biochemical markers of the L-arginine-nitric oxide pathway in the aqueous humour in glaucoma patients. *Acta Ophthalmol.Scand.* 2002;80:191-195.
136. Chang CJ, Chiang CH, Chow JC, Lu DW. Aqueous humor nitric oxide levels differ in patients with different types of glaucoma. *J.Ocul.Pharmacol.Ther.* 2000;16:399-406.
137. Loffler KU. Neovascular glaucoma: Aetiology, pathogenesis and treatment. *Ophthalmologe* 2006;103:1057-63; quiz 1064.
138. Konareva-Kostianeva M. Neovascular glaucoma. *Folia.Med.(Plovdiv)* 2005;47:5-11.
139. Gilmore ED, Hudson C, Nrusimhadevara RK, et al. Retinal arteriolar diameter, blood velocity, and blood flow response to an isocapnic hyperoxic provocation in early sight-threatening diabetic retinopathy. *Invest Ophthalmol Vis Sci.* 2007;48:1744-1750.
140. Gilmore ED, Hudson C, Nrusimhadevara RK, et al. Retinal arteriolar hemodynamic response to a combined isocapnic hyperoxia and glucose provocation in early sight-threatening diabetic retinopathy. *Invest.Ophthalmol.Vis.Sci.* 2008;49:699-705.

141. Riva CE, Titze P, Hero M, Movaffaghy A, Petrig BL. Choroidal blood flow during isometric exercises. *Invest.Ophthalmol.Vis.Sci.* 1997;38:2338-2343.
142. Kiss B, Dallinger S, Polak K, Findl O, Eichler HG, Schmetterer L. Ocular hemodynamics during isometric exercise. *Microvasc.Res.* 2001;61:1-13.
143. Garhofer G, Huemer KH, Zawinka C, Schmetterer L, Dorner GT. Influence of diffuse luminance flicker on choroidal and optic nerve head blood flow. *Curr.Eye Res.* 2002;24:109-113.
144. Schmeisser ET, Harrison JM, Sutter EE, Kiel J, Elliott WR, Sponsel WE. Modification of the heidelberg retinal flowmeter to record pattern and flicker induced blood flow changes. *Doc.Ophthalmol.* 2003;106:257-263.
145. Vo Van T, Riva CE. Variations of blood flow at optic nerve head induced by sinusoidal flicker stimulation in cats. *J.Physiol.* 1995;482 (Pt 1):189-202.
146. Hosking SL, Harris A, Chung HS, et al. Ocular haemodynamic responses to induced hypercapnia and hyperoxia in glaucoma. *Br.J.Ophthalmol.* 2004;88:406-411.
147. Sines D, Harris A, Siesky B, et al. The response of retrobulbar vasculature to hypercapnia in primary open-angle glaucoma and ocular hypertension. *Ophthalmic Res.* 2007;39:76-80.

148. Quaranta L, Manni G, Donato F, Bucci MG. The effect of increased intraocular pressure on pulsatile ocular blood flow in low tension glaucoma. *Surv.Ophthalmol.* 1994;38 Suppl:S177-81; discussion S182.
149. Harino S, Grunwald JE, Petrig BJ, Riva CE. Rebreathing into a bag increases human retinal macular blood velocity. *Br.J.Ophthalmol.* 1995;79:380-383.
150. Schmetterer L, Lexer F, Unfried C, Sattman H, Fercher AF. Topical measurement of fundus pulsations. *Opt Eng.* 1995;34:711-716.
151. Schmetterer L, Dallinger S, Findl O, et al. Non-invasive investigations of the normal ocular circulation in humans. *Invest.Ophthalmol.Vis.Sci.* 1998;39:1210-1220.
152. Fuchsjager-Mayrl G, Wally B, Georgopoulos M, et al. Ocular blood flow and systemic blood pressure in patients with primary open-angle glaucoma and ocular hypertension. *Invest.Ophthalmol.Vis.Sci.* 2004;45:834-839.
153. Polak K, Dorner G, Kiss B, et al. Evaluation of the zeiss retinal vessel analyser. *Br.J.Ophthalmol.* 2000;84:1285-1290.
154. Luksch A, Garhofer G, Imhof A, et al. Effect of inhalation of different mixtures of O(2) and CO(2) on retinal blood flow. *Br.J.Ophthalmol.* 2002;86:1143-1147.
155. Zinser G. Scanning laser doppler flowmetry: Principle and technique. Anonymous *In Current concepts on ocular blood flow in glaucoma.* The Hague, The Netherlands: Kugler Publications; 1999. 197-204 pp.

156. Michelson G, Schmauss B. Two dimensional mapping of the perfusion of the retina and optic nerve head. *Br.J.Ophthalmol.* 1995;79:1126-1132.
157. Nicoletta MT, Hnik P, Drance SM. Scanning laser doppler flowmeter study of retinal and optic disk blood flow in glaucomatous patients. *Am.J.Ophthalmol.* 1996;122:775-783.
158. Michelson G, Langhans MJ, Groh MJ. Perfusion of the juxtapapillary retina and the neuroretinal rim area in primary open angle glaucoma. *J.Glaucoma* 1996;5:91-98.
159. Hafez AS, Bizzarro RL, Lesk MR. Evaluation of optic nerve head and peripapillary retinal blood flow in glaucoma patients, ocular hypertensives, and normal subjects. *Am.J.Ophthalmol.* 2003;136:1022-1031.
160. Chauhan BC, Smith FM. Confocal scanning laser doppler flowmetry: Experiments in a model flow system. *J.Glaucoma* 1997;6:237-245.
161. Fekete GT, Yoshida A, Schepens CL. Laser based instruments for ocular blood flow assessment. *Journal of Biomedical Optics* 1998;3:415-422.
162. Venkataraman ST, Hudson C, Harvey E, Flanagan JG. Impact of simulated light scatter on scanning laser doppler flowmetry. *Br.J.Ophthalmol.* 2005;89:1192-1195.
163. Fekete GT, Goger DG, Tagawa H, Delori FC. Laser doppler technique for absolute measurement of blood speed in retinal vessels. *IEEE Trans.Biomed.Eng.* 1987;34:673-680.

164. Riva CE, Feke GT, Eberli B. Bidirectional LDV system for the absolute measurement of blood speed in retinal vessels. *Appl. Opt.* 1979;18:2301-2306.
165. Feke GT, Riva CE. Laser doppler measurements of blood velocity in human retinal vessels. *J. Opt. Soc. Am.* 1978;68:526-531.
166. Milbocker MT, Feke GT, Goger DG. Automated determination of centerline blood speed in retinal vessels from laser doppler spectra. Anonymous *In Non-invasive assessment of the visual system*. Washington D.C.: OSA Technical Digest Series, Optical Society of America; 1988. 162-165 pp.
167. Feke GT, Tagawa H, Deupree DM, Goger DG, Sebag J, Weiter JJ. Blood flow in the normal human retina. *Invest. Ophthalmol. Vis. Sci.* 1989;30:58-65.
168. Kida T, Harino S, Sugiyama T, Kitanishi K, Iwahashi Y, Ikeda T. Change in retinal arterial blood flow in the contralateral eye of retinal vein occlusion during glucose tolerance test. *Graefes Arch. Clin. Exp. Ophthalmol.* 2002;240:342-347.
169. Guan K, Hudson C, Flanagan JG. Variability and repeatability of retinal blood flow measurements using the canon laser blood flowmeter. *Microvasc. Res.* 2003;65:145-151.
170. Venkataraman ST, Hudson C, Fisher JA, Flanagan JG. Novel methodology to comprehensively assess retinal arteriolar vascular reactivity to hypercapnia. *Microvasc. Res.* 2006;72:101-107.

171. Azizi B, Buehler H, Venkataraman ST, Hudson C. Impact of simulated light scatter on the quantitative, noninvasive assessment of retinal arteriolar hemodynamics. *J.Biomed.Opt.* 2007;12:034021.
172. Kagemann L, Harris A, Kumar R, Rechtman E. Retina and optic nerve imaging. T. A. Ciulla, C. D. Regillo and A. Harris. *In New technologies for the assessment of retinal circulation.* 2003.
173. [Anonymous]. Canon inc. CLBF diameter reading system. *Personal Communication with Canon Medical Equipment Technical Services Department* (Feb. 6, 2005).
174. Jean-Louis S, Lovasik J, Kergoat H. Systemic hyperoxia and retinal vasomotor responses. *Invest.Ophthalmol.Vis.Sci.* 2005;46:1714-1720.
175. Rhoades RA. Respiratory physiology: Gas transfer and transport. Tanner GA Rhoades RA. *In Medical physiology.* Philadelphia: Lippincott Williams & Wilkins; 2003. 350-362 pp.
176. Rhoades RA. Ventilation and mechanics of breathing. Rhoades RA and Tanner GA. *In Medical Physiology.* Philadelphia: Lipincott Williams & Wilkins; 2003. 309-336 pp.
177. Ito S, Mardimae A, Han J, et al. Non-invasive prospective targeting of arterial P(CO₂) in subjects at rest. *J.Physiol.* 2008;586:3675-3682.

178. Hlastala MPB, A. Blood gas transport and tissue gas exchange. P. Hlastala and A. J. Berger. *In Physiology of Respiration*. New York: Oxford University Press; 2001. 96-113 pp.
179. Peebles K, Celi L, McGrattan K, Murrell C, Thomas K, Ainslie PN. Human cerebrovascular and ventilatory CO₂ reactivity to end-tidal, arterial and internal jugular vein PCO₂. *J. Physiol.* 2007;584:347-357.
180. Venkataraman ST, Hudson C, Fisher JA, Flanagan JG. The impact of hypercapnia on retinal capillary blood flow assessed by scanning laser doppler flowmetry. *Microvasc. Res.* 2005;69:149-155.
181. Pakola SJ, Grunwald JE. Effects of oxygen and carbon dioxide on human retinal circulation. *Invest. Ophthalmol. Vis. Sci.* 1993;34:2866-2870.
182. Chung HS, Harris A, Halter PJ, et al. Regional differences in retinal vascular reactivity. *Invest. Ophthalmol. Vis. Sci.* 1999;40:2448-2453.
183. Schmetterer L, Wolzt M, Lexer F, et al. The effect of hyperoxia and hypercapnia on fundus pulsations in the macular and optic disc region in healthy young men. *Exp. Eye Res.* 1995;61:685-690.
184. Kisilevsky M, Mardimae A, Slessarev M, Han J, Fisher J, Hudson C. Retinal arteriolar and middle cerebral artery responses to combined hypercarbic/hyperoxic stimuli. *Invest. Ophthalmol. Vis. Sci.* 2008;49:5503-5509.

185. Haefliger IO, Lietz A, Griesser SM, et al. Modulation of heidelberg retinal flowmeter parameter flow at the papilla of healthy subjects: Effect of carbogen, oxygen, high intraocular pressure, and beta-blockers. *Surv.Ophthalmol.* 1999;43 Suppl 1:S59-S65.
186. Tayyari F, Venkataraman ST, Wong T, Hudson C. The relationship between retinal vascular reactivity and arteriolar diameter. *Invest.Ophthalmol.Vis.Sci.* 2006;47:E-abstract 479.
187. Kergoat H, Faucher C. Effects of oxygen and carbogen breathing on choroidal hemodynamics in humans. *Invest.Ophthalmol.Vis.Sci.* 1999;40:2906-2911.
188. Lietz A, Hendrickson P, Flammer J, Orgül S, Haefliger IO. Effects of carbogen, oxygen and intraocular pressure on heidelberg retina flowmeter parameter 'flow' measured at the papilla. *Ophthalmologica* 1998;212:149-152.
189. Becker HF, Polo O, McNamara SG, Berthon-Jones M, Sullivan CE. Effect of different levels of hyperoxia on breathing in healthy subjects. *J.Appl.Physiol.* 1996;81:1683-1690.
190. Dean JB, Mulkey DK, Henderson RA, 3rd, Potter SJ, Putnam RW. Hyperoxia, reactive oxygen species, and hyperventilation: Oxygen sensitivity of brain stem neurons. *J.Appl.Physiol.* 2004;96:784-791.
191. Riva CE, Grunwald JE, Sinclair SH. Laser doppler velocimetry study of the effect of pure oxygen breathing on retinal blood flow. *Invest.Ophthalmol.Vis.Sci.* 1983;24:47-51.

192. Nattie E. CO₂, brainstem chemoreceptors and breathing. *Prog. Neurobiol.* 1999;59:299-331.
193. Harris A, Arend O, Wolf S, Cantor LB, Martin BJ. CO₂ dependence of retinal arterial and capillary blood velocity. *Acta Ophthalmol. Scand.* 1995;73:421-424.
194. Hosking SL, Evans DW, Embleton SJ, Houde B, Amos JF, Bartlett JD. Hypercapnia invokes an acute loss of contrast sensitivity in untreated glaucoma patients. *Br. J. Ophthalmol.* 2001;85:1352-1356.
195. Quigley HA, Broman AT. The number of people with glaucoma worldwide in 2010 and 2020. *Br. J. Ophthalmol.* 2006;90:262-267.
196. Buhrmann R, Hodge W, Gold D. Foundation for the canadian vision health strategy. Jan 2007:16.
197. Friedman DS, Wolfs RC, O'Colmain BJ, et al. Prevalence of open-angle glaucoma among adults in the united states. *Arch. Ophthalmol.* 2004;122:532-538.
198. Leske MC. Open-angle glaucoma -- an epidemiologic overview. *Ophthalmic Epidemiol.* 2007;14:166-172.
199. Rudnicka AR, Mt-Isa S, Owen CG, Cook DG, Ashby D. Variations in primary open-angle glaucoma prevalence by age, gender, and race: A bayesian meta-analysis. *Invest. Ophthalmol. Vis. Sci.* 2006;47:4254-4261.

200. Quigley HA, Enger C, Katz J, Sommer A, Scott R, Gilbert D. Risk factors for the development of glaucomatous visual field loss in ocular hypertension. *Arch.Ophthalmol.* 1994;112:644-649.
201. Lichter PR, Musch DC, Gillespie BW, et al. Interim clinical outcomes in the collaborative initial glaucoma treatment study comparing initial treatment randomized to medications or surgery. *Ophthalmology* 2001;108:1943-1953.
202. AGIS Investigators. The advanced glaucoma intervention study (AGIS): 12. baseline risk factors for sustained loss of visual field and visual acuity in patients with advanced glaucoma. *Am.J.Ophthalmol.* 2002;134:499-512.
203. Gordon MO, Beiser JA, Brandt JD, et al. The ocular hypertension treatment study: Baseline factors that predict the onset of primary open-angle glaucoma. *Arch.Ophthalmol.* 2002;120:714-20; discussion 829-30.
204. Leske MC, Nemesure B, He Q, Wu SY, Fielding Hejtmancik J, Hennis A. Patterns of open-angle glaucoma in the barbados family study. *Ophthalmology* 2001;108:1015-1022.
205. Mukesh BN, McCarty CA, Rait JL, Taylor HR. Five-year incidence of open-angle glaucoma: The visual impairment project. *Ophthalmology* 2002;109:1047-1051.
206. Kass MA, Heuer DK, Higginbotham EJ, et al. The ocular hypertension treatment study: A randomized trial determines that topical ocular hypotensive medication delays or

prevents the onset of primary open-angle glaucoma. *Arch.Ophthalmol.* 2002;120:701-13; discussion 829-30.

207.Higginbotham EJ, Gordon MO, Beiser JA, et al. The ocular hypertension treatment study: Topical medication delays or prevents primary open-angle glaucoma in african american individuals. *Arch.Ophthalmol.* 2004;122:813-820.

208.Asrani S, Zeimer R, Wilensky J, Gieser D, Vitale S, Lindenmuth K. Large diurnal fluctuations in intraocular pressure are an independent risk factor in patients with glaucoma. *J.Glaucoma* 2000;9:134-142.

209.Tielsch JM, Sommer A, Katz J, Royall RM, Quigley HA, Javitt J. Racial variations in the prevalence of primary open-angle glaucoma. the baltimore eye survey. *JAMA* 1991;266:369-374.

210.Wolfs RC, Klaver CC, Ramrattan RS, van Duijn CM, Hofman A, de Jong PT. Genetic risk of primary open-angle glaucoma. population-based familial aggregation study. *Arch.Ophthalmol.* 1998;116:1640-1645.

211.Leske MC, Heijl A, Hyman L, et al. Predictors of long-term progression in the early manifest glaucoma trial. *Ophthalmology* 2007;114:1965-1972.

212.Flammer J, Orgul S, Costa VP, et al. The impact of ocular blood flow in glaucoma. *Prog.Retin.Eye Res.* 2002;21:359-393.

213. Pache M, Flammer J. A sick eye in a sick body? systemic findings in patients with primary open-angle glaucoma. *Surv.Ophthalmol.* 2006;51:179-212.
214. Mitchell P, Smith W, Chey T, Healey PR. Open-angle glaucoma and diabetes: The blue mountains eye study, australia. *Ophthalmology* 1997;104:712-718.
215. Klein BE, Klein R, Jensen SC. Open-angle glaucoma and older-onset diabetes. the beaver dam eye study. *Ophthalmology* 1994;101:1173-1177.
216. Leibowitz HM, Krueger DE, Maunder LR. The framingham eye study monograph. *Surv of Ophthalmol.* 1980;24 (suppl):335-610.
217. Wang JJ, Mitchell P, Smith W. Is there an association between migraine headache and open-angle glaucoma? findings from the blue mountains eye study. *Ophthalmology* 1997;104:1714-1719.
218. Chauhan BC, Mikelberg FS, Balaszi AG, et al. Canadian glaucoma study: 2. risk factors for the progression of open-angle glaucoma. *Arch.Ophthalmol.* 2008;126:1030-1036.
219. Flanagan JG. Glaucoma update: Epidemiology and new approaches to medical management. *Ophthalmic Physiol.Opt.* 1998;18:126-132.
220. Neufeld AH, Liu B. Glaucomatous optic neuropathy: When glia misbehave. *Neuroscientist* 2003;9:485-495.
221. Alvarado J, Murphy C, Juster R. Trabecular meshwork cellularity in primary open-angle glaucoma and nonglaucomatous normals. *Ophthalmology* 1984;91:564-579.

222. Floyd BB, Cleveland PH, Worthen DM. Fibronectin in human trabecular drainage channels. *Invest.Ophthalmol.Vis.Sci.* 1985;26:797-804.
223. Lutjen-Drecoll E, Rittig M, Rauterberg J, Jander R, Mollenhauer J. Immunomicroscopical study of type VI collagen in the trabecular meshwork of normal and glaucomatous eyes. *Exp.Eye Res.* 1989;48:139-147.
224. de Kater AW, Melamed S, Epstein DL. Patterns of aqueous humor outflow in glaucomatous and nonglaucomatous human eyes. A tracer study using cationized ferritin. *Arch.Ophthalmol.* 1989;107:572-576.
225. Quigley HA, Addicks EM. Scanning electron microscopy of trabeculectomy specimens from eyes with open-angle glaucoma. *Am.J.Ophthalmol.* 1980;90:854-857.
226. Tripathi RC. Mechanism of the aqueous outflow across the trabecular wall of schlemm's canal. *Exp.Eye Res.* 1971;11:116-121.
227. Tripathi RC, Li J, Chan WF, Tripathi BJ. Aqueous humor in glaucomatous eyes contains an increased level of TGF-beta 2. *Exp.Eye Res.* 1994;59:723-727.
228. Sigal IA, Flanagan JG, Tertinegg I, Ethier CR. Predicted extension, compression and shearing of optic nerve head tissues. *Exp.Eye Res.* 2007;85:312-322.
229. Sigal IA, Flanagan JG, Ethier CR. Factors influencing optic nerve head biomechanics. *Invest.Ophthalmol.Vis.Sci.* 2005;46:4189-4199.

230. Sigal IA, Flanagan JG, Tertinegg I, Ethier CR. Modeling individual-specific human optic nerve head biomechanics. part I: IOP-induced deformations and influence of geometry. *Biomech. Model. Mechanobiol* 2008.
231. Lewis TL, Chronister CL. Etiology and pathophysiology of primary open - angle glaucoma. M. Fingeret and T. L. Lewis. *In Primary Care of the Glaucomas*. New York: McGraw Hill; 2001. 63-80 pp.
232. Grieshaber MC, Terhorst T, Flammer J. The pathogenesis of optic disc splinter haemorrhages: A new hypothesis. *Acta Ophthalmol. Scand.* 2006;84:62-68.
233. Plange N, Kaup M, Weber A, Arend KO, Remky A. Retrobulbar haemodynamics and morphometric optic disc analysis in primary open-angle glaucoma. *Br.J.Ophthalmol.* 2006;90:1501-1504.
234. Kaiser HJ, Schoetzau A, Stumpfig D, Flammer J. Blood-flow velocities of the extraocular vessels in patients with high-tension and normal-tension primary open-angle glaucoma. *Am.J.Ophthalmol.* 1997;123:320-327.
235. Gottanka J, Kuhlmann A, Scholz M, Johnson DH, Lutjen-Drecoll E. Pathophysiologic changes in the optic nerves of eyes with primary open angle and pseudoexfoliation glaucoma. *Invest.Ophthalmol. Vis.Sci.* 2005;46:4170-4181.
236. Kornzweig AL, Eliasoph I, Feldstein M. Selective atrophy of the radial peripapillary capillaries in chronic glaucoma. *Arch.Ophthalmol.* 1968;80:696-702.

237. Tezel G, Kass MA, Kolker AE, Wax MB. Comparative optic disc analysis in normal pressure glaucoma, primary open-angle glaucoma, and ocular hypertension. *Ophthalmology* 1996;103:2105-2113.
238. Daicker B. Selective atrophy of the radial peripapillary capillaries of the retina and glaucomatous visual fields. *Ophthalmologica* 1976;172:138.
239. Michelson G, Langhans MJ, Harazny J, Dichtl A. Visual field defect and perfusion of the juxtapapillary retina and the neuroretinal rim area in primary open-angle glaucoma. *Graefes Arch.Clin.Exp.Ophthalmol.* 1998;236:80-85.
240. Epstein DL. The patient's history; symptoms of glaucoma. D. L. Epstein, R. R. Allingham and J. S. Schuman. *In Chandler and Grant's Glaucoma*. Baltimore: Williams & Wilkins; 1997. 25-32 pp.
241. Gupta D. Patient history. Anonymous *In Glaucoma Diagnosis and Management*. Philadelphia: Lippincott Williams & Wilkins; 2004. 44-46 pp.
242. Fingeret M. Medical management of glaucoma. M. Fingeret and T. L. Lewis. *In Primary Care of the Glaucomas*. New York: McGraw Hill; 2001. 333-363 pp.
243. Brubaker RF, Liesegang TJ. Effect of trabecular photocoagulation on the aqueous humor dynamics of the human eye. *Am.J.Ophthalmol.* 1983;96:139-147.

244. Werner EB. Treatment and management: Laser procedures in the therapy of glaucoma. M. Fingeret and T. L. Lewis. *In Primary Care of the Glaucomas*. New York: McGraw Hill; 2001. 365-372 pp.
245. Gupta D. Surgical management of glaucoma. Anonymous *In Glaucoma Diagnosis and Management*. Philadelphia, PA: Lipincott Williams & Wilkins; 2004. 255-266 pp.
246. Orgul S, Mansberger S, Bacon DR, Van Buskirk EM, Cioffi GA. Optic nerve vasomotor effects of topical beta-adrenergic antagonists in rabbits. *Am.J.Ophthalmol.* 1995;120:441-447.
247. Jay WM, Aziz MZ, Green K. Effect of topical epinephrine and timolol on ocular and optic nerve blood flow in phakic and aphakic rabbit eyes. *Curr.Eye Res.* 1984;3:1199-1202.
248. Millar JC, Wilson WS, Carr RD, Humphries RG. Drug effects on intraocular pressure and vascular flow in the bovine perfused eye using radiolabelled microspheres. *J.Ocul.Pharmacol.Ther.* 1995;11:11-23.
249. Nicolela MT, Buckley AR, Walman BE, Drance SM. A comparative study of the effects of timolol and latanoprost on blood flow velocity of the retrobulbar vessels. *Am.J.Ophthalmol.* 1996;122:784-789.
250. Nicolela MT, Walman BE, Buckley AR, Drance SM. Ocular hypertension and primary open-angle glaucoma: A comparative study of their retrobulbar blood flow velocity. *J.Glaucoma* 1996;5:308-310.

251. Lubeck P, Orgul S, Gugleta K, Gherghel D, Gekkieva M, Flammer J. Effect of timolol on anterior optic nerve blood flow in patients with primary open-angle glaucoma as assessed by the heidelberg retina flowmeter. *J.Glaucoma* 2001;10:13-17.
252. Harris A, Spaeth GL, Sergott RC, Katz LJ, Cantor LB, Martin BJ. Retrobulbar arterial hemodynamic effects of betaxolol and timolol in normal-tension glaucoma. *Am.J.Ophthalmol.* 1995;120:168-175.
253. Fuchsjäger-Mayrl G, Wally B, Rainer G, et al. Effect of dorzolamide and timolol on ocular blood flow in patients with primary open angle glaucoma and ocular hypertension. *Br.J.Ophthalmol.* 2005;89:1293-1297.
254. Carenini AB, Sibour G, Boles Carenini B. Differences in the longterm effect of timolol and betaxolol on the pulsatile ocular blood flow. *Surv.Ophthalmol.* 1994;38 Suppl:S118-24.
255. Altan-Yaycioglu R, Turker G, Akdol S, Acunas G, Izgi B. The effects of beta-blockers on ocular blood flow in patients with primary open angle glaucoma: A color doppler imaging study. *Eur.J.Ophthalmol.* 2001;11:37-46.
256. Morsman CD, Bosem ME, Lusky M, Weinreb RN. The effect of topical beta-adrenoceptor blocking agents on pulsatile ocular blood flow. *Eye* 1995;9 (Pt 3):344-347.
257. Bosem ME, Lusky M, Weinreb RN. Short-term effects of levobunolol on ocular pulsatile flow. *Am.J.Ophthalmol.* 1992;114:280-286.

258. Schmetterer L, Strenn K, Findl O, et al. Effects of antiglaucoma drugs on ocular hemodynamics in healthy volunteers. *Clin.Pharmacol.Ther.* 1997;61:583-595.
259. Claridge KG. The effect of topical pilocarpine on pulsatile ocular blood flow. *Eye* 1993;7:507-510.
260. Weigert G, Resch H, Luksch A, et al. Intravenous administration of clonidine reduces intraocular pressure and alters ocular blood flow. *Br.J.Ophthalmol.* 2007;91:1354-1358.
261. Avunduk AM, Sari A, Akyol N, et al. The one-month effects of topical betaxolol, dorzolamide and apraclonidine on ocular blood flow velocities in patients with newly diagnosed primary open-angle glaucoma. *Ophthalmologica* 2001;215:361-365.
262. Costagliola C, Parmeggiani F, Ciancaglini M, D'Oronzo E, Mastropasqua L, Sebastiani A. Ocular perfusion pressure and visual field indice modifications induced by alpha-agonist compound (clonidine 0.125%, apraclonidine 1.0% and brimonidine 0.2%) topical administration. an acute study on primary open-angle glaucoma patients. *Ophthalmologica* 2003;217:39-44.
263. Jonescu-Cuypers CP, Harris A, Ishii Y, et al. Effect of brimonidine tartrate on ocular hemodynamics in healthy volunteers. *J Ocul Pharmacol Ther* 2001;17:199-205.
264. Sponsel WE, Paris G, Trigo Y, et al. Latanoprost and brimonidine: Therapeutic and physiologic assessment before and after oral nonsteroidal anti-inflammatory therapy. *Am.J.Ophthalmol.* 2002;133:11-18.

265. Simsek T, Yanik B, Conkbayir I, Zilelioglu O. Comparative analysis of the effects of brimonidine and dorzolamide on ocular blood flow velocity in patients with newly diagnosed primary open-angle glaucoma. *J.Ocul.Pharmacol.Ther.* 2006;22:79-85.
266. Sampaolesi J, Tosi J, Darchuk V, Ucha RA, Marengo J, Sampaolesi R. Antiglaucomatous drugs effects on optic nerve head flow: Design, baseline and preliminary report. *Int.Ophthalmol.* 2001;23:359-367.
267. Nicolela MT, Walman BE, Buckley AR, Drance SM. Ocular hypertension and primary open-angle glaucoma: A comparative study of their retrobulbar blood flow velocity. *J.Glaucoma* 1996;5:308-310.
268. Liu CJ, Ko YC, Cheng CY, Chou JC, Hsu WM, Liu JH. Effect of latanoprost 0.005% and brimonidine tartrate 0.2% on pulsatile ocular blood flow in normal tension glaucoma. *Br.J.Ophthalmol.* 2002;86:1236-1239.
269. Arend O, Harris A, Wolter P, Remky A. Evaluation of retinal haemodynamics and retinal function after application of dorzolamide, timolol and latanoprost in newly diagnosed open-angle glaucoma patients. *Acta Ophthalmol.Scand.* 2003;81:474-479.
270. Siesky B, Harris A, Sines D, et al. A comparative analysis of the effects of the fixed combination of timolol and dorzolamide versus latanoprost plus timolol on ocular hemodynamics and visual function in patients with primary open-angle glaucoma. *J.Ocul.Pharmacol.Ther.* 2006;22:353-361.

271. Vetrugno M, Cantatore F, Gigante G, Cardia L. Latanoprost 0.005% in POAG: Effects on IOP and ocular blood flow. *Acta Ophthalmol.Scand.Suppl.* 1998;(227):40-1.
272. Gherghel D, Hosking SL, Cunliffe IA, Armstrong RA. First-line therapy with latanoprost 0.005% results in improved ocular circulation in newly diagnosed primary open-angle glaucoma patients: A prospective, 6-month, open-label study. *Eye* 2006;.22(3):363-369.
273. Martinez A, Sanchez M. Retrobulbar haemodynamic effects of the latanoprost/timolol and the dorzolamide/timolol fixed combinations in newly diagnosed glaucoma patients. *Int.J.Clin.Pract.* 2007;61:815-825.
274. Dallinger S, Bobr B, Findl O, Eichler HG, Schmetterer L. Effects of acetazolamide on choroidal blood flow. *Stroke* 1998;29:997-1001.
275. Kiss B, Dallinger S, Findl O, Rainer G, Eichler HG, Schmetterer L. Acetazolamide-induced cerebral and ocular vasodilation in humans is independent of nitric oxide. *Am.J.Physiol.* 1999;276:R1661-7.
276. Faingold D, Hudson C, Flanagan J, et al. Assessment of retinal hemodynamics with the canon laser blood flowmeter after a single dose of 2% dorzolamide hydrochloride eyedrops. *Can.J.Ophthalmol.* 2004;39:506-510.
277. Pillunat LE, Bohm AG, Koller AU, Schmidt KG, Klemm M, Richard G. Effect of topical dorzolamide on optic nerve head blood flow. *Graefes Arch.Clin.Exp.Ophthalmol.* 1999;237:495-500.

278. Schmidt KG, Dick B, von Ruckmann A, Pillunat LE. Ocular pulse amplitude and local carbonic anhydrase inhibition. *Ophthalmologie* 1997;94:659-664.
279. Galassi F, Sodi A, Renieri G, et al. Effects of timolol and dorzolamide on retrobulbar hemodynamics in patients with newly diagnosed primary open-angle glaucoma. *Ophthalmologica* 2002;216:123-128.
280. Harris A, Arend O, Chung HS, Kagemann L, Cantor L, Martin B. A comparative study of betaxolol and dorzolamide effect on ocular circulation in normal-tension glaucoma patients. *Ophthalmology* 2000;107:430-434.
281. Harris A, Jonescu-Cuypers CP, Kagemann L, et al. Effect of dorzolamide timolol combination versus timolol 0.5% on ocular bloodflow in patients with primary open-angle glaucoma. *Am.J.Ophthalmol.* 2001;132:490-495.
282. Rolle T, Tofani F, Brogliatti B, Grignolo FM. The effects of dorzolamide 2% and dorzolamide/timolol fixed combination on retinal and optic nerve head blood flow in primary open-angle glaucoma patients. *Eye* 2008;22(9):1172-9.
283. Bergstrand IC, Heijl A, Harris A. Dorzolamide and ocular blood flow in previously untreated glaucoma patients: A controlled double-masked study. *Acta Ophthalmol.Scand.* 2002;80:176-182.
284. Sponsel WE. Topical carbonic anhydrase inhibitors and visual function. L. E. Pillunat, A. Harris, D. R. Anderson and E. L. Greve. *In Current concepts on ocular blood flow in glaucoma.* The Hague, The Netherlands: Kugler Publications; 1999. 251-265 pp.

285. Pedersen DB, Koch Jensen P, la Cour M, et al. Carbonic anhydrase inhibition increases retinal oxygen tension and dilates retinal vessels. *Graefes Arch.Clin.Exp.Ophthalmol.* 2005;243:163-168.
286. Kaup M, Plange N, Niegel M, Remky A, Arend O. Effects of brinzolamide on ocular haemodynamics in healthy volunteers. *Br.J.Ophthalmol.* 2004;88:257-262.
287. Yorio T, Krishnamoorthy R, Prasanna G. Endothelin: Is it a contributor to glaucoma pathophysiology? *J.Glaucoma* 2002;11:259-270.
288. Harris A, Kagemann L, Ehrlich R, Rospigliosi C, Moore D, Siesky B. Measuring and interpreting ocular blood flow and metabolism in glaucoma. *Can.J.Ophthalmol.* 2008;43:328-336.
289. Bjarnhall G, Tomic L, Mishima HK, Tsukamoto H, Alm A. Retinal mean transit time in patients with primary open-angle glaucoma and normal-tension glaucoma. *Acta Ophthalmol.Scand.* 2007;85:67-72.
290. Agarwal HC, Gupta V, Sihota R, Singh K. Pulsatile ocular blood flow among normal subjects and patients with high tension glaucoma. *Indian J.Ophthalmol.* 2003;51:133-138.
291. Kerr J, Nelson P, O'Brien C. A comparison of ocular blood flow in untreated primary open-angle glaucoma and ocular hypertension. *Am.J.Ophthalmol.* 1998;126:42-51.

292. Fontana L, Poinoosawmy D, Bunce CV, O'Brien C, Hitchings RA. Pulsatile ocular blood flow investigation in asymmetric normal tension glaucoma and normal subjects. *Br.J.Ophthalmol.* 1998;82:731-736.
293. James CB, Smith SE. Pulsatile ocular blood flow in patients with low tension glaucoma. *Br.J.Ophthalmol.* 1991;75:466-470.
294. Schmidt KG, Ruckmann AV, Mittag TW, Hessemer V, Pillunat LE. Reduced ocular pulse amplitude in low tension glaucoma is independent of vasospasm. *Eye* 1997;11 (Pt 4):485-488.
295. Findl O, Rainer G, Dallinger S, et al. Assessment of optic disk blood flow in patients with open-angle glaucoma. *Am.J.Ophthalmol.* 2000;130:589-596.
296. Bohdanecka Z, Orgul S, Meyer AB, Prunte C, Flammer J. Relationship between blood flow velocities in retrobulbar vessels and laser doppler flowmetry at the optic disk in glaucoma patients. *Ophthalmologica* 1999;213:145-149.
297. Logan JF, Rankin SJ, Jackson AJ. Retinal blood flow measurements and neuroretinal rim damage in glaucoma. *Br.J.Ophthalmol.* 2004;88:1049-1054.
298. Piltz-seymour JR, Grunwald JE, Hariprasad SM, Dupont J. Optic nerve blood flow is diminished in eyes of primary open-angle glaucoma suspects. *Am.J.Ophthalmol.* 2001;132:63-69.
299. Boehm AG, Pillunat LE, Koeller U, et al. Regional distribution of optic nerve head blood flow. *Graefes Arch.Clin.Exp.Ophthalmol.* 1999;237:484-488.

- 300.Sato EA, Ohtake Y, Shinoda K, Mashima Y, Kimura I. Decreased blood flow at neuroretinal rim of optic nerve head corresponds with visual field deficit in eyes with normal tension glaucoma. *Graefes Arch.Clin.Exp.Ophthalmol.* 2006;244:795-801.
- 301.Plange N, Kaup M, Arend O, Remky A. Asymmetric visual field loss and retrobulbar haemodynamics in primary open-angle glaucoma. *Graefes Arch.Clin.Exp.Ophthalmol.* 2006;244:978-983.
- 302.Birinci H, Danaci M, Oge I, Erkan ND. Ocular blood flow in healthy and primary open-angle glaucomatous eyes. *Ophthalmologica* 2002;216:434-437.
- 303.Butt Z, O'Brien C, McKillop G, Aspinall P, Allan P. Color doppler imaging in untreated high- and normal-pressure open-angle glaucoma. *Invest.Ophthalmol.Vis.Sci.* 1997;38:690-696.
- 304.Kaiser HJ, Schoetzau A, Stumpfig D, Flammer J. Blood-flow velocities of the extraocular vessels in patients with high-tension and normal-tension primary open-angle glaucoma. *Am.J.Ophthalmol.* 1997;123:320-327.
- 305.Galassi F, Nuzzaci G, Sodi A, Casi P, Vielmo A. Color doppler imaging in evaluation of optic nerve blood supply in normal and glaucomatous subjects. *Int.Ophthalmol.* 1992;16:273-276.
- 306.Huber KK, Plange N, Arend O, Remky A. Colour doppler imaging in normal pressure glaucoma patients. *Klin.Monatsbl.Augenheilkd.* 2006;223:156-160.

307. Harris A, Sergott RC, Spaeth GL, Katz JL, Shoemaker JA, Martin BJ. Color doppler analysis of ocular vessel blood velocity in normal-tension glaucoma. *Am.J.Ophthalmol.* 1994;118:642-649.
308. Galassi F, Sodi A, Ucci F, Renieri G, Pieri B, Masini E. Ocular haemodynamics and nitric oxide in normal pressure glaucoma. *Acta Ophthalmol.Scand.Suppl.* 2000;(232):37-38.
309. Butt Z, McKillop G, O'Brien C, Allan P, Aspinall P. Measurement of ocular blood flow velocity using colour doppler imaging in low tension glaucoma. *Eye* 1995;9 (Pt 1):29-33.
310. Zeitz O, Galambos P, Wagenfeld L, et al. Glaucoma progression is associated with decreased blood flow velocities in the short posterior ciliary artery. *Br.J.Ophthalmol.* 2006;90:1245-1248.
311. Yamazaki Y, Drance SM. The relationship between progression of visual field defects and retrobulbar circulation in patients with glaucoma. *Am.J.Ophthalmol.* 1997;124:287-295.
312. Martinez A, Sanchez M. A comparison of the effects of 0.005% latanoprost and fixed combination dorzolamide/timolol on retrobulbar haemodynamics in previously untreated glaucoma patients. *Curr Med Res Opin.* 2006;22:67-73.

313. Siesky B, Harris A, Cantor LB, et al. A comparative study of the effects of brinzolamide and dorzolamide on retinal oxygen saturation and ocular microcirculation in patients with primary open-angle glaucoma. *Br.J.Ophthalmol.* 2008;92:500-504.
314. Costa VP, Harris A, Stefansson E, et al. The effects of antiglaucoma and systemic medications on ocular blood flow. *Prog.Retin.Eye Res.* 2003;22:769-805.
315. Stewart WC, Holmes KT, Johnson MA. Washout periods for brimonidine 0.2% and latanoprost 0.005%. *Am.J.Ophthalmol.* 2001;131:798-799.
316. Lesk MR, Wajszilber M, Deschenes MC. The effects of systemic medications on ocular blood flow. *Can.J.Ophthalmol.* 2008;43:351-355.
317. Sampaolesi J, Tosi J, Darchuk V, Ucha RA, Marengo J, Sampaolesi R. Antiglucomatous drugs effects on optic nerve head flow: Design, baseline and preliminary report. *Int.Ophthalmol.* 2001;23:359-367.
318. Eichenberger D, Hendrickson P, Robert Y, Gloor B. Influence of ocular media on perimetric results. *Doc Ophthalmol Proc.Ser* 1987;49:9-11.
319. Johnson PC. Autoregulation of blood flow. *Circ.Res.* 1986;59:483-495.
320. Weigert G, Findl O, Luksch A, et al. Effects of moderate changes in intraocular pressure on ocular hemodynamics in patients with primary open-angle glaucoma and healthy controls. *Ophthalmology* 2005;112:1337-1342.

321. Grunwald JE, Riva CE, Stone RA, Keates EU, Petrig BL. Retinal autoregulation in open-angle glaucoma. *Ophthalmology* 1984;91:1690-1694.
322. Nagel E, Vilser W, Lanzl IM. Retinal vessel reaction to short-term IOP elevation in ocular hypertensive and glaucoma patients. *Eur.J.Ophthalmol.* 2001;11:338-344.
323. Roff EJ, Harris A, Chung HS, et al. Comprehensive assessment of retinal, choroidal and retrobulbar haemodynamics during blood gas perturbation. *Graefes Arch.Clin.Exp.Ophthalmol.* 1999;237:984-990.
324. Harris A, Zarfati D, Zalish M, et al. Reduced cerebrovascular blood flow velocities and vasoreactivity in open-angle glaucoma. *Am.J.Ophthalmol.* 2003;135:144-147.
325. Gilmore ED, Hudson C, Venkataraman ST, Preiss D, Fisher J. Comparison of different hyperoxic paradigms to induce vasoconstriction: Implications for the investigation of retinal vascular reactivity. *Invest.Ophthalmol.Vis.Sci.* 2004;45:3207-3212.
326. Riva CE, Falsini B, Logean E. Flicker-evoked responses of human optic nerve head blood flow: Luminance versus chromatic modulation. *Invest.Ophthalmol.Vis.Sci.* 2001;42:756-762.
327. Garhofer G, Resch H, Weigert G, Lung S, Simader C, Schmetterer L. Short-term increase of intraocular pressure does not alter the response of retinal and optic nerve head blood flow to flicker stimulation. *Invest.Ophthalmol.Vis.Sci.* 2005;46:1721-1725.

328. Bek T, Hajari J, Jeppesen P. Interaction between flicker-induced vasodilatation and pressure autoregulation in early retinopathy of type 2 diabetes. *Graefes Arch.Clin.Exp.Ophthalmol.* 2008;246:763-769.
329. Rosengarten B, Huwendiek O, Kaps M. Neurovascular coupling and cerebral autoregulation can be described in terms of a control system. *Ultrasound Med.Biol.* 2001;27:189-193.
330. Iadecola C. Regulation of the cerebral microcirculation during neural activity: Is nitric oxide the missing link? *Trends Neurosci.* 1993;16:206-214.
331. Delles C, Michelson G, Harazny J, Oehmer S, Hilgers KF, Schmieder RE. Impaired endothelial function of the retinal vasculature in hypertensive patients. *Stroke* 2004;35:1289-1293.
332. Riva CE, Petrig BL, Falsini B, Logean E. *Neurovascular coupling at the optic nerve head studied by laser doppler flowmetry.* Washington D.C: Optical Society of America; 2000. 64-76 pp.
333. Clark CV, Mapstone R. Systemic autonomic neuropathy in open-angle glaucoma. *Doc.Ophthalmol.* 1986;64:179-185.
334. Kumar R, Ahuja VM. A study of changes in the status of autonomic nervous system in primary open angle glaucoma cases. *Indian J.Med.Sci.* 1999;53:529-534.

335. Brown CM, Dutsch M, Michelson G, Neundorfer B, Hilz MJ. Impaired cardiovascular responses to baroreflex stimulation in open-angle and normal-pressure glaucoma. *Clin.Sci.(Lond)* 2002;102:623-630.
336. Gherghel D, Hosking SL, Cunliffe IA. Abnormal systemic and ocular vascular response to temperature provocation in primary open-angle glaucoma patients: A case for autonomic failure? *Invest.Ophthalmol.Vis.Sci.* 2004;45:3546-3554.
337. Hafez AS, Bizzarro R, Descovich D, Lesk MR. Correlation between finger blood flow and changes in optic nerve head blood flow following therapeutic intraocular pressure reduction. *J.Glaucoma* 2005;14:448-454.

2 Rationale

Vascular dysregulation is suggested to be involved in the pathogenesis of GON, in addition to increased IOP. Previous studies have shown a decrease in homeostatic blood flow in both retinal and ONH vasculature in patients with POAG. However, there is paucity of information on the response of ocular blood vessels to provocations that assess vascular reactivity. The ultimate aim of this thesis was to determine the magnitude of retinal and ONH vascular reactivity in patients with untreated POAG (uPOAG). In addition, the thesis also aimed to establish the relationship between functional vascular reactivity and biochemical markers of endothelial function in POAG. There were a number of steps and considerations that required careful evaluation and validation in achieving these ultimate aims:

2.1 Development of a safe, sustained and stable normoxic/isoxic hypercapnic provocation

Increase in inspired carbon dioxide (CO₂), which results in hypercapnia, is an appealing provocation to employ in patients with POAG in order to avoid vasoconstriction in what is often considered to be a vasospastic disease. In particular, only a few studies have used hypercapnia to assess retinal vascular reactivity, partly because of obvious safety concerns in terms of administration of increased amounts of CO₂ in human volunteers. Some of these studies have shown a decreased magnitude of vascular reactivity in retinal vessels in patients with POAG. However, most have failed to use standardised hypercapnic stimuli to assess retinal vascular reactivity. The majority of the studies have used a non re-breathing circuit to induce hypercapnia by the manual addition of CO₂ to the inspired gases. Hypercapnia

induces hyperventilation which, in turn, alters arterial oxygen (O_2) concentration, and the magnitude of this change varies between individuals resulting in a non-standardised provocation. The maintenance of normoxia / isoxia during hypercapnic provocation is important for the assessment of vascular reactivity in order to avoid confounding effects of O_2 induced vasoconstriction. The use of a non-rebreathing valve system to induce hypercapnia by manual addition of CO_2 to inspired air (known as the dynamic end-tidal forcing, DEF technique) has been shown to only raise $PETCO_2$ to the target level; however, using this technique there is a large difference between the $PETCO_2$ and the arterial concentration of CO_2 ($PaCO_2$). The sequential rebreathing circuit by the use of a rebreathing valve has been shown to avoid this problem and thereby closely matches both $PETCO_2$ and $PaCO_2$ values. In this thesis, a sequential rebreathing circuit and an automated gas flow controller (RespirAct™, Thornhill Research Inc., Toronto Canada) were used to independently alter $PETCO_2$ and stabilize $PETO_2$ and to induce normoxic/isoxic hypercapnia in patients with POAG. The development of a sustained and stable normoxic hypercapnic stimulus was essential for safety reasons.

2.2 Quantitative assessment of retinal hemodynamics

Various blood flow assessment techniques have been used in an attempt to quantify retinal hemodynamics. However, the majority of instruments that have been used to-date were not able to truly assess retinal blood flow in absolute units. Typically, these instruments would assess a component of retinal hemodynamics that was then assumed to reflect change in retinal blood flow. The Canon Laser Blood Flowmeter (CLBF, model 100, Canon, Tokyo, Japan) is the only instrument that quantifies retinal blood flow in absolute units. The CLBF

simultaneously measures diameter and blood velocity at a single point along a major retinal vessel. In this respect, the CLBF measurement is not continuous but rather is limited to a 2 second window. For this reason, we were aware from the infancy of this work of the need to develop a sustained and stable normoxic / isoxic hypercapnic provocation to induce retinal vascular reactivity so that repeated hemodynamic measurements could be obtained. Similar consideration was given to the Heidelberg Retina Flowmeter (HRF, Heidelberg Engineering GmbH, Heidelberg, Germany) which was used in this work to assess the impact of normoxic / isoxic hypercapnia on retinal capillary and ONH vascular reactivity. The HRF has a relatively high measurement variability which demands repeated measurements over a sustained period of time in order to attain a valid estimate of the hemodynamic parameter value.

2.3 Evaluation, validation and repeatability

Chapters 3, 4 and 5 of this thesis focus on the development of a safe, sustained and stable normoxic / isoxic hypercapnic stimulus and define the physiological response of the retinal and ONH vasculature to the provocation. The objective of Chapter 3 was to develop a safe, sustained and stable hypercapnic stimulus to assess retinal capillary and ONH vascular reactivity using the HRF. Accordingly, the manual addition of CO₂ to inspired air was delivered via a sequential rebreathing circuit to induce hypercapnia. This stimulus was tested in young clinically healthy individuals. The hypothesis was that retinal and ONH capillary blood flow would increase during hypercapnia. Although the hypercapnic stimulus arguably resulted in a physiologically insignificant change, there was still an increase in PETO₂ during hypercapnia.

In order to minimize the change in $PETO_2$, the objective of Chapter 4 was to utilize the sequential rebreathing circuit to induce normoxic / isoxic hypercapnia by +15% $PETCO_2$ relative to baseline and to assess retinal arteriolar vascular reactivity using the CLBF in young healthy controls. The rate of flow of inspired air was simply decreased until subjects began to partially rebreathe expired air from the rebreathed gas reservoir, thereby elevating $PETCO_2$ in a controlled manner. The requirement for a safe, sustained and stable hypercapnic stimulus was maintained. The hypothesis was that arteriolar diameter, blood velocity and blood flow would increase during normoxic / isoxic hypercapnia. The partial rebreathe technique resulted in an improved control of $PETO_2$ during hypercapnia but nevertheless there was still a statistically significant decrease in the magnitude of $PETO_2$.

The results of Chapters 3 and 4 catalysed the development of an automated gas flow controller (RespirAct™, Thornhill Research Inc., Toronto Canada) which was used in conjunction with the sequential rebreathing circuit. Using this system, $PETCO_2$ and $PETO_2$ can be independently controlled and set values are robust to changes in respiration rate and tidal volume. The objective of Chapter 5 was to assess retinal arteriolar and retinal capillary and ONH vascular reactivity in response to a normoxic / isoxic hypercapnic provocation induced using the automated gas flow controller and sequential rebreathing circuit in young healthy controls. The hypothesis was that the magnitude of vascular reactivity would be equivalent in percentage terms in the retinal arterioles and the downstream capillaries since the retinal circulation is a closed system. This technique resulted in much improved and better $PETO_2$ control during hypercapnia but nevertheless a statistically significant increase was still recorded. Since the change in $PETO_2$ was now minimal, the term normoxic

hypercapnia (i.e. change that did not have any measureable physiological impact) was adopted for all future descriptions of the provocation rather than isoxic hypercapnia (i.e. unchanged). The normoxic hypercapnic provocation was demonstrated to be repeatable.

2.4 Judicious selection of glaucoma patients to investigate vascular reactivity

The objective of Chapter 6 was to apply the evaluated and validated normoxic hypercapnic stimulus in patients with POAG. The majority of previous studies have assessed retinal hemodynamics in patients with POAG who were receiving at least one IOP lowering medication and often multiple medications, or who had undergone an insufficient wash-out period prior to assessment. As a result, we set out to investigate retinal arteriolar and ONH vascular reactivity to normoxic hypercapnia in newly diagnosed untreated POAG (uPOAG) and in healthy controls. Patients with uPOAG were recruited in order to exclude the potential confounding effects of IOP lowering medications on the assessment of retinal vascular reactivity. Patients with progressive POAG (pPOAG) and who were receiving treatment were also assessed since they are thought to most likely manifest vascular dysregulation. The hypothesis was that patients with uPOAG and pPOAG would manifest a reduced magnitude of retinal arteriolar and ONH vascular reactivity compared to healthy controls.

Previous studies have also investigated any possible beneficial effects of certain IOP lowering medications on ocular blood flow. In particular, studies have shown that treatment with Dorzolamide might improve retinal blood flow. However, none of the earlier studies have quantified the vascular reactivity in uPOAG at baseline and then followed the same

patient group after a short period of treatment, that is, newly treated POAG (ntPOAG). A second objective of Chapter 6 was to determine the effect of treatment with 2% Dorzolamide, twice daily for 2 weeks on retinal and ONH vascular reactivity in uPOAG. The second hypothesis of Chapter 6 was that treatment with Dorzolamide will improve retinal and ONH vascular reactivity in uPOAG.

2.5 Relationship between functional vascular response and biochemical measures in POAG

There is a suggestion that the potent vasoconstrictor ET-1 released by the vascular endothelium is present in higher amounts in the aqueous and plasma of patients with POAG and, in particular, in those with NTG. There is also evidence that patients with POAG exhibit reduced plasma cGMP levels which is thought to be a surrogate marker of NO expression. However, there is lack of research on the presence of these biochemical markers of endothelial function in uPOAG and pPOAG. The objective of Chapter 7 was to compare plasma levels of ET-1 and cGMP (i.e. endothelial derived markers) to the magnitude of retinal vascular reactivity in patients with uPOAG and pPOAG and in healthy controls in order to ultimately validate the functional measurement. The primary hypothesis was that plasma ET-1 will be present in higher amounts at baseline in uPOAG and pPOAG compared to age-similar controls and that hypercapnia would reduce the presence of ET-1 in all groups. In addition, cGMP was hypothesized to be lower in uPOAG and pPOAG compared to age-similar controls at baseline and that hypercapnia would increase plasma cGMP levels. In addition, the effect of treatment with 2% Dorzolamide for 2 weeks on plasma ET-1 and cGMP levels was also investigated. The secondary hypothesis was that treatment would

decrease ET-1 in patients with uPOAG, thereby explaining the restoration of vascular reactivity, while there would be a concomitant post-treatment increase in cGMP.

3 The Impact of Hypercapnia on Retinal Capillary Blood Flow Assessed by Scanning Laser Doppler Flowmetry

Venkataraman ST, Hudson C, Fisher JA, Flanagan JG. The impact of hypercapnia on retinal capillary blood flow assessed by scanning laser Doppler flowmetry. *Microvasc.Res.* 2005;69:149-155.

Reprinted by permission from Elsevier publishers.

3.1 Abstract

Aim: To determine the effect of hypercapnia on retinal capillary blood flow using scanning laser Doppler flowmetry (SLDF).

Methods: One randomly selected eye of each of 10 normal healthy subjects (mean age 25 years, SD 2.3) was studied. Subjects breathed unrestricted air for 15 minutes before (baseline) and after raising fractional (per cent) end-tidal concentration of CO₂ (FETCO₂) for 15 minutes by adding low flows of CO₂ to air entering a sequential gas delivery circuit attached to a nasal mask. Five good quality baseline SLDF images were acquired both of the optic nerve head (ONH) and of the macula. Subsequently, a minimum of 7 sequential images were acquired during hypercapnia. Five further images were acquired of the ONH, or of the macula, after returning to unlimited air breathing. The respiratory parameters of subjects were continually monitored.

Results: The group mean increase in end-tidal CO₂ was 14.13% (SD 4.10) relative to baseline. The nasal macula (p=0.028) and foveal (p=0.042) areas showed a significant

increase in retinal capillary blood flow in response to hypercapnia while no significant change was noted in the ONH or temporal macula areas. Change in blood flow significantly correlated with change of FETCO₂ and/or end-tidal PO₂ for 3 of the 4 locations.

Conclusions: Hypercapnia provoked a significant increase in retinal capillary blood flow in 2 of 4 retinal locations. Hypercapnia also induced a change in respiratory parameters that significantly correlated with change in retinal capillary blood flow in 3 of the 4 locations.

Keywords: Hypercapnia, retinal capillary blood flow, laser Doppler flowmetry.

3.2 Introduction

Change of retinal perfusion induced by the perturbation of inspired oxygen (O_2), or carbon dioxide (CO_2), can be used to provide a measure of the magnitude of retinal vascular reactivity. Hypercapnia represents a potent vasoactive stimulus ^{1,2}. The change of fractional (per cent) end-tidal CO_2 concentration (FET CO_2) reflects the change in the partial pressure of arterial CO_2 (Pa CO_2) ³. An increase in FET CO_2 has been demonstrated to produce vasodilatation in animals and humans of both the cerebral and retinal circulations using various measurement techniques ^{1, 2, 4-10}. A 1 mmHg change in Pa CO_2 produces a 3% increase in ocular blood flow in primates ⁴.

Scanning laser Doppler flowmetry (SLDF i.e. the combination of a laser Doppler flowmeter and a scanning laser system) provides a two-dimensional, quantifiable perfusion map of retinal capillary blood flow ¹¹. SLDF can be used to non-invasively visualise and quantify retinal capillary blood flow ¹¹⁻¹³. Previous studies have quantified the impact of hypercapnia on SLDF measurement of retinal capillary blood flow ⁵, on similar hemodynamic techniques ⁸ and on contrast sensitivity ¹⁴. All of these studies utilised non-standardised stimuli and/or poorly defined methodology ^{5, 8, 14}. In particular, in the study by Harris et al (1994a), any concomitant change of end-tidal O_2 concentrations are not reported ¹⁵. They state that isoxic conditions are maintained during hypercapnia although evidence to support this is absent and the gas delivery system used does not seem capable of achieving isoxic hypercapnia. Furthermore, the period of hypercapnia was brief, i.e. approximately 3 minutes ¹⁴, which would impose severe methodological limitations on any experimental design.

The aim of this study was to non-invasively assess the magnitude of vascular reactivity of the retinal, and superficial optic nerve head, capillaries in young clinically normal subjects by SLDF, in response to a standardized hypercapnic provocation. The development of a standardized stimulus will provide conditions under which changes in vascular response can be compared in a given subject from one time period to the next, between subjects and between research groups. Unique to this study, the use of a sequential re-breathing technique¹⁶ facilitated the control and manipulation of stimulus parameters.

3.3 Materials and methods

3.3.1 Subjects

The study protocol was approved by the University of Waterloo, Office of Research Ethics. All subjects signed a consent form prior to participation after explanation of the nature and possible consequences of the study according to the tenets of the Declaration of Helsinki. Ten clinically normal young subjects of mean age 25 years (SD 2.35, range 22-29) were recruited (3 males : 7 females). Exclusion criteria included habitual smoking, treatable respiratory disorders (e.g. asthma), cardiovascular disease, systemic hypertension, refractive error greater than ± 6.00 DS and greater than ± 1.50 DC, ocular pathology and family history of glaucoma or diabetes. All subjects had Snellen visual acuity of 20/20 or better. The study eye was randomly selected. Subjects were asked to abstain from caffeine containing food and drinks 2 hours prior to the second visit.

3.3.2 Visits

Subjects attended for two visits. During the first visit, both eyes were dilated and an ocular examination was undertaken to ensure eligibility criteria for the study. Intraocular pressure was measured for both eyes using Goldmann tonometry. Retinal tomograph images were acquired using the Heidelberg Retina Tomograph (HRT; Heidelberg Engineering GmbH, Dossenheim, Germany) centered at both the optic nerve head and macula. HRT assessment was performed in order to calculate the optimal retinal location (i.e. x, y) and dioptric setting (i.e. z) for subsequent capillary blood flow measurement at both the optic nerve head and

macula¹⁷. Using this technique, a preset location and focus was defined for the subsequent acquisition of SLDF images during the subsequent visit.

3.3.3 Scanning laser Doppler flowmetry

The light reflected by moving red blood cells in the retina undergoes a frequency shift while light reflected from surrounding tissue is unchanged. Using SLDF, the intensity of back-scattered laser light from the retina is measured as a function of time (to produce an intensity-time curve) for each pixel within the image. The two coherent components of light interfere resulting in an oscillation, or “beat”, of the measured light intensity. The frequency of the intensity oscillation is equal to the Doppler frequency shift. Fast Fourier transformation of the intensity-time curve generates a power spectrum of the Doppler shift to derive parameters of blood flow, volume and velocity¹⁸ at each pixel within the image.

SLDF measurements were undertaken using the Heidelberg Retina Flowmeter (HRF; Heidelberg Engineering GmbH, Dossenheim, Germany, software version 1.03W). The HRF uses a 780nm wavelength infrared diode laser to measure the intensity, and thereby calculate the Doppler shift of back-scattered light. The instrument has a spatial resolution of approximately 10 μ m and a depth resolution 300-400 μ m^{19, 20}. The laser scanning system of the HRF enables the measurement of a 10° horizontal x 2.5° vertical (i.e. approximately 2.7mm x 0.7mm) field with a resolution of 256 pixels x 64 lines, respectively. Each line of 256 pixels is scanned 128 times at a repetition rate of 4000Hz. The resulting image acquisition time is 2.048 sec.

The focus settings for each subject were kept constant throughout the experiment. HRF images of both the ONH and the macula were acquired. Subjects fixated a green light with the non-study eye. The fixation light was mounted on a stand at a distance of 3 meters. A periscope was placed in front of the non-study eye when imaging the macula in order to permit the subject to view the fixation light.

3.3.4 Procedures

At visit 2, intraocular pressure was measured in the non-study eye prior to the introduction of the hypercapnic stimulus (to avoid disturbance of image quality in the study eye) and in both eyes on completion of the breathing protocol. The results were compared to those attained at visit 1 to ensure consistency. The total duration of visit 2 was 45 minutes. Subjects accommodated to the circuit for 10 minutes to allow stabilization of cardio-vascular parameters e.g. respiration rate, heart rate and blood pressure. Subjects were then fitted with a nasal mask connected to a sequential re-breathing circuit (Hi-Ox SR, Viasys Healthcare, Yorba Linda, CA). The sequential re-breathing circuit allowed the manipulation of inspired, and thereby expired, gases as described by Vesely and co-workers (2001) and Gilmore and co-workers (2004)^{16, 21}. The circuit comprised a non-rebreathing valve and fresh gas and re-breathed gas reservoirs that were interconnected by two one-way valves and a single PEEP valve (Figure 3.1). The nasal mask was attached to the sequential re-breathing system that, in turn, was connected to the gas supply. Flow from the gas tanks was controlled using rotometers (Flowmeter 56073-11-01-000, Controls corp. of America, Virginia beach, Virginia). Inspired gases were reduced until FETCO₂ rose approximately 15% relative to baseline, a level previously documented to be safe²². Subjects were instructed not to open

their mouth during the procedure in order to achieve control of inspired gas concentration. Should the subjects experience discomfort from the hypercapnia, however, they would be able to breathe through their mouth (and the study would be aborted). It was predetermined that the procedure would be abandoned if: i). There was an increase in diastolic blood pressure of $\geq 15\text{mmHg}$; ii). Absolute diastolic blood pressure reached or exceeded 100mmHg ; and iii). Pulse rate reached or exceeded 150beats/min .

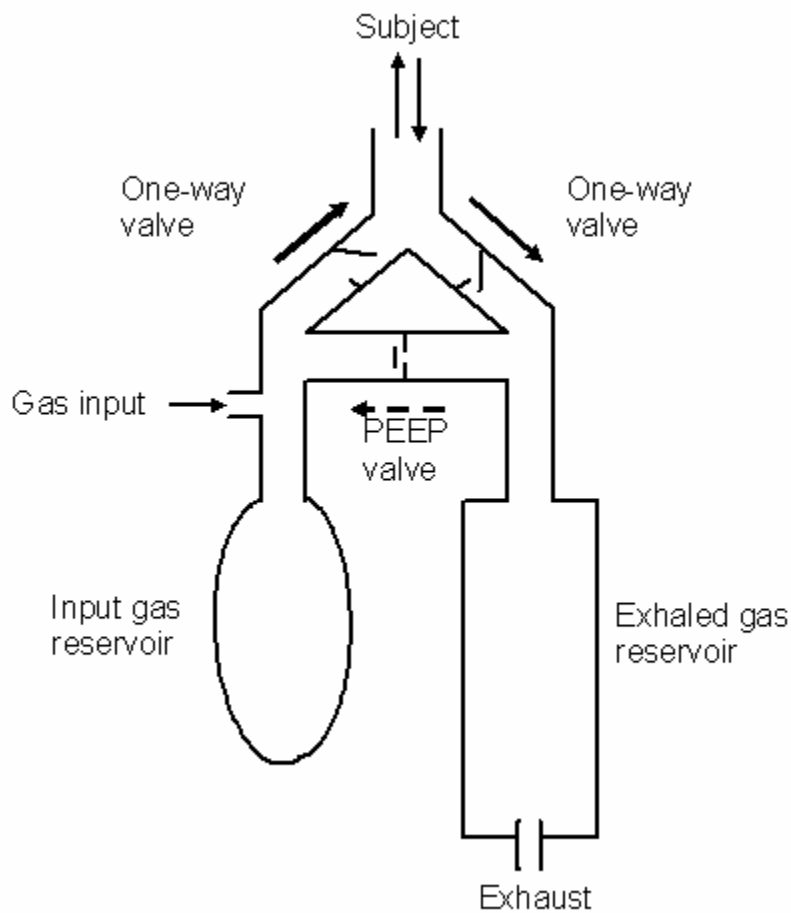


Figure 3.1 Schematic representation of the sequential rebreathing system.

During the initial 15 minutes of data collection, subjects breathed bottled air entering the mask at a rate of 6.0 to 8.0 litres per minute (LPM) allowing the development of a stable

resting FETCO₂. FETCO₂ was stabilized (preventing any changes with increases in minute ventilation) by setting the air flow equal to the subjects' resting minute ventilation (i.e. the air flow at which the fresh air reservoir *just* collapsed). Five good quality baseline SLDF images were acquired both of the optic nerve head (ONH) and of the macula (site order systematically alternated between subjects). During the next 15 minutes, 0.3 to 0.4 LPM of CO₂ was added to 5.0 to 7.0 LPM of inspired air to increase FETCO₂ by approximately 15% from baseline. A minimum of 7 sequential SLDF images were acquired at both locations once a stabilized increase of FETCO₂ was attained (site order maintained relative to baseline). During the final 15 minutes, subjects once more breathed bottled air at a rate of 6.0 to 8.0 LPM and were allowed to return to their resting FETCO₂ level. At this point, five further SLDF images were acquired of the ONH, or of the macula (systematically alternated between subjects). Tidal gas concentrations, including inspired and expired O₂ and CO₂ levels, were continuously sampled from the nasal mask using a rapid response gas analyzer (Cardiocard 5, Datex-Ohmeda, Helsinki, Finland). Over the entire procedure, systolic and diastolic blood pressure, heart rate, respiration rate, pulse rate and oxygen saturation were monitored using the critical care monitor.

Capillary blood flow values of neuro-retinal rim, nasal macula, fovea and temporal macula were generated using the Automated Full Field Perfusion Image Analysis (AFFPIA) software. The AFFPIA software has been described in detail elsewhere²³. This analysis was used to extract blood flow values from SLDF images. Using this technique, erroneous blood flow data due to saccades and large blood vessels were excluded. The AFFPIA enabled the

use of a circle to be centered on the desired retinal measurement site (i.e. the fovea or ONH) to derive capillary blood flow values for specified retinal areas (Figure 3.2).

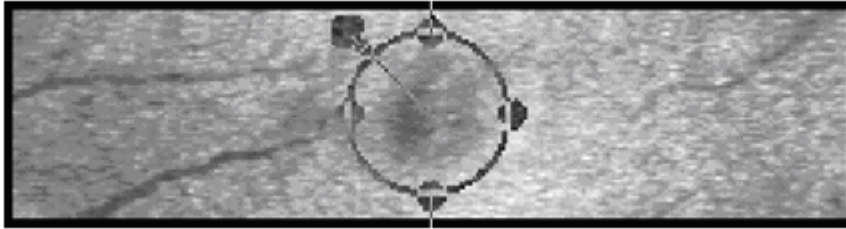


Figure 3.2 Scanning laser Doppler flowmetry image of the left macula of an individual showing the AFFPIA analysis circle centered on the fovea.

Using the AFFPIA, capillary blood flow values of the fovea (all valid pixels within the circle), nasal macula (all valid pixels nasal to the fovea) and temporal macula (all valid pixels temporal to the fovea) were generated. A similar methodology was used to generate capillary blood flow values for the ONH.

3.3.5 Statistical analysis

Repeated measures Analysis of Variance (ANOVA) was performed on each of the dependent variables using Statistical Analysis System (SAS). The dependent variables were retinal capillary blood flow, end-tidal CO₂ and O₂ gas concentrations. The within-subject factors were retinal measurement site (i.e. ONH, nasal macula, fovea and temporal macula) and time (i.e. baseline, hypercapnia and post-hypercapnia). Pearson's correlation co-efficient analysis was undertaken to determine any significant relationship of the change over time in blood flow to change of the gas parameters. Probability values of mean correlation were determined and an $R \geq 0.2$ with a corresponding $p < 0.05$ were considered to demonstrate a moderate or greater relationship. Student's two-tailed paired t-test was used to compare baseline and hypercapnic measures of systolic and diastolic blood pressure, heart rate, oxygen saturation and respiration rate.

3.4 Results

The repeated measures ANOVA demonstrated that group mean nasal and foveal capillary blood flow increased significantly ($p=0.028$ & $p=0.042$, respectively) as a result of hypercapnic provocation. The Pearson correlation co-efficient showed that change in blood flow significantly correlated with change of FETCO₂ and/or end-tidal PO₂ for 3 of the 4 locations. Change of ONH capillary blood flow showed significant correlation with change of FETO₂, while nasal macula blood flow showed significant correlation with both FETCO₂ and FETO₂. Similarly, change of foveal blood flow significantly correlated with change of FETCO₂ (Table 3.1).

Gas Parameters	ONH (p)	Macula Nasal (p)	Foveal (p)	Macula Temporal (p)
FETCO ₂	0.1808	0.0382 *	0.0377 *	0.2075
FETO ₂	0.0363 *	0.0053 *	0.7063	0.1724

Table 3.1 Statistical significance values for correlation between change in relevant gas parameters over time and change in blood flow in the optic nerve head, macula nasal, foveal and macula temporal areas of the retina.

(FETCO₂; end-tidal CO₂. FETO₂; end-tidal O₂). * represents significance at the $p<0.05$ level.

Seven of 10 subjects showed an increase in ONH capillary blood flow during hypercapnia compared to baseline. Nine subjects showed an increase in both the nasal macula and foveal capillary blood flow, while 8 subjects showed an increase at the temporal macula during hypercapnia compared to baseline (Figure 3.3). The group mean ONH capillary blood flow demonstrated an insignificant trend to increase from 190.15 a.u (SD 74.93) at baseline to 209.57 a.u. (SD 73.44) during hypercapnia ($p=0.325$). The group mean nasal macula

capillary blood flow increased from 127.17 a.u. (SD 32.59) at baseline to 151.22 a.u. (SD 36.67) during hypercapnia ($p=0.028$), while foveal blood flow increased from 92.71 a.u. (SD 28.07) to 107.39 a.u. (SD 34.43) ($p=0.042$). Temporal macula blood flow demonstrated an insignificant trend to increase from 120.21 a.u. (SD 40.28) to 140.54 a.u. (SD 41.00) ($p=0.068$), respectively.

A sustained increase in FETCO₂ was achieved in all subjects. A representative example demonstrating the change in FETCO₂ over the course of the experiment is shown in Figure 3.4. The group mean magnitude of fractional (i.e. %) end-tidal concentrations of CO₂ and O₂ for baseline, hypercapnia and post-hypercapnia (\pm SD) are presented in (Table 3.2). Group mean FETCO₂ significantly increased from 5.37% (SD 0.45) at baseline to 6.13% (SD 0.44) during hypercapnia ($p<0.0001$); this resulted in a group mean relative increase (i.e. to baseline) in end-tidal CO₂ of 14.13% (SD 4.10). The end-tidal fractional concentration of O₂ (FETO₂) increased from 14.59% (SD 0.5) at baseline to 16.48% (SD 1.0) ($p=0.0005$) but was physiologically insignificant.

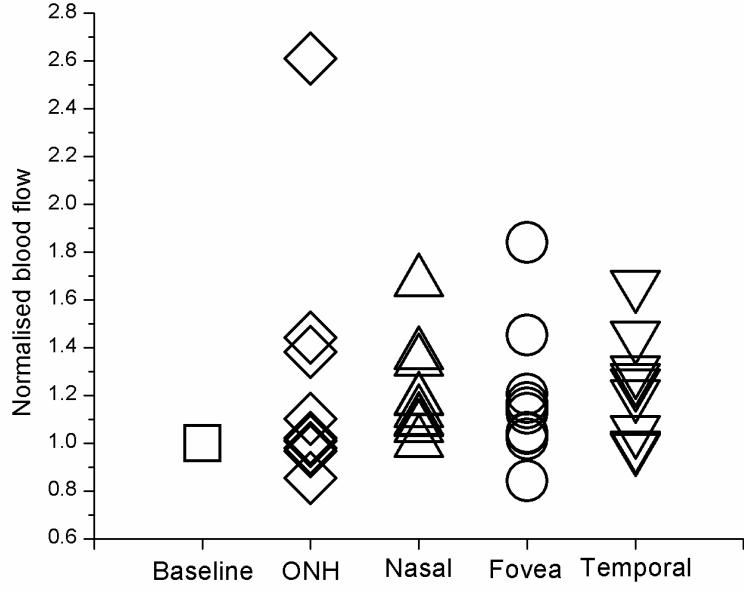


Figure 3.3 Normalised blood flow for each individual of the optic nerve head (open diamond; 5 plot symbols are overlapping), (macula nasal open triangle, 4 plot symbols are overlapping), foveal (open circle, 2 plot symbols are overlapping) and macula temporal (open inverted triangle, 5 plot symbols are overlapping) locations relative to the baseline (open square).

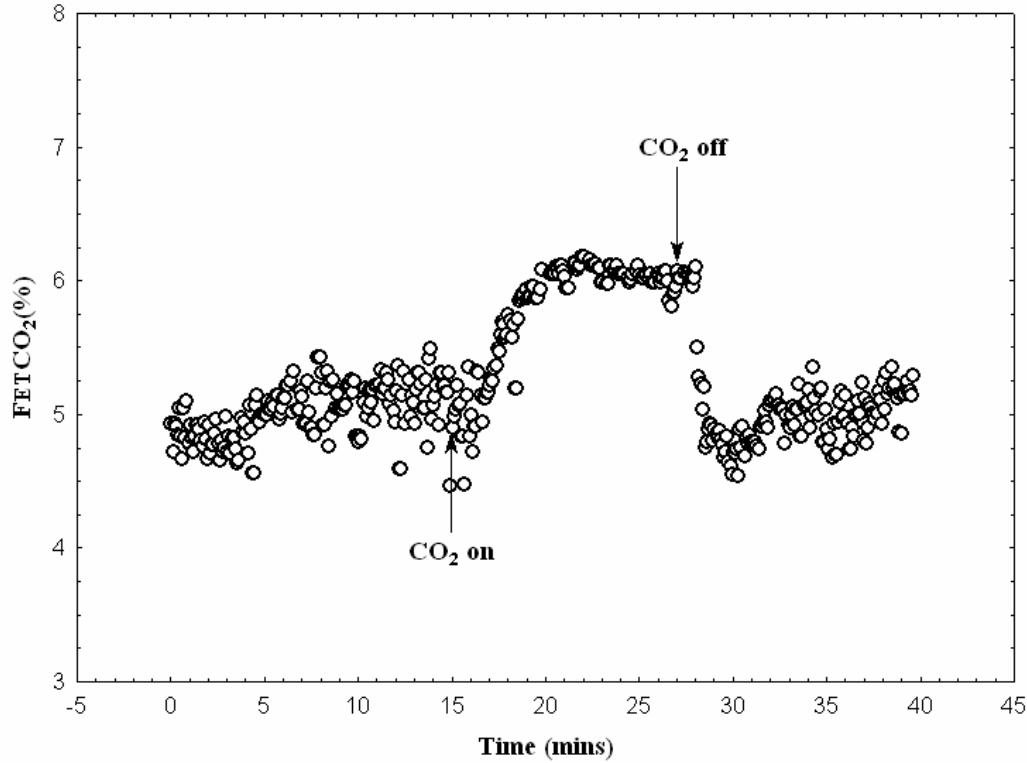


Figure 3.4 FETCO₂ plotted against time for a single individual.

Condition	FETCO ₂ (%)	FETO ₂ (%)
Baseline	5.37 ± 0.4	14.59 ± 0.5
Hypercapnia	6.13 ± 0.4	16.48 ± 1.0
Post-hypercapnia	5.24 ± 0.4	15.19 ± 0.6
p-value (Re-ANOVA)	<0.0001	=0.0005

Table 3.2 The group mean magnitude of fractional (i.e. %) end-tidal concentrations of CO₂ and O₂ for baseline, hypercapnia and post-hypercapnia (± SD).

(FETCO₂; end-tidal percentage concentration of CO₂. FETO₂; end-tidal percentage concentration of O₂).

There was no necessity to abandon the procedure in any subject as a result of increase in blood pressure or pulse rate. There was no significant change in systolic or diastolic blood

pressure and oxygen saturation during the hypercapnic provocation relative to baseline. Respiration rate ($p=0.005$) and heart rate ($p=0.049$) showed a significant increase during hypercapnia relative to baseline (Table 3.3).

Condition	Heart rate (beats/min)	Blood Pressure Systolic (mmHg)	Blood Pressure Diastolic (mmHg)	Respiration rate (breaths/min)	Oxygen saturation (%)
Baseline	73.1 ± 5.6	110.8 ± 9.0	67.7 ± 6.4	12.7 ± 2.8	98.56 ± 0.43
Hypercapnia	75.3 ± 7.5	113.3 ± 11.0	66.6 ± 9.0	14.7 ± 3.3	98.94 ± 0.47
Post-hypercapnia	72.4 ± 6.4	108.9 ± 9.6	69.2 ± 5.8	13.0 ± 2.9	98.98 ± 0.48
p-value	=0.049	>0.05	>0.05	0.005	>0.05

Table 3.3 The group mean percentage heart rate, systolic and diastolic blood pressure, respiration rate and oxygen saturation (\pm SD) as a function of condition (i.e. baseline, hypercapnia and post-hypercapnia).

3.5 Discussion

In this study, we describe the changes in retinal blood flow resulting from a 15% change in end-tidal fractional CO₂ concentration. Capillary blood flow in the nasal macula and fovea significantly increased during hypercapnia. ONH and temporal macula blood flow, however, did not show a significant increase. The increase in foveal blood flow during hypercapnia might be due to a possible vascular regulatory mechanism exhibited by the underlying choroidal vessels as this has been shown by previous researchers²⁴. Also, the difference in retinal vascular response to hypercapnia for the 4 locations (i.e. 2 locations exhibited a significant increase in blood flow while 2 did not) may be explained by variations in the relative contribution of the underlying choroid to the measured signal²⁵. The choroidal

vasculature is thought to possess a less efficient regulatory mechanism⁵. Change in blood flow significantly correlated with change of FETCO₂ and/or FETO₂ for 3 of the 4 locations. The difference in the magnitude of response to hypercapnia in various areas of the retina and ONH could also possibly be due to the inherent variability of capillary blood flow measurements using the HRF. Topographical variation in vascular reactivity to gas perturbation, however, in different areas of the retina has been noted in previous studies. Roff and co-workers (1999) showed a significant increase in retinal capillary blood flow of the superior temporal quadrant compared to baseline using SLDF, but not in the inferior temporal quadrant, in normal subjects undergoing 15% increase in FETCO₂⁵. Chung and co-workers, (1999) also found that hypercapnia resulted in a localized significant increase of retinal capillary blood flow in the superior temporal quadrant but not in the inferior temporal quadrant⁷. Similarly, topographical variation in cortical vascular reactivity to gas perturbation, has been noted. For example, cerebral plasma volume (CPV) has been assessed using magnetic resonance imaging during normocapnia and hypercapnia (partial pressure of CO₂ approximately 65mmHg) in the dorsoparietal neocortex and striatum of each hemisphere in cerebellum and in extra cerebral tissue of rats. CPV showed a significant increase in the neocortex, striatum of the cerebellum but not in the extra cerebral tissue²⁶.

This study described a safe way of administering CO₂ to young subjects using a sequential re-breathing circuit. There was no significant change in blood pressure and oxygen saturation, however, there was a significant increase in heart rate and respiration rate during hypercapnia relative to baseline, as found in previous studies^{5, 27}. Participants were able to sustain hypercapnia for 15minutes without any major discomfort during the provocation. A

sustained and a stable increase in FETCO₂ was achieved in all subjects. An important further advantage of using the sequential re-breathing circuit is that absolute FETCO₂ levels can be manipulated whilst minimizing the variability of FETCO₂²¹, thus providing stable stimulus conditions for provocation. As a result, a smaller magnitude of change of FETCO₂ will result in statistical significance.

Inhalation of CO₂ enriched gas, as in our study, dilutes and thereby reduces the O₂ concentration in the lung and thus in the blood. As O₂ is a vasoactive molecule in the ocular vasculature, changes in blood O₂ concentration will influence the vascular response to blood CO₂ concentration. However, this effect on the lung O₂ concentration is partly offset by the increased ventilation stimulated by hypercapnia. In our study, the small increase in FETO₂ concentration was statistically significant but of no physiological significance, since it represented only 1/760 of the range of a full scale of atmospheric O₂ concentration (from 1 to 760 mmHg). Previous studies utilizing hypercapnic provocation to assess ocular vascular reactivity have not reported taking any measures to maintain FETO₂ constant. In fact, most have failed to monitor or report the FETO₂ concentration^{5, 7, 14, 28}.

An increase in intra-ocular pressure and transient loss of perfusion to the optic nerve head are some of the factors that may contribute to the development of glaucomatous optic neuropathy^{29, 30}. In particular, vascular dysregulation is thought to be associated with patients with normal-tension glaucoma (NTG)³¹. Endothelin-1 (ET-1) is a 21-residue amino acid peptide with vasoconstrictive properties that is elevated in patients with NTG and primary open angle^{30, 32-34}. Under normal conditions, the vasoconstrictive effect of ET-1 is balanced by the basal

release of NO although many other vasoactive factors undoubtedly contribute to the dynamic control of vascular perfusion^{31, 35}. Interestingly, an exaggerated increase in end-diastolic flow velocity of the ophthalmic artery has been observed in response to hypercapnia in NTG patients compared to normal subjects, suggesting a possible over-expression of ET-1 at baseline and an overall dysregulation of vascular tonus control in patients with NTG³⁶. NO is produced primarily by the isoforms of nitric oxide synthase (NOS) present in the vascular endothelium³⁷. The release of NO in both vascular smooth muscle cells and pericytes triggers the release of cyclic guanosine monophosphate leading to dephosphorylation of myosin light chain resulting in vasodilatation³⁸⁻⁴⁰. Inhibition of NOS reduces the magnitude of vascular reactivity in blood vessels in response to hypercapnia³⁷. In addition, alteration in the extra cellular pH at the level of retinal pericytes may play a role in hypercapnic vasodilatation⁴¹. We intend to utilise the methodology developed in this study in patients with NTG and compare the results gained to age-matched normal controls. We anticipate that this methodology in combination with biochemical assays of endothelial derived constricting and relaxing factors will reveal the role of NO in vascular dysregulation associated with glaucoma. This work is in progress in our laboratory.

3.6 Conclusions

Hypercapnia provoked a significant increase in retinal capillary blood flow in 2 of 4 retinal locations. In addition, change in blood flow significantly correlated with change of FETCO₂ and/or FETO₂ for 3 of the 4 locations. Hypercapnic provocation typically results in changes in PO₂ which in turn can affect vascular reactivity. In our study, the use of the sequential re-breathing circuit resulted in a physiologically insignificant change in PO₂ that is, a near

isoxic hypercapnic provocation. We plan to modify our hypercapnic provocation to allow the maintenance of isoxic conditions during achievement of multiple levels of FETCO₂ and apply it to assess the vascular reactivity of the retinal vasculature in normals and individuals with vasospastic disorders.

3.7 References

1. Harris A, Arend O, Wolf S, Cantor LB, Martin BJ. CO₂ dependence of retinal arterial and capillary blood velocity. *Acta Ophthalmol.Scand.* 1995;73:421-424.
2. Sponsel WE, DePaul KL, Zetlan SR. Retinal hemodynamic effects of carbon dioxide, hyperoxia, and mild hypoxia. *Invest.Ophthalmol.Vis.Sci.* 1992;33:1864-1869.
3. Rhoades RA. Respiratory physiology: Gas transfer and transport. Tanner GA Rhoades RA. *In Medical physiology.* Philadelphia: Lippincott Williams & Wilkins; 2003. 350-362 pp.
4. Tsacopoulos M, David NJ. The effect of arterial PCO₂ on relative retinal blood flow in monkeys. *Invest.Ophthalmol.* 1973;12:335-347.
5. Roff EJ, Harris A, Chung HS, et al. Comprehensive assessment of retinal, choroidal and retrobulbar haemodynamics during blood gas perturbation. *Graefes Arch.Clin.Exp.Ophthalmol.* 1999;237:984-990.
6. Kety SS, Schmidt CF. The effect of altered arterial tensions of carbon dioxide and oxygen on cerebral blood flow and cerebral oxygen consumption of normal young men. *J.Clin.Invest.* 1948;27:484-494.
7. Chung HS, Harris A, Halter PJ, et al. Regional differences in retinal vascular reactivity. *Invest.Ophthalmol.Vis.Sci.* 1999;40:2448-2453.

8. Harris A, Anderson DR, Pillunat L, et al. Laser doppler flowmetry measurement of changes in human optic nerve head blood flow in response to blood gas perturbations. *J.Glaucoma* 1996;5:258-265.
9. Raper AJ, Kontos HA, Patterson JL. Response of pial precapillary vessels to changes in arterial carbon dioxide tension. *Circ.Res.* 1971;28:518-523.
10. Haefliger IO, Lietz A, Griesser SM, et al. Modulation of heidelberg retinal flowmeter parameter flow at the papilla of healthy subjects: Effect of carbogen, oxygen, high intraocular pressure, and beta-blockers. *Surv.Ophthalmol.* 1999;43 Suppl 1:S59-S65.
11. Michelson G, Langhans MJ, Groh MJ. Clinical investigation of the combination of a scanning laser ophthalmoscope and laser doppler flowmeter. *Ger.J.Ophthalmol.* 1995;4:342-349.
12. Michelson G, Schmauss B, Langhans MJ, Harazny J, Groh MJ. Principle, validity, and reliability of scanning laser doppler flowmetry. *J.Glaucoma* 1996;5:99-105.
13. Hafez AS, Bizzarro RL, Rivard M, Lesk MR. Changes in optic nerve head blood flow after therapeutic intraocular pressure reduction in glaucoma patients and ocular hypertensives. *Ophthalmology* 2003;110:201-210.
14. Hosking SL, Evans DW, Embleton SJ, Houde B, Amos JF, Bartlett JD. Hypercapnia invokes an acute loss of contrast sensitivity in untreated glaucoma patients. *Br.J.Ophthalmol.* 2001;85:1352-1356.

15. Harris A, Martin BJ, Shoemaker JA. Regulation of retinal blood flow during blood gas perturbation. *Journal of Glaucoma*. 1994;3:S82-90.
16. Gilmore ED, Hudson C, Venkataraman ST, Preiss D, Fisher J. Comparison of different hyperoxic paradigms to induce vasoconstriction: Implications for the investigation of retinal vascular reactivity. *Invest.Ophthalmol.Vis.Sci*. 2004;45:3207-3212.
17. Sehi M, Flanagan JG. The effect of image alignment on capillary blood flow measurement of the neuroretinal rim using the heidelberg retina flowmeter. *Br.J.Ophthalmol*. 2004;88:204-206.
18. Michelson G, Schmauss B. Two dimensional mapping of the perfusion of the retina and optic nerve head. *Br.J.Ophthalmol*. 1995;79:1126-1132.
19. Chauhan BC, Smith FM. Confocal scanning laser doppler flowmetry: Experiments in a model flow system. *J.Glaucoma* 1997;6:237-245.
20. Kagemann L, Harris A, Chung H, Jonescu-Cuyper C, Zarfati D, Martin B. Photodetector sensitivity level and heidelberg retina flowmeter measurements in humans. *Invest.Ophthalmol.Vis.Sci*. 2001;42:354-357.
21. Vesely A, Sasano H, Volgyesi G, et al. MRI mapping of cerebrovascular reactivity using square wave changes in end-tidal PCO₂. *Magn.Reson.Med*. 2001;45:1011-1013.
22. Niwa Y, Harris A, Kagemann L, et al. A new system to supply carbon dioxide safely to glaucoma patients. *Jpn.J.Ophthalmol*. 1999;43:16-19.

23. Michelson G, Welzenbach J, Pal I, Harazny J. Automatic full field analysis of perfusion images gained by scanning laser doppler flowmetry. *Br.J.Ophthalmol.* 1998;82:1294-1300.
24. Lovasik JV, Kergoat H, Riva CE, Petrig BL, Geiser M. Choroidal blood flow during exercise-induced changes in the ocular perfusion pressure. *Invest.Ophthalmol.Vis.Sci.* 2003;44:2126-2132.
25. Yu DY, Townsend R, Cringle SJ, Chauhan BC, Morgan WH. Improved interpretation of flow maps obtained by scanning laser doppler flowmetry using a rat model of retinal artery occlusion. *Invest.Ophthalmol.Vis.Sci.* 2005;46:166-174.
26. Payen JF, Vath A, Koenigsberg B, Bourlier V, Decorps M. Regional cerebral plasma volume response to carbon dioxide using magnetic resonance imaging. *Anesthesiology* 1998;88:984-992.
27. Harino S, Grunwald JE, Petrig BJ, Riva CE. Rebreathing into a bag increases human retinal macular blood velocity. *Br.J.Ophthalmol.* 1995;79:380-383.
28. Hilton EJ, Hosking SL, Cubbidge RP, Morgan AJ. Regional variability in visual field sensitivity during hypercapnia. *Am.J.Ophthalmol.* 2003;136:272-276.
29. Flammer J. To what extent vascular factors are involved in pathogenesis of glaucoma. H. J. Kaiser, J. Flammer and P. Hendrickson. *In Ocular blood flow. Glaucoma-meeting 1995.* Basel, Karger; 1996. 12-39 pp.
30. Haefliger IO, Dettmann E, Liu R, et al. Potential role of nitric oxide and endothelin in the pathogenesis of glaucoma. *Surv.Ophthalmol.* 1999;43 Suppl 1:S51-S58.

31. Drance SM, Sweeney VP, Morgan RW, Feldman F. Studies of factors involved in the production of low tension glaucoma. *Arch.Ophthalmol.* 1973;89:457-465.
32. Kaiser HJ, Flammer J, Wenk M, Luscher T. Endothelin-1 plasma levels in normal-tension glaucoma: Abnormal response to postural changes. *Graefes Arch.Clin.Exp.Ophthalmol.* 1995;233:484-488.
33. Sugiyama T, Moriya S, Oku H, Azuma I. Association of endothelin-1 with normal tension glaucoma: Clinical and fundamental studies. *Surv.Ophthalmol.* 1995;39 Suppl 1:S49-S56.
34. Yorio T, Krishnamoorthy R, Prasanna G. Endothelin: Is it a contributor to glaucoma pathophysiology? *J.Glaucoma* 2002;11:259-270.
35. Jarajapu YP, Grant MB, Knot HJ. Myogenic tone and reactivity of the rat ophthalmic artery. *Invest.Ophthalmol.Vis.Sci.* 2004;45:253-259.
36. Harris A, Sergott RC, Spaeth GL, Katz JL, Shoemaker JA, Martin BJ. Color doppler analysis of ocular vessel blood velocity in normal-tension glaucoma. *Am.J.Ophthalmol.* 1994;118:642-649.
37. Schmetterer L, Findl O, Strenn K, et al. Role of NO in the O₂ and CO₂ responsiveness of cerebral and ocular circulation in humans. *Am.J.Physiol.* 1997;273:R2005-R2012.
38. Orgul S, Gugleta K, Flammer J. Physiology of perfusion as it relates to the optic nerve head. *Surv.Ophthalmol.* 1999;43 Suppl 1:S17-S26.

39. Haefliger IO, Meyer P, Flammer J. Endothelium-dependent vasoactive factors. H. J. Kaiser, J. Flammer and P. Hendrickson. *In Ocular blood flow*. Glaucoma-meeting 1995. Basel, Karger; 1996. 51-63 pp.
40. Meyer P, Haefliger IO, Flammer J, Luscher TF. Endothelium-dependent regulation in ocular vessels. H. J. Kaiser, J. Flammer and P. Hendrickson. *In Ocular Blood Flow - New Insights into the Pathogenesis of Ocular Diseases*. Basel, Switzerland: Karger Publishers; 1996. 64-73 pp.
41. Chen Q, Anderson DR. Effect of CO₂ on intracellular pH and contraction of retinal capillary pericytes. *Invest.Ophthalmol.Vis.Sci.* 1997;38:643-651.

4 Novel Methodology to Comprehensively Assess Retinal Arteriolar Vascular Reactivity to Hypercapnia

Venkataraman ST, Hudson C, Fisher JA, Flanagan JG. Novel methodology to comprehensively assess retinal arteriolar vascular reactivity to hypercapnia. *Microvasc.Res.* 2006;72:101-107.

Reprinted by permission from Elsevier publishers

4.1 Abstract

Purpose: 1). Describe a new methodology that permits the comprehensive assessment of retinal arteriolar vascular reactivity in response to a sustained and stable hypercapnic stimulus. 2). Determine the magnitude of the vascular reactivity response of the retinal arterioles to hypercapnic provocation in healthy, young subjects.

Methodology: Eleven healthy subjects of mean age 27years (SD 3.43) participated in the study and one eye was randomly selected. A mask attached to a sequential re-breathing circuit, and connected to a gas delivery system, was fitted to the face. To establish baseline values, subjects breathed bottled air for 15 minutes and at least 6 blood flow measurements of the supero-temporal arteriole were acquired using the Canon Laser Blood Flowmeter (CLBF). Air flow was then decreased until a stable increase in fractional end-tidal CO₂ concentration (F_{ET}CO₂) of 10-15% was achieved. CLBF measurements were acquired every minute (minimum of 6 measurements) during the 20 minute period of elevated F_{ET}CO₂. F_{ET}CO₂ was then reduced to baseline levels and 6 further CLBF measurements were

acquired. Respiratory rate, blood pressure, pulse rate and oxygen saturation were monitored continuously.

Results: Retinal arteriolar diameter, blood velocity and blood flow increased during hypercapnia relative to baseline ($p=0.0045$, $p<0.0001$ & $p<0.0001$, respectively). Group mean $F_{ET}CO_2$ showed an increase of 12.0% (SD 3.6) relative to baseline ($p<0.0001$).

Conclusions: This study describes a new methodology that permits the comprehensive assessment of retinal arteriolar vascular reactivity in response to a sustained and stable hypercapnic stimulus. Retinal arteriolar diameter, blood velocity and blood flow increased significantly in response to a hypercapnic provocation in young, healthy subjects.

Keywords: Vascular reactivity, hypercapnia, retinal arterioles, bi-directional laser Doppler velocimetry.

4.2 Introduction

Vascular reactivity is the magnitude of change of hemodynamic parameters to a provocative stimulus, for example, an increase in partial pressure of oxygen or carbon dioxide in the blood. It has been shown that both the retinal and the cerebral vessels react similarly by constricting to oxygen (O₂) and by dilating to carbon dioxide (CO₂)¹⁻⁴. Hypercapnia, that is an increased partial pressure of CO₂ (PaCO₂) in systemic arterial blood, is known to be a potent vasodilatory stimulus. For the purpose of non-invasive studies in healthy subjects at rest, the end-tidal partial pressure of CO₂ (P_{ET}CO₂) is considered to be within 2 mmHg of the arterial PCO₂ (PaCO₂) and tracks it closely when P_{ET}CO₂ is varied⁵. In this paper, we will also refer to F_{ET}CO₂ which is the *fractional* end-tidal concentration of CO₂; P_{ET}CO₂ = F_{ET}CO₂ x barometric pressure.

The vascular reactivity response of the retina to a 10 - 15% increase in F_{ET}CO₂, achieved by the use of various methods of modulating inspired CO₂, has been quantified using laser Doppler based techniques⁶⁻⁹. The response of the ocular vasculature to breathing a mixture of 95% air and 5% CO₂, or 95% O₂ and 5% CO₂ (i.e. carbogen), has also been assessed using the Oculix and Retinal Vessel Analyser (RVA)^{1, 10}, blue field entoptic technique¹¹ and the Pulsatile Ocular Blood Flowmeter (POBF)¹². In addition, Harino and co-workers¹³ determined change in macular blood velocity, by rebreathing into a bag to elevate F_{ET}CO₂, using the blue field entoptic technique. Recently, our group has determined the effect of hypercapnia, induced using a sequential re-breathing circuit, on retinal capillary blood flow⁹. Unlike previous studies, the use of a sequential re-breathing circuit permitted a sustained and a stable increase in F_{ET}CO₂ with minimal concomitant change in end-tidal PO₂

concentrations. In addition, all of the hemodynamic assessment techniques detailed above assess only one aspect of hemodynamics (i.e. vessel diameter or *effectively* blood velocity).

The determination of quantitative retinal blood flow necessitates the simultaneous measurement of vessel diameter and blood velocity. The Canon Laser Blood Flowmeter (CLBF), model 100 (Canon, Tokyo, Japan), is the only retinal hemodynamic instrument that can simultaneously measure vessel diameter and centerline blood velocity, and therefore for the first time, quantify volumetric blood flow in absolute units ¹⁴. It utilizes bidirectional photodetectors to quantify centerline blood velocity, densitometry to measure vessel diameter and an eye tracker system to minimize the impact of eye movement ^{15, 16}. Using the CLBF and a sequential re-breathing circuit, our group has recently defined the timeline response of the retinal arterioles to isocapnic hyperoxia ¹⁷ and have demonstrated that retinal blood flow varies directly with the arterial PCO₂, as reflected in the P_{ET}CO₂ ¹⁸. However, the magnitude of the vascular reactivity response to hypercapnia has not been systematically addressed in previous work.

The aims of the study were to: 1). Describe a new methodology that permits the comprehensive assessment of retinal arteriolar vascular reactivity in response to a standardized, sustained and stable hypercapnic stimulus with minimal concomitant change in end-tidal PO₂. The concomitant change in end-tidal pO₂ during hypercapnia is a problem that previous studies have typically ignored. 2). Determine the magnitude of change in vessel diameter, blood velocity and flow of the retinal arterioles in response to sustained and stable hypercapnic provocation in young, healthy subjects. The magnitude of retinal arteriolar

vascular reactivity will be used as a reference for future studies that investigate the impact of disease upon this hypercapnic provocation. A sequential re-breathing circuit was used to induce a stable, sustainable change in $F_{ET}CO_2$ ^{18,19}.

4.3 Materials and methods

4.3.1 Sample

The study was approved by the University Health Network, Research Ethics Board, University of Toronto and by the University of Waterloo, Office of Research Ethics. All subjects signed a consent form prior to participation after explanation of the nature and possible consequences of the study according to the tenets of the declaration of Helsinki. Eleven healthy subjects (7 males and 4 females) of mean age 27years (SD 3.43, range 24 – 36years) participated in the study. One eye was chosen randomly for the study. All subjects had a visual acuity 20/20 or better. Exclusion criteria included habitual smoking, treatable respiratory disorders (e.g. asthma), cardiovascular diseases, systemic hypertension, a refractive error greater than $\pm 6.00\text{DS}$ and $\pm 1.50\text{DC}$, any ocular pathology, no immediate family history of glaucoma or diabetes or medications with known effects on blood flow (e.g. anticonvulsants, muscle relaxants, or anti-inflammatory medications). All participants were asked to refrain from caffeine-containing drinks or snacks for at least 12 hours prior to their study visit.

4.3.2 Visits

Subjects attended for two visits. During the first visit, both pupils were dilated using Mydracyl 1% (Alcon Canada Inc. Mississauga, Canada) and a health profile and ocular examination were performed to ensure eligibility for the study. The study eye was then randomly chosen and one CLBF image was acquired of a supero-temporal arteriole to determine a suitable measurement site. The site of CLBF measurement was approximately 1

disc diameter distant from the edge of the optic nerve head along a relatively straight segment of the supero-temporal arteriole and distant from any bifurcations. The measurement site selected at visit 1 was stored in the memory of the PC for subsequent imaging at visit 2. At the first visit, intra ocular pressure was measured in both eyes, followed by axial length measurement of the study eye. During the second visit, intra ocular pressure was measured only in the non-study eye to maintain the optical quality of the cornea for CLBF imaging. At visit 2, subjects underwent hypercapnic provocation and assessment of retinal vascular reactivity.

4.3.3 Instrumentation

4.3.3.1 Quantitative retinal blood flow assessment

The principle underlying the quantitative retinal blood flow assessment technique is based on the Doppler effect. Laser light scattered from a stationary object such as a vessel wall remains unaltered in frequency, while light reflected by a moving red blood cell undergoes a frequency shift (Δf). This shift in frequency is proportional to the velocity of the moving particle. A vessel that exhibits Poiseuille flow will have a range of velocities and thus a range of frequency shifts up to a maximum frequency shift (Δf_{\max}) that corresponds to the maximum velocity of the blood moving at the centre of the vessel lumen. Δf_{\max} can be referenced to the frequency of laser light reflected from stationary tissue to calculate relative change in velocity²⁰. By utilizing two photo-detectors separated by a known angle, the maximum frequency shift detected by each photo-detector is subtracted to allow the absolute quantification of centre-line blood velocity, irrespective of the angle between the moving particle and reflected beam^{21,22}. The resulting Doppler signal is analysed using a previously

described algorithm^{21, 23}. The frequency shift is determined as the frequency at which there is an abrupt reduction in the amplitude of the fluctuations in the Doppler-shift power spectrum. This determination does not depend on any presumed shape of the average power spectral density curve.

Briefly, the CLBF simultaneously measures blood velocity (mm/sec) and vessel diameter (μm) to calculate the rate of blood flow ($\mu\text{L}/\text{min}$). The operating principles of the quantitative blood flow assessment technique have been described in detail elsewhere^{17, 24-27}. Hemodynamic measurements are corrected for magnification effects associated with axial and refractive ametropia^{25, 26}. In combination with the average velocity (V_{mean}) over a pulse cycle and diameter (D), flow (F) through the vessel can be calculated using the formula:

$$F = 1/2 \cdot \pi \cdot D^2/4 \cdot V_{\text{mean}} \cdot 60$$

where V_{mean} is the time average of the centerline blood velocity.

4.3.3.2 Sequential re-breathing circuit

The sequential re-breathing circuit design has been described in detail elsewhere^{9, 17}. It comprises a fresh gas reservoir and an expiratory gas reservoir. Each reservoir is connected to a face mask with separate one way valves. The face mask covers the mouth and nose of the subject. In turn, the two reservoirs are inter-connected using a positive end-expiratory pressure (PEEP) valve which allows subjects to breath exhaled gas (i.e. re-breathe CO_2 enriched gas) when the fresh gas reservoir is depleted^{18, 28}. This unique feature permits the sustained and stable manipulation of $F_{\text{ET}}\text{CO}_2$ in a subject by adjusting the air flow into the circuit and is independent of the minute ventilation.

4.3.4 Procedures

Subjects rested for 10 minutes prior to the start of the procedure to achieve stable baseline cardiovascular and respiratory parameters. A commercially available face mask (HiOx^{SR} Viasys Healthcare, Yorba Linda, CA), securely sealed to the subjects face using Tegaderm (Health Care, Minnesota, USA), was connected to the sequential re-breathing circuit. Flow from a gas tank containing air was controlled using generic rotometers as flowmeters. The relative concentrations of inhaled and exhaled O₂ and CO₂ were sampled continuously using a critical care gas monitor (CardiCap 5, Datex-Ohmeda, Helsinki, Finland).

For the first 15 minutes, subjects breathed bottled air at a flow equal to their minute ventilation ensuring a stable F_{ET}CO₂ and at least six CLBF measurements at the predetermined arteriolar measurement site were acquired. During the next 20 minutes, air flow was reduced until a stable increase in F_{ET}CO₂ of approximately 10-15% relative to the baseline value was achieved. CLBF measurements were acquired every minute (minimum of 6 measurements). The sequential gas delivery circuit, with a constant inflow of air, assured stable conditions during repeated CLBF measurements since it maintained the F_{ET}CO₂ constant, independent of changes in ventilation. During the final 15 minute period, air flow was again increased to restore F_{ET}CO₂ to the baseline level and at least 6 CLBF measurements were acquired. Pulse rate, blood pressure, respiration rate and finger oxygen saturation were continuously monitored.

4.3.5 Analysis

4.3.5.1 CLBF velocity waveform analysis

CLBF analysis software was used to analyze each acquired velocity waveform. A standardized protocol was used to remove aberrant portions of each waveform due to eye movements or improper vessel tracking. The maximum number of acceptable cycles for each acquisition was included in the analysis, while a minimum of one complete systolic-diastolic cycle was required for inclusion of a given waveform.

4.3.5.2 Statistical Analysis

Group mean hemodynamic and systemic parameter values of each individual were calculated for each condition (i.e. baseline, hypercapnia and post-hypercapnia). A repeated measures Analysis of Variance (reANOVA) of the mean hemodynamic and systemic parameters was performed using Statistical Analysis System (SAS v.8.02). The dependent variables were retinal arteriolar diameter, blood velocity, blood flow, systolic and diastolic blood pressure, pulse rate, respiration rate and oxygen saturation. Time (baseline, hypercapnia and post-hypercapnia) was the within subject factor. Fisher's least significant difference (LSD) protected post-hoc test was used to determine the level of significance for each hemodynamic parameter that was found to have changed significantly by re ANOVA.

4.4 Results

A sustained and stable hypercapnic provocation was achieved in all subjects ($p < 0.0001$). There was a 12.0 ± 3.6 % relative increase in $F_{ET}CO_2$ during hypercapnia. The group mean magnitude of $F_{ET}CO_2$ and fractional (i.e. %) end-tidal concentrations of O_2 ($F_{ET}O_2$) for baseline, hypercapnia and post-hypercapnia (\pm SD) are presented in (Table 4.1). There was also a concomitant statistically significant decrease in the $F_{ET}O_2$ during hypercapnia in all subjects (Figure 4.1).

Condition	$F_{ET}CO_2$ (%)	$F_{ET}O_2$ (%)
Baseline	5.1 ± 0.4	15.0 ± 0.4
Hypercapnia	5.7 ± 0.3	14.1 ± 0.6
Post-hypercapnia	5.0 ± 0.3	15.3 ± 0.3
p-value (Re ANOVA)	<0.0001	<0.0001

Table 4.1 The group mean fractional concentration of expired CO_2 and O_2 (\pm SD) as a function of condition (i.e. baseline, hypercapnia and post-hypercapnia) expressed as per cent.

The repeated measures ANOVA p-value, indicating the significance of the change of expired CO_2 and O_2 over the course of the provocation, is shown on the bottom row ($F_{ET}CO_2$; end-tidal percentage concentration of CO_2 ; $F_{ET}O_2$ end-tidal percentage concentration of O_2).

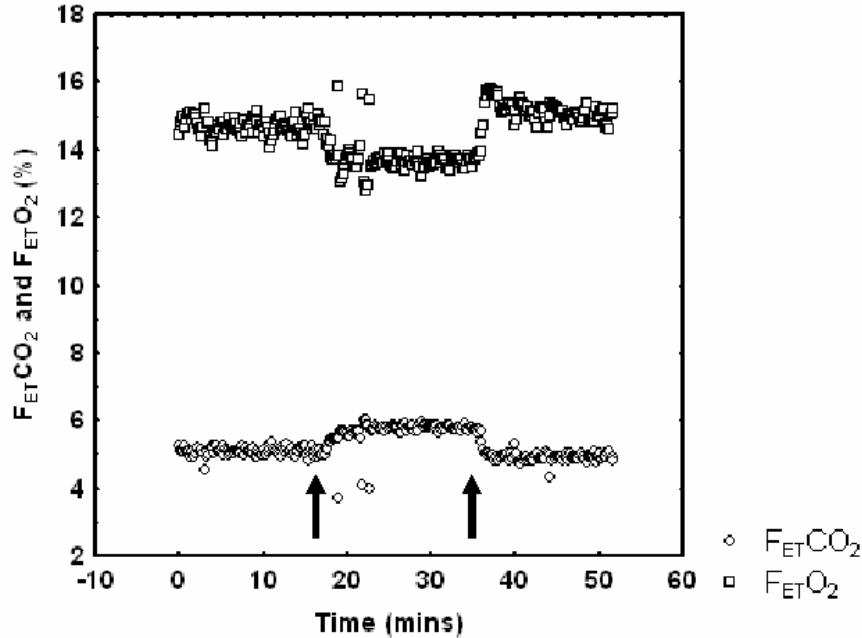


Figure 4.1 Change in $F_{ET}CO_2$ (open circles) and $F_{ET}O_2$ (open squares) of a single individual over the course of the study.

The black arrows represent the start and end of the hypercapnic stimulus.

During hypercapnia, group mean (\pm SD) retinal arteriolar diameter increased from $108.7 \pm 10.8 \mu\text{m}$ to $112.2 \pm 10.9 \mu\text{m}$ ($p=0.0045$) (Figure 4.2A) and group mean blood velocity also increased from $28.1 \pm 4.1 \text{ mm/sec}$ to $35.4 \pm 4.9 \text{ mm/sec}$ ($p<0.0001$) (Figure 4.2B). The resulting group mean arteriolar blood flow increased from $7.9 \pm 1.9 \mu\text{l/min}$ to $10.7 \pm 2.9 \mu\text{l/min}$ ($p<0.0001$) (Figure 4.2C). The magnitude of increase in retinal arteriolar diameter, blood velocity and blood flow during hypercapnia relative to baseline was $3.2 \pm 1.4 \%$, $26.4 \pm 7.0 \%$ and $34.9 \pm 8.1 \%$, respectively. Baseline magnitudes of group mean retinal arteriolar diameter, blood velocity and flow were not significantly different from recovery values.

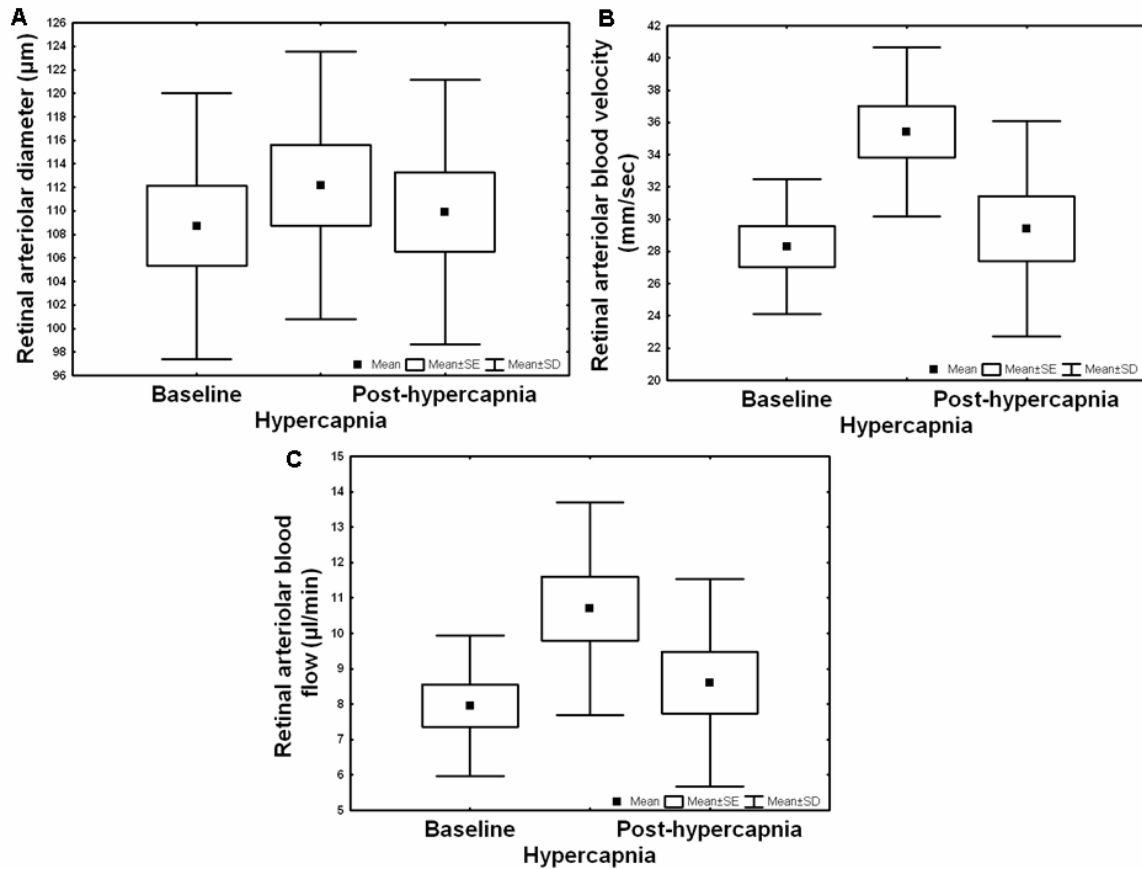


Figure 4.2 Box plot of group mean change in: A). Retinal arteriolar diameter; B). Blood velocity; and C). Blood flow as a function of condition (i.e. baseline, hypercapnia and post-hypercapnia).

Subjects did not complain of any discomfort prior to, during or post-hypercapnia. There was no significant change observed in the systolic and diastolic blood pressure, respiration rate, and oxygen saturation during hypercapnia relative to baseline (Table 4.2). However, the group mean pulse rate increased slightly from 72 beats/min to 75 beats/min during hypercapnia relative to baseline ($p=0.0120$).

Condition	Pulse Rate (beats/min)	Blood Pressure Systolic (mmHg)	Blood Pressure Diastolic (mmHg)	Respiration Rate (breaths/min)	Oxygen Saturation (%)
Baseline	72.4 ± 10.4	111.1 ± 12.0	69.8 ± 9.0	15.8 ± 2.4	97.4 ± 1.7
Hypercapnia	75.1 ± 11.1	112.1 ± 12.8	70.6 ± 8.3	15.1 ± 2.9	97.8 ± 1.5
Post-hypercapnia	73.1 ± 10.3	112.8 ± 11.9	71.1 ± 9.9	15.4 ± 1.9	98.0 ± 1.3
p-value (Re ANOVA)	p=0.0120	NS	NS	NS	NS

Table 4.2 The group mean (\pm SD) pulse rate, systolic and diastolic blood pressure, respiration rate and oxygen saturation as a function of condition (i.e. baseline, hypercapnia and post-hypercapnia).

The repeated measures ANOVA p-value, indicating the significance of the change of each parameter over the course of the provocation, is shown on the bottom row (NS; non-significant).

4.5 Discussion

This study describes a new methodology that permits the comprehensive assessment of retinal arteriolar vascular reactivity in response to a standardized, sustained and stable hypercapnic stimulus with minimal concomitant change in end-tidal PO_2 . As far as we are aware, this improvement in the standardization of the hypercapnic provocation is unique amongst the ocular blood flow literature. It also establishes the magnitude of response of the retinal arterioles to hypercapnic provocation in healthy, young subjects. We have previously demonstrated that retinal blood flow varies directly with the arterial PCO_2 , as reflected in the $P_{ET}CO_2$ ¹⁸. However, this is the first study to systematically quantify the magnitude of increase in retinal arteriolar vascular reactivity in terms of change in vessel diameter, blood velocity and flow, during sustained and stable hypercapnia.

The magnitude of increase in retinal arteriolar diameter following hypercapnic provocation found in this study is similar to previous work. Dorner and co-workers¹ determined the impact of breathing 5% CO_2 and 95% air on retinal arteriolar diameter, macular leucocyte velocity and temporal retinal vein velocity using the RVA, blue field entoptic technique and Oculix, respectively. An increase in retinal arteriolar diameter of 4.2 % (SD 1.6) was reported in their study following an approximately 21% increase in $F_{ET}CO_2$, in general agreement with our study.

Capillaries act primarily as exchange vessels while the arterioles drive the vascular reactivity response i.e. diameter is adjusted in the arteriolar resistance vessels by smooth muscle in the vessel wall resulting in gross downstream regulation of blood flow²⁹. The magnitude of

response produced by retinal capillaries during hypercapnic provocation is less⁹ compared to the magnitude of change in retinal arteriolar hemodynamics found in the present study. Using a similar sample of subjects, we have recently⁹ demonstrated a significant increase of capillary hemodynamics in the macular nasal and the foveal areas of the retina during hypercapnia using scanning laser Doppler flowmetry (SLDF) but no change was observed in the optic nerve head (ONH) and temporal macular areas. The regional differences in capillary response might be due to variations in the relative contribution of the underlying choroid to the measured signal³⁰. Also, the measurement of capillary hemodynamics using SLDF has a less favorable signal-to-noise ratio. The strong statistical outcomes in this study (e.g. $p < 0.0001$) indicate that the arteriolar vasodilation amongst the sample is consistent and the variability of the CLBF measurements merely represents the spread of homeostatic hemodynamic values.

An increase in the arterial blood CO₂ concentration has also been shown to vasodilate retinal capillaries in humans. Sponzel and co-workers¹¹ found a 26% increase in perimacular leukocyte velocity using the blue field entoptic technique after breathing carbogen. Roff and co-workers⁸ demonstrated a mean increase of 11% and 13% in blood velocity and flow using SLDF during hypercapnia but no change was observed in the ophthalmic and central retinal arteries determined by color Doppler imaging. Another study that used the SLDF to assess the hemodynamic response of the retinal vessels in young subjects showed a 15.4% and 21.2% increase in blood velocity and flow, respectively, in the superior retina in response to a 15% increase in F_{ET}CO₂⁶. The reason for the differences in magnitude of the capillary response between studies is probably explained by differences in magnitude of

hypercapnia, the stability of the provocation and the variability of SLDF measurements. In contrast to previous work, the present study assessed the magnitude of the response of the retinal arterioles (i.e. the site of vascular resistance) to a sustained and stable hypercapnic provocation.

A similar magnitude of increase in retinal blood flow in response to hypercapnia has been shown in monkeys ³¹. In addition, assessment of cerebral vascular reactivity during elevated PaCO₂ levels have also shown vasodilatation in both humans and animals ^{2, 4, 32}. Alterations in the hemodynamic parameters of retinal and cerebral blood vessels might be mediated by changes in extra cellular pH and/or release of vasoactive mediators particularly nitric oxide, but also including prostacyclin and prostaglandins, produced by the vascular endothelium ³³⁻³⁶.

Factors that regulate the tone of the retinal vasculature include endothelin derivatives and nitric oxide, both produced by the vascular endothelium ^{37, 38}. In hypercapnia induced vasodilatation, nitric oxide produced by the enzyme nitric oxide synthase is thought to be a major mediating factor ³⁹. Nitric oxide produces vasodilatation by the release of 3'5'-cyclic guanosine monophosphate (cGMP) in the smooth muscle cells leading to a decrease in intracellular calcium and dephosphorylation of myosin light chains ³⁴. Inhibition of nitric oxide synthase activity has been shown to result in a decrease of hypercapnia induced vasodilation in humans ³⁵.

In this study, sustained and stable hypercapnia was achieved with the aid of a sequential re-breathing circuit. The magnitude of hypercapnia was safe since it was well within the range experienced on a day-to-day basis. Subjects experienced no discomfort and there was no physiologically significant change observed in the blood pressure and heart rate during the provocation (Table 4.2). Only pulse rate increased by 2 to 3 beats / minute during hypercapnia, in agreement with previous studies ^{7, 13}. The concomitant decrease in $F_{ET}O_2$ during the hypercapnic period was secondary to change in $F_{ET}CO_2$. In our study, the small change in $F_{ET}O_2$ was statistically significant but nevertheless physiologically irrelevant. Hypoxia-stimulated changes in blood flow in a tissue occur in response to changes in blood oxygen saturation (SaO_2). In this study, the change in $F_{ET}O_2$ was too small to affect the SaO_2 . Furthermore, the SaO_2 was in the normal range in our subjects and was far from the threshold of the vascular response which for cerebral vessels is known to be at 88 % oxygen saturation ⁴⁰.

Harino and co-workers (1995) used the blue field entoptic technique to assess macular leukocyte velocity and a total re-breathing technique to achieve an increase in $F_{ET}CO_2$ of 33% leading to a concomitant decrease in $F_{ET}O_2$ of approximately 37%. In our study, however, $F_{ET}CO_2$ increased only by 12% with a concomitant 6% decrease in $F_{ET}O_2$. This relatively subtle increase in $F_{ET}CO_2$ was sufficient to demonstrate a substantial increase in retinal arteriolar hemodynamics. Interestingly, other studies that have used hypercapnic provocation have failed to report any change of $F_{ET}O_2$ concentration ^{41, 42}, although we anticipate such change to be greater than a 6% decrease in $F_{ET}O_2$ since none of the previous studies have utilized a sequential re-breathing circuit. Change in $F_{ET}O_2$ will act as a

confounding factor for vascular reactivity measurements during hypercapnia⁴³. Furthermore, we have developed in-house a computer driven gas flow controller that enables the independent manipulation of $F_{ET}CO_2$ and of $F_{ET}O_2$, thereby facilitating and automating the attainment of isoxic hypercapnia⁴⁴. On-going work will define the retinal vascular reactivity response to isoxic hypercapnia⁴⁵ and the influence of age and disease upon the magnitude of vascular reactivity.

4.6 Conclusions

This study describes a new methodology that permits the comprehensive assessment of retinal arteriolar vascular reactivity in response to a standardized, sustained and stable hypercapnic stimulus. It also defines the magnitude of response of the retinal arterioles to the hypercapnic provocation in healthy, young subjects. Retinal arteriolar diameter, blood velocity and blood flow increased by 3.2% (SD 1.4), 26.4% (SD 7.0) and 34.9% (SD 8.1), respectively, in response to a 12.0% (SD 3.6) rise in $F_{ET}CO_2$. These values may be used as a reference for future studies that investigate the impact of disease upon our hypercapnic provocation.

4.7 References

1. Dorner GT, Garhofer G, Zawinka C, Kiss B, Schmetterer L. Response of retinal blood flow to CO₂-breathing in humans. *Eur.J.Ophthalmol.* 2002;12:459-466.
2. Kety SS, Schmidt CF. The effect of altered arterial tensions of carbon dioxide and oxygen on cerebral blood flow and cerebral oxygen consumption of normal young men. *J.Clin.Invest.* 1948;27:484-494.
3. Meadows GE, Dunroy HM, Morrell MJ, Corfield DR. Hypercapnic cerebral vascular reactivity is decreased, in humans, during sleep compared with wakefulness. *J.Appl.Physiol.* 2003;94:2197-2202.
4. Raper AJ, Kontos HA, Patterson JL. Response of pial precapillary vessels to changes in arterial carbon dioxide tension. *Circ.Res.* 1971;28:518-523.
5. Robbins PA, Conway J, Cunningham DA, Khamnei S, Paterson DJ. A comparison of indirect methods for continuous estimation of arterial PCO₂ in men. *J.Appl.Physiol.* 1990;68:1727-1731.
6. Chung HS, Harris A, Halter PJ, et al. Regional differences in retinal vascular reactivity. *Invest.Ophthalmol.Vis.Sci.* 1999;40:2448-2453.
7. Harris A, Anderson DR, Pillunat L, et al. Laser doppler flowmetry measurement of changes in human optic nerve head blood flow in response to blood gas perturbations. *J.Glaucoma* 1996;5:258-265.

8. Roff EJ, Harris A, Chung HS, et al. Comprehensive assessment of retinal, choroidal and retrobulbar haemodynamics during blood gas perturbation. *Graefes Arch.Clin.Exp.Ophthalmol.* 1999;237:984-990.
9. Venkataraman ST, Hudson C, Fisher JA, Flanagan JG. The impact of hypercapnia on retinal capillary blood flow assessed by scanning laser doppler flowmetry. *Microvasc.Res.* 2005;69:149-155.
10. Luksch A, Garhofer G, Imhof A, et al. Effect of inhalation of different mixtures of O₂ and CO₂ on retinal blood flow. *Br.J.Ophthalmol.* 2002;86:1143-1147.
11. Sponsel WE, DePaul KL, Zetlan SR. Retinal hemodynamic effects of carbon dioxide, hyperoxia, and mild hypoxia. *Invest.Ophthalmol.Vis.Sci.* 1992;33:1864-1869.
12. Kergoat H, Faucher C. Effects of oxygen and carbogen breathing on choroidal hemodynamics in humans. *Invest.Ophthalmol.Vis.Sci.* 1999;40:2906-2911.
13. Harino S, Grunwald JE, Petrig BJ, Riva CE. Rebreathing into a bag increases human retinal macular blood velocity. *Br.J.Ophthalmol.* 1995;79:380-383.
14. Harris A, Jonescu-Cuypers CP, Kagemann L, Ciulla TA, Kreiglstein GK. Measurement of blood flow. Anonymous *In Atlas of Ocular Blood Flow Vascular Anatomy, Pathophysiology and Metabolism.* Butterwoth Heinemann; 2003. 19-70 pp.
15. Feke GT, Yoshida A, Schepens CL. Laser based instruments for ocular blood flow assessment. *Journal of Biomedical Optics* 1998;3:415-422.

16. Yoshida A, Feke GT, Mori F, et al. Reproducibility and clinical application of a newly developed stabilized retinal laser doppler instrument. *Am.J.Ophthalmol.* 2003;135:356-361.
17. Gilmore ED, Hudson C, Preiss D, Fisher J. Retinal arteriolar diameter, blood velocity, and blood flow response to an isocapnic hyperoxic provocation. *Am J Physiol Heart Circ Physiol* 2005;288:H2912-H2917.
18. Gilmore ED, Hudson C, Venkataraman ST, Preiss D, Fisher J. Comparison of different hyperoxic paradigms to induce vasoconstriction: Implications for the investigation of retinal vascular reactivity. *Invest.Ophthalmol.Vis.Sci.* 2004;45:3207-3212.
19. Sommer LZ, Iscoe S, Robicsek A, et al. A simple breathing circuit minimizing changes in alveolar ventilation during hyperpnoea. *Eur.Respir.J.* 1998;12:698-701.
20. Feke GT, Riva CE. Laser doppler measurements of blood velocity in human retinal vessels. *J.Opt.Soc.Am.* 1978;68:526-531.
21. Feke GT, Goger DG, Tagawa H, Delori FC. Laser doppler technique for absolute measurement of blood speed in retinal vessels. *IEEE Trans.Biomed.Eng.* 1987;34:673-680.
22. Riva CE, Feke GT, Eberli B. Bidirectional LDV system for the absolute measurement of blood speed in retinal vessels. *Appl.Opt.* 1979;18:2301-2306.
23. Milbocker MT, Feke GT, Goger DG. Automated determination of centerline blood speed in retinalvessels from laser doppler spectra. Anonymous *In Non-invasive assessment of the visual system.* Washington D.C.: OSA Technical Digest Series, Optical Society of America; 1988. 162-165 pp.

24. Guan K, Hudson C, Flanagan JG. Variability and repeatability of retinal blood flow measurements using the canon laser blood flowmeter. *Microvasc.Res.* 2003;65:145-151.
25. Kida T, Harino S, Sugiyama T, Kitanishi K, Iwahashi Y, Ikeda T. Change in retinal arterial blood flow in the contralateral eye of retinal vein occlusion during glucose tolerance test. *Graefes Arch.Clin.Exp.Ophthalmol.* 2002;240:342-347.
26. Nagaoka T, Mori F, Yoshida A. Retinal artery response to acute systemic blood pressure increase during cold pressor test in humans. *Invest.Ophthalmol.Vis.Sci.* 2002;43:1941-1945.
27. Sato E, Fekete GT, Menke MN, Wallace McMeel J. Retinal haemodynamics in patients with age-related macular degeneration. *Eye* 2006;20:697-702.
28. Vesely A, Sasano H, Volgyesi G, et al. MRI mapping of cerebrovascular reactivity using square wave changes in end-tidal PCO₂. *Magn.Reson.Med.* 2001;45:1011-1013.
29. Rooke TW, Sparks HVJ. An overview of the circulation and hemodynamics. R. A. Rhoades and G. A. Tanner. *In Medical Physiology.* Lippincott Williams and Wilkins; 2003. 210-218 pp.
30. Yu DY, Townsend R, Cringle SJ, Chauhan BC, Morgan WH. Improved interpretation of flow maps obtained by scanning laser doppler flowmetry using a rat model of retinal artery occlusion. *Invest.Ophthalmol.Vis.Sci.* 2005;46:166-174.
31. Tsacopoulos M, David NJ. The effect of arterial PCO₂ on relative retinal blood flow in monkeys. *Invest.Ophthalmol.* 1973;12:335-347.

32. Bayerle-Eder M, Wolzt M, Polska E, et al. Hypercapnia-induced cerebral and ocular vasodilation is not altered by glibenclamide in humans. *Am.J.Physiol.Regul.Integr.Comp.Physiol.* 2000;278:R1667-R1673.
33. Lindauer U, Vogt J, Schuh-Hofer S, Dreier JP, Dirnagl U. Cerebrovascular vasodilation to extraluminal acidosis occurs via combined activation of ATP-sensitive and Ca²⁺-activated potassium channels. *J.Cereb.Blood Flow Metab.* 2003;23:1227-1238.
34. Orgul S, Gugleta K, Flammer J. Physiology of perfusion as it relates to the optic nerve head. *Surv.Ophthalmol.* 1999;43 Suppl 1:S17-S26.
35. Schmetterer L, Findl O, Strenn K, et al. Role of NO in the O₂ and CO₂ responsiveness of cerebral and ocular circulation in humans. *Am.J.Physiol.* 1997;273:R2005-R2012.
36. Wang Q, Bryowsky J, Minshall RD, Pelligrino DA. Possible obligatory functions of cyclic nucleotides in hypercapnia-induced cerebral vasodilation in adult rats. *Am.J.Physiol.* 1999;276:H480-H487.
37. Yorio T, Krishnamoorthy R, Prasanna G. Endothelin: Is it a contributor to glaucoma pathophysiology? *J.Glaucoma* 2002;11:259-270.
38. Orgul S, Cioffi GA, Wilson DJ, Bacon DR, Van Buskirk EM. An endothelin-1 induced model of optic nerve ischemia in the rabbit. *Invest.Ophthalmol.Vis.Sci.* 1996;37:1860-1869.
39. Haefliger IO, Dettmann E, Liu R, et al. Potential role of nitric oxide and endothelin in the pathogenesis of glaucoma. *Surv.Ophthalmol.* 1999;43 Suppl 1:S51-S58.

40. Gupta AK, Menon DK, Czosnyka M, Smielewski P, Jones JG. Thresholds for hypoxic cerebral vasodilation in volunteers. *Anesth.Analg.* 1997;85:817-820.
41. Harris A, Martin BJ, Shoemaker JA. Regulation of retinal blood flow during blood gas perturbation. *Journal of Glaucoma.* 1994;3:S82-90.
42. Hosking SL, Evans DW, Embleton SJ, Houde B, Amos JF, Bartlett JD. Hypercapnia invokes an acute loss of contrast sensitivity in untreated glaucoma patients. *Br.J.Ophthalmol.* 2001;85:1352-1356.
43. Fallon TJ, Maxwell D, Kohner EM. Retinal vascular autoregulation in conditions of hyperoxia and hypoxia using the blue field entoptic phenomenon. *Ophthalmology* 1985;92:701-705.
44. Slessarev M, Fisher JA, Volgyesi G, et al. A new method and apparatus to reliably attain and maintain target end tidal gas concentrations. 2005;PCT/CA2005/001166 (In submission).
45. Venkataraman ST, Hudson C, Flanagan JG, Rodrigues L, Mardimae A, Fisher JA. Retinal arteriolar and capillary vascular reactivity assessment in response to isoxic hypercapnia. *Invest.Ophthalmol.Vis.Sci.* 2006;47:E-Abstract 490.

5 Retinal Arteriolar and Capillary Vascular Reactivity in Response to Isoxic Hypercapnia

Venkataraman ST, Hudson C, Fisher JA, et al. Retinal arteriolar and capillary vascular reactivity in response to isoxic hypercapnia. *Exp. Eye Res.* 2008. Dec; 87 (6): 535-542.

Reprinted by permission from Elsevier publishers.

5.1 Abstract

The aim of the study was to compare the magnitude of vascular reactivity of the retinal *arterioles* in terms of percentage change to that of the retinal *capillaries* using a novel, standardized methodology to provoke isoxic hypercapnia.

Ten healthy subjects (mean age 25yrs, range 21–31) were recruited. Subjects attended for a single visit comprising two study sessions separated by 30 minutes. Subjects were fitted with a sequential re-breathing circuit connected to a computer-controlled gas blender. Each session consisted of breathing at rest for 10min (baseline), increase of PETCO₂ (maximum partial pressure of CO₂ during expiration) by 15% above baseline whilst maintaining isoxia for 20 minutes, and return to baseline conditions for 10 minutes. Retinal hemodynamic measurements were performed using the Canon Laser Blood Flowmeter and the Heidelberg Retina Flowmeter in random order across sessions.

Retinal *arteriolar* diameter, blood velocity and flow increased by 3.3%, 16.9% and 24.9% ($p < 0.001$), respectively, during isoxic hypercapnia. There was also an increase of *capillary*

blood flow of 34.8%, 21.6%, 24.9% ($p \leq 0.006$) at the optic nerve head neuroretinal rim, nasal macula and fovea, respectively. The co-efficient of repeatability (COR) was 5% of the average PETCO₂ both at baseline and during isoxic hypercapnia and was 10% and 7% of the average PETO₂ (minimum partial pressure of oxygen at end exhalation), respectively.

The magnitude of retinal *capillary* vascular reactivity was equivalent to the *arteriolar* vascular reactivity with respect to percentage change of flow. The magnitude of isoxic hypercapnia was repeatable.

Keywords: Retina, blood flow, laser Doppler flowmetry, hypercapnia, PETCO₂, PETO₂.

5.2 Introduction

Vascular reactivity is the magnitude of change in retinal hemodynamic measurements to provocative stimuli, such as that elicited by change in arterial blood partial pressure of carbon dioxide (PaCO_2) or oxygen (PaO_2). As the measurement of PaCO_2 is invasive and painful, the partial pressure of CO_2 in end-tidal gas (PETCO_2) is often used as a surrogate for PaCO_2 ¹. Previous research has used various techniques to raise PETCO_2 including the addition of CO_2 to inspired air²⁻¹⁵, and the total rebreathing of exhaled gas¹⁶. Each of these methods is associated with a variable concomitant change in end-tidal PO_2 (PETO_2). Inhaling CO_2 results in an unpredictable increase in ventilation and thereby an unpredictable increase in PETO_2 ¹⁷. Previous studies have failed to consider concomitant changes in PaO_2 during hypercapnia and the derived vascular reactivity values thereby represent change induced by manipulation of PaO_2 as well as PaCO_2 . In our experience, inducing a 10-15% increase in PETCO_2 by the manual addition of CO_2 to inspired air increased PETO_2 by 13%¹³, while PETO_2 was reduced by 6% when using a manually controlled partial re-breathing technique¹⁴.

We have developed a partial re-breathing approach that utilizes computer control of inspired gases to achieve consistent changes in PETCO_2 and in PETO_2 in a subject independent of each other and independent of minute ventilation, in order to primarily study retinal and cerebral vascular reactivity (RespirAct™, Thornhill Research Inc., Toronto Canada). The aim of the current study was to compare the percentage change of the magnitude of vascular reactivity of retinal *arterioles* to that of the retinal *capillaries* using a novel, standardized methodology to provoke isoxic hypercapnia. The magnitude of vascular reactivity in response to isoxic

hypercapnia is hypothesized to be equivalent in retinal arterioles and capillaries since the retinal circulation is a closed system, i.e. any percentage change in flow in the arterioles would be expected to be similarly reflected in the downstream capillaries. In addition, it is critical to use a repeatable magnitude of PETCO₂ elevation during hypercapnia to reduce the variability in vascular reactivity assessment. A secondary aim therefore was to assess the repeatability of targeted PETCO₂ in normocapnic and hypercapnic phases.

5.3 Materials and methods

5.3.1 Sample

The study was approved by the Research Ethics Boards of the University Health Network, University of Toronto, and the Office of Research Ethics, University of Waterloo. All subjects provided signed informed consent prior to agreeing to participate, after explanation of the nature and possible consequences of the study according to the tenets of the Declaration of Helsinki. Ten healthy subjects (8 females) of mean age 25 years (SD 3.2, range 21-31 years) participated in this study. Subjects had corrected visual acuity of 6/6 or better. Exclusion criteria included respiratory disorders, cardiovascular diseases, systemic hypertension, habitual smoking, refractive error greater than $\pm 6.00\text{DS}$ and $\pm 1.50\text{DC}$, any ocular disease, immediate family history of glaucoma, and/or diabetes, and medications with known effects on blood flow (e.g. antihypertensive medication and medication with activity at autonomic receptors, smooth muscles, or those affecting NO release).

5.3.2 Instrumentation

5.3.2.1 Gas delivery system

A sequential gas delivery (SGD) breathing circuit (Hi-Ox⁸⁰, ViasysHealthcare, Yorba Linda CA) was assembled by placing a rebreathing bag on the expiratory port of a commercial 3-valve oxygen delivery system. This breathing circuit has been described in detail elsewhere^{13, 14, 18, 19}. The SGD allows subjects to breath exhaled gas (i.e. re-breathe CO₂ enriched gas) when the fresh gas reservoir is depleted²⁰.

Algorithms have previously been derived relating subject minute CO₂ production and O₂ consumption, gas flow and composition entering the SGD circuit to values of PETCO₂ and PETO₂²¹. These algorithms have been set up in a computer-controlled gas blender to provide the gas flow to the SGD (RespirAct™, Thornhill Research Inc., Toronto Canada) (Figure 5.1). The software allows the user to choose a series of target PETCO₂ and PETO₂ and the duration of each targeted phase.

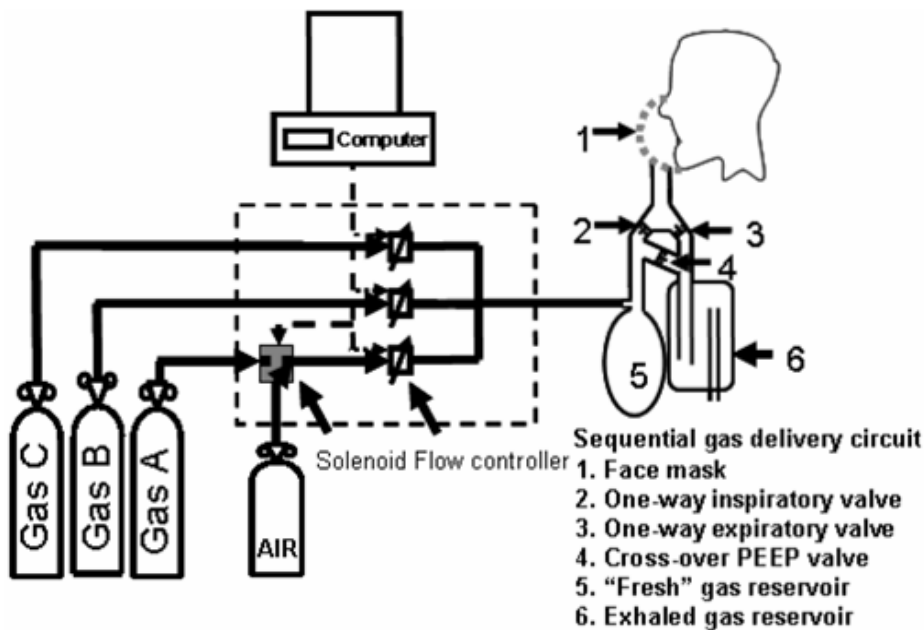


Figure 5.1 Schematic representation of the gas flow controller attached to a sequential gas delivery system.

5.3.2.2 Retinal blood flow assessment

5.3.2.2.1 Scanning Laser Doppler Flowmetry of Capillaries

The principle and details of the SLDF have been detailed elsewhere^{2, 13, 22}. It is based on the principle of the Doppler effect. SLDF measurements were undertaken using the Heidelberg

Retina Flowmeter (HRF; Heidelberg Engineering GmbH, Dossenheim, Germany, software version 1.03W). The HRF-derived assessment of capillary flow and vascular reactivity represents an indirect measurement of vascular function since it measures the frequency of the intensity oscillation attributable to red blood cell movement in a volume of tissue.

5.3.2.2.2 Laser Doppler Flowmetry of Arterioles

The principle and technical details of the Canon Laser Blood Flowmeter (CLBF; Model 100, Canon, Tokyo, Japan) have been detailed elsewhere ^{14, 18, 23-28}. It is based on the principle of bi-directional laser Doppler velocimetry and simultaneous vessel densitometry. The CLBF simultaneously measures blood velocity (mm/sec) and vessel diameter (μm) to calculate the rate of blood flow ($\mu\text{L}/\text{min}$).

5.3.3 Procedures

Subjects were asked to refrain from caffeine-containing food or drinks for 24 hours prior to the study. Subjects were rested for 15 minutes prior to the start of the breathing paradigm. The study was performed during a single visit using two sessions separated by at least 30 minutes in order to measure retinal vascular reactivity with both the CLBF and the HRF: the order of use of the instruments was systematically varied between sessions. Each session lasted approximately 40 minutes.

All participants underwent Heidelberg Retina Tomograph (HRT) imaging before the start of the protocol to determine the difference in the focus between the temporal rim of the optic

nerve head (ONH) and the peripapillary retina. This data was then used to establish the optimal focus setting during the HRF imaging of the temporal rim, thereby optimizing the sampling of the anterior ONH capillaries²⁹. The HRF focus and sensitivity settings were maintained constant during all phases of the breathing paradigm.

The mask of the breathing circuit was sealed to the face using adhesive tape (Tegaderm, 3M Health Care, St Paul, MN, USA). Initially air flow was set to exceed minute ventilation and thus prevent rebreathing. Tidal gas concentrations were monitored continuously. When PETCO₂ became stable (less than 2 mmHg change over 2 min), end-tidal and mixed exhaled O₂ and CO₂ partial pressures were calculated from gas sampled from the face mask and the exhaled gas reservoir, respectively. CO₂ production was calculated automatically by the computer-controlled gas blender as the product of air flow entering the breathing circuit and the mixed expired concentrations of CO₂^{30 31}. O₂ consumption was calculated as the product of air flow and the difference in O₂ concentration in air and mixed exhaled gas. Three gas stages were implemented at each session. In the first stage, gas flow into the breathing circuit was adjusted to provide a PETCO₂ of 38 mmHg at resting PETO₂ (baseline) and this stage was maintained for 10 min (or longer if stability of end-tidal gases or systemic parameters could not be attained). In the second stage, PETCO₂ was raised by 15% while maintaining isoxia for 20 min. In the third stage, PETCO₂ was returned to baseline levels for a further 10 min while again maintaining isoxia. An example of the change in PETCO₂ over time and the concomitant stable PETO₂ in one subject is shown in (Figure 5.2).

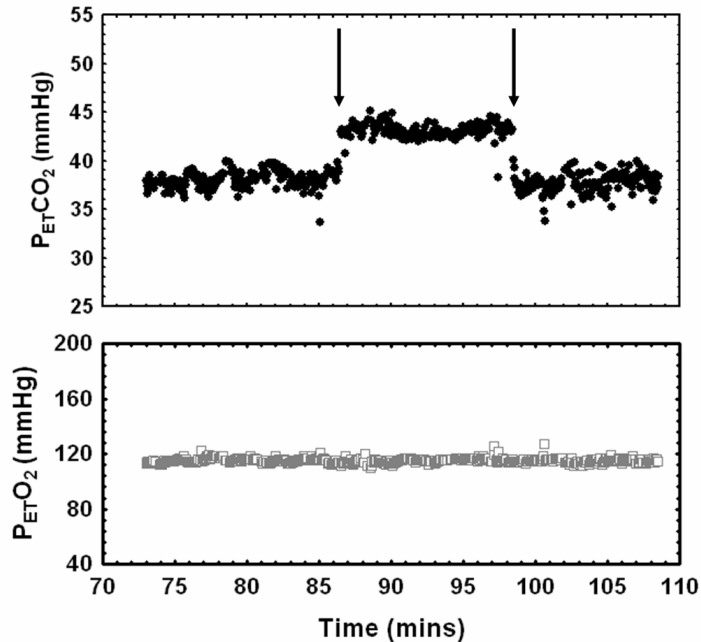


Figure 5.2 Change in P_{ETCO_2} (upper) and simultaneous constant P_{ETO_2} (lower) in one individual using the gas flow controller.

The arrows in the P_{ETCO_2} graph represent start and end of isoxic hypercapnia.

Retinal blood flow measurements were acquired at each stage. At least 3 good quality HRF images each centered on the ONH and at least 3 images centered on the macula were acquired at each stage. HRF images of the ONH were acquired to subsequently calculate temporal neuroretinal rim capillary blood flow, while macular images were acquired to calculate capillary blood flow for the nasal, foveal and temporal areas. At the other session, 5 CLBF measurements of a relatively straight segment, distant from bifurcations of the superior or inferior temporal arteriole were acquired at each stage. Blood pressure was monitored every 2.5 minutes while pulse rate and oxygen saturation was measured every minute during the breathing period using a rapid response critical care gas analyzer (Cardiocap 5, Datex-Ohmeda, Helsinki, Finland).

5.3.4 Analysis

5.3.4.1 Gas parameters analysis

The gas parameters were analysed using Lab view software (National Instruments, version 7.1). Tidal concentrations of CO₂ and O₂ were measured continuously. PETCO₂ and PETO₂ were calculated breath-by-breath as the maximum PCO₂ value and minimum PETO₂ value, respectively, during exhalation. PETCO₂ and PETO₂ values were averaged over the time of blood flow measurement at each stage.

5.3.4.2 SLDF image analysis

Capillary blood flow values of the temporal ONH neuroretinal rim, macula nasal, foveal and macula temporal areas were analysed using the Automated Full Field Perfusion Image Analysis (AFFPIA) software version 3.3²². The analysis software comprised two concentric circles of variable radius, up to a maximum of 2.5°, that were placed in the measurement areas. Capillary blood flow was calculated within the areas defined by the measurement circles. Using this technique, capillary blood flow values of the various macular areas were calculated using the total area within a 2.5° diameter outer circle only. Blood flow values were calculated for the temporal rim of the ONH based upon the radius area defined by the outer and inner circles placed and adjusted in diameter to define the outer and inner edge of the temporal neural rim, respectively. AFFPIA avoids any possible influence of larger retinal blood vessels by excluding Doppler signals that are outside the valid measurement range of the HRF photodetector and erroneous blood flow data due to eye movements are also excluded^{22, 32, 33}.

5.3.4.3 CLBF velocity waveform analysis

CLBF analysis software was used to analyze each acquired velocity waveform. A standardized protocol was employed to remove aberrant portions of each waveform due to eye movements or improper vessel tracking. The maximum number of acceptable waveforms in each measurement was included for analysis (minimum of one complete cycle required).

5.3.4.4 Statistical Analysis

A Repeated Measures Analysis of Variance (reANOVA) with Greenhouse-Geisser correction was used to determine the significance of any change of each of the dependent variables using SAS version 9.1. The dependent variables for retinal capillary hemodynamics were ONH blood flow, macula nasal, foveal and macula temporal blood flow, while the dependent variables for retinal arteriolar hemodynamics were diameter, blood velocity and flow. In addition, separate ANOVAs were performed to determine the significance of any change of PETCO₂, PEO₂, respiration rate, pulse rate, systolic and diastolic blood pressure and oxygen saturation. Statistical significance was Bonferroni adjusted to a level of $p < 0.01$ due to multiple reANOVAs performed on the gas, systemic and retinal hemodynamic parameters. The PETCO₂ and PEO₂ measurements of each subject at baseline and hypercapnia in both sessions were compared using reANOVA with session and condition as within factors. A Bland and Altman ^{34, 35} approach was used to assess the repeatability of the PETCO₂ and PEO₂ measurements across the study sessions during baseline and hypercapnic provocation.

5.4 Results

Retinal arteriolar and capillary vascular reactivity increased during isoxic hypercapnia. There was a 3.3% (SD 2.0, $p < 0.001$), 16.9% (SD 9.0, $p < 0.001$) and 24.9% (SD 7.0, $p < 0.001$) increase in retinal arteriolar diameter, blood velocity and blood flow in response to isoxic hypercapnia (Figure 5.3). Retinal capillary blood flow showed a 34.8% (SD 31.0, $p < 0.001$) increase at the rim of the ONH (Figure 5.4) and a 21.6% (SD 15.4, $p < 0.001$) and 24.9% (SD 18.4, $p = 0.006$) increase at the macula nasal and foveal areas (Figure 5.5), respectively. There was a non-significant 8.2% (SD 7.9, $p = 0.028$) trend for capillary blood flow to increase in the macula temporal area. The combined percent change in flow of retinal capillary vascular reactivity (i.e. all 4 analyzed areas = 22.4%) was similar to the magnitude of arteriolar (= 24.9%) vascular reactivity.

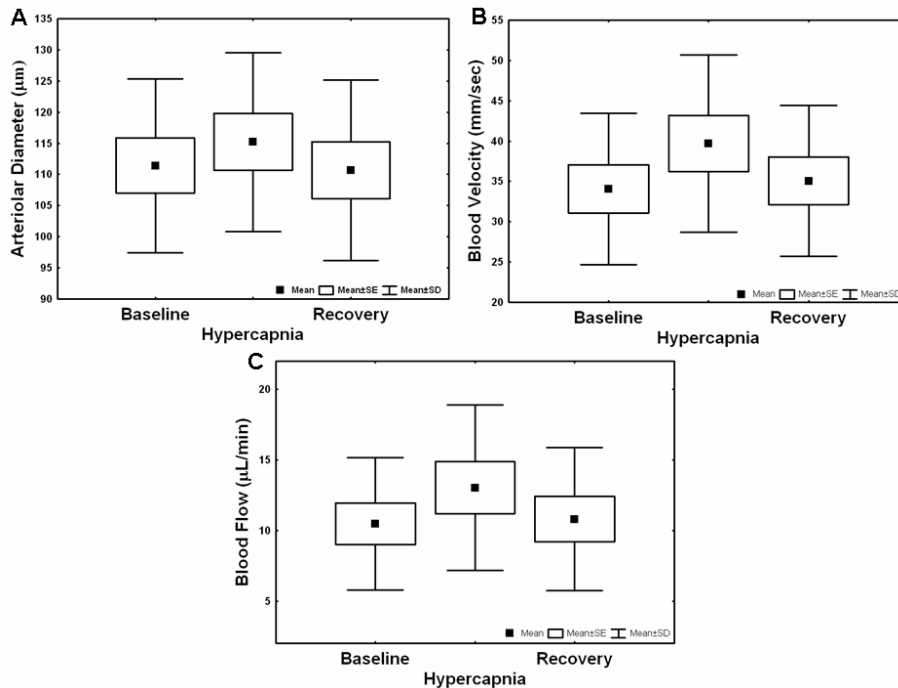


Figure 5.3 Box plot represents the group mean: A) retinal arteriolar diameter; B) blood velocity; and C) blood flow at baseline, isoxic hypercapnia and recovery.

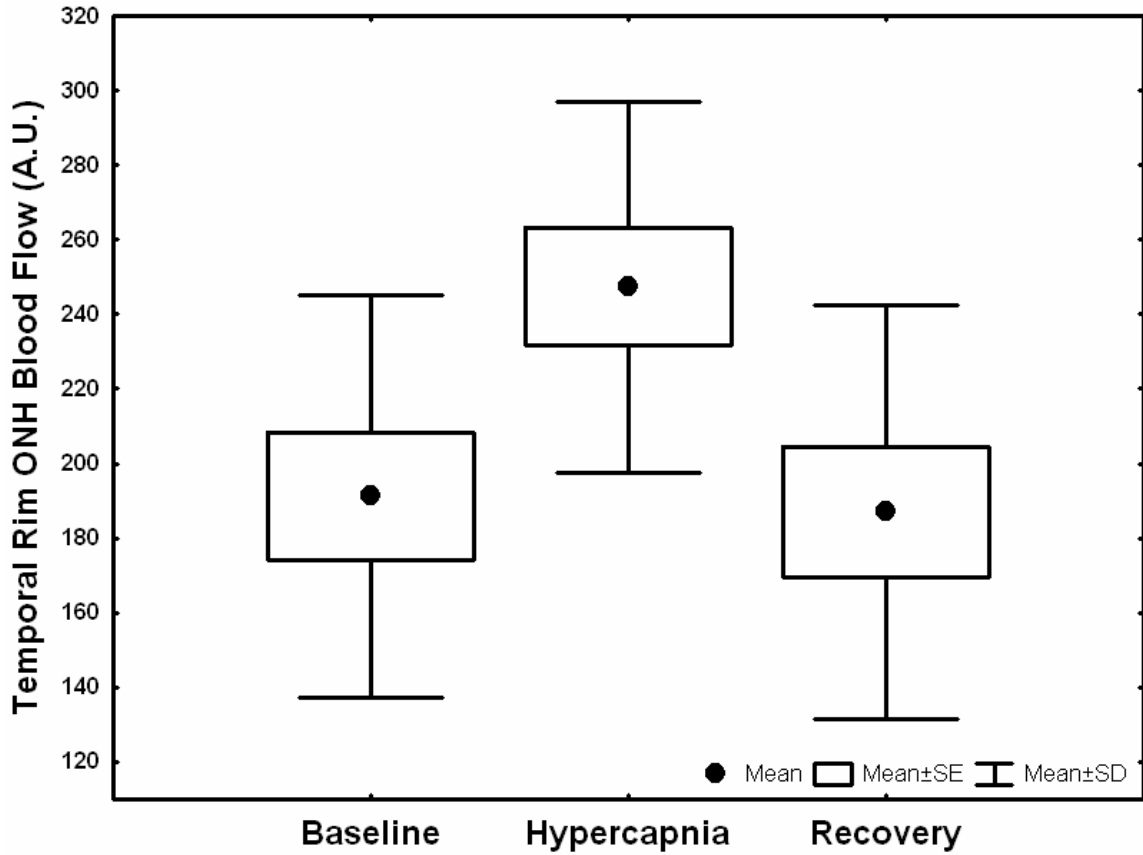


Figure 5.4 Box plot represents the group mean capillary blood flow at the temporal rim of the ONH at baseline, isoxic hypercapnia and recovery.

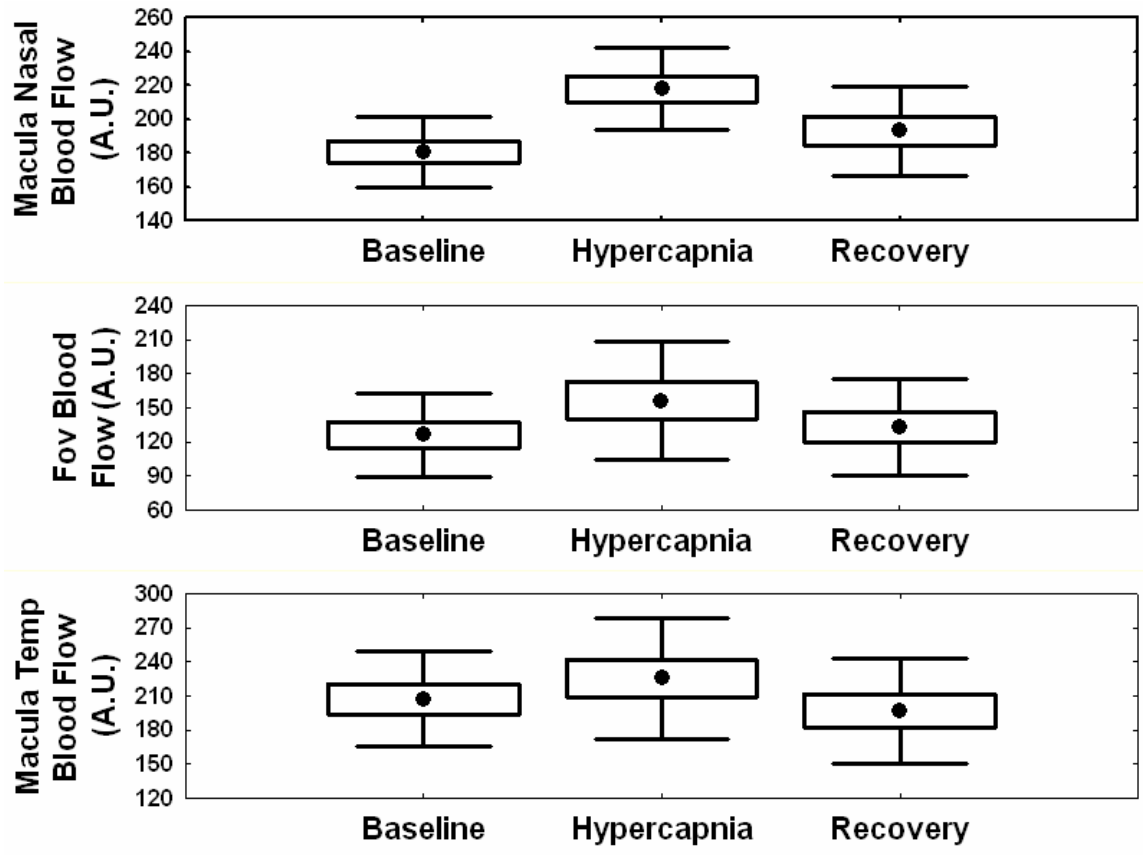


Figure 5.5 Box plot represents the group mean capillary blood flow at the macula nasal, foveal and macula temporal areas at baseline, isoxic hypercapnia and recovery.

Participants were comfortable and were able to sustain hypercapnia during the study. A 14.1% (SD 2.4) ($p < 0.001$) and 14.6% (SD 2.2) ($p < 0.001$) increase in $PETCO_2$ was achieved during the first and the second study sessions, respectively. There was a 4.2% ($p < 0.001$) and 4.4% ($p < 0.001$) concomitant increase in $PETO_2$ at the first and second sessions, respectively. The group mean magnitude of end-tidal CO_2 and O_2 concentrations at baseline, hypercapnia and recovery across the two study sessions are shown in (Tables 5.1 & 5.2).

Pulse rate ($p = 0.002$) and systolic blood pressure ($p = 0.005$) showed an increase during hypercapnia at session 1 but only pulse rate showed a significant increase at session 2

($p=0.003$). There was no other change observed in any of the measured systemic parameters (Tables 5.1 & 5.2).

The coefficient of repeatability (COR) in PETCO₂ measurements across the two sessions at baseline was 2mmHg and during isoxic hypercapnia was 2.4mmHg relative to a group mean PETCO₂ of 39mmHg and 44.5mmHg, respectively (Figure 5.6). The COR in PETO₂ measurements across the two study sessions at baseline was 10.5mmHg and during isoxic hypercapnia was 7.7mmHg relative to a group mean PETO₂ of 106.4mmHg and 110.6mmHg, respectively (Figure 5.6). Repeated measures ANOVA of the magnitude of change in PETCO₂ and PETO₂ measurements during hypercapnia did not show a significant difference across the two study sessions.

Parameters (n=10)	Baseline	Hypercapnia	Recovery	Re ANOVA
PETCO ₂ (mmHg)	39.1 ± 1.1	44.6 ± 1.4	38.6 ± 1.1	p<0.001
PETO ₂ (mmHg)	106.5 ± 5.8	110.7 ± 3.7	107.5 ± 5.0	p<0.001
Respiration rate (breaths/min)	19.5 ± 5.4	22.5 ± 4.2	22.3 ± 5.1	NS
Pulse rate (beats/min)	74.4 ± 12.1	79.3 ± 13.8	77.0 ± 14.1	p=0.002
Blood pressure (Systolic) mmHg	110.4 ± 9.3	114.6 ± 8.0	112.9 ± 9.0	p=0.005
Blood pressure (Diastolic) mmHg	71.1 ± 4.8	73.7 ± 5.1	72.6 ± 5.9	NS
O ₂ saturation (%)	99.2 ± 0.6	99.2 ± 0.5	99.3 ± 0.4	NS

Table 5.1 Group mean (± SD) end-tidal partial pressure of CO₂ & O₂, respiration rate, pulse rate, systolic & diastolic blood pressure and oxygen saturation across different breathing conditions (i.e., baseline, isoxic hypercapnia and recovery) in the first session.

Parameters (n=10)	Baseline	Hypercapnia	Recovery	Re ANOVA
PETCO ₂ (mmHg)	38.9 ± 1.1	44.5 ± 0.9	38.6 ± 1.0	p<0.001
PETO ₂ (mmHg)	106.2 ± 3.4	110.8 ± 3.1	107.6 ± 3.6	p<0.001
Respiration rate (breaths/min)	22.0 ± 6.3	22.5 ± 5.0	22.4 ± 5.3	NS
Pulse rate (beats/min)	76.6 ± 11.7	80.8 ± 13.8	79.1 ± 12.4	p=0.003
Blood pressure (Systolic) mmHg	111.5 ± 9.3	113.8 ± 8.6	112.0 ± 8.2	NS
Blood pressure (Diastolic) mmHg	69.9 ± 6.6	72.3 ± 6.0	72.4 ± 6.2	NS
O ₂ saturation (%)	99.0 ± 0.6	99.2 ± 0.5	99.3 ± 0.4	NS

Table 5.2 Group mean (± SD) end-tidal partial pressure of CO₂ & O₂, respiration rate, pulse rate, systolic & diastolic blood pressure and oxygen saturation across different breathing conditions (i.e., baseline, isoxic hypercapnia and recovery) in the second session.

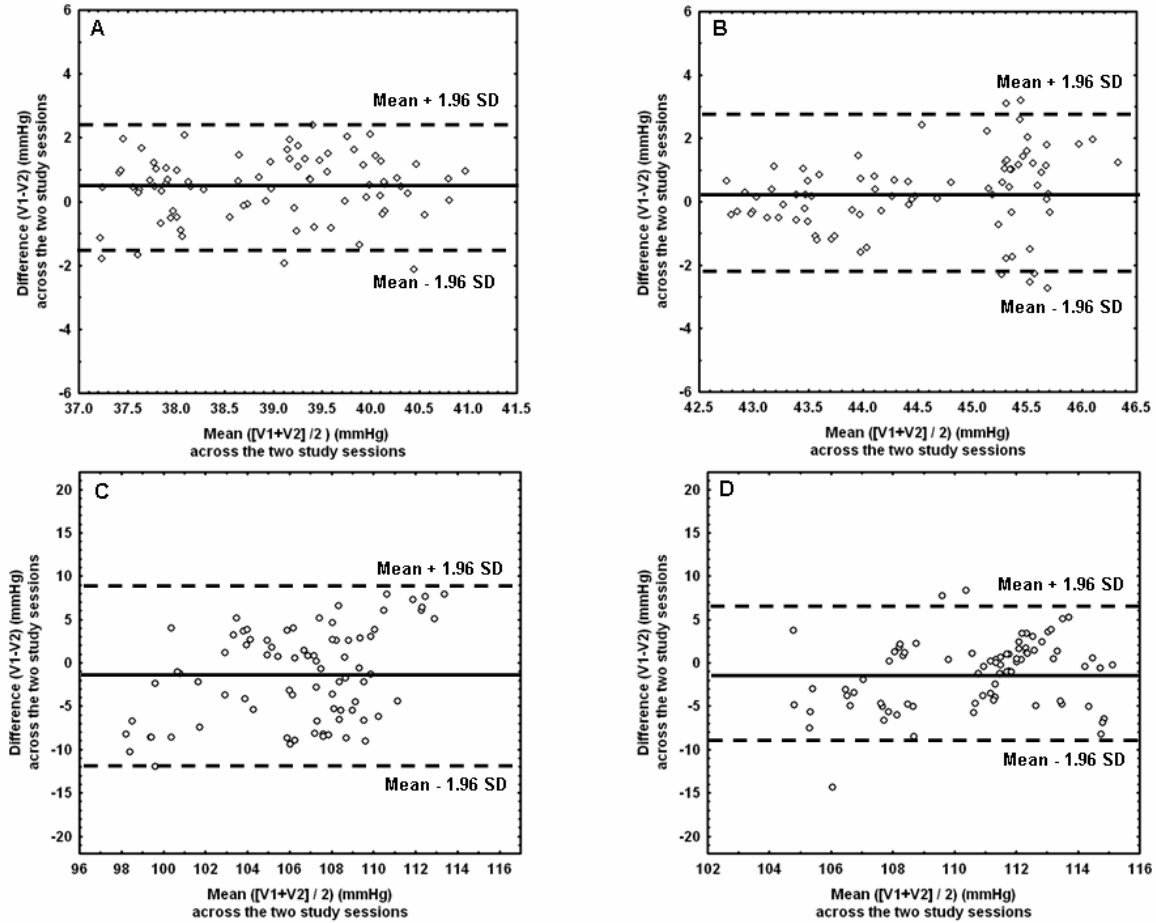


Figure 5.6 Bland and Altman plot of the difference (V1-V2) (mmHg) plotted against the mean $\{[V1 + V2]\} / 2$ (mmHg) across the two study sessions.

A) PETCO₂ (mmHg) at baseline; B) PETCO₂ (mmHg) during isoxic hypercapnia; C) PETO₂ (mmHg) at baseline; and D) PETO₂ (mmHg) during isoxic hypercapnia.

The solid line represents mean of the difference in the PETCO₂ and PETO₂ parameters. The dotted lines represent $\pm 1.96SD$ of the mean difference.

5.5 Discussion

In this study, we provided an automated, standardized and repeatable isoxic hypercapnic stimulus to provoke retinal *capillary* and *arteriolar* vascular reactivity. Vascular reactivity was calculated as the change between baseline and effect in retinal diameter, velocity and blood flow for arterioles and retinal and ONH blood flow for capillaries, for a given change in PETCO₂. Retinal arterioles and capillaries showed a significant increase in hemodynamics in response to an approximately 14% increase in PETCO₂. The overall magnitude of retinal capillary vascular reactivity (i.e. all 4 analyzed areas = 22.4%) was comparable to the arteriolar (= 24.9%) vascular reactivity in terms of percentage change of flow.

The results of the present study define the magnitudes of vascular reactivity with only minimal change in PETO₂. The magnitude of isoxic hypercapnia induced using the computer controlled gas blender was repeatable. Previous work in our laboratory showed a 13% increase in PETO₂ using the manual addition of CO₂ to inspired air¹³ and a 6% decrease in P_{ET}O₂ concentration using a manually controlled partial re-breathing technique¹⁴. In the few studies that have given consideration to concomitant changes in PaO₂ during hypercapnia, there has been a large concomitant change in PETO₂ reported. Gugleta and co-workers³⁶ showed an approximately 23% increase in PaO₂ as a result of 19% increase in PaCO₂ using the addition of 5% CO₂ to inspired air. To our knowledge, the current study is the first to have concomitantly assessed retinal arteriolar and capillary vascular reactivity using a highly repeatable hypercapnic provocation that reduces the disturbance of PETO₂ to a minimum (i.e. +4%). Although statistically significant, the +4% change in PETO₂ in this study is physiologically irrelevant. To explain, Gilmore and co-workers (2005) increased PETO₂ from

15.1% to 86.2% whilst maintaining isocapnia; this provoked a reduction in retinal arteriolar blood flow of $-4.3\mu\text{L}/\text{min}$. Therefore, a +4% change in PETO_2 would be anticipated to reduce retinal blood flow by approximately $0.24\mu\text{L}/\text{min}$ (assuming linear response characteristics)

18

The improved control of PETO_2 during hypercapnic provocation can be attributed to the combination of the sequential re-breathing circuit and the computer controlled gas blender. The use of the computer controlled gas blender permitted the normalization of all subjects' baseline PETCO_2 measurements to approximately 38mmHg, thereby facilitating a standardised increase in PETCO_2 during hypercapnia. Another advantage of using the computer controlled gas blender is the ability to achieve target end-tidal gas values within a short period of time, thereby minimizing subject discomfort, and this resulted in a sustained "square wave" increase in PETCO_2 levels. The isoxic hypercapnic provocation achieved using the computer controlled gas blender was repeatable. The COR was 5% of the average PETCO_2 both at baseline and during isoxic hypercapnia. Similarly, the COR was 10% and 7% of the average PETO_2 at baseline and during isoxic hypercapnia, respectively.

Breathing CO_2 has been shown to increase blood pressure in healthy subjects³⁷. In the present study, we observed an increase in systolic blood pressure during the first session and an increase in pulse rate at both sessions. The magnitude of increase in blood pressure during hypercapnia, however, was small and well within the range of autoregulation of the retinal vessels and would not be expected to have an influence on vascular reactivity^{38, 39}. Similar

changes in the magnitude of blood pressure and pulse rate have been observed in other studies during hypercapnia in healthy subjects and patients with vasospasm^{3, 5, 36, 40, 41}.

Evidence from the cerebral vasculature suggests that smaller diameter vessels produce a relatively larger magnitude of vascular reactivity in response to gas provocations^{42, 43}. A few studies have found the same relationship between retinal vascular reactivity and vessel diameter in the retinal microvasculature⁴⁴⁻⁴⁶. In addressing the primary aim of the present study, however, the magnitude of retinal capillary vascular reactivity in terms of change in blood flow was generally comparable to that of the retinal arterioles in percentage change. The results of our study might not be directly comparable to previous work due to the differences in both the provocation and methods of quantifying the hemodynamic responses. In addition, some studies have also failed to monitor and / or report concomitant changes in PETO₂. Jeppesen and co-workers⁴⁶ investigated the diameter response of retinal vessels to change in systemic blood pressure and showed that smaller diameter retinal arterioles have a larger magnitude of vascular reactivity.

The magnitude of retinal vascular reactivity achieved in this study is in broad agreement with previous work. Harino and co-workers¹⁶ used a subjective-based blue field entoptic methodology and a total re-breathing technique to induce hypercapnia and showed a 53% increase in leucocyte velocity. Dorner and co-workers⁵ achieved a 21% increase in PETCO₂ and, as a result, retinal arteriolar diameter and venular diameter increased by 4.2% and 3.2%, respectively. Recent work in our laboratory showed a 3.2%, 26% and 35% increase in

arteriolar diameter, blood velocity and flow in response to hypercapnia, produced using a manually controlled partial re-breathing technique ¹⁴.

Few studies have investigated retinal capillary vascular reactivity in response to hypercapnia using the SLDF technique. Chung and co-workers (1999) ⁸ observed an increase in supero-temporal capillary blood flow with a 15% increase in PETCO₂. Roff and co-workers ² showed a 39% increase in capillary blood flow in the supero-temporal retina. Previous research from our own laboratory showed a 10.2% increase in ONH, 18.9%, 15.8% and 16.9% in the macula nasal, foveal and macula temporal areas, respectively, using a partial re-breathing technique to induce hypercapnia ¹³. In the current study, we observed a similar magnitude of capillary vascular reactivity in the macula nasal and foveal areas and a relatively larger magnitude of change in the ONH.

The SLDF is used typically to assess capillary blood flow in the anterior ONH but also in other retinal areas. The blood supply to the pre-laminar portion of the ONH is derived from the branches of short posterior ciliary arteries (SPCAs) ^{47, 48}. The superficial nerve fiber layer of the ONH transitions from principally the SPCA supply next to the pre-laminar region to predominantly the central retinal artery supply at the level of the internal limiting membrane. The measured ONH vascular reactivity reported in this study primarily reflects the response of the SPCAs and the downstream branch arterioles. There is evidence that blood flow measured in the macular and foveal areas using the HRF might have a contribution from the underlying choroid ⁴⁹. We were careful, however, to focus the HRF at the level of the retinal nerve fibre layer or superficial temporal rim of the ONH. Nevertheless, choroidal

contribution to the measured signal could possibly be the reason for the regional variations in the magnitude of capillary vascular reactivity. Previous studies have shown that the choroidal vessels fail to show any metabolic regulation. More recently, Lovasik and co-workers (2003)⁵⁰ have demonstrated that choroidal vessels do indeed respond to changes in ocular perfusion pressure but to a lesser degree than the inner retinal vessels. As a result, the HRF-derived measurements of capillary vascular reactivity may represent the combined responses of the inner and outer retinal vessels.

Recently, studies have shown that the HRF results might be influenced by extraneous factors including measurement position and sampling depth in the retina^{49, 51, 52}. The results of our study cannot be compared to any of these papers because the retinal area imaged was carefully chosen to avoid large diameter blood vessels. In addition, AFFPIA was used to obtain retinal and ONH perfusion values which effectively eliminated flow signals from large blood vessels (retinal vessel diameter >30 μm) and also removed data from image pixels influenced by eye movements. Optimal focus setting was established from tomographic depth measurements, thereby optimizing the sampling of the anterior ONH capillaries²⁹.

In this study, the use of the computer controlled gas blender provided a standardised means of provoking isoxic hypercapnia in young, healthy subjects. This standardised stimulus could be used in a clinical setting to investigate diseases that are thought to result in vascular dysregulation such as glaucoma, diabetic retinopathy and age-related macular degeneration to accurately assess vascular reactivity and function.

5.6 Conclusions

In this study, a computer controlled gas blender was utilized to induce isoxic hypercapnia and the magnitude of retinal capillary and arteriolar vascular reactivity was quantified. Retinal arterioles and capillaries showed an increase in hemodynamic parameters to approximately a 14% increase in $PETCO_2$. The magnitude of retinal *capillary* vascular reactivity was comparable to the *arteriolar* vascular reactivity in terms of percentage change of flow, consistent with expectation based upon the fact that the retinal circulation is a closed system. The magnitude of isoxic hypercapnia induced using the gas flow controller was repeatable and the concomitant change in $PETO_2$ was physiologically irrelevant.

5.7 References

1. Robbins PA, Conway J, Cunningham DA, Khamnei S, Paterson DJ. A comparison of indirect methods for continuous estimation of arterial PCO₂ in men. *J.Appl.Physiol.* 1990;68:1727-1731.
2. Roff EJ, Harris A, Chung HS, et al. Comprehensive assessment of retinal, choroidal and retrobulbar haemodynamics during blood gas perturbation. *Graefes Arch.Clin.Exp.Ophthalmol.* 1999;237:984-990.
3. Luksch A, Garhofer G, Imhof A, et al. Effect of inhalation of different mixtures of O₂ and CO₂ on retinal blood flow. *Br.J.Ophthalmol.* 2002;86:1143-1147.
4. Kergoat H, Faucher C. Effects of oxygen and carbogen breathing on choroidal hemodynamics in humans. *Invest.Ophthalmol.Vis.Sci.* 1999;40:2906-2911.
5. Dorner GT, Garhoefer G, Zawinka C, Kiss B, Schmetterer L. Response of retinal blood flow to CO₂-breathing in humans. *Eur.J.Ophthalmol.* 2002;12:459-466.
6. Pakola SJ, Grunwald JE. Effects of oxygen and carbon dioxide on human retinal circulation. *Invest.Ophthalmol.Vis.Sci.* 1993;34:2866-2870.
7. Arend O, Harris A, Martin BJ, Holin M, Wolf S. Retinal blood velocities during carbogen breathing using scanning laser ophthalmoscopy. *Acta Ophthalmol (Copenh)* 1994;72:332-336.

8. Chung HS, Harris A, Halter PJ, et al. Regional differences in retinal vascular reactivity. *Invest.Ophthalmol.Vis.Sci.* 1999;40:2448-2453.
9. Fallon TJ, Maxwell D, Kohner EM. Retinal vascular autoregulation in conditions of hyperoxia and hypoxia using the blue field entoptic phenomenon. *Ophthalmology* 1985;92:701-705.
10. Hosking SL, Harris A, Chung HS, et al. Ocular haemodynamic responses to induced hypercapnia and hyperoxia in glaucoma. *Br.J.Ophthalmol.* 2004;88:406-411.
11. Sponsel WE, DePaul KL, Zetlan SR. Retinal hemodynamic effects of carbon dioxide, hyperoxia, and mild hypoxia. *Invest.Ophthalmol.Vis.Sci.* 1992;33:1864-1869.
12. Tsacopoulos M, David NJ. The effect of arterial PCO₂ on relative retinal blood flow in monkeys. *Invest.Ophthalmol.* 1973;12:335-347.
13. Venkataraman ST, Hudson C, Fisher JA, Flanagan JG. The impact of hypercapnia on retinal capillary blood flow assessed by scanning laser doppler flowmetry. *Microvasc.Res.* 2005;69:149-155.
14. Venkataraman ST, Hudson C, Fisher JA, Flanagan JG. Novel methodology to comprehensively assess retinal arteriolar vascular reactivity to hypercapnia. *Microvasc.Res.* 2006;72:101-107.
15. Harris A, Anderson DR, Pillunat L, et al. Laser doppler flowmetry measurement of changes in human optic nerve head blood flow in response to blood gas perturbations. *J.Glaucoma* 1996;5:258-265.

16. Harino S, Grunwald JE, Petrig BJ, Riva CE. Rebreathing into a bag increases human retinal macular blood velocity. *Br.J.Ophthalmol.* 1995;79:380-383.
17. Rhoades RA. Ventilation and mechanics of breathing. Rhoades RA and Tanner GA. *In Medical Physiology*. Philadelphia: Lipincott Williams & Wilkins; 2003. 309-336 pp.
18. Gilmore ED, Hudson C, Preiss D, Fisher J. Retinal arteriolar diameter, blood velocity, and blood flow response to an isocapnic hyperoxic provocation. *Am J Physiol Heart Circ Physiol* 2005;288:H2912-H2917.
19. Gilmore ED, Hudson C, Venkataraman ST, Preiss D, Fisher J. Comparison of different hyperoxic paradigms to induce vasoconstriction: Implications for the investigation of retinal vascular reactivity. *Invest.Ophthalmol.Vis.Sci.* 2004;45:3207-3212.
20. Slessarev M, Somogyi R, Preiss D, Vesely A, Sasano H, Fisher JA. Efficiency of oxygen administration: Sequential gas delivery versus "flow into a cone" methods. *Crit.Care Med.* 2006;34:829-834.
21. Slessarev M, Prisman E, Han J, et al. Prospective targeting and control of end-tidal CO₂ and O₂ concentrations. *J Physiol.* 2007;581:1207-1219.
22. Michelson G, Welzenbach J, Pal I, Harazny J. Automatic full field analysis of perfusion images gained by scanning laser doppler flowmetry. *Br.J.Ophthalmol.* 1998;82:1294-1300.
23. Guan K, Hudson C, Flanagan JG. Variability and repeatability of retinal blood flow measurements using the canon laser blood flowmeter. *Microvasc.Res.* 2003;65:145-151.

24. Nagaoka T, Mori F, Yoshida A. Retinal artery response to acute systemic blood pressure increase during cold pressor test in humans. *Invest.Ophthalmol.Vis.Sci.* 2002;43:1941-1945.
25. Kida T, Harino S, Sugiyama T, Kitanishi K, Iwahashi Y, Ikeda T. Change in retinal arterial blood flow in the contralateral eye of retinal vein occlusion during glucose tolerance test. *Graefes Arch.Clin.Exp.Ophthalmol.* 2002;240:342-347.
26. Riva CE, Feke GT, Eberli B. Bidirectional LDV system for the absolute measurement of blood speed in retinal vessels. *Appl.Opt.* 1979;18:2301-2306.
27. Feke GT, Goger DG, Tagawa H, Delori FC. Laser doppler technique for absolute measurement of blood speed in retinal vessels. *IEEE Trans.Biomed.Eng.* 1987;34:673-680.
28. Sato E, Feke GT, Menke MN, Wallace McMeel J. Retinal haemodynamics in patients with age-related macular degeneration. *Eye* 2006;20:697-702.
29. Sehi M, Flanagan JG. The effect of image alignment on capillary blood flow measurement of the neuroretinal rim using the heidelberg retina flowmeter. *Br.J.Ophthalmol.* 2004;88:204-206.
30. Jones NL. Evaluation of a microprocessor-controlled exercise testing system. *Journal of Applied Physiology* 1984;57:1312-1318.
31. Pennock BE, Donohoe M. Indirect calorimetry with a hood: Flow requirements, accuracy, and minute ventilation measurement. *Journal of Applied Physiology* 1993;74:485-491.
32. Venkataraman ST, Hudson C, Harvey E, Flanagan JG. Impact of simulated light scatter on scanning laser doppler flowmetry. *Br.J.Ophthalmol.* 2005;89:1192-1195.

33. Hafez AS, Bizzarro RL, Rivard M, Lesk MR. Changes in optic nerve head blood flow after therapeutic intraocular pressure reduction in glaucoma patients and ocular hypertensives. *Ophthalmology* 2003;110:201-210.
34. Bland JM, Altman DG. Measuring agreement in method comparison studies. *Stat Methods Med Res* 1999;8:135-160.
35. Bland JM, Altman DG. Statistical methods for assessing agreement between two methods of clinical measurement. *Lancet* 1986;1:307-310.
36. Gugleta K, Orgul S, Hasler P, Flammer J. Circulatory response to blood gas perturbations in vasospasm. *Invest.Ophthalmol.Vis.Sci.* 2005;46:3288-3294.
37. Alexopoulos D, Christodoulou J, Toulgaridis T, Sitafidis G, Klinaki A, Vagenakis AG. Hemodynamic response to hyperventilation test in healthy volunteers. *Clin.Cardiol.* 1995;18:636-641.
38. Dumskyj MJ, Eriksen JE, Dore CJ, Kohner EM. Autoregulation in the human retinal circulation: Assessment using isometric exercise, laser doppler velocimetry, and computer-assisted image analysis. *Microvasc.Res.* 1996;51:378-392.
39. Riva CE, Grunwald JE, Petrig BL. Autoregulation of human retinal blood flow. an investigation with laser doppler velocimetry. *Invest.Ophthalmol.Vis.Sci.* 1986;27:1706-1712.
40. Schmetterer L, Wolzt M, Lexer F, et al. The effect of hyperoxia and hypercapnia on fundus pulsations in the macular and optic disc region in healthy young men. *Exp.Eye Res.* 1995;61:685-690.

41. Huber KK, Adams H, Remky A, Arend KO. Retrobulbar haemodynamics and contrast sensitivity improvements after CO₂ breathing. *Acta Ophthalmol.Scand.* 2006;84:481-487.
42. Raper AJ, Kontos HA, Patterson JL. Response of pial precapillary vessels to changes in arterial carbon dioxide tension. *Circ.Res.* 1971;28:518-523.
43. Giller CA, Bowman G, Dyer H, Mootz L, Krippner W. Cerebral arterial diameters during changes in blood pressure and carbon dioxide during craniotomy. *Neurosurgery* 1993;32:737-41; discussion 741-2.
44. Kiss B, Polska E, Dorner G, et al. Retinal blood flow during hyperoxia in humans revisited: Concerted results using different measurement techniques. *Microvasc.Res.* 2002;64:75-85.
45. Knudtson MD, Klein BE, Klein R, et al. Variation associated with measurement of retinal vessel diameters at different points in the pulse cycle. *Br.J.Ophthalmol.* 2004;88:57-61.
46. Jeppesen P, Sanye-Hajari J, Bek T. Increased blood pressure induces a diameter response of retinal arterioles that increases with decreasing arteriolar diameter. *Invest.Ophthalmol.Vis.Sci.* 2007;48:328-331.
47. Lewis T, Wing J. Anatomy and physiology of the optic nerve head. M. Fingeret and T. Lewis. *In Primary care of the glaucomas.* New York: Mcgraw Hill; 2001. 43-61 pp.
48. Hayreh SS. Blood flow in the optic nerve head and factors that may influence it. *Prog.Retin.Eye Res.* 2001;20:595-624.

49. Yu DY, Townsend R, Cringle SJ, Chauhan BC, Morgan WH. Improved interpretation of flow maps obtained by scanning laser doppler flowmetry using a rat model of retinal artery occlusion. *Invest.Ophthalmol.Vis.Sci.* 2005;46:166-174.
50. Lovasik JV, Kergoat H, Riva CE, Petrig BL, Geiser M. Choroidal blood flow during exercise-induced changes in the ocular perfusion pressure. *Invest.Ophthalmol.Vis.Sci.* 2003;44:2126-2132.
51. Chauhan BC, Yu PK, Cringle SJ, Yu DY. Confocal scanning laser doppler flowmetry in the rat retina: Origin of flow signals and dependence on scan depth. *Arch.Ophthalmol.* 2006;124:397-402.
52. Townsend R, Cringle SJ, Morgan WH, Chauhan BC, Yu DY. Confocal laser doppler flowmeter measurements in a controlled flow environment in an isolated perfused eye. *Exp.Eye Res.* 2006;82:65-73.

6 Retinal Arteriolar Vascular Reactivity in Untreated and Progressive Primary Open Angle Glaucoma

Venkataraman ST, Hudson C, Rachmiel R, Buys YM, Markowitz SN, Fisher JA, Trope GE, Flanagan JG. Retinal arteriolar vascular reactivity in untreated and progressive primary open angle glaucoma. Invest Ophthalmol. Vis. Sci. (Under review).

6.1 Abstract

Aim: The primary aim was to determine the magnitude of retinal arteriolar vascular reactivity to normoxic hypercapnia in patients with untreated primary open angle glaucoma (uPOAG), progressive POAG (pPOAG) and controls.

Methods: The sample comprised 11 patients with uPOAG, 17 patients with pPOAG and 17 age-similar controls. pPOAG patients manifested optic disc hemorrhage within the previous 24 months. During the baseline 10 min phase, PETCO₂ was maintained at approximately 38mmHg. Normoxic hypercapnia (15% increase in PETCO₂ relative to baseline and PETO₂ maintained as baseline ~105mmHg) was then induced for 15 mins using an automated gas flow controller (RespirAct™, Thornhill Research Inc. Toronto, Canada). A third 10 min recovery phase was then implemented. Retinal arteriolar hemodynamics were assessed using the Canon Laser Blood Flowmeter.

Results: There was no difference in baseline arteriolar hemodynamics across groups. In healthy controls, diameter increased by +2.3% (Re-ANOVA p<0.001) and velocity and flow increased by +17.9% (p<0.001) and +22.4% (p<0.001), respectively, in response to normoxic

hypercapnia. There was no change in the hemodynamic parameters to normoxic hypercapnia in uPOAG. Retinal arteriolar diameter and blood velocity did not change in pPOAG but blood flow increased by +9.1% ($p=0.030$). The vascular reactivity to hypercapnia was different in terms of blood velocity (ANOVA $p=0.004$) and blood flow ($p=0.013$) across groups; the vascular reactivity was decreased in uPOAG and in pPOAG compared to controls (Fishers LSD post hoc test).

Conclusions: The arteriolar vascular reactivity to normoxic hypercapnia was reduced in uPOAG and in pPOAG compared to healthy subjects.

Keywords: Retinal arterioles, vascular reactivity, optic nerve head, normoxic hypercapnia, primary open angle glaucoma.

6.2 Introduction

Glaucomatous optic neuropathy (GON) is characterized by the apoptotic loss of retinal ganglion cells and their axons¹. The factors responsible for the pathogenesis of primary open angle glaucoma (POAG) are not completely understood. Elevated intra-ocular pressure (IOP) has been identified as the primary risk factor in the development and progression of POAG. However, a subset of patients with POAG maintain a “normal” IOP, termed normal tension glaucoma (NTG), while many patients with ocular hypertension (OHT) fail to develop GON. In addition, some POAG patients manifest progression of GON, while other POAG patients remain stable over many years.

Abnormal vascular regulation has been suggested to be involved in the development of POAG¹⁻⁶. Previous studies have shown that optic nerve head (ONH) and retinal blood flow is decreased in patients with POAG and NTG measured using fundus fluorescein angiography⁷, color Doppler imaging (CDI)⁷⁻⁹ and the Canon Laser Blood Flowmeter (CLBF)¹⁰. Histopathological evidence suggests that there is a decrease in the number of capillaries in the ONH in POAG¹¹. Atrophy of the peripapillary capillaries supplying the retinal nerve fibre layer (RNFL) has also been reported in POAG^{12, 13}. Using CDI, Liu and co-workers¹⁴ have shown reduced peak systolic and end-diastolic velocities in the central retinal artery (CRA) and nasal posterior ciliary artery (PCA) and increased resistive index in the CRA in patients with advanced glaucoma compared to healthy controls and early glaucoma. In addition, there is also a reduction in the cerebrovascular blood velocities noted in POAG¹⁵. However, the effect of IOP lowering medications on ocular blood flow remains poorly understood. In particular, treatment with carbonic anhydrase inhibitors has been

reported to increase aspects of ocular hemodynamics in POAG¹⁶⁻²¹, while others have found no change^{22, 23}. However, previous studies have not assessed the effect of treatment on vascular reactivity in POAG patients.

Increase in the arterial partial pressure of CO₂ (PaCO₂) above normal resting values (hypercapnia) results in vasodilation of retinal vessels in healthy volunteers²⁴⁻²⁹. The retinal vascular reactivity response to inhaled CO₂ in patients with POAG is not well established. Some studies have shown reduced vascular reactivity using CDI^{9, 30}, while another study has shown a normal magnitude of vasodilation of the short posterior ciliary arteries (SPCA)³¹. An absence of vascular reactivity of the middle cerebral artery (MCA) to hyperoxia (increased amounts of inspired oxygen) in patients with POAG has also been reported¹⁵ but recent work has shown an absence of MCA response to hyperoxia in healthy controls³².

Hypercapnia also results in hyperventilation leading to an unpredictable change in the arterial partial pressure of O₂ (PaO₂)³³. Fisher and co-workers have developed hypercapnic provocations that simultaneously stabilize PaO₂³⁴ and this normoxic hypercapnic stimulus has been applied in our laboratory to assess retinal and ONH vascular reactivity in healthy volunteers^{27, 29}. In this study, we induced normoxic hypercapnia, such that the partial pressure of end-tidal O₂ in exhaled breath (PETO₂) was maintained at physiological resting levels throughout the provocation. The primary aim of this study was to assess the magnitude of retinal arteriolar vascular reactivity to normoxic hypercapnia in patients with untreated POAG (uPOAG) and progressive POAG (pPOAG) and healthy controls. The secondary aim

of the study was to quantify vascular reactivity in newly treated POAG (ntPOAG) patients after topical treatment with 2% Dorzolamide for two weeks.

6.3 Methods

6.3.1 Sample

The study was approved by the Research Ethics Boards of the University Health Network, University of Toronto, and the Office of Research Ethics of the University of Waterloo. All subjects provided signed informed consent prior to participation after explanation of the nature and possible consequences of the study according to the tenets of the Declaration of Helsinki. The sample comprised 11 patients with newly diagnosed previously untreated POAG (uPOAG), 17 patients with pPOAG and 17 healthy age-similar control subjects. Patients with pPOAG were identified as having an optic disc hemorrhage within the previous 24 months. The uPOAG group were treated with one drop of 2% Dorzolamide twice daily for 2 weeks to form the newly treated POAG (ntPOAG) group (n=11).

All participants had a visual acuity of 20/40, or better, and a refractive error less than ± 6.00 DS and ± 1.50 DC. They were free of other ocular disease and were non-smokers. Participants with cardiovascular disorders, uncontrolled systemic hypertension and diabetes were excluded from the study. Healthy control subjects had no family history of glaucoma or diabetes. All participants were asked to abstain from caffeine containing food or drinks and were asked to adhere to a low nitrate diet for at least 12 hours before the study visit(s). An impact of caffeine on cerebral blood flow is well established ³⁵, while a recent study also showed the influence of caffeine on retrobulbar blood velocity ³⁶. Consumption of saturated fats are also known to influence vascular reactivity ³⁷.

6.3.2 Gas delivery system

A sequential gas delivery (SGD) breathing circuit (Hi-Ox⁸⁰, Viasys Healthcare, Yorba Linda CA) was modified by placing a rebreathing bag on the exhalation port of a commercial 3-valve oxygen delivery system. This breathing circuit has been described in detail elsewhere ^{27-29, 38, 39}.

6.3.3 Retinal blood flow assessment

The principle and technical details of the Canon Laser Blood Flowmeter (CLBF; Model 100, Canon, Tokyo, Japan) have been detailed elsewhere and in Chapter-1 of this Thesis ^{27, 38, 40-45}.

6.3.4 Procedures

All participants attended for 2 visits. Patients with uPOAG returned for an additional third visit and were then designated into the ntPOAG group. Both eyes were dilated using Mydracyl 1% (Alcon Canada Inc., Mississauga, Canada) at visit 1 and only the study eye was dilated during subsequent visits. Visit 1 consisted of an assessment of visual acuity, central visual field assessment (24-2 SITA-standard, Humphrey Visual Field Analyser 740, Carl Zeiss Meditec, Dublin, CA), scanning laser tomography (Heidelberg Retina Tomograph 2, v3, Heidelberg Engineering, Heidelberg, Germany) and stereo fundus photography (TOPCON, Model TRC-50VT, Japan) of the ONH and measurement of the IOP. Based on the results of the above tests and clinical assessment, the diagnosis was confirmed by a glaucoma specialist (YB or GT). One eye was randomly chosen as the study eye assuming both eyes met the study criteria.

During the second visit, IOP and blood pressure (BP) were assessed. The pupil of the chosen eye was dilated using Mydracyl 1% (Alcon Canada Inc., Mississauga, Canada). Participants rested for an initial 15 minutes before the start of the breathing paradigm. They were then fitted with a face mask connected to the automated gas flow controller. During the first 10 minutes, participants breathed air and baseline PETCO₂ was standardised to approximately 38mmHg. Following this, normoxic hypercapnia (consisting of a 15% increase in PETCO₂ from baseline and PETO₂ maintained at resting levels) was induced and sustained for the next 15 minutes. Participants were then allowed to breathe air for 10 minutes and re-establish their baseline end-tidal values (post-hypercapnia). At least, 3 CLBF measurements of either the superior or inferior temporal arteriole were obtained in each of the breathing phases. PETCO₂, PETO₂ and respiration rate were monitored by the automated gas flow controller (RespirAct™, Thornhill Research Inc., Toronto Canada). PETCO₂ and PETO₂ are accurate measurements of PaCO₂ and PaO₂, respectively, when breathing via a sequential gas delivery circuit ⁴⁶. Pulse rate, oxygen saturation, heart rate and BP (every 2.5 minutes), were monitored using the rapid response critical care gas analyzer (Cardiicap 5, Datex-Ohmeda, Helsinki, Finland).

Patients with uPOAG were then prescribed 2% Dorzolamide (Trusopt) (Merck Frosst, Canada Ltd), one drop every 12 hours in the study eye for two weeks. After 2 weeks, the ntPOAG patients were re-tested using the identical procedures described above.

6.3.5 Analysis

6.3.5.1 Retinal Blood Flow Analysis

CLBF analysis software was used to analyze the velocity waveforms. A minimum of one complete waveform was required to be included in the analysis. A standardised protocol was used in order to eliminate aberrant waveforms⁴⁰. Mean Ocular Perfusion Pressure (MOPP) was calculated using the formula:

$$\text{MOPP} = 2/3 [\text{diastolic} + 1/3(\text{systolic} - \text{diastolic})] - \text{IOP}$$

6.3.5.2 Gas Parameters Analysis

The gas parameters were analyzed using customized software (Labview, National Instruments, version 7.1). PETCO₂ and PETO₂ were calculated breath-by-breath as the maximum PETCO₂ value and minimum PETO₂ value, respectively, during exhalation.

6.3.5.3 Statistical Analysis

A repeated measures analysis of variance (reANOVA) with Greenhouse-Geiser correction was used to determine any significant change in retinal arteriolar diameter, blood velocity and blood flow across the breathing paradigm within each group. A one-way ANOVA was used to determine the significance of any difference in the baseline arteriolar hemodynamics, IOP, MOPP, age and the magnitude of change in vascular reactivity of arteriolar diameter, blood velocity and blood flow during normoxic hypercapnia across groups. Fishers least significant difference (LSD) post hoc test (SAS) was used for comparison between the groups. The Fisher's LSD post hoc test identifies groups that are significantly different from

other groups at a significance level of $p < 0.05$. It does not provide one specific p-value per se for each group that is significantly different. A separate reANOVA was performed to determine any significant change in pulse rate, systolic and diastolic BP, oxygen saturation, $PETCO_2$, $PETO_2$ and respiration rate across the breathing paradigm within each group.

6.4 Results

There was no difference in the baseline retinal arteriolar diameter, blood velocity and blood flow across groups.

Figures 6.1A, 6.1B and 6.1C show the vascular reactivity to normoxic hypercapnia in terms of percentage change in diameter, velocity and flow, respectively. In healthy controls, diameter increased by +2.3% (ReANOVA $p < 0.001$, Figure 6.1A), blood velocity increased by +17.9% ($p < 0.001$, Figure 6.1B) and blood flow increased by +22.4% ($p < 0.001$, Figure 6.1C). There was no change in any of the hemodynamic parameters to normoxic hypercapnia in the uPOAG group (Figure 6.1). Diameter and blood velocity did not change in the pPOAG group (Figure 6.1) but blood flow manifested an increase of +9.1% ($p = 0.030$, Figure 6.1C).

The change in vascular reactivity in response to normoxic hypercapnia was different in terms of velocity (one-way ANOVA $p = 0.004$) and blood flow ($p = 0.013$) across groups. Velocity and flow were decreased in uPOAG and pPOAG compared to controls and ntPOAG (Fishers LSD post hoc test).

Following Dorzolamide treatment, diameter increased by +3% ($p = 0.040$, Figure 6.1A), velocity increased by +19% ($p < 0.001$, Figure 6.1B) and flow increased by +26% ($p < 0.001$, Figure 6.1C) in the ntPOAG group (previously the uPOAG group) in response to normoxic hypercapnia.

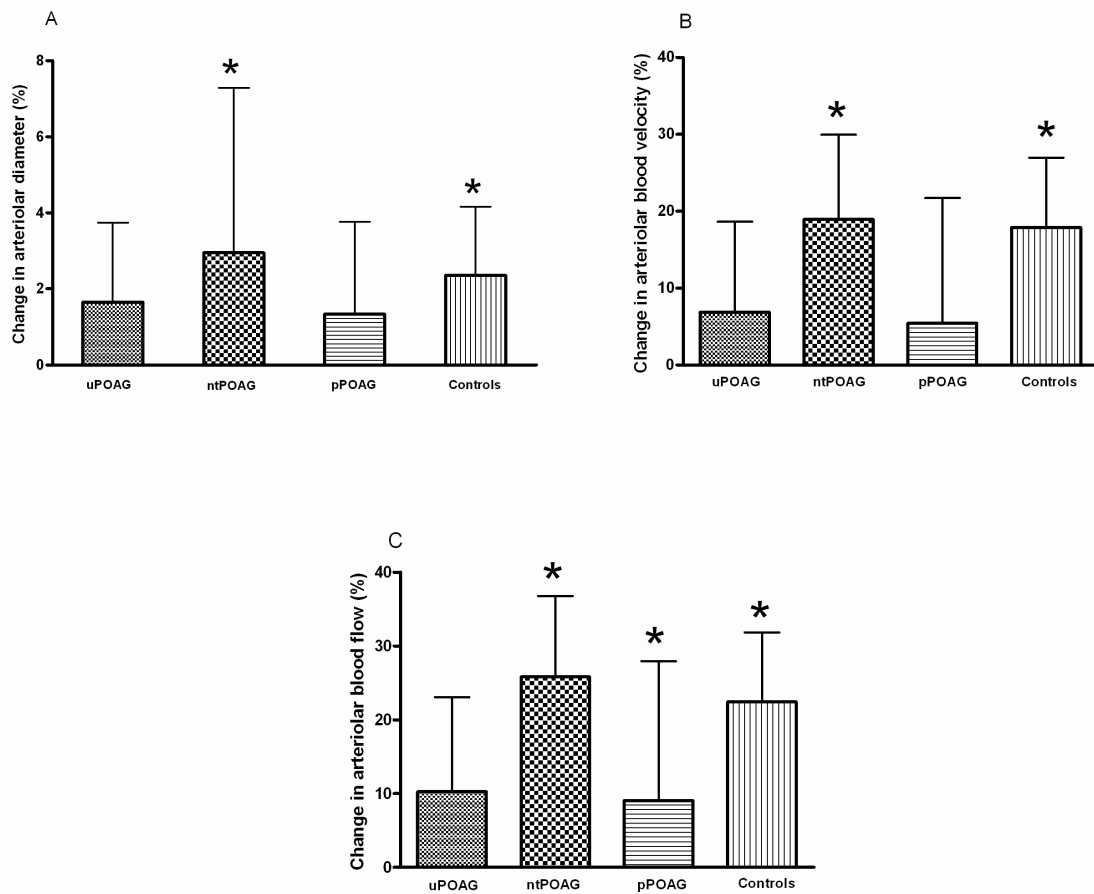


Figure 6.1 The percentage change from baseline in group mean A) retinal arteriolar diameter; B) blood velocity; and C) blood flow in response to normoxic hypercapnia in patients with uPOAG, ntPOAG, pPOAG and controls.

Error bar represents standard deviation (%) (uPOAG, untreated POAG; ntPOAG, newly treated POAG; pPOAG, progressive POAG). Note: * represents significance when compared across the three breathing conditions (baseline, normoxic hypercapnia and post-hypercapnia) within the group at the level of $p < 0.05$.

The mean age, IOP and MOPP as a function of group is detailed in Table 6.1. The group average visual field mean deviation (MD) was -1.4 (SD 1.6) in uPOAG/ntPOAG, -2.1 (SD 2.0) in pPOAG and -0.3 (SD 1.0) in controls. The group mean pattern standard deviation (PSD) in uPOAG /ntPOAG, pPOAG and controls was 2.6 (SD 2.7), 5.0 (SD 3.0) and 2.0 (SD 0.4), respectively.

Parameter	uPOAG	ntPOAG	pPOAG	Controls	p-value
Age (yrs)	54.0 ± 11.4	54.0 ± 11.4	65.0 ± 7.7*	55.0 ± 6.7	0.0022
IOP (mmHg)	22.5 ± 2.2**	18.0 ± 2.0**†	12.1 ± 2.0	13.0 ± 2.1	<0.001
MOPP (mmHg)	39.0 ± 8.2**	37.6 ± 4.5**	46.7 ± 7.8	44.9 ± 4.5	0.0010

Table 6.1 The group mean ± SD of the age, IOP and MOPP in all the groups.

(IOP, intra-ocular pressure; MOPP, mean ocular perfusion pressure; uPOAG, untreated POAG; ntPOAG, newly treated POAG; pPOAG, progressive POAG).

p-value denotes significance across all groups using one-way ANOVA. * denotes the group that is significantly different when compared to other groups. ** denotes the group that is significantly different when compared to pPOAG and controls. † denotes the group that is significantly different when compared to uPOAG.

Tables 6.2, 6.3, 6.4 & 6.5 detail the systemic parameters measured during the breathing paradigm in all the groups. The mean percentage increase in PETCO₂ during hypercapnia in all groups (i.e. uPOAG, pPOAG and controls) was 15.4% (SD 2.5, p<0.001) (Tables 6.2 to 6.5). In ntPOAG, PETCO₂ increased by 15.9% (SD 4.6, p<0.001). During normoxic hypercapnia, there was a concomitant increase in the mean PETO₂ of 3.1% (SD 2.0) (p≤0.02).

Gas and Systemic parameters	Baseline	Hypercapnia	Post-hypercapnia	p-value
PETCO ₂ (mmHg)	38.9 ± 0.7	44.9 ± 1.1	39.2 ± 0.9	<0.001
PETO ₂ (mmHg)	105.4 ± 2.6	108.6 ± 2.7	107.4 ± 2.2	<0.001
Respiration rate (breaths/min)	17.2 ± 5.4	19.0 ± 3.6	19.0 ± 4.7	NS
Pulse rate (beats/min)	71.9 ± 10.4	73.6 ± 11.3	72.7 ± 10.5	NS
Systolic BP (mmHg)	133 ± 17.4	136.9 ± 17.7	134.0 ± 18.6	<0.001
Diastolic BP (mmHg)	81.8 ± 8.7	83.8 ± 8.4	82.8 ± 9.3	NS
O ₂ saturation (%)	97.8 ± 1.1	98.1 ± 1.0	98.0 ± 1.0	NS

Table 6.2 The group mean ± SD of PETCO₂, PETO₂, respiration rate, pulse rate, systolic and diastolic BP and O₂ saturation in uPOAG.

(PETCO₂, partial pressure of end-tidal carbon dioxide; PETO₂, partial pressure of end-tidal oxygen, BP, blood pressure; O₂ saturation, oxygen saturation). Note: The p-value denotes significance of each parameter across the three breathing conditions using reANOVA. NS denotes not significant.

Gas and Systemic parameters	Baseline	Hypercapnia	Post-hypercapnia	p-value
PETCO ₂ (mmHg)	39.1 ± 1.4	45.2 ± 1.0	38.7 ± 1.4	<0.001
PETO ₂ (mmHg)	103.9 ± 5.0	106.5 ± 4.6	106.5 ± 5.2	0.020
Respiration rate (breaths/min)	18.6 ± 5.9	19.4 ± 4.7	20.2 ± 7.1	NS
Pulse rate (beats/min)	70.8 ± 8.7	72.5 ± 8.7	72.0 ± 9.1	NS
Systolic BP (mmHg)	124.0 ± 12.3	131.1 ± 11.7	129.0 ± 13.2	0.009
Diastolic BP (mmHg)	78.6 ± 10.8	78.9 ± 10.7	78.5 ± 10.9	NS
O ₂ saturation (%)	98.1 ± 0.8	98.3 ± 0.5	98.6 ± 0.7	0.003

Table 6.3 The group mean ± SD of PETCO₂, PETO₂, respiration rate, pulse rate, systolic and diastolic BP and O₂ saturation in ntPOAG.

(PETCO₂, partial pressure of end-tidal carbon dioxide; PETO₂, partial pressure of end-tidal oxygen, BP, blood pressure; O₂ saturation, oxygen saturation). Note: The p-value denotes significance of each parameter across the three breathing conditions using reANOVA. NS denotes not significant.

Gas and Systemic parameters	Baseline	Hypercapnia	Post-hypercapnia	p-value
PETCO ₂ (mmHg)	38.9 ± 1.2	45.0 ± 1.5	38.6 ± 1.0	<0.001
PETO ₂ (mmHg)	104.8 ± 2.9	108.0 ± 2.9	106.8 ± 2.7	<0.001
Respiration rate (breaths/min)	19.9 ± 4.25	20.2 ± 4.8	20.3 ± 4.7	NS
Pulse rate (beats/min)	66.0 ± 8.7	67.2 ± 8.1	67.8 ± 7.2	NS
Systolic BP (mmHg)	128.9 ± 13.9	139.4 ± 12.5	134.6 ± 14.9	<0.001
Diastolic BP (mmHg)	80.9 ± 6.0	85.2 ± 6.8	83.1 ± 9.1	0.004
O ₂ saturation (%)	98.5 ± 0.9	98.6 ± 0.8	98.8 ± 0.8	0.020

Table 6.4 The group mean ± SD of PETCO₂, PETO₂, respiration rate, pulse rate, systolic and diastolic BP and O₂ saturation in pPOAG.

(PETCO₂, partial pressure of end-tidal carbon dioxide; PETO₂, partial pressure of end-tidal oxygen, BP, blood pressure; O₂ saturation, oxygen saturation). Note: The p-value denotes significance of each parameter across the three breathing conditions using reANOVA. NS denotes not significant.

Gas and Systemic parameters	Baseline	Hypercapnia	Post-hypercapnia	p-value
PETCO ₂ (mmHg)	39.0 ± 1.6	45.0 ± 1.4	38.9 ± 1.6	<0.001
PETO ₂ (mmHg)	106.1 ± 4.8	109.1 ± 4.3	107.9 ± 4.7	<0.001
Respiration rate (breaths/min)	21.0 ± 4.8	21.2 ± 3.8	21.8 ± 3.9	NS
Pulse rate (beats/min)	65.5 ± 7.9	67.5 ± 8.7	67.0 ± 8.9	0.020
Systolic BP (mmHg)	118.5 ± 13.5	125.2 ± 15.7	124.2 ± 12.2	<0.001
Diastolic BP (mmHg)	77.6 ± 7.7	80.7 ± 9.1	79.0 ± 6.6	0.007
O ₂ saturation (%)	98.1 ± 1.0	98.5 ± 0.8	98.5 ± 0.9	0.005

Table 6.5 The group mean ± SD of PETCO₂, PETO₂, respiration rate, pulse rate, systolic and diastolic BP and O₂ saturation in controls.

(PETCO₂, partial pressure of end-tidal carbon dioxide; PETO₂, partial pressure of end-tidal oxygen, BP, blood pressure; O₂ saturation, oxygen saturation). Note: The p-value denotes significance of each parameter across the three breathing conditions using reANOVA. NS denotes not significant.

6.5 Discussion

The primary finding of this study was that retinal vascular reactivity was reduced in uPOAG and pPOAG compared to controls. A hypercapnic protocol that simultaneously maintained normoxia was undertaken to avoid additional vasoconstriction in what is a potentially vasospastic disease. The use of a sustained and stable normoxic hypercapnic stimulus was essential for the assessment of retinal arteriolar vascular reactivity so that repeated hemodynamic measurements could be obtained.

Various studies have shown a decrease in homeostatic blood flow in POAG/NTG using the CLBF¹⁰ color Doppler imaging^{9, 47-49} and pulsatile ocular blood flowmeter (POBF)⁵⁰. In this study, however, there was no difference between baseline diameter, blood velocity and blood flow in uPOAG compared to the other groups. The techniques used in previous studies have limitations. CDI requires an experienced operator to obtain reliable measurements, is unable to quantify volumetric blood flow and it can be difficult to differentiate responses between the CRA and SPCA⁵¹. Similarly, the results of the POBF can be influenced by ocular rigidity and the measurement is dominated by the choroidal circulation⁵². The use of the CLBF in this study offered an alternative approach since it objectively quantifies volumetric retinal blood flow in real units. The results of this study are not directly comparable to earlier work in that the vascular reactivity was assessed in the retinal arterioles of untreated POAG patients, while in most other studies patients were already receiving IOP lowering medications. O'Brien and co-workers (1999) assessed blood flow using the POBF in a group of 28 NTG patients of which there were 12 previously treated patients (stopped treatment 1month prior to the study) and only 16 patients with newly diagnosed NTG.

However, the blood flow results of the two groups were not separated in the analysis of the study⁵⁰.

Most previous studies have only assessed homeostatic blood flow in POAG or NTG patients, often using CDI^{7-9, 14}. The few studies that have assessed retinal and ONH vascular reactivity in POAG have found contradictory results. Gugleta and co-workers (2005) showed an increase in ONH blood flow in patients with vasospasm and a decrease in ONH blood flow in patients without vasospasm assessed using laser Doppler flowmetry in response to hypercapnia⁵³. In this study, a decrease in the magnitude of vascular reactivity to normoxic hypercapnia was noted in both uPOAG and pPOAG but all the groups, apart from uPOAG, showed evidence of increased retinal blood flow in response to normoxic hypercapnia. Similarly, a reduction in the vascular reactivity of the CRA using CDI has also been shown in patients with open angle glaucoma³⁰. Hosking and co-workers (2004) showed vasodilation of the retrobulbar vessels assessed using the CDI during hypercapnia in POAG³¹. Interestingly, Harris and co-workers (1994) have reported that patients with NTG showed an increase in the peak systolic velocity of the CRA and posterior ciliary artery (PCA) and also end-diastolic velocity of the OA during hypercapnia. There was no change in the velocities of the CRA and OA in controls in response to hypercapnia⁹. Using the CLBF, Feke and co-workers (2007) also showed evidence of abnormal retinal arteriolar response in POAG to posture change compared to controls⁵⁴. This altered response was only seen in a sub-group of patients and, in addition, patients in their study were treated with IOP lowering medications.

As glaucoma is primarily characterized by either compromise of the ONH perfusion and / or mechanical compression of the lamina cribrosa, we also assessed the response of the capillaries at the temporal rim of the ONH to normoxic hypercapnia. Several studies have demonstrated a decrease in blood flow in the ONH in POAG using different assessment techniques⁵⁵⁻⁵⁸. In this study, ONH capillary vascular reactivity was assessed in a sub-set of patients with POAG using the Heidelberg Retina Flowmeter (Heidelberg Engineering GmbH, Dossenheim, Germany, software version 1.03W). The vascular reactivity of the capillaries at the temporal rim of the ONH showed a +6%, +11% and +20% increase in blood flow to normoxic hypercapnic provocation in uPOAG (n=5), pPOAG (n=12) and controls (n=12), respectively (Figure 6.2). In ntPOAG (n=5), the magnitude of ONH vascular reactivity was +18%. We have previously shown that the percentage change of capillary vascular reactivity is comparable to arteriolar vascular reactivity in young healthy volunteers²⁹. An interesting finding of the ONH sub-study was that the vascular reactivity of the ONH capillary bed was reduced in percentage terms in uPOAG and pPOAG, to a similar extent as that of the superior/inferior temporal arteriole. The vascular reactivity of the control group was similar between the arteriolar and ONH sites and the recovery of vascular reactivity following Dorzolamide treatment was also similar between ONH capillaries and retinal arterioles for the ntPOAG group.

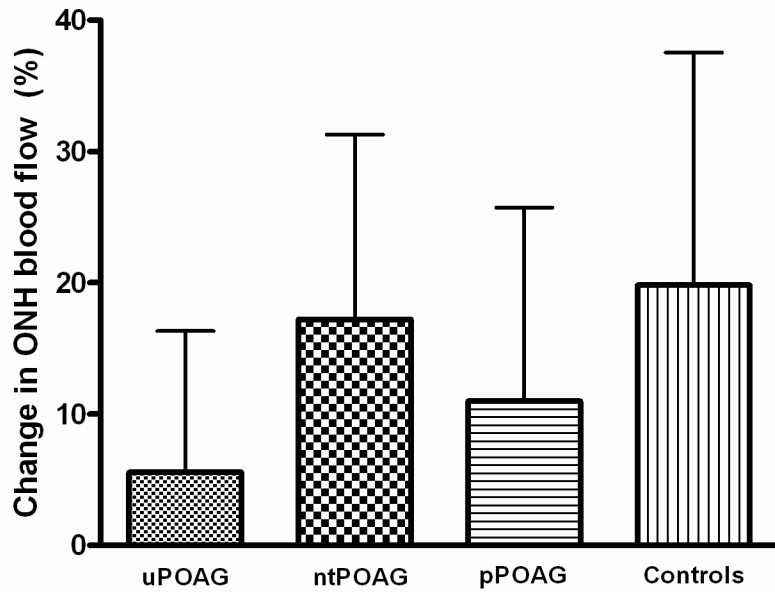


Figure 6.2 The percentage change from baseline in group mean temporal rim ONH blood flow in response to normoxic hypercapnia in patients with uPOAG and ntPOAG, pPOAG and controls.

Error bar represents standard deviation (%) (ONH, optic nerve head; uPOAG, untreated POAG; ntPOAG, newly treated POAG; pPOAG, progressive POAG). The sample comprised of 5 patients with uPOAG of mean age 54yrs (SD 8.6), 12 patients with pPOAG of mean age 65yrs (SD 7.5) and 12 healthy controls of mean age of 55yrs (SD 7.4). Normoxic hypercapnia was induced identical to the protocol described for retinal arteriolar vascular reactivity assessment.

A secondary finding of this study was that vascular reactivity improved to the level of the controls in the ntPOAG group, following 2 weeks of treatment with 2% Dorzolamide. Recently, a number of studies have focused on the assessment of the retinal blood flow after treatment with IOP lowering medications. It has been thought that carbonic anhydrase inhibitors, in particular, Dorzolamide might improve blood flow. However, many of these studies used an additional IOP lowering medication simultaneously with Dorzolamide¹⁹⁻²¹ or used untypical methods of drug delivery¹⁶. In this study, vascular reactivity was assessed in patients who had never undergone treatment with IOP lowering medications. The inclusion of previously untreated patients was essential to avoid any residual vascular effects of medication on the response of the vasculature. In addition, we also assessed vascular reactivity in patients with progressive disease (i.e. currently receiving treatment, have achieved target IOP reduction and have a history of optic disc hemorrhage) as there is evidence that this group of patients exhibit vascular dysregulation^{59, 60}. This study supports the previous findings since patients with pPOAG exhibited a reduced vascular reactivity reserve.

Previous studies have assessed the effect of treatment on homeostatic retinal blood flow, rather than on vascular reactivity *per se*, in POAG. Retinal vascular reactivity in response to hypercapnia has been previously assessed using scanning laser ophthalmoscopy, fluorescein angiography and the blue field entoptic technique in healthy subjects after treatment with Dorzolamide and no change was found in vascular reactivity⁶¹. This study is the first to investigate the effect of Dorzolamide on retinal vascular reactivity in patients with POAG. Vascular reactivity improved after short term treatment of POAG with Dorzolamide.

However, there was no difference across the groups in the baseline arteriolar hemodynamics after treatment. The controversy in terms of baseline hemodynamic findings of our study and previous reports is probably due to differences in experimental design and blood flow quantification techniques, including the concomitant use of other medications, and also due to variation in the duration of Dorzolamide administration. In the absence of a non-pharmacological control group that exhibited a similar reduction in IOP, such as laser trabeculoplasty, it is not evident whether the improvement in vascular reactivity following treatment is due to the reduction in IOP or a direct effect of Dorzolamide on the vasculature. Nevertheless, in this study, there was no difference in the MOPP between uPOAG and ntPOAG, indicating that the improvement in retinal vascular reactivity seen in the uPOAG might be due, in part, to a direct beneficial effect of Dorzolamide on the retinal vasculature. Obviously, this finding needs to be interpreted with caution until an adequate control group is established. This work is in progress.

In a related study⁶² from our laboratory, plasma levels of biochemical markers of endothelial function, namely endothelin-1 (ET-1) and cyclic guanosine monophosphate (cGMP i.e. a surrogate marker of nitric oxide), were assessed in uPOAG, ntPOAG, pPOAG and controls at baseline and during the normoxic hypercapnic provocation. A relationship was found between the change in the magnitude of vascular reactivity and the change in biochemical markers during normoxic hypercapnia in the controls. ET-1 levels were found to be repeatedly lower at baseline in uPOAG and ntPOAG, suggesting that there is a systemic endothelial dysfunction in uPOAG that remained unaltered even after short-term treatment. In addition, there was also a strong association between baseline arteriolar blood flow and

baseline levels of cGMP in uPOAG and ntPOAG. These results further validate the functional vascular reactivity abnormalities seen in this study.

Previous studies claim to have administered isoxic hypercapnia to provoke an increase in retinal blood flow in healthy subjects and in POAG^{9, 24, 31, 63, 64}. However, these studies have failed to report, and / or, monitor concomitant changes in PETO₂. In addition, elevated PETCO₂ levels were achieved by dynamic end-tidal forcing (DEF), an integral proportional feedback system to make breath-by-breath corrections to inspired gases, but this technique does not actually target the arterial concentration of CO₂ (PaCO₂). DEF requires a complex set-up including multiple large gas tanks and tubing. In contrast, the Respiract™ system (automated gas flow controller) is about the size of a desk-top computer and supplies gas at about the subject's minute ventilation to a relatively small fitted face mask. An additional advantage of the Respiract™ over DEF is that it uses a sequential gas delivery breathing circuit whereby PETCO₂ has been shown to be equal to PaCO₂. This allows the provocative stimulus (PaCO₂) to be known from exhaled gas (PETCO₂) without the need for invasive arterial punctures. With DEF, there is a large variation between PETCO₂ and PaCO₂ so the latter is not precisely known from non-invasive measures^{46, 65}.

A number of limitations exist in this study. There was a significant increase in systolic BP in uPOAG, and ntPOAG and in both systolic and diastolic BP in pPOAG and controls. The magnitude of increase in BP during normoxic hypercapnia, however, was small ($\leq 8\%$) and well within the range of autoregulation of the retinal vessels and would not be expected to have a major influence on vascular reactivity^{66, 67}. In addition, there was a small increase in

peripheral O₂ saturation (SpO₂) (defined as the ratio of the amount of O₂ that is bound to hemoglobin to the amount that can be potentially bound) in ntPOAG, pPOAG and controls during normoxic hypercapnia. To put this in perspective, one can typically measure physiologic responses to changes in SpO₂ that reach about 70%^{68, 69}. There are no known physiological responses to changes of 1% in the range of nearly saturated hemoglobin (97-99%). Also, the controls were not age-matched to the pPOAG group. The reason for this was that patients with pPOAG were those who had relatively long standing glaucoma compared to uPOAG and also those who showed progression of the disease. Previous work in our laboratory has shown negligible difference in the magnitude of the vascular reactivity in healthy subjects over the range of ages used in this study⁷⁰. Also, there was no significant difference noted in the baseline arteriolar hemodynamics across the groups.

6.6 Conclusions

Arteriolar vascular reactivity was reduced in uPOAG and in pPOAG compared to healthy subjects. Whether or not this functional deficit of vascular reactivity reflects endothelial dysfunction is equivocal. A normoxic hypercapnic protocol was undertaken that avoided additional and uncontrolled vasoconstriction in what is a potentially vasospastic disease. Vascular reactivity improved after short-term treatment of uPOAG with Dorzolamide. However, it is not clear whether this improvement was a direct effect of the medication or a secondary effect due to decrease in IOP. Based upon a sub-study, the ONH capillary bed provided similar findings to those of the retinal arterioles.

6.7 References

1. Mozaffarieh M, Grieshaber MC, Flammer J. Oxygen and blood flow: Players in the pathogenesis of glaucoma. *Mol.Vis.* 2008;14:224-233.
2. Henry E, Newby DE, Webb DJ, Hadoke PW, O'Brien CJ. Altered endothelin-1 vasoreactivity in patients with untreated normal-pressure glaucoma. *Invest.Ophthalmol.Vis.Sci.* 2006;47:2528-2532.
3. Haefliger IO, Dettmann E, Liu R, et al. Potential role of nitric oxide and endothelin in the pathogenesis of glaucoma. *Surv.Ophthalmol.* 1999;43 Suppl 1:S51-S58.
4. Chung HS, Harris A, Evans DW, Kagemann L, Garzosi HJ, Martin B. Vascular aspects in the pathophysiology of glaucomatous optic neuropathy. *Surv.Ophthalmol.* 1999;43 Suppl 1:S43-S50.
5. Flammer J, Haefliger IO, Orgul S, Resink T. Vascular dysregulation: A principal risk factor for glaucomatous damage? *J.Glaucoma* 1999;8:212-219.
6. Flammer J, Orgul S. Optic nerve blood-flow abnormalities in glaucoma. *Prog.Retin.Eye Res.* 1998;17:267-289.
7. Plange N, Kaup M, Weber A, Arend KO, Remky A. Retrobulbar haemodynamics and morphometric optic disc analysis in primary open-angle glaucoma. *Br.J.Ophthalmol.* 2006;90:1501-1504.

8. Kaiser HJ, Schoetzau A, Stumpfig D, Flammer J. Blood-flow velocities of the extraocular vessels in patients with high-tension and normal-tension primary open-angle glaucoma. *Am.J.Ophthalmol.* 1997;123:320-327.
9. Harris A, Sergott RC, Spaeth GL, Katz JL, Shoemaker JA, Martin BJ. Color doppler analysis of ocular vessel blood velocity in normal-tension glaucoma. *Am.J.Ophthalmol.* 1994;118:642-649.
10. Berisha F, Feke GT, Hirose T, McMeel JW, Pasquale LR. Retinal blood flow and nerve fiber layer measurements in early-stage open-angle glaucoma. *Am.J.Ophthalmol.* 2008;146:466-472.
11. Gottanka J, Kuhlmann A, Scholz M, Johnson DH, Lutjen-Drecoll E. Pathophysiologic changes in the optic nerves of eyes with primary open angle and pseudoexfoliation glaucoma. *Invest.Ophthalmol.Vis.Sci.* 2005;46:4170-4181.
12. Kornzweig AL, Eliasoph I, Feldstein M. Selective atrophy of the radial peripapillary capillaries in chronic glaucoma. *Arch.Ophthalmol.* 1968;80:696-702.
13. Tezel G, Kass MA, Kolker AE, Wax MB. Comparative optic disc analysis in normal pressure glaucoma, primary open-angle glaucoma, and ocular hypertension. *Ophthalmology* 1996;103:2105-2113.
14. Liu CJ, Chiou HJ, Chiang SC, Chou JC, Chou YH, Liu JH. Variations in ocular hemodynamics in patients with early and late glaucoma. *Acta Ophthalmol.Scand.* 1999;77:658-662.

15. Harris A, Zarfati D, Zalish M, et al. Reduced cerebrovascular blood flow velocities and vasoreactivity in open-angle glaucoma. *Am.J.Ophthalmol.* 2003;135:144-147.
16. Rassam SM, Patel V, Kohner EM. The effect of acetazolamide on the retinal circulation. *Eye* 1993;7 (Pt 5):697-702.
17. Fuchsjager-Mayrl G, Wally B, Rainer G, et al. Effect of dorzolamide and timolol on ocular blood flow in patients with primary open angle glaucoma and ocular hypertension. *Br.J.Ophthalmol.* 2005;89:1293-1297.
18. Zeitz O, Matthiessen ET, Reuss J, et al. Effects of glaucoma drugs on ocular hemodynamics in normal tension glaucoma: A randomized trial comparing bimatoprost and latanoprost with dorzolamide [ISRCTN18873428]. *BMC Ophthalmol.* 2005;5:6.
19. Martinez A, Sanchez M. A comparison of the effects of 0.005% latanoprost and fixed combination dorzolamide/timolol on retrobulbar haemodynamics in previously untreated glaucoma patients. *Curr Med Res Opin.* 2006;22:67-73.
20. Uva MG, Longo A, Reibaldi M, Reibaldi A. The effect of timolol-dorzolamide and timolol-pilocarpine combinations on ocular blood flow in patients with glaucoma. *Am.J.Ophthalmol.* 2006;141:1158-1160.
21. Siesky B, Harris A, Cantor LB, et al. A comparative study of the effects of brinzolamide and dorzolamide on retinal oxygen saturation and ocular microcirculation in patients with primary open-angle glaucoma. *Br.J.Ophthalmol.* 2008;92:500-504.

22. Simsek T, Yanik B, Conkbayir I, Zilelioglu O. Comparative analysis of the effects of brimonidine and dorzolamide on ocular blood flow velocity in patients with newly diagnosed primary open-angle glaucoma. *J.Ocul.Pharmacol.Ther.* 2006;22:79-85.
23. Bergstrand IC, Heijl A, Harris A. Dorzolamide and ocular blood flow in previously untreated glaucoma patients: A controlled double-masked study. *Acta Ophthalmol.Scand.* 2002;80:176-182.
24. Chung HS, Harris A, Halter PJ, et al. Regional differences in retinal vascular reactivity. *Invest.Ophthalmol.Vis.Sci.* 1999;40:2448-2453.
25. Arend O, Harris A, Martin BJ, Holin M, Wolf S. Retinal blood velocities during carbogen breathing using scanning laser ophthalmoscopy. *Acta Ophthalmol (Copenh)* 1994;72:332-336.
26. Dorner GT, Garhofer G, Zawinka C, Kiss B, Schmetterer L. Response of retinal blood flow to CO₂-breathing in humans. *Eur.J.Ophthalmol.* 2002;12:459-466.
27. Venkataraman ST, Hudson C, Fisher JA, Flanagan JG. Novel methodology to comprehensively assess retinal arteriolar vascular reactivity to hypercapnia. *Microvasc.Res.* 2006;72:101-107.
28. Venkataraman ST, Hudson C, Fisher JA, Flanagan JG. The impact of hypercapnia on retinal capillary blood flow assessed by scanning laser doppler flowmetry. *Microvasc.Res.* 2005;69:149-155.

29. Venkataraman ST, Hudson C, Fisher JA, et al. Retinal arteriolar and capillary vascular reactivity in response to isoxic hypercapnia. *Exp.Eye Res.* 2008; 87(6):535-542.
30. Sines D, Harris A, Siesky B, et al. The response of retrobulbar vasculature to hypercapnia in primary open-angle glaucoma and ocular hypertension. *Ophthalmic Res.* 2007;39:76-80.
31. Hosking SL, Harris A, Chung HS, et al. Ocular haemodynamic responses to induced hypercapnia and hyperoxia in glaucoma. *Br.J.Ophthalmol.* 2004;88:406-411.
32. Kisilevsky M, Mardimae A, Slessarev M, Han J, Fisher J, Hudson C. Retinal arteriolar and middle cerebral artery responses to combined hypercarbic/hyperoxic stimuli. *Invest.Ophthalmol.Vis.Sci.* 2008;49:5503-5509.
33. Rhoades RA. Ventilation and mechanics of breathing. Rhoades RA and Tanner GA. *In Medical Physiology.* Philadelphia: Lipincott Williams & Wilkins; 2003. 309-336 pp.
34. Slessarev M, Fisher JA, Volgyesi G, et al. A new method and apparatus to reliably attain and maintain target end tidal gas concentrations. 2005;PCT/CA2005/001166 (In submission).
35. Field AS, Laurienti PJ, Yen YF, Burdette JH, Moody DM. Dietary caffeine consumption and withdrawal: Confounding variables in quantitative cerebral perfusion studies? *Radiology* 2003;227:129-135.
36. Ozkan B, Yuksel N, Anik Y, Altintas O, Demirci A, Caglar Y. The effect of caffeine on retrobulbar hemodynamics. *Curr.Eye Res.* 2008;33:804-809.

37. Nicholls SJ, Lundman P, Harmer JA, et al. Consumption of saturated fat impairs the anti-inflammatory properties of high-density lipoproteins and endothelial function. *J.Am.Coll.Cardiol.* 2006;48:715-720.
38. Gilmore ED, Hudson C, Preiss D, Fisher J. Retinal arteriolar diameter, blood velocity, and blood flow response to an isocapnic hyperoxic provocation. *Am J Physiol Heart Circ Physiol* 2005;288:H2912-H2917.
39. Gilmore ED, Hudson C, Venkataraman ST, Preiss D, Fisher J. Comparison of different hyperoxic paradigms to induce vasoconstriction: Implications for the investigation of retinal vascular reactivity. *Invest.Ophthalmol.Vis.Sci.* 2004;45:3207-3212.
40. Guan K, Hudson C, Flanagan JG. Variability and repeatability of retinal blood flow measurements using the canon laser blood flowmeter. *Microvasc.Res.* 2003;65:145-151.
41. Nagaoka T, Mori F, Yoshida A. Retinal artery response to acute systemic blood pressure increase during cold pressor test in humans. *Invest.Ophthalmol.Vis.Sci.* 2002;43:1941-1945.
42. Kida T, Harino S, Sugiyama T, Kitanishi K, Iwahashi Y, Ikeda T. Change in retinal arterial blood flow in the contralateral eye of retinal vein occlusion during glucose tolerance test. *Graefes Arch.Clin.Exp.Ophthalmol.* 2002;240:342-347.
43. Riva CE, Feke GT, Eberli B. Bidirectional LDV system for the absolute measurement of blood speed in retinal vessels. *Appl.Opt.* 1979;18:2301-2306.
44. Feke GT, Goger DG, Tagawa H, Delori FC. Laser doppler technique for absolute measurement of blood speed in retinal vessels. *IEEE Trans.Biomed.Eng.* 1987;34:673-680.

45. Sato E, Fekete GT, Menke MN, Wallace McMeel J. Retinal haemodynamics in patients with age-related macular degeneration. *Eye* 2006;20:697-702.
46. Ito S, Mardimae A, Han J, et al. Non-invasive prospective targeting of arterial P(CO₂) in subjects at rest. *J.Physiol.* 2008;586:3675-3682.
47. Cellini M, Possati GL, Profazio V, Sbrocca M, Caramazza N, Caramazza R. Color doppler imaging and plasma levels of endothelin-1 in low-tension glaucoma. *Acta Ophthalmol.Scand.Suppl.* 1997:11-13.
48. Bjarnhall G, Tomic L, Mishima HK, Tsukamoto H, Alm A. Retinal mean transit time in patients with primary open-angle glaucoma and normal-tension glaucoma. *Acta Ophthalmol.Scand.* 2007;85:67-72.
49. Zeitz O, Galambos P, Wagenfeld L, et al. Glaucoma progression is associated with decreased blood flow velocities in the short posterior ciliary artery. *Br.J.Ophthalmol.* 2006;90:1245-1248.
50. Colm O' Brien. Pulsatile ocular blood flow in normal pressure glaucoma. Pillunat L.E, Harris A, Anderson D.R and Greve E.L. *In Current concepts on ocular blood flow in glaucoma.* The Hague, The Netherlands: Kugler Publications; 1999. 111-117 pp.
51. Harris A, Kagemann L, Ehrlich R, Rospigliosi C, Moore D, Siesky B. Measuring and interpreting ocular blood flow and metabolism in glaucoma. *Can.J.Ophthalmol.* 2008;43:328-336.

52. Garzozzi HJ, Shoham N, Chung HS, Kagemann L, Harris A. Ocular blood flow measurements and their importance in glaucoma and age-related macular degeneration. *Isr.Med.Assoc.J.* 2001;3:443-448.
53. Gugleta K, Orgul S, Hasler P, Flammer J. Circulatory response to blood gas perturbations in vasospasm. *Invest.Ophthalmol.Vis.Sci.* 2005;46:3288-3294.
54. Feke GT, Pasquale LR. Retinal blood flow response to posture change in glaucoma patients compared with healthy subjects. *Ophthalmology* 2007.
55. Kerr J, Nelson P, O'Brien C. A comparison of ocular blood flow in untreated primary open-angle glaucoma and ocular hypertension. *Am.J.Ophthalmol.* 1998;126:42-51.
56. Grunwald JE, Piltz J, Hariprasad SM, DuPont J. Optic nerve and choroidal circulation in glaucoma. *Invest.Ophthalmol.Vis.Sci.* 1998;39:2329-2336.
57. Nicolela MT, Hnik P, Drance SM. Scanning laser doppler flowmeter study of retinal and optic disk blood flow in glaucomatous patients. *Am.J.Ophthalmol.* 1996;122:775-783.
58. Schwartz B, Rieser JC, Fishbein SL. Fluorescein angiographic defects of the optic disc in glaucoma. *Arch. Ophthalmol.* 1977;95:1961-1974.
59. Grieshaber MC, Terhorst T, Flammer J. The pathogenesis of optic disc splinter haemorrhages: A new hypothesis. *Acta Ophthalmol.Scand.* 2006;84:62-68.
60. Siegner SW, Netland PA. Optic disc hemorrhages and progression of glaucoma. *Ophthalmology* 1996;103:1014-1024.

61. Sponsel WE. Topical carbonic anhydrase inhibitors and visual function. L. E. Pillunat, A. Harris, D. R. Anderson and E. L. Greve. *In Current concepts on ocular blood flow in glaucoma*. The Hague, The Netherlands: Kugler Publications; 1999. 251-265 pp.
62. Venkataraman ST, Hudson C, Rachmiel R, et al. Plasma endothelin-1 and cyclic GMP in response to normoxic hypercapnia in primary open angle glaucoma. *Invest.Ophthalmol.Vis.Sci*. 2009 (In submission).
63. Harris A, Anderson DR, Pillunat L, et al. Laser doppler flowmetry measurement of changes in human optic nerve head blood flow in response to blood gas perturbations. *J.Glaucoma* 1996;5:258-265.
64. Hosking SL, Evans DW, Embleton SJ, Houde B, Amos JF, Bartlett JD. Hypercapnia invokes an acute loss of contrast sensitivity in untreated glaucoma patients. *Br.J.Ophthalmol*. 2001;85:1352-1356.
65. Robbins PA, Conway J, Cunningham DA, Khamnei S, Paterson DJ. A comparison of indirect methods for continuous estimation of arterial PCO₂ in men. *J.Appl.Physiol*. 1990;68:1727-1731.
66. Dumskyj MJ, Eriksen JE, Dore CJ, Kohner EM. Autoregulation in the human retinal circulation: Assessment using isometric exercise, laser doppler velocimetry, and computer-assisted image analysis. *Microvasc.Res*. 1996;51:378-392.
67. Riva CE, Grunwald JE, Petrig BL. Autoregulation of human retinal blood flow. an investigation with laser doppler velocimetry. *Invest.Ophthalmol.Vis.Sci*. 1986;27:1706-1712.

68. Lucy SD, Kowalchuk JM, Hughson RL, Paterson DH, Cunningham DA. Blunted cardiac autonomic responsiveness to hypoxemic stress in healthy older adults. *Can.J.Appl.Physiol.* 2003;28:518-535.
69. Radwan L, Koziorowski A, Maszczyk Z, et al. Respiratory response to inspiratory resistive load changes in patients with obstructive sleep apnea syndrome. *Pneumonol.Alergol.Pol.* 2000;68:44-56.
70. Rose PA, Hudson C. The impact of age on retinal vascular reactivity and the relationship with cardiovascular risk factors. *Invest.Ophthalmol.Vis.Sci.* 2007;E-abstract 2266.

7 Plasma Endothelin-1 and Cyclic GMP in Response to Normoxic Hypercapnia in Primary Open Angle Glaucoma

Venkataraman ST, Hudson C, Rachmiel R, Buys YM, Fisher JA, Vogl R, Tong J, Markowitz SN, Trope GE, Flanagan JG. Plasma endothelin-1 and cyclic GMP in response to normoxic hypercapnia in primary open angle glaucoma. Invest. Ophthalmol. Vis. Sci. (In submission).

7.1 Abstract

Aim: The aim of the study was to compare plasma endothelin-1 (ET-1) and cyclic guanosine monophosphate (cGMP) levels between patients with untreated primary open angle glaucoma (uPOAG), progressive POAG (pPOAG), newly treated POAG (ntPOAG) and controls at baseline and during hypercapnia.

Methods: The sample comprised 11 patients with uPOAG (mean age 54yrs, SD 11), 12 patients with pPOAG (63yrs, SD 9.0) and 16 healthy control subjects (55yrs, SD 7.0). The uPOAG group were treated with 2% topical Dorzolamide for 2 weeks to form the ntPOAG group. At each visit, blood samples were collected from the cubital vein (with PETCO₂ standardized to 38mmHg). ET-1 and cGMP levels were determined using immunoassay. Normoxic hypercapnia was then induced for 15 minutes and blood samples were collected during hypercapnia.

Results: Baseline ET-1 levels were different between the groups ($p=0.0012$), being lower in uPOAG ($1.21\text{pg/mL} \pm 0.56$) compared to pPOAG ($p=0.040$, $1.78\text{pg/mL} \pm 0.54$) and compared to controls ($p=0.028$, $1.77\text{pg/mL} \pm 0.43$). Similarly, ntPOAG exhibited lower ET-1

levels ($1.13\text{pg/mL} \pm 0.45$) compared to the pPOAG ($p=0.015$) and controls ($p=0.009$). During normoxic hypercapnia, uPOAG and ntPOAG exhibited lower ET-1 levels than pPOAG and controls. cGMP at baseline and during normoxic hypercapnia was not different between the groups. Baseline cGMP in uPOAG and ntPOAG ($r \geq +0.65$, $p \leq 0.030$) was associated with baseline blood flow. In the control group, reduced change in ET-1 from baseline to hypercapnia was associated with increased change in retinal blood flow ($r = -0.52$, $p = 0.04$). The change in ET-1 and cGMP in response to normoxic hypercapnia did not differ between the groups.

Conclusions: Plasma ET-1 levels were lower in uPOAG and ntPOAG groups at baseline and during normoxic hypercapnia. A relationship was demonstrated between biochemical markers of endothelial function and retinal blood flow and vascular reactivity in POAG and in controls.

Keywords: Endothelin-1, cyclic guanosine monophosphate, nitric oxide, uPOAG, pPOAG, retinal arterioles.

7.2 Introduction

A transient reduction of optic nerve head (ONH) perfusion and retinal ischemia are thought to be implicated in the pathogenesis of primary open angle glaucoma (POAG), in addition to the established risk factor of increased intra-ocular pressure (IOP) ¹⁻⁵. Endothelin-1 (ET-1) and nitric oxide (NO) are involved in the regulation of blood flow in the eye ⁶. ET-1 receptors have been located in the retina and the ONH ⁷. ET-1 promotes vasoconstriction in the retina by the stimulation of the ET-A receptor that is present in the vascular smooth muscle cells and pericytes ⁸⁻¹¹. In porcine eyes, ET-1 can also result in vasodilatation via the prostacyclin pathway, through the stimulation of ET-B receptors in the ophthalmic vasculature ⁹. Conversely, NO driven relaxation of the retinal smooth muscle cells is thought to occur via an increase in cyclic guanosine monophosphate (cGMP, i.e. a surrogate marker of NO) ^{8, 12}, although other vasodilating factors such as cyclic adenosine monophosphate (cAMP) ¹³ and prostacyclin might also be responsible for vasodilation ¹⁴. A basal release of NO is essential for the regulation of retinal vascular tone ¹⁵⁻¹⁹.

There is lack of information regarding the response of biochemical markers of endothelial function in POAG to systemic provocation. Nicolela and co-workers (2003) assessed plasma levels of ET-1 before and after cold provocation and showed an increase in ET-1 after provocation in patients with treated POAG ²⁰. However, the study failed to show any significant correlation between change in biochemical markers of endothelial function and retinal capillary vascular reactivity. In addition, an abnormal decrease in ET-1 level has been found during posture change in NTG (from a supine to upright position) ²¹.

A number of limitations exist regarding previous research in this area. In particular: 1) Studies have often used patients who were being treated with IOP lowering medications or did not report the treatment status of patients ²²⁻²⁹ 2) Studies have typically determined homeostatic ET-1 ^{22-25, 30-32} and NO levels ^{26-29, 33, 34} in patients with glaucoma, rather than using some form of provocation to assess functional vascular regulation. 3) Only a few studies have adopted the approach of simultaneously assessing functional vascular regulation (Chapter 6) ^{35,20} and biochemical markers of endothelial function in POAG patients. The development of a combined vascular function and biochemical endothelial function approach is essential in order to further our understanding of the patho-physiology of POAG. 4) Patients with progressive (p)POAG are thought to be especially prone to vascular dysregulation ³⁶⁻³⁸ and the majority of studies have failed to look at this susceptible group.

The ambiguity of the work to date in this area mandates further investigation to better understand some of the mechanisms involved in the pathogenesis of POAG. The aim of this study was to compare plasma ET-1 and cGMP levels between groups of patients with untreated primary open angle glaucoma (uPOAG), progressive POAG (pPOAG), newly treated POAG (ntPOAG) and controls. The effect of systemic hypercapnic provocation, whilst maintaining normoxia, on plasma ET-1 and cGMP was assessed in all the groups. We then followed-up on the uPOAG group after treatment with a single drop of 2% Dorzolamide, twice daily for 2 weeks (who then formed the ntPOAG group). The study also aimed to correlate biochemical markers of endothelial function and functional measures of retinal blood flow and vascular reactivity in all the groups.

7.3 Methods

7.3.1 Sample

The study was approved by the Research Ethics Boards of the University Health Network, University of Toronto, and the Office of Research Ethics of the University of Waterloo. All subjects provided signed informed consent prior to participation after explanation of the nature and possible consequences of the study according to the tenets of the Declaration of Helsinki. The sample comprised 4 groups, including 11 patients with uPOAG (i.e. newly diagnosed POAG) of mean age 54 yrs (SD 11; 3 males : 8 females) and 12 patients with progressive POAG (pPOAG) of age 63 yrs (SD 9.0, 6 males : 6 females). The uPOAG group were treated with 2% topical Dorzolamide for 2 weeks to form the newly treated POAG (ntPOAG) group. Sixteen healthy control subjects of age 55 yrs (SD 7.0, 6males :10 females) formed the control group. There was a significant difference in the mean age of the pPOAG group compared to the controls ($p=0.003$, one tailed, unpaired t-test). pPOAG patients were classified based on the occurrence of optic disc hemorrhage within the past 24 months.

All participants had a visual acuity of 20/40, or better, and a refractive error less than ± 6.00 DS and ± 1.50 DC. The participants were free of other ocular pathologies and were non-smokers. Participants with cardiovascular disorders, uncontrolled systemic hypertension and diabetes were excluded from the study. Healthy control subjects had no family history of glaucoma and diabetes. All participants were asked to abstain from caffeine containing food or drinks and red meat at least 12 hours before the study visit. An impact of caffeine on

cerebral blood flow is well established ³⁹, while a recent study also showed the influence of caffeine on retrobulbar blood velocity ⁴⁰. Consumption of saturated fats is also known to influence vascular reactivity ⁴¹.

7.3.2 Procedures

7.3.2.1 ET-1 and cGMP assays

The blood sample was collected and prepared according to the manufacturer's instructions. ET-1 (R&D systems, Human Endothelin-1 Immunoassay, MN USA) and cGMP (Cayman Chemicals, Ann Arbor, MI USA) were assessed using immunoassay. The intra-assay Coefficient of Variation (CoV) of three samples of mean ET-1 of 14.4pg/mL, 32.8pg/mL and 68.7pg/mL were 4.6%, 4.5% and 4.2%, respectively. The inter-assay CoV of three samples of mean ET-1 of 16.2pg/mL, 33.9pg/mL and 70pg/mL were 6.5%, 5.5% and 5.1%, respectively. The intra-assay CoV for cGMP in the mid-range 0.55 to 30 pmol/mL ranges from 2% (at 5pmol/mL) to 20% (at 0.3pmol/mL). The inter-assay CoV ranges from 7% (at 5pmol/mL) to 28% (at 0.3pmol/mL).

Further details of the blood preparation procedures and the ET-1 and cGMP assays are included in the thesis Appendix.

7.3.2.2 Normoxic hypercapnia provocation

The technique used to induce normoxic hypercapnia has been fully described in previous publications from our group ^{42, 43 35}. Briefly, an automated gas flow controller (RespirActTM,

Thornhill Research Inc., Toronto Canada) was attached to a sequential rebreathing circuit to induce normoxic hypercapnia in all the groups^{42, 43}.

7.3.3 Procedures

Eligibility to participate in the study was assessed during the first visit. The diagnosis of POAG was confirmed by a glaucoma specialist (GT or YB). During the second visit, participants rested for 15 minutes before the start of the breathing paradigm. Following this, PETCO₂ (partial end-tidal concentration of CO₂) was normalized to 38mmHg for 10minutes and a blood sample was then collected from the cubital vein. Normoxic hypercapnia (consisting of a 15% increase in PETCO₂ from baseline and PETO₂ maintained at resting levels) was then induced and stabilized for 15 minutes while a second blood sample was collected when both PETCO₂ and PETO₂ were stable. Patients with uPOAG were then treated with a single drop of 2% topical Dorzolamide twice daily for 2 weeks. At the end of this 2 week period, the procedures were replicated in the ntPOAG group.

7.3.4 Statistical Analysis

A one-way Analysis of Variance (ANOVA) was performed to compare ET-1 and cGMP levels at baseline and during hypercapnia in all the groups (Statistica, Statsoft version 7.0). Tukey's honestly significant differences (HSD) post-hoc test was used to compare between patient groups. Any difference in the change of ET-1 and cGMP in response to normoxic hypercapnia was compared using a one-way ANOVA followed by Tukey's HSD post hoc test for between groups comparison.

Correlation Analysis: The plasma ET-1 and cGMP results were correlated to functional measures of retinal arteriolar blood flow and vascular reactivity simultaneously assessed in response to normoxic hypercapnia in the same sample of patients (Chapter 6) ³⁵. Pearson correlation analysis (GraphPad Prism version 5) was performed to correlate absolute ET-1 and cGMP levels at baseline and during hypercapnia to absolute retinal arteriolar blood flow in all the groups. The change in ET-1 and cGMP in response to normoxic hypercapnia was also correlated to the vascular reactivity in all the groups. Only conservative correlations with an $r > 0.40$ (represents 16% of the variance within the correlation) and a $p < 0.05$ have been reported in order to avoid false-positive results.

7.4 Results

Baseline ET-1 levels were different across groups ($p=0.0012$) (Table 7.1). ET-1 levels were lower in uPOAG compared to pPOAG ($p=0.040$) and controls ($p=0.028$). Similarly, ntPOAG also showed lower ET-1 levels compared to pPOAG ($p=0.015$) and controls ($p=0.009$). The group mean baseline plasma ET-1 in the uPOAG and ntPOAG groups was 1.21pg/mL (SD 0.56) and 1.13pg/mL (SD 0.45), respectively, while in the pPOAG group and in the controls it was 1.78pg/mL (SD 0.54) and 1.77pg/mL (SD 0.43).

ET-1 levels during normoxic hypercapnia were also different across groups ($p=0.0014$) (Table 7.1). ET-1 levels in uPOAG were lower than the pPOAG ($p=0.017$) and controls ($p=0.013$). Similarly, the ET-1 levels were lower in ntPOAG compared to pPOAG ($p=0.032$) and controls ($p=0.026$) during hypercapnia.

There was no difference in cGMP at baseline and during normoxic hypercapnia across the groups (Table 7.2). The group mean baseline cGMP in the uPOAG, and ntPOAG groups was 3.23pmol/mL (SD 0.54) and 3.06pmol/mL (SD 0.98), respectively, while in pPOAG and controls it was 2.96pmol/mL (SD 1.06) and 2.92pmol/mL (SD 0.76).

Condition	uPOAG	ntPOAG	pPOAG	Controls	p-value
Baseline	1.21 ± 0.56*	1.13 ± 0.45*	1.78 ± 0.54	1.77 ± 0.43	0.0012
Hypercapnia	1.09 ± 0.72*	1.13 ± 0.52*	1.78 ± 0.53	1.76 ± 0.41	0.0014

Table 7.1 Represents group mean ± SD of the ET-1 values (pg/mL) at baseline and during normoxic hypercapnia in uPOAG (untreated POAG), ntPOAG (newly treated POAG), pPOAG (progressive POAG), and controls.

The p-value represents significant difference across groups (One-way ANOVA.) * denotes the groups that were significantly different when compared between groups using Tukey's honestly significant difference (HSD) post-hoc test (significance at the level of $p < 0.05$).

Condition	uPOAG	ntPOAG	pPOAG	Controls	p-value
Baseline	3.23 ± 0.54	3.06 ± 0.98	2.96 ± 1.06	2.92 ± 0.76	NS
Hypercapnia	2.86 ± 0.88	2.97 ± 0.97	2.86 ± 1.03	2.62 ± 0.81	NS

Table 7.2 Represents group mean ± SD of the cGMP values (pmol/mL) at baseline and during normoxic hypercapnia in uPOAG (untreated POAG), ntPOAG (newly treated POAG), pPOAG (progressive POAG), and controls.

NS denotes not significant.

A significant correlation between plasma cGMP and retinal arteriolar blood flow at baseline in uPOAG ($r = +0.68$, $p = 0.023$) and ntPOAG ($r = +0.65$, $p = 0.030$) was noted (Figures 7.1A & 7.1B), suggesting that higher cGMP was associated with higher blood flow. Conversely, there was a relatively weak non-significant negative correlation between the ET-1 and arteriolar blood flow at baseline in uPOAG ($r = -0.45$, $p = 0.164$) and a negative non-

significant correlation in ntPOAG ($r = -0.59$, $p = 0.061$) (Figures 7.2A & 7.2B), suggesting that higher ET-1 level was associated with lower blood flow. In ntPOAG, ET-1 during normoxic hypercapnia negatively correlated to blood flow ($r = -0.65$, $p = 0.043$), suggesting that higher ET-1 was associated with lower blood flow, while there was no correlation in uPOAG ($r = -0.31$, $p = 0.354$) during hypercapnia (Figures 7.3A & 7.3B).

In the control group only, there was a significant negative correlation between the change in ET-1 from baseline to normoxic hypercapnia and the change in arteriolar blood flow ($r = -0.52$, $p = 0.04$, Figure 7.4A), suggesting that as the change in ET-1 reduced, the change in blood flow increased. There was also a relatively weak non-significant positive correlation between the change in cGMP from baseline to normoxic hypercapnia and the change in blood flow in the control group ($r = +0.45$, $p = 0.08$, Figure 7.4B), possibly indicating that as the change in cGMP increased, the change in blood flow also increased.

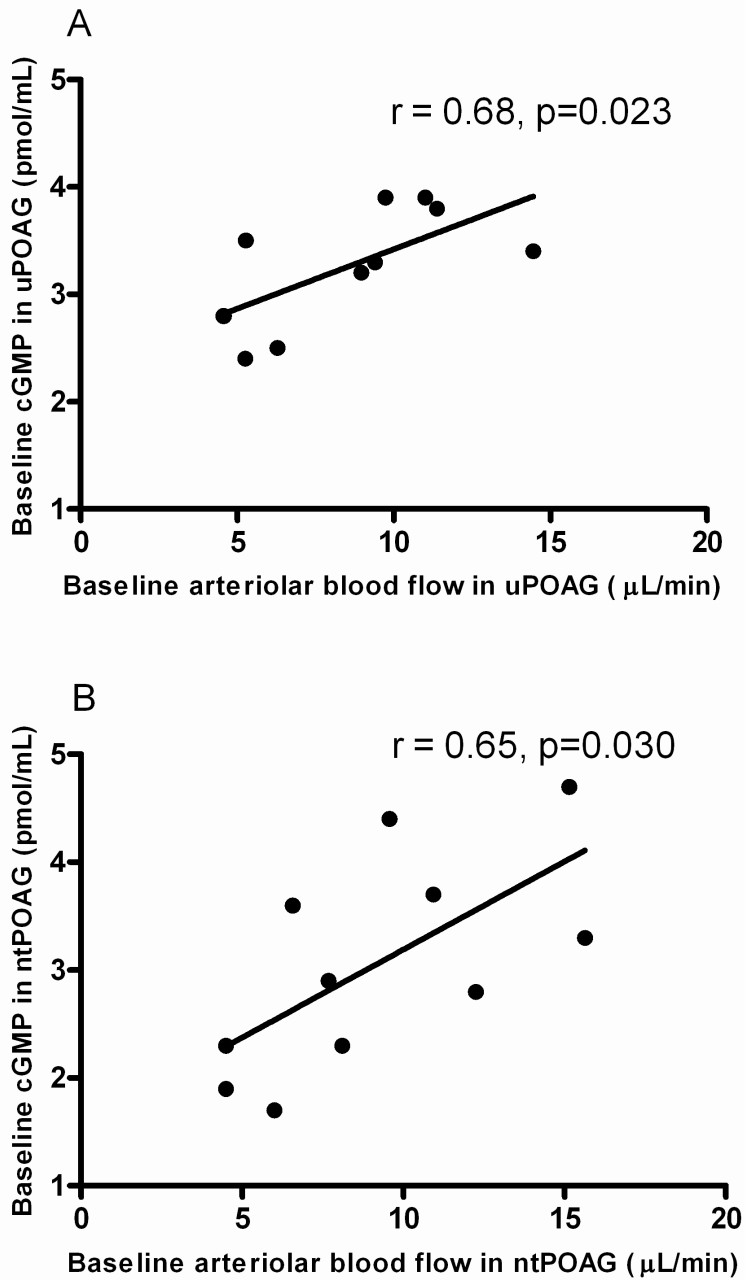


Figure 7.1 Correlation analysis of the baseline cGMP and retinal arteriolar blood flow in A) uPOAG (untreated POAG) and B) ntPOAG (newly treated POAG).

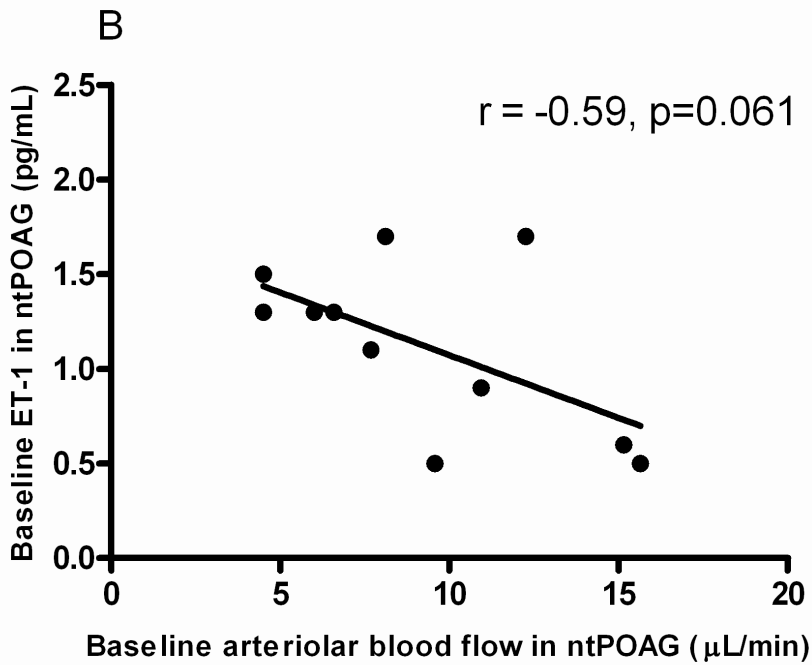
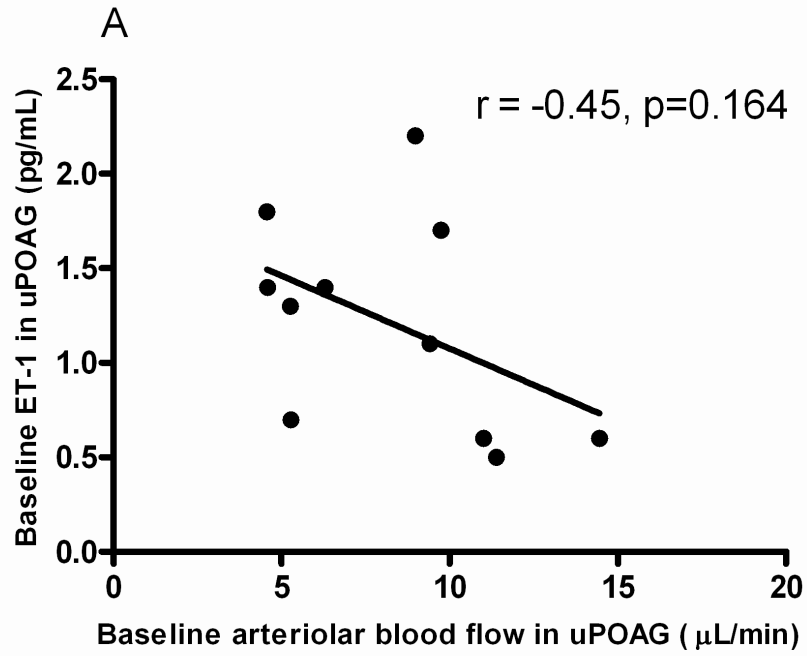


Figure 7.2 Correlation analysis of the baseline ET-1 concentration and retinal arteriolar blood flow in A) uPOAG (untreated POAG) and B) ntPOAG (newly treated POAG).

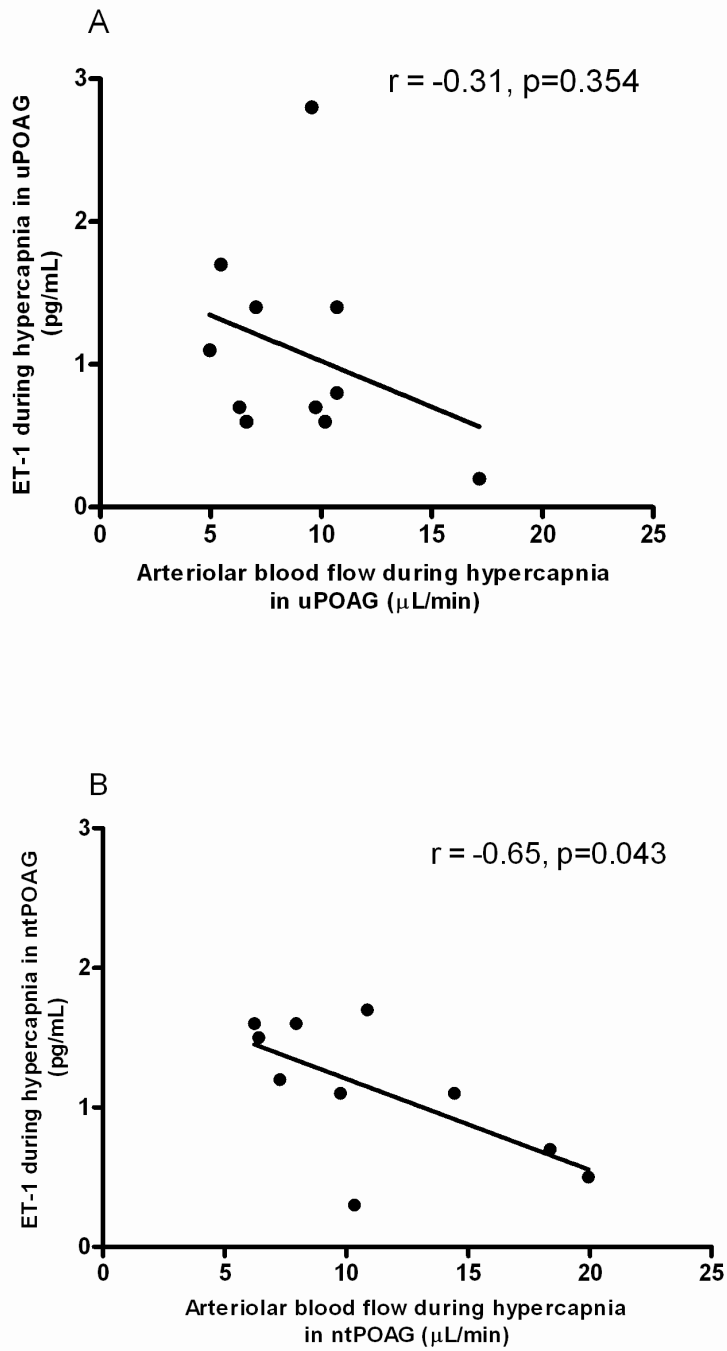


Figure 7.3 Correlation analysis of the hypercapnic ET-1 and retinal arteriolar blood flow in A) uPOAG (untreated POAG) and B) ntPOAG (newly treated POAG).

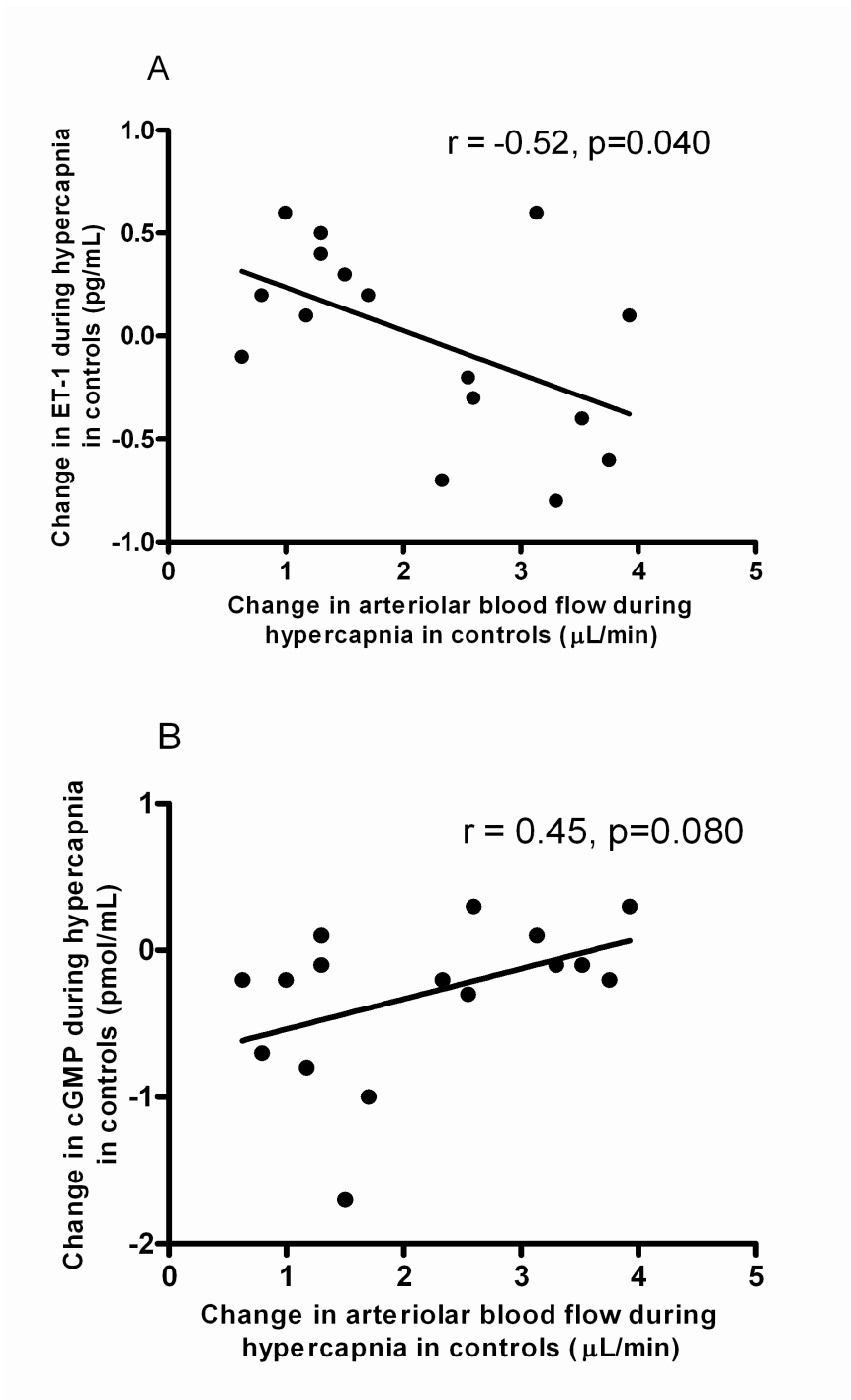


Figure 7.4 Correlation analysis of the change in response to normoxic hypercapnia of A) ET-1 and B) cGMP to the change in arteriolar blood flow in controls.

There was no difference in the change in ET-1 and in cGMP in response to normoxic hypercapnia across groups (Figures 7.5 and 7.6, respectively). In terms of percentage change in ET-1, uPOAG showed a greater trend to decrease (-9.60%) in response to normoxic hypercapnia than the other groups (ntPOAG = -1.61%, pPOAG = +2.86% and controls = +2.84%). In uPOAG (-11.23%), the percentage change in cGMP also showed a greater trend to decrease compared to ntPOAG (+4.04%) and pPOAG (-0.88%). In the controls, however, the magnitude of change in cGMP (-9.62%) due to hypercapnia was similar to that of uPOAG.

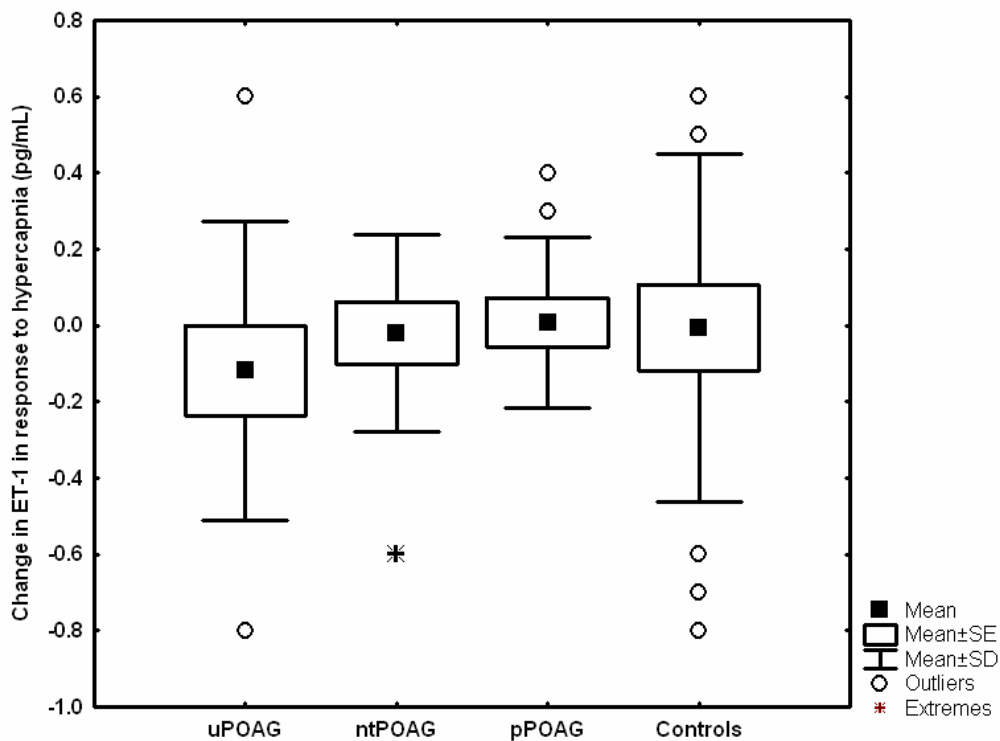


Figure 7.5 Box plots represent change in plasma ET-1 in response to normoxic hypercapnia in uPOAG (untreated POAG), ntPOAG (newly treated POAG), pPOAG (progressive POAG) and controls.

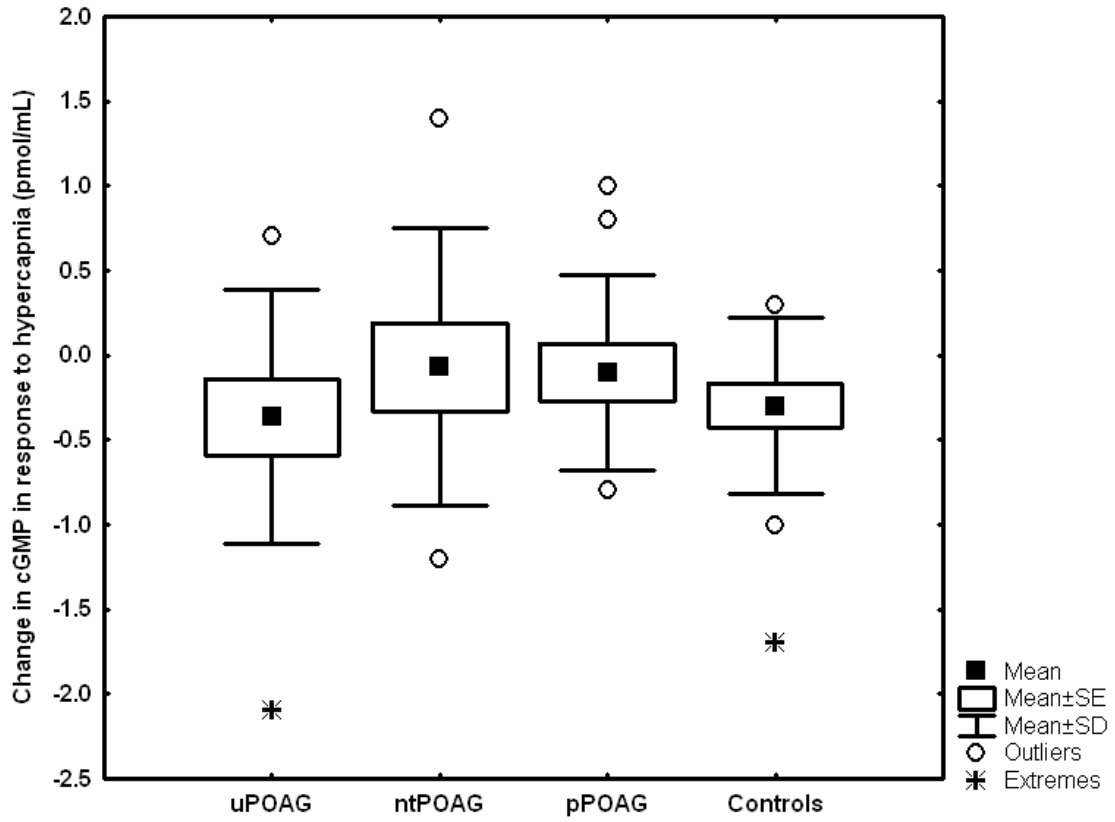


Figure 7.6 Box plots represent change in plasma cGMP in response to normoxic hypercapnia in uPOAG (untreated POAG), ntPOAG (newly treated POAG), pPOAG (progressive POAG) and controls.

7.5 Discussion

This study found that baseline ET-1 levels were lower in the uPOAG and ntPOAG groups compared to the pPOAG group and controls. The ET-1 levels were repeatedly lower in the uPOAG and ntPOAG groups in response to normoxic hypercapnia. These results suggest that there is an overall reduction in ET-1 in uPOAG. This is the first study to show a reduction in ET-1 levels in uPOAG at baseline and after short-term treatment with 2% Dorzolamide. Interestingly, there was an improvement in functional retinal vascular reactivity after Dorzolamide treatment ³⁵, possibly suggesting that Dorzolamide treatment does not immediately impact systemic measures of ET-1 and cGMP, although the functional assessment of retinal vascular reactivity had recovered at this point in time. Alternatively, this finding might indicate that the recovery of vascular reactivity following Dorzolamide treatment occurs as a result of IOP reduction. In addition, the correlation results in the controls showed that as the change in ET-1 reduced during normoxic hypercapnia, the change in blood flow increased.

Previously, higher baseline plasma levels of ET-1 have been reported in patients with treated NTG ^{22, 23} and pPOAG ²⁴. while others showed no difference in POAG ^{20, 21, 25, 30-32} and in untreated NTG ³². In our study, however, there was a reduced ET-1 in newly diagnosed, untreated patients compared to controls and pPOAG. The finding of higher levels of plasma ET-1 in pPOAG (patients on IOP lowering medications) than uPOAG in our study is consistent with previous reports of ET-1 levels in treated patients ²¹⁻²⁴. Only one previous study has assessed ET-1 in patients with NTG without prior treatment and found no difference in baseline ET-1 levels compared to controls ³². Certain IOP lowering medications

have also been suggested to improve ocular blood flow via a mechanism that is independent of the change in ocular perfusion pressure^{44,45} and may improve retinal vascular reactivity in untreated POAG^{46,35}. In this study, we found evidence of the effect of treatment on the expression of biochemical markers of endothelial function. Based on the results of this study, it is likely that the findings of earlier studies are confounded by the influence of IOP lowering medications.

A decrease in the baseline surrogate markers of NO in the aqueous of treated POAG has been reported^{26,29,33} and also in the plasma of patients with treated NTG³⁴. However, there have also been reports of an increase in NO markers in the plasma²⁷ and aqueous²⁸ of treated POAG. In this study, we did not see any difference in cGMP levels at baseline and during normoxic hypercapnia in any of the POAG groups when compared to controls. The discrepancies seen between studies that measured biochemical markers of endothelial function might be due to the differences in assay procedures and their cross-reactivities. Furthermore, the role of NO in the patho-physiology of POAG is controversial and, due to its short half-life, direct assessment of NO is challenging. NO is thought to produce vasodilation by a decrease in intracellular Ca^{2+} and an increase in cGMP levels^{9,15,47-49}. Recently, a less pronounced decrease in retinal blood flow was reported in POAG compared to the controls after systemic inhibition of NO, suggesting that other biochemical vascular factors might be involved in effecting vaso-dilation⁵⁰.

Previous studies have only assessed homeostatic blood flow in POAG and there is lack of work on the assessment of retinal vascular reactivity. In addition, patients with progressive

POAG have been suggested to be more susceptible to vascular dysregulation but studies have failed to look at retinal vascular reactivity and biochemical markers of endothelial function. In an earlier study, we showed a reduced magnitude of vascular reactivity in uPOAG and pPOAG compared to controls in response to normoxic hypercapnia. We also found that treatment with 2% Dorzolamide, for 2 weeks improved the magnitude of retinal vascular reactivity in ntPOAG (Chapter 6) ³⁵. A decrease in extracellular pH has been suggested as a possible mechanism for a reported increase in homeostatic blood flow after Dorzolamide treatment ^{44, 51-53}. Also, a reduced involvement of NO during acetazolamide induced vasodilation in humans has been reported ⁵². However, the mechanism responsible for the improvement in vascular reactivity after Dorzolamide treatment is still not clear and we continue to investigate this question in our on-going research. It is possible that the reduction in IOP would improve vascular reactivity, although a direct effect of Dorzolamide on the retinal vessels cannot be excluded.

This study found significant correlations between homeostatic blood flow and biochemical markers of endothelial function. A strong relationship was noted between baseline cGMP levels and arteriolar blood flow in uPOAG and ntPOAG, suggesting an association between increase in cGMP and increase in blood flow. A negative correlation was noted in uPOAG and ntPOAG between ET-1 and baseline blood flow, while a stronger negative correlation was observed between ET-1 and blood flow during hypercapnia only in the ntPOAG. These associations suggest that increased expression of ET-1 inhibits blood flow in POAG; this association was repeated in response to hypercapnic provocation and after treatment with

Dorzolamide. These correlations show that ET-1 and cGMP are involved in the regulation of blood flow in POAG but clearly the situation is complex and much remains to be revealed.

The study also correlated the functional vascular reactivity to biochemical markers of endothelial function. In healthy subjects, an association was found such that as the change in ET-1 from baseline to hypercapnia decreases, there is an increase in the vascular reactivity of arteriolar blood flow. In addition, as the change in cGMP increases, there is an increase in the change of arteriolar blood flow in healthy subjects. Previously, Nicoleta and co-workers (2003) correlated the change in ET-1 levels to the change in finger blood flow after cold provocation in treated POAG patients and failed to show any significant relationship²⁰. To the best of our knowledge, this is the first study where an association between biochemical markers of endothelial function and functional vascular reactivity in response to hypercapnia has been established. This approach can be used to further our understanding about the patho-physiology of POAG. The correlation observed in healthy subjects in this study further validates the functional measures of vascular reactivity and provides evidence of the underlying physiological mechanisms responsible for the functional measures (Chapter 6)³⁵.

There was no significant difference in the magnitude of change in ET-1 and cGMP between baseline and normoxic hypercapnia across groups. However, there was a trend towards a greater percentage decrease of ET-1 (i.e. 4 times greater) in response to normoxic hypercapnia in uPOAG than the other groups. In the ntPOAG group, there was no such decrease seen, possibly indicating an effect of Dorzolamide on the expression of ET-1. Similarly, a trend towards a greater percentage decrease of cGMP in response to normoxic

hypercapnia was seen in uPOAG that was not repeated after treatment with Dorzolamide, although in a related study functional vascular reactivity increased in response to normoxic hypercapnia after treatment with Dorzolamide (Chapter 6)³⁵. Interestingly, the controls also showed a similar magnitude of decrease in cGMP during hypercapnia as the uPOAG group.

It is possible that endothelium derived vasodilating factors other than cGMP might be involved in retinal vasodilation^{8, 54}. The role of NO during hypercapnic vasodilation in the cerebral vessels of animal models is established^{13, 55-57}. In the retinal circulation, however, the involvement of NO is still controversial^{19, 58, 59}.

We noted some discrepancies in the correlation results between biochemical markers of endothelial function and functional vascular reactivity. A difference in the time of recovery of vascular reactivity in POAG after short term treatment with Dorzolamide compared to any measureable changes in the biochemical markers of endothelial function may well explain such discrepancy. That is, functional vascular reactivity could be decreased in pPOAG and uPOAG earlier than any quantifiable changes in the biochemical markers of endothelial function. Furthermore, it is not known whether systemic levels of ET-1 and cGMP can be related to the concentrations present in the ocular circulation. The blood flow in the retina and the ONH is regulated by locally mediated mechanisms^{6, 54}. Some of the earlier studies have assessed aqueous levels of ET-1 or cGMP in POAG and NTG which is also thought to represent expression of biochemical markers of endothelial function under local conditions. Nevertheless, a linear relationship has been reported between aqueous and plasma cGMP²⁶ in POAG but any association for aqueous derived ET-1 remains elusive.

Limitations: In this study, 2 patients in the uPOAG and 2 patients in the pPOAG groups were taking systemic anti-hypertensive drugs. Also, the patients in the pPOAG group were on topical IOP lowering medications including beta-blockers, carbonic anhydrase inhibitors and prostaglandin analogues, all of which potentially might influence the expression of endothelial derived vasoactive factors. The pPOAG group was older than the controls and uPOAG groups, primarily because patients with pPOAG had relatively long standing glaucoma. It has been suggested that ET-1 levels may increase with age³¹. However, there was no difference in the baseline ET-1 and cGMP levels in pPOAG compared to the controls. Furthermore, the major limiting factor in the assessment of cGMP as a surrogate marker of NO is the influence of diet. Studies have shown increased variability of NO with uncontrolled diet, while a low-nitrate diet helps to accurately assess NO^{60, 61}. Apart from a single previous study²⁶, the majority of the studies have failed to control the dietary intake of participants. In this study, patients avoided the intake of food rich in saturated fats and nitrates such as red meat for at least 12 hours before the study visit, assuming adequate compliance.

7.6 Conclusions

Plasma ET-1 levels at baseline and during normoxic hypercapnia were significantly lower in the uPOAG and ntPOAG groups compared to controls and pPOAG and this reduced expression of ET-1 was unaltered after short-term treatment. There was no difference in the baseline cGMP across groups. This is the first study to report a correlation between retinal vascular reactivity and biochemical markers of endothelial function. There was a negative correlation between the expression of ET-1 in response to normoxic hypercapnia and the

magnitude of vascular reactivity in controls. The assessment of ET-1, and to a lesser extent, cGMP in patients with POAG provides useful information about the function of retinal blood vessels at baseline and during hypercapnic provocation. Clearly, the relationship between functional vascular reactivity and biochemical markers of endothelial function is complex and much remains to be revealed.

7.7 References

1. Flammer J, Mozaffarieh M. What is the present pathogenetic concept of glaucomatous optic neuropathy? *Surv.Ophthalmol.* 2007;52:S162-73.
2. Anderson DR. Introductory comments on blood flow autoregulation in the optic nerve head and vascular risk factors in glaucoma. *Surv.Ophthalmol.* 1999;43 Suppl 1:S5-9.
3. Chung HS, Harris A, Evans DW, Kagemann L, Garzosi HJ, Martin B. Vascular aspects in the pathophysiology of glaucomatous optic neuropathy. *Surv.Ophthalmol.* 1999;43 Suppl 1:S43-S50.
4. Grieshaber MC, Mozaffarieh M, Flammer J. What is the link between vascular dysregulation and glaucoma? *Surv.Ophthalmol.* 2007;52:S144-54.
5. Butt Z, O'Brien C, McKillop G, Aspinall P, Allan P. Color doppler imaging in untreated high- and normal-pressure open-angle glaucoma. *Invest.Ophthalmol.Vis.Sci.* 1997;38:690-696.
6. Cioffi GA, Granstam E, Alm A. Ocular circulation. P. Kaufman and A. Alm. *In Adler's physiology of the eye.* Elsevier; 2002. 747-784 pp.
7. Yorio T, Krishnamoorthy R, Prasanna G. Endothelin: Is it a contributor to glaucoma pathophysiology? *J.Glaucoma* 2002;11:259-270.
8. Haefliger IO, Flammer J, Beny JL, Luscher TF. Endothelium-dependent vasoactive modulation in the ophthalmic circulation. *Prog.Retin.Eye Res.* 2001;20:209-225.

9. Meyer P, Flammer J, Luscher TF. Endothelium-dependent regulation of the ophthalmic microcirculation in the perfused porcine eye: Role of nitric oxide and endothelins. *Invest.Ophthalmol.Vis.Sci.* 1993;34:3614-3621.
10. Zhu Y, Park TS, Gidday JM. Mechanisms of hyperoxia-induced reductions in retinal blood flow in newborn pig. *Exp.Eye Res.* 1998;67:357-369.
11. Dallinger S, Dorner GT, Wenzel R, et al. Endothelin-1 contributes to hyperoxia-induced vasoconstriction in the human retina. *Invest.Ophthalmol.Vis.Sci.* 2000;41:864-869.
12. Haefliger IO, Zschauer A, Anderson DR. Relaxation of retinal pericyte contractile tone through the nitric oxide-cyclic guanosine monophosphate pathway. *Invest.Ophthalmol.Vis.Sci.* 1994;35:991-997.
13. Wang Q, Bryowsky J, Minshall RD, Pelligrino DA. Possible obligatory functions of cyclic nucleotides in hypercapnia-induced cerebral vasodilation in adult rats. *Am.J.Physiol.* 1999;276:H480-H487.
14. Haefliger IO, Meyer P, Flammer J. Endothelium-dependent vasoactive factors. H. J. Kaiser, J. Flammer and P. Hendrickson. *In Ocular blood flow. Glaucoma-meeting 1995.* Basel, Karger; 1996. 51-63 pp.
15. Haefliger IO, Flammer J, Luscher TF. Heterogeneity of endothelium-dependent regulation in ophthalmic and ciliary arteries. *Invest.Ophthalmol.Vis.Sci.* 1993;34:1722-1730.
16. Jarajapu YP, Grant MB, Knot HJ. Myogenic tone and reactivity of the rat ophthalmic artery. *Invest.Ophthalmol.Vis.Sci.* 2004;45:253-259.

17. Dorner GT, Garhofer G, Kiss B, et al. Nitric oxide regulates retinal vascular tone in humans. *Am.J.Physiol.Heart Circ.Physiol.* 2003;285:H631-H636.
18. Pechanova O, Simko F. The role of nitric oxide in the maintenance of vasoactive balance. *Physiol.Res.* 2007;56 Suppl 2:S7-S16.
19. Donati G, Pournaras CJ, Munoz JL, Tsacopoulos M. The role of nitric oxide in retinal vasomotor regulation. *Klin.Monatsbl.Augenheilkd.* 1994;204:424-426.
20. Nicolela MT, Ferrier SN, Morrison CA, et al. Effects of cold-induced vasospasm in glaucoma: The role of endothelin-1. *Invest.Ophthalmol.Vis.Sci.* 2003;44:2565-2572.
21. Kaiser HJ, Flammer J, Wenk M, Luscher T. Endothelin-1 plasma levels in normal-tension glaucoma: Abnormal response to postural changes. *Graefes Arch.Clin.Exp.Ophthalmol.* 1995;233:484-488.
22. Sugiyama T, Moriya S, Oku H, Azuma I. Association of endothelin-1 with normal tension glaucoma: Clinical and fundamental studies. *Surv.Ophthalmol.* 1995;39 Suppl 1:S49-S56.
23. Cellini M, Possati GL, Profazio V, Sbrocca M, Caramazza N, Caramazza R. Color doppler imaging and plasma levels of endothelin-1 in low-tension glaucoma. *Acta Ophthalmol.Scand.Suppl.* 1997:11-13.
24. Emre M, Orgul S, Haufschild T, Shaw SG, Flammer J. Increased plasma endothelin-1 levels in patients with progressive open angle glaucoma. *Br.J.Ophthalmol.* 2005;89:60-63.
25. Kanimatsu S, Mayama C, Tomidokoro A, Araie M. Plasma endothelin-1 level in japanese normal tension glaucoma patients. *Curr.Eye Res.* 2006;31:727-731.

26. Galassi F, Renieri G, Sodi A, Ucci F, Vannozzi L, Masini E. Nitric oxide proxies and ocular perfusion pressure in primary open angle glaucoma. *Br.J.Ophthalmol.* 2004;88:757-760.
27. Kotikoski H, Moilanen E, Vapaatalo H, Aine E. Biochemical markers of the L-arginine-nitric oxide pathway in the aqueous humour in glaucoma patients. *Acta Ophthalmol.Scand.* 2002;80:191-195.
28. Tsai DC, Hsu WM, Chou CK, et al. Significant variation of the elevated nitric oxide levels in aqueous humor from patients with different types of glaucoma. *Ophthalmologica* 2002;216:346-350.
29. Kosior-Jarecka E, Gerkowicz M, Latalaska M, Koziol-Montewka M, Szczepanik A. Nitric oxide level in aqueous humor in patients with glaucoma. *Klin.Oczna* 2004;106:158-159.
30. Hollo G, Lakatos P, Farkas K. Cold pressor test and plasma endothelin-1 concentration in primary open-angle and capsular glaucoma. *J.Glaucoma* 1998;7:105-110.
31. Tezel G, Kass MA, Kolker AE, Becker B, Wax MB. Plasma and aqueous humor endothelin levels in primary open-angle glaucoma. *J.Glaucoma* 1997;6:83-89.
32. Henry E, Newby DE, Webb DJ, Hadoke PW, O'Brien CJ. Altered endothelin-1 vasoreactivity in patients with untreated normal-pressure glaucoma. *Invest.Ophthalmol.Vis.Sci.* 2006;47:2528-2532.
33. Doganay S, Evereklioglu C, Turkoz Y, Er H. Decreased nitric oxide production in primary open-angle glaucoma. *Eur.J.Ophthalmol.* 2002;12:44-48.

34. Colm O' Brien. Pulsatile ocular blood flow in normal pressure glaucoma. Pillunat L.E, Harris A, Anderson D.R and Greve E.L. *In Current concepts on ocular blood flow in glaucoma*. The Hague, The Netherlands: Kugler Publications; 1999. 111-117 pp.
35. Venkataraman ST, Hudson C, Rachmiel R, et al. Retinal arteriolar vascular reactivity in untreated and progressive primary open angle glaucoma. *Invest Ophthalmol Vis Sci*. 2009 (In submission).
36. Budenz DL, Anderson DR, Feuer WJ, et al. Detection and prognostic significance of optic disc hemorrhages during the ocular hypertension treatment study. *Ophthalmology* 2006; 113(12): 2137-2143.
37. Mozaffarieh M, Flammer J. Is there more to glaucoma treatment than lowering IOP? *Surv.Ophthalmol*. 2007;52 Suppl 2:S174-9.
38. Siegner SW, Netland PA. Optic disc hemorrhages and progression of glaucoma. *Ophthalmology* 1996;103:1014-1024.
39. Field AS, Laurienti PJ, Yen YF, Burdette JH, Moody DM. Dietary caffeine consumption and withdrawal: Confounding variables in quantitative cerebral perfusion studies? *Radiology* 2003;227:129-135.
40. Ozkan B, Yuksel N, Anik Y, Altintas O, Demirci A, Caglar Y. The effect of caffeine on retrobulbar hemodynamics. *Curr.Eye Res*. 2008;33:804-809.

41. Nicholls SJ, Lundman P, Harmer JA, et al. Consumption of saturated fat impairs the anti-inflammatory properties of high-density lipoproteins and endothelial function. *J.Am.Coll.Cardiol.* 2006;48:715-720.
42. Venkataraman ST, Hudson C, Fisher JA, et al. Retinal arteriolar and capillary vascular reactivity in response to isoxic hypercapnia. *Exp.Eye Res.* 2008; 87(6):535-542.
43. Slessarev M, Prisman E, Han J, et al. Prospective targeting and control of end-tidal CO₂ and O₂ concentrations. *J Physiol.* 2007;581:1207-1219.
44. Fuchsjager-Mayrl G, Wally B, Rainer G, et al. Effect of dorzolamide and timolol on ocular blood flow in patients with primary open angle glaucoma and ocular hypertension. *Br.J.Ophthalmol.* 2005;89:1293-1297.
45. Uva MG, Longo A, Reibaldi M, Reibaldi A. The effect of timolol-dorzolamide and timolol-pilocarpine combinations on ocular blood flow in patients with glaucoma. *Am.J.Ophthalmol.* 2006;141:1158-1160.
46. Venkataraman ST, Hudson C, Fisher JA, et al. Retinal arteriolar and capillary response to isoxic hypercapnia in primary open angle glaucoma pre-& post-treatment. *Invest.Ophthalmol.Vis.Sci.* 2007;48:E-Abstract 4395.
47. Haefliger IO, Flammer J, Luscher TF. Nitric oxide and endothelin-1 are important regulators of human ophthalmic artery. *Invest.Ophthalmol.Vis.Sci.* 1992;33:2340-2343.
48. Koss MC. Functional role of nitric oxide in regulation of ocular blood flow. *Eur.J.Pharmacol.* 1999;374:161-174.

49. Neufeld AH, Hernandez MR, Gonzalez M. Nitric oxide synthase in the human glaucomatous optic nerve head. *Arch.Ophthalmol.* 1997;115:497-503.
50. Polak K, Luksch A, Berisha F, Fuchsjager-Mayrl G, Dallinger S, Schmetterer L. Altered nitric oxide system in patients with open-angle glaucoma. *Arch.Ophthalmol.* 2007;125:494-498.
51. Stefansson E, Jensen PK, Eysteinnsson T, et al. Optic nerve oxygen tension in pigs and the effect of carbonic anhydrase inhibitors. *Invest.Ophthalmol.Vis.Sci.* 1999;40:2756-2761.
52. Kiss B, Dallinger S, Findl O, Rainer G, Eichler HG, Schmetterer L. Acetazolamide-induced cerebral and ocular vasodilation in humans is independent of nitric oxide. *Am.J.Physiol.* 1999;276:R1661-7.
53. Reber F, Gersch U, Funk RW. Blockers of carbonic anhydrase can cause increase of retinal capillary diameter, decrease of extracellular and increase of intracellular pH in rat retinal organ culture. *Graefes Arch.Clin.Exp.Ophthalmol.* 2003;241:140-148.
54. Orgul S, Gugleta K, Flammer J. Physiology of perfusion as it relates to the optic nerve head. *Surv.Ophthalmol.* 1999;43 Suppl 1:S17-S26.
55. Estevez AY, Phillis JW. Hypercapnia-induced increases in cerebral blood flow: Roles of adenosine, nitric oxide and cortical arousal. *Brain Res.* 1997;758:1-8.
56. Heinert G, Nye PC, Paterson DJ. Nitric oxide and prostaglandin pathways interact in the regulation of hypercapnic cerebral vasodilatation. *Acta Physiol.Scand.* 1999;166:183-193.

57. Parfenova H, Shibata M, Zuckerman S, Leffler CW. CO₂ and cerebral circulation in newborn pigs: Cyclic nucleotides and prostanoids in vascular regulation. *Am.J.Physiol.* 1994;266:H1494-501.
58. Gidday JM, Zhu Y. Nitric oxide does not mediate autoregulation of retinal blood flow in newborn pig. *Am.J.Physiol.* 1995;269:H1065-72.
59. Schmetterer L, Findl O, Strenn K, et al. Role of NO in the O₂ and CO₂ responsiveness of cerebral and ocular circulation in humans. *Am.J.Physiol.* 1997;273:R2005-R2012.
60. Tsikas D. Methods of quantitative analysis of the nitric oxide metabolites nitrite and nitrate in human biological fluids. *Free Radic.Res.* 2005;39:797-815.
61. Wang J, Brown MA, Tam SH, Chan MC, Whitworth JA. Effects of diet on measurement of nitric oxide metabolites. *Clin.Exp.Pharmacol.Physiol.* 1997;24:418-420.

8 General Discussion

In this thesis, a safe, sustained and a repeatable normoxic hypercapnic stimulus was developed that was then used to assess the vascular reactivity of the retinal arterioles and change in the systemic biochemical markers of endothelial function in POAG. The maintenance of normoxia/isoxia during hypercapnic provocation is important for the assessment of vascular reactivity in order to avoid variable and uncontrolled confounding effects of O₂ induced vasoconstriction. There is lack of comprehensive assessment of vascular reactivity in POAG, especially uPOAG. The assessment of retinal vascular reactivity without any influence of IOP lowering medications aided the better understanding of the pathophysiology of POAG. This is the first study to assess all aspects of retinal vascular reactivity (i.e. diameter, velocity and flow) to a standardised normoxic hypercapnic provocation. It was found that there was a decrease in vascular reactivity in uPOAG and pPOAG compared to controls. In addition, this work also showed that vascular reactivity improved after treatment with 2% Dorzolamide for two weeks in ntPOAG (newly treated POAG). Another major finding of this work was decreased levels of ET-1 in uPOAG at baseline, during normoxic hypercapnia and after short term treatment with Dorzolamide. This is the first study to also establish an association between functional vascular reactivity and biochemical markers of endothelial function.

A number of limitations exist in terms of the previous studies that have assessed homeostatic blood flow and/or vascular reactivity in POAG. The majority of previous studies have 1) used non-standardised provocation techniques to assess retinal vascular reactivity; 2) used techniques that fail to comprehensively assess blood flow or vascular reactivity 3) included

patients who were already receiving IOP lowering medications 4) have not investigated patients with pPOAG, whom are thought to be more susceptible to vascular dysregulation 5) have not investigated the association between functional vascular reactivity and biochemical markers of endothelial function.

Studies in the past have used a non-rebreathing circuit connected to a gas mixing chamber to induce hypercapnia. The manual addition of CO₂ to room air (combined in a mixing chamber) to increase PETCO₂ is known as Dynamic End-Tidal Forcing (DEF). Recently, it was shown that there is a wide variation between the arterial partial pressure of CO₂ (PaCO₂) and PETCO₂ using the DEF in combination with a non-rebreathing circuit. The use of a sequential rebreathing circuit allows the intake of exhaled gas from the rebreathed reservoir during a decrease in the inspired air. This unique feature has been shown to closely match PETCO₂ and PaCO₂ and also reduce the intra-breath fluctuations in PETCO₂. Accordingly, the objective of this thesis was to develop a safe, sustained and a repeatable normoxic/isoxic hypercapnic stimulus in order to ultimately assess retinal vascular reactivity in POAG.

Chapter 3 describes the use of the manual addition of CO₂ via a sequential rebreathing circuit to a controlled level of inspired air to achieve a 15% increase in PETCO₂. The vascular response of the ONH and macular areas to normoxic/isoxic hypercapnia was assessed using the Heidelberg Retina Flowmeter (HRF) in young healthy subjects. A 14% increase in PETCO₂ with a +13% concomitant increase in PETO₂ was noted. A significant increase in the group mean macular nasal and foveal capillary blood flow was shown in response to normoxic/isoxic hypercapnia. There was no change in the blood flow of the temporal rim of

the ONH and macula temporal areas in response to normoxic/isoxic hypercapnia. Previous studies have also noted regional variation in the vascular reactivity to hypercapnia. *This study concluded that there was a difference in the magnitude of vascular reactivity of the retinal areas assessed in response to normoxic/isoxic hypercapnia. Although the hypercapnic stimulus arguably resulted in a physiologically insignificant change, there was still a distinct increase in $PETO_2$ during hypercapnia.*

In chapter 4, a new manual methodology was used to assess retinal arteriolar vascular reactivity in response to a modified normoxic/isoxic hypercapnic stimulus. In addition, the CLBF allowed a comprehensive assessment of the retinal hemodynamics in young healthy subjects. Normoxic/isoxic hypercapnia was induced by simply decreasing inspired air until subjects began to partially rebreath expired air from the rebreathed gas reservoir, thereby elevating $PETCO_2$ in a controlled manner. The modified hypercapnic stimulus resulted in a 12% increase in $PETCO_2$ while there was a concomitant 6% decrease in $PETO_2$. A significant increase in the magnitude of retinal arteriolar diameter, blood velocity and blood flow in response to hypercapnia was noted. The changes in the retinal hemodynamics in this study were comparable to other research, however, to the best of our knowledge, this is the first study to comprehensively assess retinal hemodynamics. *The partial rebreathing technique resulted in an improved control of $PETO_2$ during hypercapnia compared to the manual addition of CO_2 to inspired air. Nevertheless, there was still a statistically significant decrease in the magnitude of $PETO_2$. The arteriolar vascular reactivity results of this study will serve as a reference point for future studies using the CLBF.*

The results of Chapters 3 & 4 aided in the development of an automated gas flow controller (RespirAct™, Thornhill Research Inc., Toronto Canada). Chapter 5 describes the use of an automated gas flow controller in combination with the sequential rebreathing circuit to induce normoxic/isoxic hypercapnia. This stimulus was used to assess retinal arteriolar and ONH capillary vascular reactivity in young healthy subjects. Using this system, PETCO₂ and PETO₂ can be independently controlled and set values are robust to changes in respiration rate and tidal volume. A group mean 15% increase in PETCO₂ with only a 2-3% increase in PETO₂ was achieved. As a result, there was a significant increase in the retinal arteriolar diameter, blood velocity and blood flow and in capillary blood flow of the temporal rim of the ONH, nasal macula and foveal areas. The magnitude of changes noted in the ONH using the new normoxic/isoxic hypercapnic stimulus was greater when compared to the response to the previously described hypercapnic stimulus (Chapter 3). There was also an increase in nasal macula and foveal area blood flow and a non-significant trend towards increase in the temporal macular area in response to normoxic/isoxic hypercapnia. Theoretically the vascular reactivity of the retinal capillaries and the arterioles will be comparable as the retinal circulation is a closed system. However, this is the first study to show that the overall magnitude of capillary vascular reactivity in terms of percentage change of flow was comparable to the provoked change in arteriolar blood flow. In addition, the PETCO₂ and PETO₂ levels achieved using the automated gas flow controller were also repeatable. *The study concluded that the use of an automated gas flow controller provided much improved control of end-tidal CO₂ and O₂ but still resulted in minimal changes in PETO₂ during hypercapnia. For this reason the term “normoxic hypercapnia” (i.e. change that did not cause any measurable physiological impact) was used to describe the stimulus in the*

following chapters of this thesis and in all subsequent publications. The vascular reactivity of the retinal capillaries and arterioles was comparable in terms of percentage change of flow.

Chapter 6 describes the use of the standardised and repeatable normoxic hypercapnic stimulus to assess retinal vascular reactivity in patients with uPOAG, pPOAG and control subjects. The chapter also describes the effect of treatment with 2% Dorzolamide for 2 weeks in a ntPOAG group. The magnitude of retinal arteriolar vascular reactivity was reduced in uPOAG and pPOAG compared to controls. Treatment with 2% Dorzolamide for 2 weeks improved retinal vascular reactivity in ntPOAG. As glaucoma is a condition whose primary site of damage is at the ONH, a sub-study was undertaken to also assess the vascular response of the ONH using the HRF in a small sample. A decreased ONH capillary vascular response in uPOAG and pPOAG was observed. Similarly, in the ntPOAG group, treatment with 2% Dorzolamide for two weeks improved ONH vascular reactivity. Some of the previous studies have assessed retinal vascular reactivity in previously treated patients. The inclusion of previously untreated patients is essential to avoid any residual direct, or indirect, vascular effects of IOP lowering medications. In addition, this study also assessed vascular reactivity in patients with pPOAG (i.e. currently receiving treatment and currently manifesting optic disc hemorrhage) as there is increasing evidence that this group of patients are more susceptible to vascular dysregulation. *This study revealed impairment of retinal vascular reactivity in uPOAG and pPOAG and that short term treatment with Dorzolamide improved retinal and ONH vascular reactivity in uPOAG. It is not very clear whether this improvement is a direct effect of treatment or due to the decrease in IOP in uPOAG. However, in our study there was no change in the mean ocular perfusion pressure (MOPP)*

during pre- & post-treatment, suggesting that the improvement in vascular reactivity might be due to the effect of Dorzolamide. The magnitude of vascular reactivity of the arterioles and ONH capillaries was comparable in terms of percentage change of flow in POAG and controls subjects.

Chapter 7 assessed systemic levels of biochemical markers of endothelial function (ET-1 and cGMP) in uPOAG, pPOAG and controls at baseline and during normoxic hypercapnia. Furthermore, the study also quantified biochemical markers of endothelial function after treatment with 2% Dorzolamide (ntPOAG). The study showed lower levels of ET-1 at baseline in uPOAG and ntPOAG compared to pPOAG and controls. This finding repeated during normoxic hypercapnia. These results suggest that there is an overall reduction in the endothelial constricting factors in uPOAG. The plasma cGMP level was positively associated with blood flow at baseline in both uPOAG and ntPOAG, suggesting that when there is an increase in cGMP there is also an increase in blood flow. Similarly, a weak negative association was noted between ET-1 and blood flow at baseline in uPOAG and ntPOAG that also repeated during normoxic hypercapnia in ntPOAG. These results suggest that an increase in ET-1 results in a decrease in blood flow. In the controls only, the change in plasma ET-1 during normoxic hypercapnia showed a negative association to the change in arteriolar blood flow. These associations further validate the functional vascular reactivity measures in Chapter 6. *The study concluded that there was a decrease in endothelial derived vasoconstricting factor in uPOAG and this finding remained unchanged even after short term treatment with 2% Dorzolamide. A relationship was established between functional vascular reactivity and change in biochemical markers of endothelial function in response to*

normoxic hypercapnia in controls. The assessment of ET-1 in patients with POAG provides useful information about the function of retinal blood vessels at baseline and during hypercapnic provocation. The relationship between functional vascular reactivity and systemic biochemical markers is complex and much remains to be revealed.

8.1 Future work

1. Future work will investigate the mechanism involved in the improvement of vascular reactivity in POAG after treatment with 2% Dorzolamide. It is not known whether the improvement of vascular reactivity in POAG after short term treatment of Dorzolamide is due to the direct effect of Dorzolamide or as a result of a decrease in IOP. Future study will determine retinal vascular reactivity in response to normoxic hypercapnia in uPOAG patients who were treated with primary Selective Laser Trabeculoplasty (SLT) to reduce IOP. The study will also assess biochemical markers of endothelial function in POAG pre-and post-laser treatment. This work is in progress in our laboratory.
2. Future studies should also quantify systemic levels of nitrates and nitrites (surrogate markers of the presence of nitric oxide). It is possible that endothelial derived biochemical factors other than ET-1 and NO might be responsible for the regulation of blood flow in the retina. In the cerebral literature, prostacyclin pathway induced vasodilation has been proposed during hypercapnia. There is a need for a complete understanding of the various biochemical markers of endothelial function in the retina in addition to ET-1 and cGMP. Furthermore, prostacyclin induced release of cyclic adenosine monophosphate (cAMP) should also be quantified to provide more information about the regulation of the retinal vasculature in POAG in response to normoxic hypercapnia.

3. There is increasing evidence for vascular dysregulation in patients with POAG and associated systemic vasospastic symptoms such as cold hands, cold feet and migraine. Future work should assess retinal and ONH vascular reactivity and also systemic biochemical markers of endothelial function in NTG. This work is in progress in our laboratory.
4. Recently, oxidative stress has been proposed as an important factor responsible for the development of glaucomatous optic neuropathy (GON) in POAG. Glutathione (GSH) is a non-enzymatic antioxidant that also facilitates the bioavailability of NO (a vasodilator). The assessment of systemic GSH levels in POAG at baseline and during normoxic hypercapnia will provide a better understanding of the regulation of blood flow in the retina.
5. Retinal vascular reactivity measurements can be combined with retinal oximetry assessment in POAG. This will provide information about the retinal oxygen saturation and metabolism in POAG that will help to better understand the pathophysiology of the disease.

8.2 Summary of new knowledge and findings from this work

1. This work resulted in the development of a novel and standardised normoxic hypercapnic stimulus. The new stimulus can now be safely used to also determine functional vascular response of other ocular and systemic conditions that exhibit vascular dysregulation.
2. This is the first study to show that the magnitude of retinal *capillary* vascular reactivity was equivalent to the *arteriolar* vascular reactivity with respect to percentage change of flow.
3. This work provides a comprehensive assessment of retinal vascular reactivity in POAG in response to normoxic hypercapnia. Patients with uPOAG and pPOAG revealed a reduced response to normoxic hypercapnia compared to controls. Treatment with 2% Dorzolamide for two weeks improved retinal vascular reactivity in the previously untreated group.

4. This work found an overall reduction in vasoconstrictive factor in uPOAG that remained unchanged during normoxic hypercapnia and after short term treatment with 2% Dorzolamide. In addition, the study also established an association between functional vascular reactivity and biochemical markers of endothelial function (i.e. ET-1 and cGMP) in POAG and controls. These findings further validate the assessment of retinal vascular reactivity assessment in patients with POAG and provide a better understanding of the pathophysiology of the disease.

9 Appendix A: Impact of Simulated Light Scatter on Scanning Laser Doppler Flowmetry

Venkataraman ST, Hudson C, Harvey E, Flanagan JG. Impact of simulated light scatter on scanning laser Doppler flowmetry. Br.J.Ophthalmol. 2005; Sep, 89(9): 1192-1195.

Reprinted by permission from BMJ publishing group.

9.1 Abstract

Aim: To determine the impact of simulated light scatter on scanning laser Doppler flowmetry (SLDF) assessment of retinal capillary blood flow and retinal image quality.

Methodology: One eye of 10 normal subjects (mean age 24years, SD 1.7, range 22-27) was randomly selected. Varying concentrations of polystyrene microspheres (Polybead® Polysciences Inc., USA) were suspended in optically clear cells to simulate light scatter. The microsphere concentrations used were 0.05%, 0.03%, 0.02%, 0.01% and a cell containing only water. LogMAR visual acuity and contrast sensitivity was measured both with and without the cells. Optimal focus and alignment was established by acquiring 3 SLDF images each of the optic nerve head (ONH) and of the macula using the Heidelberg Retina Flowmeter (HRF) with no cell in place. Subsequently, SLDF images were acquired with each of the light scatter cells mounted in front of the HRF. The group mean retinal capillary blood flow was compared using repeated measures Analysis of Variance (reANOVA) as a function of microsphere concentration.

Results: Retinal capillary blood flow was significantly higher in the ONH, nasal macula, fovea and temporal macula with increase in microsphere concentration ($p < 0.0001$). Using Dunnett's post hoc test, retinal capillary blood flow was found to be significantly increased relative to no cell for the 0.03% and 0.05% cell concentrations.

Conclusions: Simulated light scatter produced an artifactual increase in retinal capillary blood flow. The impact of cataract on SLDF measurements has yet to be determined.

Keywords: Light scatter, polystyrene microspheres, cataract, retina, capillary blood flow.

9.2 Introduction

Cataract results in intra-ocular light scatter due to change in refractive index and opacification of the crystalline lens leading to degradation of retinal image quality^{1, 2}. In humans, the aggregation of lens crystallins form high molecular weight (HMW) aggregates of 300 to 500nm diameter resulting in cataract^{3, 4}. Degradation of retinal image quality and contrast in a cataractous eye is primarily due to forward light scatter⁵.

Non-invasive digital imaging techniques designed to improve the detection and clinical management of retinal disease are now used commonly. Assessment of the influence of ocular media opacities on the outcome of these new imaging techniques is important because cataract frequently occurs concomitantly with retinal disease. A number of reports have studied the influence of simulated light scatter on visual field performance and have shown a resulting decrease in visual field sensitivity⁶⁻⁸. We have recently developed a simulated light scatter model and have demonstrated its' impact on fundus visualization using a digital retinal camera⁹.

The purpose of the study was to determine the influence of simulated light scatter on scanning laser Doppler flowmetry (SLDF) assessment of retinal capillary blood flow and retinal image quality.

9.3 Materials and methods

9.3.1 Sample

The study protocol was approved by the University of Waterloo, Office of Research Ethics. Ten subjects of mean age 24 years (SD 1.7, range 22-27) participated in the study. All participants had a LogMAR visual acuity of 0.0, or better. Subjects with the following Lens Opacity Classification System (LOCS) III ¹⁰ grading were excluded from the study: Nuclear color > NC2, Nuclear opalescence > NO2; Cortical > C2; and Posterior sub-capsular \geq P1.

9.3.2 Scanning laser Doppler flowmetry

The light reflected by moving red blood cells in the retina undergoes a frequency shift while light reflected from surrounding tissue remain unchanged. Using SLDF, the intensity of back-scattered laser light from the retina is measured as a function of time (to produce an intensity-time curve) for each pixel within the image. The two coherent components of light interfere resulting in an oscillation or “*beat*”, of the measured light intensity. The frequency of the intensity oscillation is equal to the Doppler frequency shift. Fast Fourier transformation of the intensity-time curve generates a power spectrum of the Doppler shift to derive parameters of blood flow, volume and velocity at each pixel within the image ¹¹.

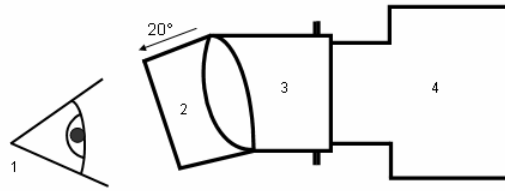
SLDF measurements were undertaken using the Heidelberg Retina Flowmeter (HRF; Heidelberg Engineering GmbH, Dossenheim, Germany, version 1.03W). The HRF uses a 780nm wavelength diode laser to measure the intensity, and thereby calculate the Doppler shift of back-scattered light. The instrument has a spatial resolution of approximately 10 μ m

and a depth resolution 300-400 μm ¹²⁻¹⁴. The laser scanning system of the HRF enables the measurement of a 10° horizontal x 2.5° vertical (i.e. approximately 2.7mm x 0.7mm) field with a resolution of 256 pixels x 64 lines, respectively. Each line of 256 pixels is scanned 128 times at a repetition rate of 4000Hz. The resulting image acquisition time is 2.048 sec.

9.3.3 Simulated light scatter model

Light scatter was induced using various concentrations of 500nm diameter polystyrene microspheres (Polybead® Polysciences Inc., USA) suspended in sterile water. The diameter of the microspheres was chosen to be similar to the diameter of HMW aggregates in a cataractous lens^{4, 5, 8}. Microsphere concentrations of 0.05%, 0.03%, 0.02% and 0.01%, and water only were prepared under sterile conditions (surfactant poloxamer 407 was included to prevent coagulation)¹⁵. The stability of the light scatter model was determined by assessing HRF measurements against a plain white paper background for the 0.05% cell which had not been disturbed for 24hours and then after vigorous shaking. The mean value (3 repeats) for 10x10 pixels was 47735 a.u. (SD 373) and immediately after shaking was not significantly different i.e. 47335 a.u. (SD 431).

The various microsphere concentrations were injected into cells constructed from two 35mm removable CR39 plano lenses mounted on opposite ends of a plastic ring (inner diameter 25 mm), with a spacing of 4.5mm between the lenses and a thickness of 2.04mm each. The total volume of each cell was 2.2mL. The cells were mounted to the objective of the HRF using a custom made adaptor that incorporated a 20° tilt to minimize surface reflections (Figure 9.1).



1 – Subject's eye, 2 – Light scatter cell
 3 – Custom made adaptor used to tilt the cell by 20°, 4 – Heidelberg Retina Flowmeter

Figure 9.1 Schematic representation of the light scatter cell mounted in front of the objective of the HRF using a custom designed adaptor to produce a standard 20° tilt.

9.3.4 Procedures

All participants underwent a preliminary eye examination followed by dilation of the study eye with a single drop of 0.5% tropicamide. LOCS III grading was undertaken after dilation. Three SLDF images of the optic nerve head (ONH) and 3 images of the macula were acquired with no cell in place in order to establish optimal focus settings and image alignment. Subsequently, 3 SLDF images both of the ONH and of the macula were acquired with the various cells in place. The order of cells and also the measurement site were randomized between subjects and a constant focus setting and alignment was maintained based upon that of the no cell situation. The eye to camera distance was kept constant during image acquisition.

Fundus photographs of the study eye of one subject were acquired for all conditions using a digital fundus camera (Canon CR6-45NM, Canon, Lake Success, New York), in order to illustrate the clinical relevance of the simulated light scatter model.

9.3.5 Analysis

Automated full field perfusion image analysis (AFFPIA) software version 3.3 and HRF custom analysis were used to generate retinal capillary blood flow values. AFFPIA excludes erroneous blood flow values due to saccades and major blood vessels ¹⁶. The AFFPIA software was used to delineate the temporal neuroretinal rim of the ONH. In addition, a 2.5° circle was centred to delineate the foveal macular area. All points temporal to the circle delineated the temporal macular area while those nasal of the circle delineated the nasal macular area. Capillary blood flow values were derived for the temporal neuroretinal rim and the various macular areas.

A custom analysis was developed partly due to the limitation of the AFFPIA software to generate blood flow values with the higher microsphere concentrations. The HRF custom analysis preserved sample size especially with the high concentration light scatter cells. The HRF custom analysis consisted of a 10 x 10 pixel measurement window that was placed within the areas of interest. Care was taken to place the 10 x 10 pixel window at the same location for all images of a given subject and also within the same area that was used for AFFPIA using a transparent sheet to mark the relevant land marks and the AFFPIA area. Capillary blood flow for each pixel of the area of interest was obtained along with the brightness index of the image (DC value). A total of 100 flow (with corresponding DC) values were produced for each area analysed. Flow values with a DC range of 70-200 arbitrary units (a.u) were included in the analysis since this range is within the acceptable level of retinal image illumination ¹⁷⁻¹⁹. The data was then sorted in ascending order and any

artifactual zero flow values were excluded, along with an equal number of the highest flow values. Only images with at least 35 flow values were included.

Repeated measures analysis of variance (reANOVA) of the retinal capillary blood flow values for all microsphere concentrations and all measurement regions were performed for both AFFPIA and HRF custom analyses using SAS (v.8.02). Since AFFPIA failed to generate blood flow values in the majority of the subjects for 0.05% microsphere concentration it was not included in the statistical analysis. It was assumed that there was minimal light scatter and degradation of retinal image quality without any cell in place. Dunnett's post hoc test was performed to determine the microsphere concentration that resulted in a significant change. The DC values obtained using the HRF custom analysis for the various microsphere concentrations were also analysed in an identical manner. Pearson's correlation procedure was performed to determine whether there was a significant linear relationship between blood flow values with no cell and with increase in microsphere concentration in all subjects.

9.4 Results

The group mean baseline capillary blood flow with the AFFPIA and HRF analysis of the ONH, nasal macula, fovea and temporal macula is shown in Table 9.1.

Analyses	ONH	Nasal macula	Fovea	Temporal macula
AFFPIA	228.86 ± 62.84	151.96 ± 30.30	120.25 ± 26.08	155.88 ± 47.90
HRF custom	226.68 ± 191.63	176.52 ± 39.46	192.65 ± 53.92	163.89 ± 83.11

Table 9.1 Group mean baseline capillary blood flow values (\pm SD) of the ONH, nasal macula, fovea and temporal macula using the AFFPIA and HRF custom analysis.

The reANOVA for the AFFPIA demonstrated a significant increase in capillary blood flow with increase in microsphere concentration for the ONH ($p < 0.0001$), nasal macula ($p = 0.0003$), fovea ($p = 0.0004$), temporal macula ($p = 0.0003$). The reANOVA for the HRF analysis also demonstrated a significant increase in capillary blood flow with increase in microsphere concentration for the ONH ($p < 0.0001$), nasal macula ($p < 0.0001$), fovea ($p < 0.0001$) and temporal macula ($p < 0.0001$).

Dunnett's post-hoc analysis of the AFFPIA data revealed a significant increase in capillary blood flow with the 0.03% cell concentration while HRF custom analysis revealed a significant increase with both 0.03% and 0.05% cell concentrations for the ONH, nasal macula, fovea and temporal macula relative to baseline. Capillary blood flow values of the

ONH, nasal macula, fovea and temporal macula extracted using the AFFPIA and HRF custom analysis followed a similar trend for all light scatter cell situations (Figures 9.2A-D).

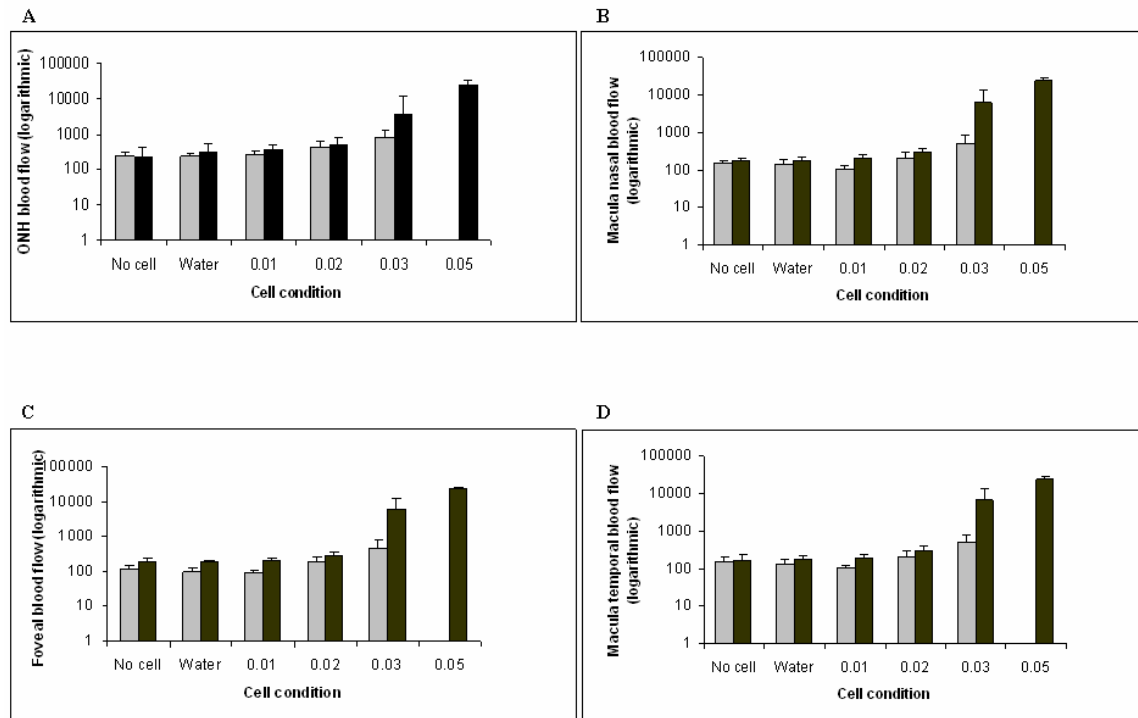


Figure 9.2 Group mean capillary blood flow (+SD) with no cell, water only, 0.01%, 0.02%, 0.03%, 0.05% microsphere concentrations of the A) optic nerve head B) macula nasal C) foveal and D) macula temporal areas using SLDF (grey bars) and custom HRF (black bars) analysis.

The re-ANOVA for the DC values obtained using the HRF custom analysis for all the measured regions demonstrated a significant difference across the various microsphere concentrations ($p=0.0001$) (Figure 9.3). Dunnett's post-hoc analysis of the DC values revealed a significant decrease in DC values with the 0.05% cell concentrations for the ONH, nasal macula, fovea and temporal macula relative to baseline. Pearson's correlation procedure did not show any significant linear association between blood flow values for the no cell situation and with increase in microsphere concentration. There was no consistent offset observed in the effect produced by the increasing microsphere concentration.

With no light scatter cell in place and with the cell containing only water, optimal fundus visualisation was achieved. Cells containing polystyrene microsphere concentrations of 0.01% and 0.02% allowed a blurred outline of the ONH to be visible (Figure 9.4). With higher microsphere concentrations, visualisation of fundus details were increasingly difficult.

The results of one subject were excluded due to excessive eye movement and poor image quality. AFFPIA failed to generate capillary blood flow values for ≤ 5 and 9 subjects with the 0.03% and 0.05% microsphere concentrations, respectively. The HRF custom analysis resulted in incomplete sets of data only for the ONH measurement site (due to our requirement of a minimum 35 flow values per pixel window) in 2 subjects.

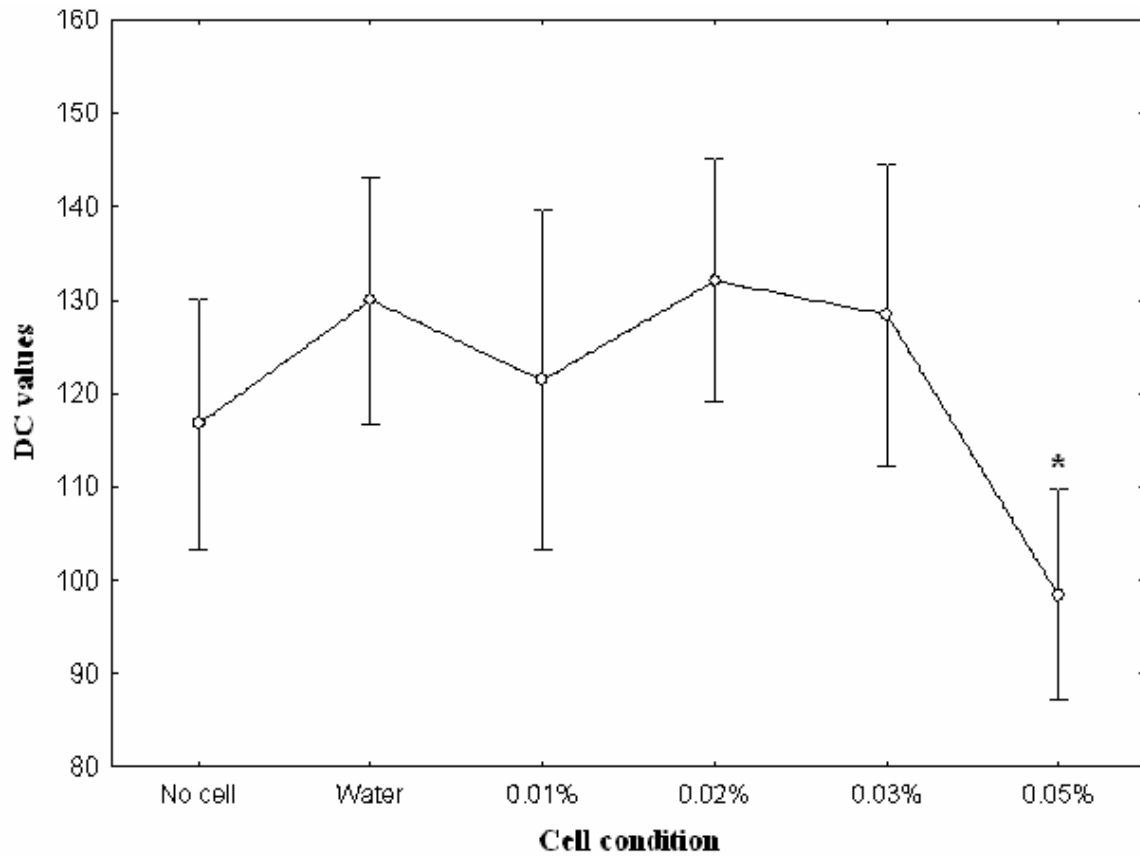
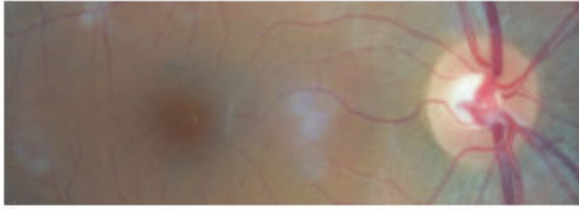


Figure 9.3 Group mean DC values for all the measured regions with no cell, water only, 0.01%, 0.02%, 0.03%, 0.05% microsphere concentrations.

Vertical bars denote 95% confidence interval. (* represents significance $p < 0.05$).

A



B



C



D



Figure 9.4 Fundus image of a normal subject acquired with various cell microsphere concentrations placed in front of a digital fundus camera.

(A. with no cell in place, B. cell with only water, C. cell with 0.01% microsphere concentration, D. cell with 0.02% concentration).

9.5 Discussion

To the best of our knowledge, this is the first study to investigate the effect of artificial light scatter on retinal capillary blood flow and image quality using the HRF. AFFPIA and the HRF custom analyses both demonstrated a significant artifactual increase in capillary blood flow with increasing light scatter. Post-hoc analysis of the AFFPIA data revealed a significant increase in capillary blood flow with the 0.03% cell concentration while HRF custom data revealed a significant increase with both 0.03% and 0.05% cell concentrations for all the measured regions relative to baseline. There was a significant decrease in the DC values demonstrated with the 0.05% microsphere concentration relative to baseline. The cell with water only was included as one of the conditions because it would induce some degree of image degradation and light scatter; however, the analysis demonstrated that there was no significant difference between the no cell condition and the cell with water only. Although the increase in capillary blood flow with lower light scatter microsphere concentrations did not reach statistical significance it might have clinical implications.

The HRF is sensitive to change in photodetector setting. Change in image brightness has already been shown to impact SLDF derived estimates of retinal capillary blood flow^{13, 17, 19, 20}. In the current study, increase in light scatter decreased the image brightness for all subjects leading to an increase in the HRF gain setting by the operator to optimise the view of various retinal structures, as would occur in a clinical situation. This produced a significant decrease in DC values with the highest microsphere concentration resulting in a significant increase in blood flow values. DC related error in HRF measurements has been observed in both in-vitro models and in images of the human fundus. Tsang and co-workers

(1999) suggested that darker backgrounds resulted in higher blood velocity values in an in-vitro blood flow model using the HRF. Increase in retinal capillary blood flow as a result of DC changes has already been demonstrated in normal subjects using the HRF²⁰. However, it should be noted that both the AFFPIA and our custom HRF analyses attempted to eliminate unacceptable DC values from the raw HRF measurements.

There was a light scatter induced shift observed in the y-axis of the power spectrum with 0.03% and 0.05% artificial light scatter microsphere concentrations. Careful examination of the SLDF power spectrum is required to eliminate images with DC shifts beyond the valid measurement range of the HRF. The HRF has a high zero offset due to random variation of backscattered light and internal noise leading to change in flow values¹². In this study, increase in simulated light scatter exaggerated the high zero offset. This explains the significant artifactual increase in capillary blood flow with increasing light scatter.

AFFPIA resulted in exclusion of a majority of subjects as it failed to generate blood flow values for higher light scatter cell concentrations due to invalid zero offset. On the other hand, our HRF custom analysis provided capillary blood flow values for nearly all possible cell situations with the operator defined acceptable range of DC values for all images. This feature of the HRF custom analysis produced apparently valid capillary blood flow values even for the higher light scatter cell concentrations.

9.6 Conclusion

Simulated light scatter produced an artifactual increase in capillary blood flow in the ONH and in various macular regions of the retina. Artificial light scatter resulted in a shift in the y-axis of the SLDF power spectrum. Both AFFPIA and our HRF custom analysis produced remarkably similar capillary blood flow values. SLDF images need to be analysed with caution to exclude unacceptable DC values and power spectrum shifts to derive accurate capillary blood flow values. The impact of cataract on SLDF measurements has yet to be determined: this work is in progress in our lab.

9.7 References

1. Bettelheim FA. Physical basis of lens transparency. Maisel H. *In The Ocular Lens, Structure, Function and Pathology*. New York: Marcel Dekker; 1985. 265-300 pp.
2. Benedek GB. Theory of the transparency of the eye. *Appl.Opt.* 1971;10:459-473.
3. Bettelheim FA, Siew E. Biological and physical basis of lens transparency. McDevitt. *In Cell biology of the eye*. Academic Press, New York; 1982. 243-297 pp.
4. Dengler-Harles M, Wild JM, Cole MD, O'Neill EC, Crews SJ. The influence of forward light scatter on the visual field indices in glaucoma. *Graefes Arch.Clin.Exp.Ophthalmol.* 1990;228:326-331.
5. Moss ID, Wild JM. The influence of induced forward light scatter on the normal blue-on-yellow perimetric profile. *Graefes Arch.Clin.Exp.Ophthalmol.* 1994;232:409-414.
6. Eichenberger D, Hendrickson P, Robert Y, Gloor B. Influence of ocular media on perimetric results. *Doc Ophthalmol Proc.Ser* 1987;49:9-11.
7. Heuer DK, Anderson DR, Knighton RW, Feuer WJ, Gressel MG. The influence of simulated light scattering on automated perimetric threshold measurements. *Arch.Ophthalmol.* 1988;106:1247-1251.
8. Wood JM, Wild JM, Crews SJ. Induced intraocular light scatter and the sensitivity gradient of the normal visual field. *Graefes Arch.Clin.Exp.Ophthalmol.* 1987;225:369-373.

9. Hudson C, Khanna CJ, Miller A, Gilmore E. A method to establish the clinical relevance of a simulated cataract model. *The Journal of Ophthalmic Photography* 2003;25:80-83.
10. Chylack LT,Jr, Wolfe JK, Singer DM, et al. The lens opacities classification system III. the longitudinal study of cataract study group. *Arch.Ophthalmol.* 1993;111:831-836.
11. Michelson G, Schmauss B. Two dimensional mapping of the perfusion of the retina and optic nerve head. *Br.J.Ophthalmol.* 1995;79:1126-1132.
12. Chauhan BC, Smith FM. Confocal scanning laser doppler flowmetry: Experiments in a model flow system. *J.Glaucoma* 1997;6:237-245.
13. Kagemann L, Harris A, Chung H, Jonescu-Cuypers C, Zarfati D, Martin B. Photodetector sensitivity level and heidelberg retina flowmeter measurements in humans. *Invest.Ophthalmol.Vis.Sci.* 2001;42:354-357.
14. Haefliger IO, Lietz A, Griesser SM, et al. Modulation of heidelberg retinal flowmeter parameter flow at the papilla of healthy subjects: Effect of carbogen, oxygen, high intraocular pressure, and beta-blockers. *Surv.Ophthalmol.* 1999;43 Suppl 1:S59-S65.
15. Portoles M, Austin F, Nos-Barbera S, Paterson C, Refojo MF. Effect of poloxamer 407 on the adherence of pseudomonas aeruginosa to corneal epithelial cells. *Cornea* 1995;14:56-61.
16. Michelson G, Welzenbach J, Pal I, Harazny J. Automatic full field analysis of perfusion images gained by scanning laser doppler flowmetry. *Br.J.Ophthalmol.* 1998;82:1294-1300.

17. Jonescu-Cuypers CP, Chung HS, Kagemann L, Ishii Y, Zarfati D, Harris A. New neuroretinal rim blood flow evaluation method combining heidelberg retina flowmetry and tomography. *Br.J.Ophthalmol.* 2001;85:304-309.
18. Kagemann L, Harris A, Chung HS, Evans D, Buck S, Martin B. Heidelberg retinal flowmetry: Factors affecting blood flow measurement. *Br.J.Ophthalmol.* 1998;82:131-136.
19. Hosking SL, Embleton S, Kagemann L, Chabra A, Jonescu-Cuypers C, Harris A. Detector sensitivity influences blood flow sampling in scanning laser doppler flowmetry. *Graefes Arch.Clin.Exp.Ophthalmol.* 2001;239:407-410.
20. Tsang AC, Harris A, Kagemann L, Chung HS, Snook BM, Garzozzi HJ. Brightness alters heidelberg retinal flowmeter measurements in an in vitro model. *Invest.Ophthalmol.Vis.Sci.* 1999;40:795-799.

10 Appendix B: Endothelin – 1 (ET- 1) assay procedure

10.1 Sample preparation

1. Blood samples were collected in a K3 EDTA sprayed vacutainer and kept in ice for about 30mins.
2. The samples were then centrifuged at 1800 x g (gravity) and 4° C.
3. 100µL of Aprotinin ((from bovine lung, Sigma-Aldrich, ST.Louis, MO) was added to each 2mL plasma and stored at -70° C.
4. A minimum of 2mL was required for the test.

10.2 Principle of the assay

The assay kit contains a microplate that is pre-coated with an antibody specific for ET-1. Standards, Samples, Control and Conjugate are pipetted into the wells and any ET-1 present is sandwiched by the immobilized antibody and the enzyme-linked antibody specific for ET-1. Following a wash to remove any unbound substances from the plate, Substrate is added to the wells and color develops in proportion to the amount of bound ET-1. That is, the intensity of the color developed is directly proportional to the amount of bound ET-1. Table 10.1 details the reagents used for the ET-1 assay.

ET-1 microplate	96 well microplate (12 strips of 8 wells) coated with rat antibody to human ET-1.
ET-1 Standards	6 vials of lyophilized synthetic human ET-1 containing blue dye.
Sample Diluent	20mL of buffered protein base, with blue dye and preservative.
ET-1 Conjugate Concentrate	0.3mL of antibody to ET-1 conjugated to horseradish peroxidase (HRP) in buffer.
Conjugate Diluent	11mL of diluent for HRP-Conjugate concentrate, with red dye and preservative.
ET-1 Control	1 vial of lyophilized human ET-1. The concentration of the control was within the range specified on the vial label.
Wash Buffer Concentrate	20mL of 25-fold concentrated buffered surfactant with preservative.
Substrate	11mL of stabilized tetramethylbenzidine solution.
Stop solution	11mL of hydrochloric acid (HCl) solution 2N.
Plate sealers	8 adhesive plate sealers.

Table 10.1 Details the various reagents in the endothelin-1 (ET-1) assay kit provided by the manufacturer that was used for the ET-1 assay procedure.

10.3 Reagent preparation

All reagents were prepared based on the manufacturer's (R&D systems, MN USA) guidelines.

1. 20mL of Wash Buffer Concentrate was diluted with deionized water to prepare 500mL of Wash Buffer

2. The ET-1 Standards and ET-1 Control was reconstituted immediately before use with 1.0mL of deionized water and was kept at room temperature.
3. 250 μ L of Conjugate Concentrate (HRP) was transferred into the bottle of Conjugate Diluent and mixed gently by inversion.

10.4 Assay procedure

The samples, Standards and the ET-1 Control were assayed in duplicate according to the manufacturer guidelines.

1. 100 μ L of diluted Conjugate was added to each microplate well (total of 96 wells).
2. 100 μ L each of the Standard and Control were added to each well without any interruption and this procedure was completed within 10mins.
3. The plate was covered with a plate sealer and then incubated for 1 hour at room temperature.
4. The contents were then aspirated from each well and washed six times by adding 300 μ L of Wash Buffer in each well.
5. 100 μ L of Substrate (tetramethylbenzidine) was added to each well and the plate was sealed using a new plate sealer and incubated at room temperature for 30mins.
6. 100 μ L of Stop solution (HCl solution, 2N) was added to each well in the same order as the Substrate was added.
7. The optical density of each well was determined using a microplate reader spectrophotometer (Spectramax Plus 384, Molecular Devices) set at 450nm wavelength.
8. A standard curve was then generated with ET- 1 concentration on the x-axis and mean absorbance on the y-axis. The concentration for each unknown sample was calculated based

on the mean absorbance in the standard curve. The minimum detectable ET-1 was 0.3 pg/mL.

11 Appendix C: 3',5' cyclic guanosine monophosphate (cGMP)

assay procedure

11.1 Sample preparation

1. Blood samples were collected in a K3 EDTA sprayed vacutainer and kept in ice for about 30mins.
2. The samples were then centrifuged at 1800 x g (gravity) and 4° C.
3. The centrifuged blood samples were aliquoted in test tubes and stored at -70 ° C.
4. A minimum of 1mL was required for the test.

11.2 Reagents used for the assay procedure and other contents in the

Enzyme Immunoassay (EIA) kit

1. cGMP EIA Antiserum
2. cGMP acetylcholinesterase (AChE) Tracer
3. cGMP EIA Standard
4. 10mL EIA Buffer Concentrate
5. 5mL Wash Buffer Concentrate
6. 3mL Tween 20
7. Mouse Anti-rabbit antibody (IgG) coated Plate
8. Plate Cover

9. Ellman's Reagent (consists of acetylthiocholine and 5,5'-dithiobis-(2-nitrobenzoic acid)):
Reconstitution of Ellman's reagent was done before the development stage by adding 20mL of deionised water to the Ellman's reagent vial.
10. 2.5mL Acetic Anhydride
11. Ethanol 95%
12. Potassium hydroxide (KOH)
13. EIA Tracer Dye
14. EIA Antiserum Dye

11.3 Principle of the assay

The EIA is based on the competition between free cGMP and a cGMP- AChE Conjugate (cGMP tracer) for a limited number of cGMP specific rabbit antibody binding sites. The concentration of cGMP tracer is constant while the concentration of cGMP in the standard or samples varies. As a result, the cGMP tracer that is bound to the rabbit antibody is inversely proportional to the concentration of cGMP in the well.

11.4 Definition of terminologies in the assay procedure

Blank: background absorbance caused by Ellman's Reagent. The blank absorbance was subtracted from the absorbance readings of all the other wells.

Total Activity: total enzymatic activity of the AChE linked tracer.

NSB (Non-Specific Binding): non-immunological binding of the cGMP tracer to the well. Even in the absence of an anti-serum a very small amount of cGMP tracer still binds to the well. NSB is the measure of this low binding.

B₀ (Maximum binding): maximum amount of the tracer that the antiserum can bind in the absence of free analyte.

%B/B₀ (%Bound/Maximum Bound): ratio of the absorbance of a particular sample of standard well to that of the maximum binding (B₀) well.

Standard Curve: a plot of the %B/B₀ values versus concentration of a series of wells containing various known amounts of analyte.

11.5 Reagent preparation

1. The EIA Buffer Concentrate in the kit was diluted with 90ml of ultra pure water and the vial was rinsed to dissolve any precipitated salts.
2. The Wash Buffer Concentrate was diluted to a total volume of 5 liters with ultra pure water and 2.5ml of Tween 20 (Detergent, to decrease non-specific binding) was added.
3. cGMP AChE tracer and cGMP antiserum were each reconstituted with 6ml EIA Buffer and stored at 4 ° C.

11.6 Sample preparation

1. 500μL of each collected plasma sample was transferred into individually labelled test tubes. 2mL of ice-cold ethanol was added to each tube and vortexed.
2. The tubes were centrifuged at 3000rpm for 10minutes.
3. The supernatant was transferred into labelled test tubes and dried using SPEED VAC rotor evaporator at medium drying rate.
4. The residue was reconstituted in 500μL EIA Buffer.

11.7 Standard preparation

1. cGMP Stock Standard: The cGMP standard (concentration 300pmol/mL) in the kit was reconstituted with 1mL of EIA Buffer. The stock standard was aliquoted in order to avoid repeated freezing and thawing.
2. cGMP diluted Stock Standard: 100µL of stock standard (300pmol/mL) was aliquoted into 9.9mL of EIA Buffer. The concentration of the diluted stock standard was 3pmol/mL.
3. cGMP Working Standards: 500µL of EIA Buffer was added to each of 9 clean test tubes (labelled #1 to #9). The following concentrations of working standard were prepared before the acetylation procedure, 0.00, 0.023, 0.046, 0.093, 0.187, 0.375, 0.75, 1.5 and 3.0pmol/mL using serial dilution procedure (Table 11.1).

Working Standard	Diluted Standard Volume (µL)	EIA Buffer Volume (µL)	cGMP Concentration (pmol/mL)
S9	500µL of 3.0pmol/mL	-	3.0
S8	500µL of 3.0pmol/mL	500	1.5
S7	500 µL of S8	500	0.75
S6	500 µL of S7	500	0.375
S5	500 µL of S6	500	0.187
S4	500 µL of S5	500	0.093
S3	500 µL of S4	500	0.046
S2	500 µL of S3	500*	0.023
S1		500	0

* after mixing S2, the last 500 µL was discarded.

Table 11.1 Details the serial dilution procedure that was followed to prepare various concentrations of working standards.

11.8 Acetylation procedure

Acetylation procedure was performed to improve the sensitivity of the assay to detect even lower amounts of cGMP (i.e. cGMP of less than 1pmol/mL). All samples and standards were acetylated individually. 100µL of prepared 4M (4 molar) KOH was added to 500µL of

standards and sample followed by 25 μ L of acetic anhydride in quick succession. After mixing for 15 sec on a vortex mixer, 25 μ L 4 M KOH was added and all tubes were vortexed again. This procedure was repeated for all samples and standards.

11.9 Assay procedure

1. The pre-coated microtiter plate consists of 12 removable strips (Figure 11.1). The standards and samples were done in duplicates.
2. 50 μ L of acetylated EIA buffer (Standard 1) was added into each of the NSB wells, the B₀ wells and the S₁ wells.
3. 50 μ L of EIA buffer was added into each of the NSB wells followed by addition of 50 μ L of standards and samples into the appropriate wells.
4. 50 μ L of sample was added to the corresponding wells in duplicate. cGMP AchE Tracer was added to each well except the TA and the Blank wells.
5. cGMP antiserum was added to each well except TA, NSB and Blank wells. The microplate was then covered and incubated at room temperature for 18hours.
6. The wells were then rinsed six times with wash buffer and reconstituted Ellman's reagent was added to each well. The development of the plate was obtained in the dark using an orbital shaker. The assay typically develops in 60-90mins.
7. The plate was read at a wavelength of 405nm using a spectrophotometer (Spectramax Plus 384, Molecular Devices) after optimum development (i.e. when B₀ wells equal 0.3 AU after Blank subtraction).

	1	2	3	4	5	6	7	8	9	10	11	12
	BLK	S 2	S 6	1	5	9	13	17	21	25	29	33
B	NSB	S 2	S 6	1	5	9	13	17	21	25	29	33
C	NSB	S 3	S 7	2	6	10	14	18	22	26	30	34
D	B ₀	S 3	S 7	2	6	10	14	18	22	26	30	34
E	B ₀	S 4	S 8	3	7	11	15	19	23	27	31	35
F	TA	S 4	S 8	3	7	11	15	19	23	27	31	35
G	S 1	S 5	S 9	4	8	12	16	20	24	28	32	36
H	S 1	S 5	S 9	4	8	12	16	20	24	28	32	36

Figure 11.1 Map of the microplate wells used for cGMP assay procedure.

Blk; blank NSB; non-specific binding, B₀; maximum binding, TA; total activity, S1-S9 denotes standards in duplicates with concentrations ranging from 0 to 3.0pmol/mL. # 1-36 represents samples with unknown concentration.

11.10 Calculation of results

A standard curve was generated using the concentration of acetylated cGMP in the x-axis and the percentage of Standard (or sample) bound/maximum bound (i.e. cGMP/maximum bound) in the y-axis to calculate the concentration of cGMP. The %B/B₀ value for each sample was calculated and the concentration of each sample (pmol/mL) was calculated by identifying the %B/B₀ on the standard curve and reading the corresponding values on the x-axis.